

AD A103530

NSWC TR 80-417

12

LEVEL III
H10345

SPACE SHUTTLE RANGE SAFETY COMMAND
DESTRUCT SYSTEM ANALYSIS AND VERIFICATION
PHASE III – BREAKUP OF SPACE SHUTTLE CLUSTER VIA
RANGE SAFETY COMMAND DESTRUCT SYSTEM

MARCH 1981

PREPARED FOR THE
NATIONAL AERONAUTICS AND SPACE ADMINISTRATION
GEORGE C. MARSHALL SPACE FLIGHT CENTER, ALABAMA

NASA DEFENSE PURCHASE REQUEST H-13047B, AMENDMENT 6
NAVSURFWPNCEN TASK NO. WR14ZAN01

Approved for public release, distribution unlimited.

DTIC
ELECTED
SEP 1 1981
S D
D



NAVAL SURFACE WEAPONS CENTER

Dahlgren, Virginia 22448 • Silver Spring, Maryland 20910

ONE FILE COPY

81 9 01 013

UNCLASSIFIED

SECURITY CLASSIFICATION OF THIS PAGE (When Data Entered)

REPORT DOCUMENTATION PAGE		READ INSTRUCTIONS BEFORE COMPLETING FORM	
1. REPORT NUMBER 14 NSWC/TR-80-417	2. GOVT ACCESSION NO. AD-A103530	3. RECIPIENT'S CATALOG NUMBER 9	
4. TITLE (and Subtitle) Phase I - SPACE SHUTTLE RANGE SAFETY COMMAND / DESTRUCT SYSTEM ANALYSIS AND VERIFICATION, Phase I. Breakup of Space Shuttle Cluster via Range Safety Command		5. TYPE OF REPORT & PERIOD COVERED Final rep't	
6. AUTHOR(s) W. M. Hinckley, D. L. Letho, N. L. Coleburn, A. J. Gorechlad, J. M. Ward, and J. Petes (10)		7. PERFORMING ORG. REPORT NUMBER Destruct System	
8. PERFORMING ORGANIZATION NAME AND ADDRESS Naval Surface Weapons Center White Oak Laboratory Silver Spring, MD 20910		10. PROGRAM ELEMENT, PROJECT, TASK AREA & WORK UNIT NUMBERS NASA 0,0,R15KA	
11. CONTROLLING OFFICE NAME AND ADDRESS 12 166		12. REPORT DATE March 1981	
14. MONITORING AGENCY NAME & ADDRESS (if different from Controlling Office)		15. SECURITY CLASS. (of this report) UNCLASSIFIED	
		16a. DECLASSIFICATION/DOWNGRADING SCHEDULE	
16. DISTRIBUTION STATEMENT (of this Report) Approved for public release; distribution unlimited.			
17. DISTRIBUTION STATEMENT (of the abstract entered in Block 20, if different from Report)			
18. SUPPLEMENTARY NOTES			
19. KEY WORDS (Continue on reverse side if necessary and identify by block number) space shuttle solid rocket booster finite elements fragments destruct system structural response flight dynamics detonation linear shaped charge explosion debris external tank aerodynamic drag hydrogen-oxygen-air orbiter stress analysis blast			
20. ABSTRACT (Continue on reverse side if necessary and identify by block number) The Triplex Destruct System (LSC's on each SRB and on ET) was analyzed for effectiveness for the entire ascent portion of the flight. LSC size/placements were established, LOX/LH ₂ vent times were predicted, SRB depressurization times were calculated, and SRB/ET/Crbiter structural breakup pattern and times were determined. Further, debris weight and aerodynamic characteristics are presented for use in future hazard analyses.			

UNCLASSIFIED

SECURITY CLASSIFICATION OF THIS PAGE (When Data Entered)

UNCLASSIFIED

SECURITY CLASSIFICATION OF THIS PAGE (When Data Entered)

Accession For	
NTIS GRA&I	<input checked="" type="checkbox"/>
DTIC TAB	<input type="checkbox"/>
Unannounced	<input type="checkbox"/>
Justification	
By _____	
Distribution/ _____	
Availability Codes	
Dist	Avail and/or Special
A	

NSWC TR 80-417

DTIC
SELECTED
S D
SEP 1 1981
D

FOREWORD

This report is submitted to the National Aeronautics and Space Administration (NASA), George C. Marshall Space Flight Center, Alabama, in fulfillment of NASA-Defense Purchase Request H-13047-B, dated 15 May 1975, and as modified by Amendment 6 on 12 August 1976. This Phase III study deals with the breakup of the Space Shuttle configurations upon activation of the Triplex Command Destruct system.

The findings of earlier Phase I and II studies conducted by the Naval Surface Weapons Center (NSWC), White Oak Laboratory, are utilized in this study. In Phase I, the aerodynamic loads imposed on the Space Shuttle components were determined for the nominal cluster configuration and in case of inadvertent loss of either a solid rocket booster or the orbiter vehicle. The Phase II study, in part, resulted in the design of the current Triplex Command Destruct System.

This Phase III study analyzes in detail the breakup of the cluster components. The breakup pieces are identified and their characteristics, e.g., size, shape, weight, and ballistic properties, are described. This information can be used to estimate the trajectories of the pieces and the debris pattern formed on the surface of the earth. This, in turn, leads to an estimate of the hazards encountered in the unlikely event that destruct action has to be taken.

The authors acknowledge and appreciate the excellent technical contributions of many of their colleagues at the White Oak Laboratory. M.A. Brown, L.E. Crogan, C.W. Smith, J.W. Watt, and T.J. Young provided much of the structural analysis for the breakup models. A.J. Gorechlad, J. Knott, R.E. Lee, and W. Ragsdale supplied the bulk of the aerodynamics data. These contributions form an intrinsic part of the substance of this report. The professional guidance and leadership of J.A. Roach, MSFC, EL-42, and NASA technical coordinator of this task, are also recognized and appreciated. As in our earlier associations with him on Phases I and II of this program, his patient and cooperative actions made working on this task both productive and pleasurable.

D.L. LEHTO
W.M. HINCKLEY
J. PETES, Team Leader

J. F. PROCTOR
By direction

CONTENTS

<u>Chapter</u>		<u>Page</u>
1	BACKGROUND..... INTRODUCTION..... OBJECTIVES..... DISCUSSION.....	1-1 1-1 1-2 1-4
2	EXECUTIVE SUMMARY..... INTRODUCTION..... SRB BREAKUP..... ET BREAKUP..... ORBITER BREAKUP..... LOX-LH ₂ EXPLOSION..... CONCLUSION.....	2-1 2-1 2-1 2-2 2-3 2-3 2-5
3	BLAST EFFECTS FROM ET DESTRUCT..... INTRODUCTION..... JET OUTFLOW..... JET BREAKUP..... RATE OF BUBBLE GROWTH..... STRIPPING OF LIQUID JET..... DROPLET EVAPORATION TIME..... CLUSTER WITH ORBITER..... MIXING UNDER ORBITER..... IMPACT OF LH ₂ PANCAKE ON LOX JET..... CLUSTER WITHOUT ORBITER..... TURBULENT MIXING IN WAKE OF CLUSTER..... DETONABILITY OF HYDROGEN-OXYGEN-AIR MIXTURES..... HYDROGEN-AIR MIXTURES..... HYDROGEN-OXYGEN MIXTURES..... LH ₂ -LOX MIXTURES..... PROPAGATION OF BURNING..... BLAST.....	3-1 3-1 3-2 3-2 3-27 3-29 3-30 3-31 3-33 3-34 3-36 3-36 3-37 3-37 3-40 3-41 3-41 3-42
4	SRE, ET, AND ORBITER BREAKUP..... INTRODUCTION..... SRB BREAKUP..... ET BREAKUP..... ORBITER BREAKUP..... DEBRIS FRAGMENTS..... RELOCATION OF LH ₂ TANK LSC.....	4-1 4-1 4-1 4-10 4-15 4-16 4-24

CONTENTS — Continued

<u>Chapter</u>	<u>Page</u>
Appendix A LISTING OF SRB DEBRIS FRAGMENTS.....	A-1
Appendix B LISTING OF ET DEBRIS FRAGMENTS.....	B-1
Appendix C LISTING OF ORBITER DEBRIS FRAGMENTS.....	C-1

ILLUSTRATIONS

<u>Figure</u>	<u>Page</u>
2-1 LOX/LH ₂ MIXING AND EXPLOSION SITES.....	2-2
3-1 THRUST VS. TIME FOR LOX JET.....	3-3
3-2 THRUST VS. TIME FOR LH ₂ JET.....	3-4
3-3 PORTION OF LOX PLUME PASSING UNDER ORBITER.....	3-32
3-4 SHAPE OF LH ₂ JET UNDER ORBITER.....	3-33
3-5 DETONATION LIMITS OF H ₂ AIR MIXTURES.....	3-38
3-6 DETONABILITY OF H ₂ AIR MIXTURE AT ALTITUDE OF 831 FT (10 SEC).....	3-38
3-7 DETONABILITY OF H ₂ AIR MIXTURE AT ALTITUDE OF 24.49 KFT (50 SEC)...	3-39
3-8 DETONABILITY OF H ₂ AIR MIXTURE AT ALTITUDE OF 90.57 KFT (T = 100 SEC).....	3-39
3-9 DETONATION LIMITS OF H ₂ -O ₂ MIXTURES.....	3-40
3-10 FRACTION OF H ₂ DETONABLE IN TURBULENT PLUME.....	3-43
3-11 PRESSURE VS. DISTANCE FOR 7,400-LB TNT CHARGE.....	3-44
3-12 IMPULSE VS. DISTANCE FOR 7,400-LB TNT CHARGE.....	3-45
4-1 SRB COMMAND DESTRUCT SYSTEM.....	4-2
4-2 FRAGMENTATION OF SYSTEM TUNNEL BY LSC'S.....	4-2
4-3 INITIAL SRB PERFORATION PATTERN.....	4-3
4-4 PROPELLANT FRAGMENT SIZE DISTRIBUTIONS.....	4-5
4-5 EFFECT OF FLAME SPREAD RATE ON CHAMBER PRESSURE DURING PROPELLANT BREAKUP.....	4-6
4-6 CHAMBER PRESSURE VS. TIME AFTER DESTRUCT ACTION.....	4-7
4-7 MAXIMUM RELATIVE VELOCITY OF PROPELLANT FRAGMENTS.....	4-8
4-8 FORWARD FRUSTUM AND SKIRT.....	4-9
4-9 AFT CASE, AFT SKIRT AND NOZZLE.....	4-9
4-10 AFT SRB/ET ATTACH STRUT.....	4-9
4-11 ET COMMAND DESTRUCT SYSTEM.....	4-11
4-12 ET SKIN FRAGMENTS.....	4-12
4-13 FRAGMENTATION OF CABLE TRAY.....	4-12
4-14 INITIAL HOLING OF LH ₂ TANK.....	4-13
4-15 MAJOR ET FRAGMENTS.....	4-14
4-16 BLAST LOADING ON ORBITER.....	4-15
4-17 FORWARD FUSELAGE STRUCTURE.....	4-17
4-18 ASCENT VEHICLE AXIS SYSTEM.....	4-19
4-19 ASCENT TRAJECTORY PARAMETERS FOR INTEGRATED VEHICLE WITH INADVERTENT RIGHT SRB SEPARATION 10 SECONDS AFTER LIFT-OFF.....	4-20
4-20 ASCENT TRAJECTORY PARAMETERS FOR INTEGRATED VEHICLE WITH INADVERTENT RIGHT SRB SEPARATION 50 SECONDS AFTER LIFT-OFF.....	4-20

ILLUSTRATIONS -- Continued

<u>Figure</u>		<u>Page</u>
4-21	ASCENT TRAJECTORY PARAMETERS FOR INTEGRATED VEHICLE WITH INADVERTENT RIGHT SRB SEPARATION 100 SECONDS AFTER LIFT-OFF.....	4-21
4-22	ASCENT TRAJECTORY PARAMETERS FOR INTEGRATED VEHICLE WITH INADVERTENT ORBITER SEPARATION 10 SECONDS AFTER LIFT-OFF.....	4-21
4-23	ASCENT TRAJECTORY PARAMETERS FOR INTEGRATED VEHICLE WITH INADVERTENT ORBITER SEPARATION 50 SECONDS AFTER LIFT-OFF.....	4-22
4-24	ASCENT TRAJECTORY PARAMETERS FOR INTEGRATED VEHICLE WITH INADVERTENT ORBITER SEPARATION 100 SECONDS AFTER LIFT-OFF.....	4-22
4-25	ΔV VS. DESTRUCT ACTION TIME FOR SELECTED FRAGMENTS.....	4-23
4-26	10-FT LSC INSTALLATION SPANNING RING FRAME X_T 1624.....	4-25
4-27	X_T 1624 FRAME CROSS SECTION AT LSC.....	4-26
4-28	LH ₂ TANK RESPONSE TO LSC CUT AT EARLY TIMES DURING ASCENT.....	4-30
A-1	DRAG COEFFICIENT FOR AFT CASE AND NOZZLE.....	A-22
A-2	DRAG COEFFICIENT FOR FORWARD FRUSTUM AND SKIRT.....	A-23
A-3	DRAG COEFFICIENT FOR AFT SRB/ET ATTACH STRUTS.....	A-24
A-4	DRAG COEFFICIENT FOR SRB MOTOR CASE SEGMENTS.....	A-25
A-5	DRAG COEFFICIENT FOR CLEVIS PINS.....	A-26
A-6	DRAG COEFFICIENT FOR LONG, SLENDER SRM CASE, SYSTEMS TUNNEL, AND LSC SEGMENTS.....	A-27
A-7	DRAG COEFFICIENT FOR SHORT SRB SYSTEMS TUNNEL SEGMENTS.....	A-27
A-8	DRAG COEFFICIENT FOR SRM PROPELLANT CUBES.....	A-28
B-1	LIFT AND DRAG COEFFICIENTS FOR FORWARD ET SECTION.....	B-24
B-2	LIFT AND DRAG COEFFICIENTS FOR MID ET SECTION.....	B-25
B-3	LIFT AND DRAG COEFFICIENTS FOR AFT ET SECTION.....	B-26
B-4	DRAG COEFFICIENT FOR PIPE SECTIONS.....	B-27
B-5	DRAG COEFFICIENT FOR VENT VALVE, PURGE, AND HELIUM INJECTION LINES.	B-27
B-6	DRAG COEFFICIENT FOR ET SKIN SECTIONS.....	B-28
B-7	DRAG COEFFICIENT FOR RING FRAME STABILIZERS (LH ₂ TANK).....	B-28
B-8	DRAG COEFFICIENT FOR STABILITY RINGS (LH ₂ TANK), STRINGERS AND TENSION STRAPS (SLOSH BAFFLE), CABLE TRAY SEGMENTS, AND LSC SHEATH SEGMENTS.....	B-29
B-9	DRAG COEFFICIENT FOR SLOSH BAFFLE SEGMENTS AND INDIVIDUAL BAFFLE WEBS.....	B-29
C-1	DRAG COEFFICIENT FOR FUSELAGE MID SECTION.....	C-8
C-2	DRAG COEFFICIENT FOR FUSELAGE AFT SECTION (BODY, WING, TAIL, NOZZLES).....	C-9
C-3	DRAG COEFFICIENT FOR NOSE LANDING GEAR.....	C-10
C-4	DRAG COEFFICIENT FOR RCS NOZZLES.....	C-10
C-5	DRAG COEFFICIENT FOR RCS FUEL, OXIDIZER, AND PRESSURIZATION TANKS..	C-11
C-6	DRAG COEFFICIENT FOR ORBITER/ET ATTACH STRUTS.....	C-11
C-7	DRAG COEFFICIENT FOR BEAMS, TRUSSES, AND PIPES.....	C-12
C-8	DRAG COEFFICIENT FOR PAYLOAD BAY DOORS, LANDING GEAR DOORS, SKIN SECTIONS, AND THERMAL TILES.....	C-12
C-9	DRAG COEFFICIENT FOR C-C THERMAL MATERIAL.....	C-13

TABLES

<u>Table</u>		<u>Page</u>
1-1	RSS ACTIVATION SCOPE OF WORK.....	1-3
3-1	CRYOGEN DATA.....	3-5
3-2	FLIGHT DATA.....	3-5
3-3	DUMPING OF LOX TANK.....	3-6
3-4	AERODYNAMIC STRIPPING OF LOX JET.....	3-6
3-5	DUMPING OF LH ₂ TANK.....	3-7
3-6	AERODYNAMIC STRIPPING OF LH ₂ JET.....	3-7
3-7	PROPERTIES OF PLUME FROM 1 CM SECTION OF LOX JET.....	3-8
3-8	COMPOSITION OF PLUME FROM 1 CM SECTION OF LOX JET.....	3-8
3-9	AERODYNAMIC STRIPPING OF LH ₂ BY LOX-AIR PLUME.....	3-9
3-10	DETONATION PROPERTIES OF LOX+AIR FLOW ON LH ₂ PANCAKE.....	3-9
3-11	VENTING OF LOX TANK AT 10 SECONDS FLIGHT TIME.....	3-10
3-12	VENTING OF LOX TANK AT 20 SECONDS FLIGHT TIME.....	3-11
3-13	VENTING OF LOX TANK AT 50 SECONDS FLIGHT TIME.....	3-12
3-14	VENTING OF LOX TANK AT 65 SECONDS FLIGHT TIME.....	3-13
3-15	VENTING OF LOX TANK AT 100 SECONDS FLIGHT TIME.....	3-14
3-16	VENTING OF LOX TANK AT 115 SECONDS FLIGHT TIME.....	3-15
3-17	VENTING OF LOX TANK AT 350 SECONDS FLIGHT TIME.....	3-16
3-18	VENTING OF LOX TANK AT 450 SECONDS FLIGHT TIME.....	3-17
3-19	VENTING OF LH ₂ TANK AT 10 SECONDS FLIGHT TIME.....	3-18
3-20	VENTING OF LH ₂ TANK AT 20 SECONDS FLIGHT TIME.....	3-19
3-21	VENTING OF LH ₂ TANK AT 50 SECONDS FLIGHT TIME.....	3-20
3-22	VENTING OF LH ₂ TANK AT 65 SECONDS FLIGHT TIME.....	3-21
3-23	VENTING OF LH ₂ TANK AT 100 SECONDS FLIGHT TIME.....	3-22
3-24	VENTING OF LH ₂ TANK AT 115 SECONDS FLIGHT TIME.....	3-23
3-25	VENTING OF LH ₂ TANK AT 350 SECONDS FLIGHT TIME.....	3-24
3-26	VENTING OF LH ₂ TANK AT 450 SECONDS FLIGHT TIME.....	3-25
3-27	VENTING TIMES FOR LOX AND LH ₂ TANKS	3-26
3-28	IMPACT OF LH ₂ ON LOX JET.....	3-35
3-29	MIXING OF JETS WITH ORBITER SEPARATED.....	3-35
4-1	VELOCITY, ANGLE OF ATTACK, AND ANGLE OF SIDESLIP AT DESTRUCT ACTION TIME FOR SELECTED TIMES.....	4-18

CHAPTER 1

BACKGROUND

INTRODUCTION

The Space Shuttle cluster includes a Triplex Command Destruct System to be activated by the range safety officer to terminate certain conditions of aberrant flight. This system evolved partly as a result of two studies made by the Naval Surface Weapons Center, White Oak Laboratory, for the George C. Marshall Space Flight Center (MSFC), Code EL-42.

The first study (Phase I), initiated in mid-1975, determined that the destruct system as then designed was inadequate to assure the required catastrophic destruct of the Space Shuttle cluster and rapid dumping of the LOX and LH₂ in the external tank (ET) at all times into flight from 10 seconds after lift-off to 300 seconds.¹ This initial destruct system used linear-shaped charges (LSC's) mounted outboard on the two solid rocket boosters (SRB's). Destruct action of the SRB's was to bring about destruct of the ET.

It is particularly important to destruct the ET; its large quantities of LOX and LH₂ present a considerable potential explosion hazard upon ground impact should the ET fall to the surface relatively intact. Specifically, the Air Force Eastern Test Range Manual, AFETRM-127-1, in paragraph 4.3.1.3.1.2 states: "For liquid propellant stages using non-toxic propellants, the destruct charges must cause penetration of the propellant tanks, both fuel and oxidizer, to the extent necessary for rapid dispersion of the propellants. The intent of this requirement is to ensure the maximum amount of propellants are dispersed before vehicle impact with the ground. This will reduce the impact area hazard by reducing the explosive yield."

A Phase II study explored about a dozen different explosive systems to accomplish the desired destruct and dumping at all times of interest.² A number of criteria were

¹"Study Report on Space Shuttle Range Safety Command Destruct System Analysis and Verification," Naval Surface Weapons Center, White Oak Laboratory, Silver Spring, Maryland, for George C. Marshall Space Flight Center, Marshall Space Flight Center, Alabama, under NASA-Defense Purchase Request H-13047 B of 15 May 1975. Report dated 2 Feb 1976. (Now published as Phase I of this report.)

²"Ordnance Options for a Space Shuttle Range Safety Command Destruct System," Naval Surface Weapons Center, White Oak Laboratory, Silver Spring, Maryland, for George C. Marshall Space Flight Center, Marshall Space Flight Center, Alabama, under NASA-Defense Purchase Request H-13047 B, Amendment 3, 8 Mar 1976. Report dated 10 Dec 1976. (Now published as Phase II of this report.)

keyed to the requirements to help evaluate each system studied. These requirements were: (1) rapid dumping of the LOX and LH₂ at altitude; (2) minimum mixing of the LOX and LH₂, so that (3) minimum potential blast yield of the mixture results; (4) minimum weight of the ordnance devices; (5) commonality of the ordnance devices; and (6) easy placement of the ordnance items. The recommended system, the one that best met the criteria, added explosively loaded LSC's to the ET, dedicated to the direct and independent destruct of the ET. This, in conjunction with the LSC's aboard the two SRB's, comprises the Triplex Command Destruct System.

Destruct of the Space Shuttle and dumping of the LOX and LH₂ are but the starting points for other range and ground safety (or hazards) considerations. The destruct products have to be quantified and identified. How many SRB, ET, and orbiter vehicle (OV) pieces are formed? Of what shape, size, and weight are they? And what are the aerodynamic characteristics of these thousands of pieces, their drag and lift coefficients? This information is required to permit calculation of the debris pattern at the surface of the earth and estimates of the extent of surface hazards. Because much of the information developed in Phases I and II is applicable to answering the questions on the Space Shuttle breakup, MSFC added Phase III to develop a breakup model and determine the properties of the resulting pieces. That work is the subject of this report.

OBJECTIVES. The technical objectives of this study, along with some of the ground rules, are stated in the Statement of Work issued by MSFC.

I. Scope of Work

For the cases indicated in the accompanying matrix (Table 1-1) determine the following:

- (a) Number of pieces resulting from Range Safety Action
- (b) Size, area, and weight and shape of pieces
- (c) ΔV imparted to pieces
- (d) Aerodynamic Characteristics, C_D and C_L vs. Mach Number of pieces

II. Discussion

- (a) The starting point for developing the breakup model for the SRBs, ET, and Orbiter will be the action of the explosive destruct systems aboard the SRBs and the ET as determined in Phases I and II of this study. These systems will rupture, tear, hole, or in general, weaken the structural integrity of the SRBs and the ET.
- (b) These weakened structures will be subject to further destruction and breakup through the application of explosion, inertia, aerodynamic, and body forces applied to the full and partial clusters. The Orbiter will experience its breakup through the application of these same forces.

TABLE 1-1 RSS ACTIVATION SCOPE OF WORK

1. Analyze the following cases:

Component	Nominal			One SRB Lost				Orbiter Lost		Percentage of Propellant Remaining	
	SRB	ET	OV	SRB		ET	OV	SRB	ET	SRB	ET
Time or Propellant Level				Free	Cluster						
10 sec after lift-off	X	X	X							90	98
20 sec*				X	X	X	X	X	X		
50 sec, max Q-region	X	X	X							45	88
52 sec*				X	X	X	X				
65 sec*								X	X		
100 sec, just prior to SRB burnout	X	X	X							<1	75
115 sec*				X	X	X	X	X	X		
350 sec flight time		X									25
450 sec, propellant depletion	X										<1

*The cases were added at a later time.

2. Define:

- a. Number of pieces resulting from Range Safety Action.
- b. Size (area and weight) and shape (consistent with aerodynamic curves).
- c. ΔV imparted to pieces.
- d. Aerodynamics (C_D and C_L vs. Mach Number).

(c) Breakup of the nominal configuration will start upon activation of the range command destruct system. However, to realistically account for the time between inadvertent initial and subsequent separation of various cluster elements (as determined in the Phase I study) and the activation of the range command destruct system, the major structural breakup analysis for the cluster elements will start at the following times:

- 10 sec at 10 sec after lift off
- 15 sec at all other times except under such circumstances arising from an

inadvertent separation in which subsequent structural failure will occur in less time; the delta times of Phase I will then be used.

- (d) A normal flight path will be used in the analysis, i.e., the altitude and velocity of the cluster or components of the cluster are as defined in normal flight, or close to these values.
- (e) Vehicle dynamics will be those predicted in the Phase I study at the appropriate times for command destruct.
- (f) C_D and C_L will be time average or spectrum values as functions of Mach number.
- (g) The ΔV imparted to the pieces will be the vector sum of the velocity of the cluster at the time range destruct is initiated and the velocity imparted by the explosion and other forces.

DISCUSSION. The objectives of the task are straightforward. It should be noted that only initial breakup pieces and the aerodynamics of these pieces are called for in the task, not the subsequent trajectories and possible further breakup. Some elaboration on the "Discussion" portion of the Statement of Work, particularly with reference to the starting times for considering command-destruct-initiated breakup, may be useful. For the nominal configuration of the cluster (with the two SRB's, the ET, and the OV all attached), the starting time for breakup can be at whatever time the destruct signal is given. The flight condition times in the matrix are appropriate. In the modified matrix, these times are translated into approximate times in seconds into flight. (Note that only a modified matrix (Table 1-1) is presented in this report; the original matrix had only the flight times without asterisks. The reasons for the added times, shown with asterisks, are reflected in the following paragraphs.)

When an SRB or the OV is inadvertently lost, the starting times have to be slightly modified. This is necessary to account for the time between initial loss of the SRB or OV and the time when the destruct command signal to activate the LSC destructor explosives is given. Eastern Test Range personnel estimate that a few seconds may elapse before it is definitely determined that the cluster has lost a major component. Additional seconds may be consumed in consolidating and evaluating all information pertinent to the loss. As a consequence, it may be 10 to 15 seconds after the initial loss that the command destruct signal is given. During this time, as shown in Phase I, substantial separation and damage of the cluster elements have occurred under the influence of the aerodynamic flight loads. When the destruct signal is given, the major catastrophic breakup is initiated and superimposed on the separated and structurally weakened cluster units. These new and realistic times for starting the destruct through activation of the LSC ordnance are included in the modified matrix as asterisked items.

Chapter 2 of this report summarizes the results of the study. It is patently impossible to characterize all of the thousands of pieces created by the breakup for all conditions of cluster configuration at the different times of interest in anything but a qualitative way. Similarly, the assumptions going into the calculations

for the breakup models, the details of the structural analyses, and the mixing and detonation of the dumped LOX and LH₂ are treated mainly in qualitative terms. The details of these assumptions and calculations are presented in Chapters 3 and 4. Chapter 3 treats the LOX-LH₂ dumping, mixing, and explosion. Chapter 4 provides the breakup models and structural analyses. Listings of breakup pieces are broken down into three groups, one each for the SRB, ET, and OV. The breakup pieces for the SRB are presented in Appendix A, those for the ET in Appendix B, and those for the OV in Appendix C. Within each group, the lists are arranged according to time into flight.

CHAPTER 2

EXECUTIVE SUMMARY

INTRODUCTION

Upon activation of the Range Safety System (RSS), explosively loaded, linear-shaped charges (LSC's) on the two solid rocket boosters (SRB's) and the external tank (ET) of the Space Shuttle cluster rupture the SRB and ET skins along their lengths. This initial weakening of the structural integrity of the SRB's and ET leads to a major breakup of the SRB's, the ET, and the orbiter vehicle (OV). The many forces — mechanical, aerodynamic, and explosive — contributing to this breakup and the characteristics (size, shape, weight, number, C_D , C_L , and ΔV) of the pieces or fragments are the subject of this report.

The breakup model considers activation of the RSS from 10 seconds after lift-off through 450 seconds into flight. Both the normal configuration of the Space Shuttle cluster and the abnormal situation where either one SRB or the OV is inadvertently released are considered. Table 1-1 indicates in matrix form the Shuttle configurations and times of concern covered in this study.

After the longitudinal cuts of the SRB and ET skins by the LSC's, many interacting and strong forces operate to break the Space Shuttle cluster into many thousands of pieces of various sizes and shapes. Mechanical and aerodynamic forces produce the major breakup of the main propulsion system components, while mechanical and blast forces cause damage and some breakup of the OV. First, consider the breakup model with only mechanical and aerodynamic forces being the breakup mechanisms. Later, the explosive blast forces generated by the mixing and detonation of the LOX and LH₂ escaping from the ET will be introduced.

SRB BREAKUP

Upon severing the solid rocket motor (SRM) skin along 70 percent of its length, the internal pressure created by the burning propellant is sufficient to open the SRB case and propellant grain in a clamshell-like fashion. This now weakened SRB structure breaks along seven major segment joints. The six cylindrical segments of the motor case cut by the LSC break into twelve pieces, each segment breaking in half at the clamshell hinge. The forward frustum and skirt and the aft case and nozzle separate as individual large pieces: The equipment tunnel and its contents also contribute to fragment production.

The opening up of the motor case segments fractures the propellant into a spectrum of sizes from about 1-inch cubes to a few pieces in the 35-inch cube range. The SRB breakup is the same whether the SRB is in its normal configuration or in a free mode, having been inadvertently separated. It should be noted that the solid propellant is not expected to detonate under the action of the LSC or the subsequent rapid burning due to breakup.

The breakup mechanism of the SRB is essentially the same at 10 seconds after lift-off as at 115 seconds into flight, except for propellant fragmentation. At the later times, less propellant with thinner wall thickness is available for fragmentation. Hence, most of the propellant pieces will be clustered at the small end of the size spectrum. The C_D and ballistic factors for the pieces change somewhat with time because of the Mach number dependence of these factors.

ET BREAKUP

After initial longitudinal ruptures of the LOX and LH₂ tanks by the LCS's, the breakup analysis of the ET is similar to that of the SRB breakup. What differs are the magnitudes of the forcing functions producing the fragments and the structural parameters of the two tanks. For instance, the LSC ruptures of the ET are relatively small, about 20 feet along the LH₂ tank and 8 feet along the LOX tank. This compares with an about 72-foot cut in the SRB skin.

Although the initial rupture of the LOX skin is only 8 feet long, a maximum hole size of about 160 ft²* is predicted for dumping the LOX. Through circumferential crack propagation of the original LSC cut and gross yielding of the tank brackets and cable tray pads, the tank skin and structure will be peeled back about a quarter of the circumference of the tank. Superior strength of the barrel panels forward of the SRB beam limits the extent of this initial hole size. The extent of subsequent damage and breakup are controlled by the energy in the tank, the damage to the LH₂ tank, and the lateral thrust on ET resulting from the expelled LOX and LH₂.

The initial hole size in the LH₂ tank depends on essentially the same factors as those influencing the LOX tank hole: size of the LSC cut and linear crack extension in the skin. At times of 50 seconds into flight and later, the hole size is calculated to be 620 ft²;* at earlier times, e.g., 10 seconds, because of the lack of sufficient tensile axial stress, the initial hole size is only about 300 ft².*

These combined forces -- the LSC cut, the opening of the LOX and LH₂ tanks through crack propagation and internal tank pressures, the thrust of the LOX and LH₂ jets -- coupled with the flight-induced loads, break the ET into many pieces. Some are quite large, e.g., the forward section of the LOX tank (6,500 pounds), the mid-section comprising the intertank and part of the LH₂ tank (42,000 pounds), and the aft section of the LH₂ tank (20,000 pounds). Other pieces, e.g., fragments of the cable tray and piping, longitudinal stringers, stability ring segments, etc., are considerably smaller but more numerous.

*Area of skin removed.

The number and size of pieces of the ET breakup will not be influenced much as a function of time into flight and altitude when destruct action is taken. The ballistic characteristics of the pieces, however, are influenced because of Mach number dependence. Loss of an SRB or the OV will not change the breakup model of the ET.

ORBITER BREAKUP

The orbiter does not have a dedicated destruct system; SRB breakup is not expected to affect the orbiter. However, even with the initial conditions considered -- no LOX-LH₂ explosion -- the OV will sustain damage and breakup through ET destruct. The impact force of the LH₂ jet, on the order of 10⁶ pounds, exerted on the bottom of the orbiter will result in failures of the OV/ET attach fittings, and the OV fuselage will be failed in bending near the mid-point of the cargo bay (just forward of the wing).

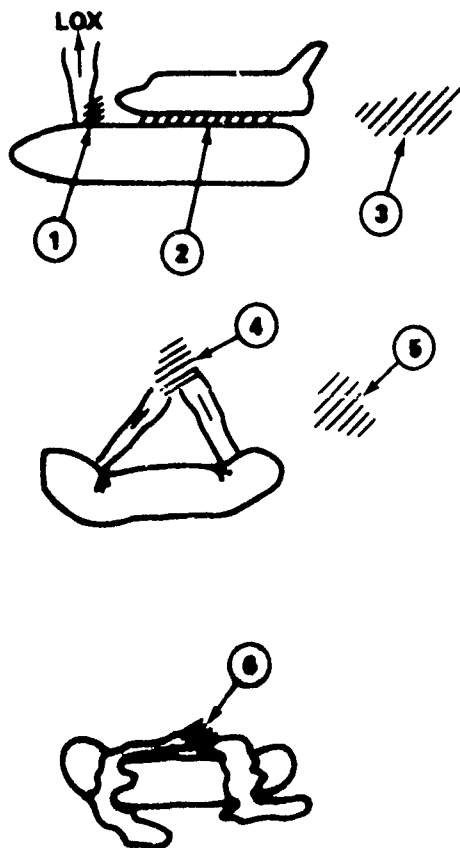
If the orbiter is inadvertently lost prior to RSS activation, of course, no damage will be sustained by the OV except that which may have contributed to the inadvertent loss.

LOX-LH₂ EXPLOSION

The preceding discussions did not consider breakup in the presence of an explosion of the vented LOX and LH₂. There are a number of such potential sources of explosion when the LOX and LH₂ are dumped through the large holes in the ET tanks. In the nominal cluster with the orbiter still attached, the LH₂ in hitting the underside of the orbiter can expand laterally in a pancake-like fashion. The leading edge of this high velocity mass of LH₂ will intersect the LOX jet forward of it, and, through auto-ignition, an explosion can take place (Fig. 2-1, Item 1). The evaporating and stripped LOX and LH₂ can mix with the air underneath the orbiter, and in the presence of some ignition source (e.g., a burning piece of propellant) and explosion can occur (Fig. 2-1, Item 2). A third possibility exists in the vaporous hydrogen mixing with the air in the wake of the cluster and, with some ignition source, resulting in an explosion (Fig. 2-1, Item 3).

If the OV is lost to the cluster before RSS activation, there are several additional scenarios for possible explosions. The jetting LOX and LH₂ streams can mix at high velocity when the ET distorts during its destruct so that the jet intersect; through auto-ignition, the mixture will explode (Fig. 2-1, Item 4). Items 5 and 6 in Figure 2-1 indicate the other possibilities for mixing the LOX and LH₂. In Item 5, the hydrogen mixes with air and stripped oxygen in the wake of the jets and cluster, and in Item 6 mixing occurs after gross ET breakup. In each of these two cases, a source of ignition is required to initiate the explosion.

The largest explosion in terms of TNT equivalence and the one most damaging in its ability to produce additional fragments from the already broken-up cluster is that illustrated by Item 1 in Figure 2-1 -- the high velocity laterally expanding pancake of LH₂ impacting on the LOX stream. Since this mixing model does not invoke the necessity for an outside ignition source, it is a probable model. It is estimated that this explosion will have an upper limit TNT explosion energy equivalence of 7,400 pounds.

FIGURE 2-1 LOX/LH₂ MIXING AND EXPLOSION SITES

This is a rather large explosive force; however, there are factors which mitigate its effects somewhat in terms of further cluster breakup. At early times into flight, it takes about 1-1/4 seconds for sufficient LH₂ to mix with the LOX to produce auto-ignition. In this time, the SRB pieces have moved sufficiently far from the explosion source to reduce the effect to only modest additional damage. Because of the proximity of the LOX tank and intertank sections of the ET to the blast, they are expected to sustain considerably more damage. However, these structures are capable of absorbing the blast energy through large deformation (plastic flow) and while distorted will not be further fragmented. At later times into flight and at the higher altitudes attained, the blast pressures are greatly reduced (at 100,000-foot altitude it is only about 1/10 of that at sea level). Thus, little additional damage occurs to the SRB and ET pieces. The orbiter, however, fares differently. Because of the proximity of its nose to the explosion origin, substantial damage and breakup in this area is expected. For instance, the forward landing gear and parts of the nose skin and structure will come off. But much beyond about 10-feet, particularly at the higher altitudes, the OV is expected to sustain only modest blast damage.

The other models for potential sources of explosion, treated in some detail in the text, are not considered to be as significant as the pancaking LH₂-LOX model. Down-stream mixing (Models 3 and 5) is not significant in terms of cluster breakup because it occurs at too great a distance from the cluster. Similarly, Model 4 is not particularly important because it occurs at too great a distance from the cluster debris. Models 2 and 6 present probable sources of explosions at distances of concern, but the resulting explosion or explosions are expected to be relatively smaller than the largest explosion predicted, i.e., considerably less than the 7,400-pound TNT equivalence. Model 2 will contribute to debris production mainly by loosening pieces of the thermal insulation tile from the OV. This, however, will be but a small addition to the total debris production.

CONCLUSION

In both nominal and aberrant configurations, the triplex RSS explosive destruct system will break the components of the Space Shuttle cluster into many thousands of pieces, some large, but most relatively small. Major breakup of the SRB and ET components is initiated by the LSC's mounted on these components. Subsequent breakup occurs largely through failure of the skin and structural members under the impetus of normal internal pressures, flight loads, and mechanical stress. The OV will break just forward of the wing under the forces of the jetting LH₂ and will also sustain blast damage to its nose.

The blast force considered most probable is that generated by the auto-ignition of the high velocity, lateral pancaking expansion of the LH₂ stream impinging and mixing with the LOX jet forward of it. The maximum credible explosion is expected to be about 7,400 pounds TNT equivalence. This blast will fracture and break the nose section of the orbiter and will cause some additional damage to the previously fractured ET tanks and SRB's.

The time into flight when destruct action is initiated influences the ballistic characteristics of the structure fragment pieces more than it does their number, size, and shape. The propellant pieces, however, are in all characteristics dependent on time of flight and the amount of propellant available for fracturing.

The characteristics of all the pieces of the Space Shuttle cluster formed by the destruct action are listed in the text of this report for both nominal and aberrant configurations and for flight times of 10 to 450 seconds.

CHAPTER 3

BLAST EFFECTS FROM ET DESTRUCT

INTRODUCTION

In this chapter, effects on the LOX and LH₂ after ET rupture are calculated and explosive effects that might arise from their mixing are estimated.

The LOX and LH₂ jets are exposed to the airflow about the cluster. This airflow generates capillary waves which crest and break into droplets that are swept back with the airflow. The LOX droplets quickly evaporate, and the oxygen-air mixture sweeps back toward the LH₂. The LH₂ jet impacts the bottom of the orbiter vehicle (OV) and spreads out in all directions as a pancake under the OV. Only about two meters of the LOX jet contribute to the flow that gets under the OV and reaches the LH₂. Most of the LOX is carried beyond the OV and never comes into contact with hydrogen.

The potential sources of explosion when the orbiter is still present are, Fig. 2-1:

1. The hydrogen-oxygen-air mixture under the orbiter.
2. The LH₂-LOX mixture at the LOX jet when the expanding pancake of LH₂ strikes it.
3. Mixing of hydrogen with air in the wake of the cluster. This is regarded as being too far back to have significant effects on the breakup or trajectories of the cluster fragments.

The potential sources of explosion after the orbiter has left the cluster are, Fig. 2-1:

4. The mixing of the LH₂ and LOX jets when the ET distorts causing intersection of the jets.
5. Mixing of hydrogen with air and stripped oxygen in the wake of the jets and cluster.
6. Mixing of LOX and LH₂ after gross ET breakup.

Thrust versus time for the LOC jet is illustrated in Figure 3-1, and the thrust versus time for the LH₂ jet is shown in Figure 3-2.

JET OUTFLOW

The method of calculating the two-phase flow from the ruptured tanks was described in Phase II. The cyrogen properties are shown in Table 3-1 and the flight conditions in Table 3-2. The calculations are based on ullage pressures of 21 psig for the LOX tank and 33 psia for the LH₂ tank. The vapor pressures of both liquids were taken as 15.7 psia. Tables 3-3 through 3-10 present the initial outflow conditions. The initial high outflow rate is caused by the pressure of the ullage gas. When the pressure in the tank drops below the vapor pressure, the liquid boils and the outflow is driven by the vapor pressure. The time-dependent outflow is presented in Tables 3-11 through 3-26.

The LH₂ tank vents more rapidly than the LOX tank (the hole is larger and the flow velocity is higher). Table 3-27 gives the vent times and final vent fractions. The venting stops when the pressures inside and outside the tank become equal. Any further dumping will be incidental sloshing through the vent or by gross breakup of the tank. At the lower altitudes, a large fraction of the LOX and LH₂ is still in the tanks when venting stops and will not come out unless there is gross tank rupture due to ground impact or aerodynamic or blast forces. At flight times of 350 and 450 seconds, about 4000 pounds of hydrogen will freeze in the tank. The amount of frozen LOX in the LOX tank is under 100 pounds. The LOX jet will continue for several seconds after the LH₂ jet has stopped. If there is gross breakup of the tanks, the amount of mixing near the cluster will depend strongly on the details of the breakup.

JET BREAKUP

The exiting jet is subjected to the airflow about the vehicle. The liquid part of the jet is subjected to stripping by tearing off of small droplets from capillary waves on its sides. The bubbly part of the jet (due to boiling) has a rough surface that gives the airstream a good grip on it, and is probably stripped faster than a liquid jet. Stripping rather than bag breakup will occur because the Weber number is about 10⁶, and stripping breakup occurs for Weber numbers above about 20.

When the vehicle is supersonic (beyond about 50 seconds into flight), there will be a bow shock on each of the jets. Its effects are not considered significant. Therefore, its presence will be ignored in this analysis.

After moving out some distance, the jets are completely broken up by boiling and stripping and are swept back with the airflow to form plumes. If the cluster is in approximately normal flight, the oxygen plume will impact the LH₂ jet and plume (or the LH₂ pancake, if the orbiter is still attached). Some LH₂ will evaporate, and part or all of the oxygen and entrained air may condense to liquid or solid. As evaporation of the LH₂ proceeds, the plume will increase because of the expansion of the hydrogen gas. The plume diameter will expand until its internal pressure equals the ambient air and eventually dissipates, if it is not burned or detonated before then.

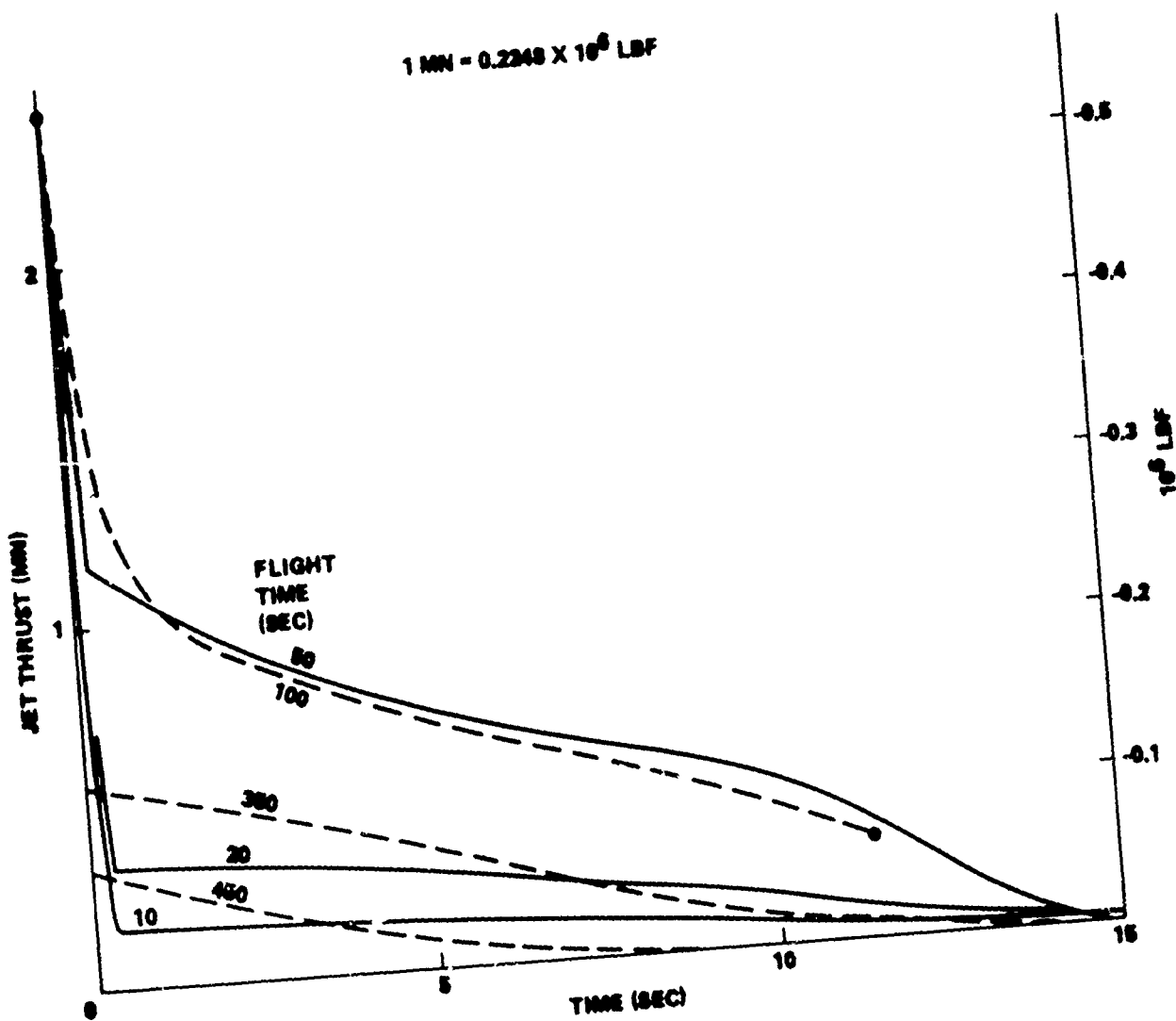


FIGURE 3-1 THRUST VS. TIME FOR LOX JET

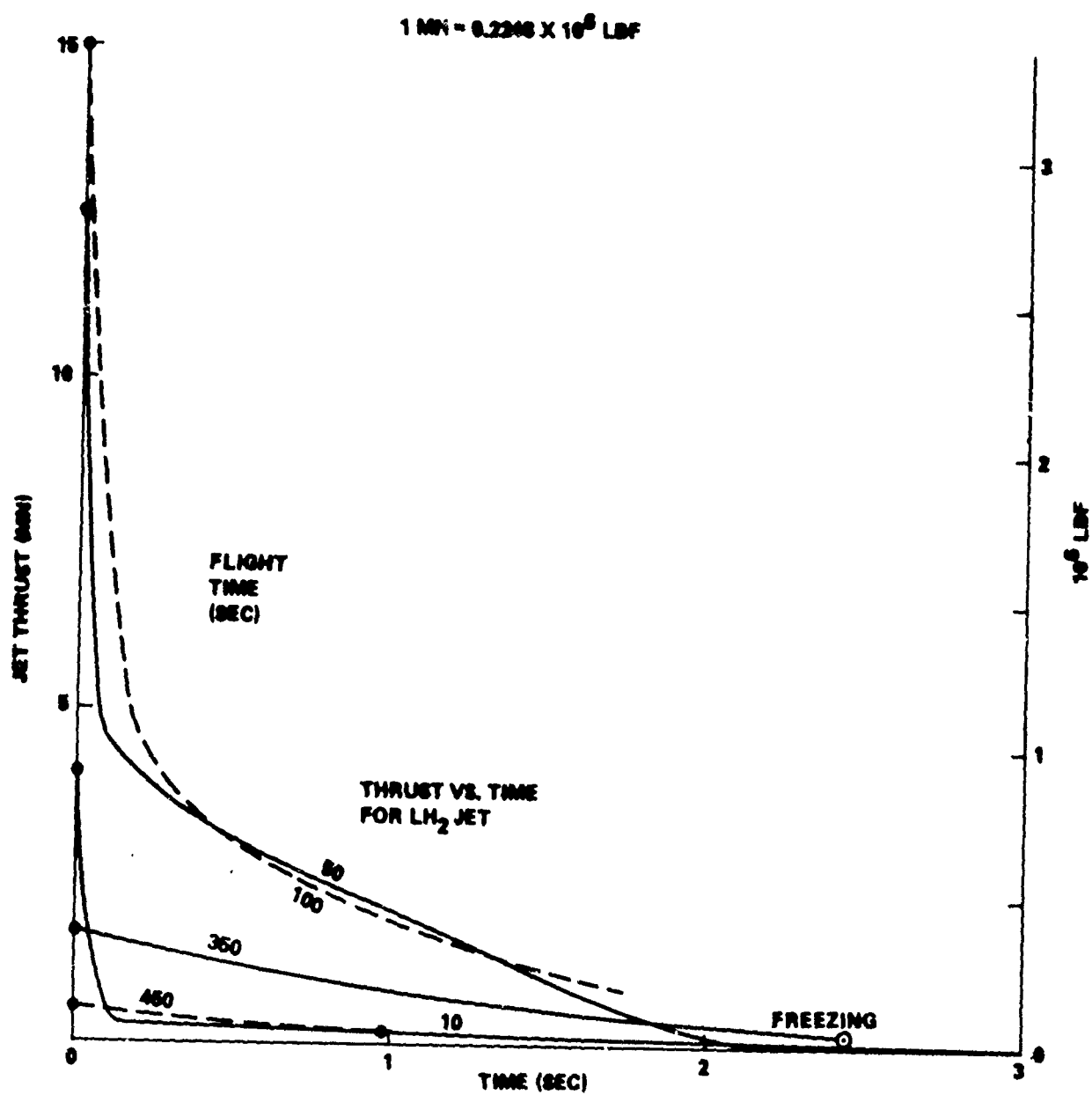


FIGURE 3-2 THRUST VS. TIME FOR LH₂ JET

TABLE 3-1 CRYOGEN DATA

	DENSITY G/CM ³	VISCOSITY G/CM.S	SURF TENS DYNE/CM	P BOIL BAR	T BOIL K
L02	1.147	.00870	13.2	1,0822	90.81
LH2	.070	.00024	2.0	1,0822	20.47

BOILING POINTS AT AMBIENT PRESSURE

TIME (S)	PRESSURE (BAR)	----BOILING POINTS (K)---		
		LOX	LH2	N2
10	9.833-1	89.89	20.16	77.10
20	8.816-1	88.87	19.79	76.18
30	7.234-1	87.08	19.17	74.59
40	4.867-1	83.72	18.02	71.61
50	3.844-1	81.85	17.36	69.97
60	2.510-1	78.69	16.31	67.55
65	1.956-1	76.97	15.76	65.66
70	1.488-1	75.17	15.18	64.09
80	8.003-2	71.39	14.02	63.15(S)
90	3.887-2	67.48	13.96(S)	63.15(S)
100	1.719-2	63.58	13.96(S)	63.15(S)
110	6.989-3	59.80	13.96(S)	63.15(S)
115	3.675-3	57.37	13.96(S)	63.15(S)
120	2.813-3	56.42	13.96(S)	63.15(S)
350	2.967-8	54.35(S)		
450	3.903-8	54.35(S)	(S)=SOLID	

TABLE 3-2 FLIGHT DATA

TIME (S)	ALTITUDE (FT)	SPEED (FT/S)	SPEED (CM/S)	PRESSURE (BAR)	DENSITY (G/CM ³)	TEMP (K)	L02 P (PSIA)	LH2 P (PSIA)
10	831.	184.	5608.	9.833E-01	1.196E-03	286.5	35.3	33.0
20	3800.	430.	13106.	8.816E-01	1.095E-03	280.6	33.8	33.0
30	9037.	677.	20635.	7.234E-01	9.325E-04	270.3	31.5	33.0
40	18957.	887.	27036.	4.867E-01	6.765E-04	250.6	28.1	33.0
50	24490.	1073.	32705.	3.844E-01	5.589E-04	239.7	26.6	33.0
60	33915.	1277.	38923.	2.510E-01	3.957E-04	221.0	24.6	33.0
65	39196.	1412.	43053.	1.956E-01	2.568E-04	216.7	23.8	32.0
70	44905.	1578.	48097.	1.488E-01	2.393E-04	216.6	23.2	33.0
80	57881.	1997.	60869.	8.003E-02	1.287E-04	216.6	22.2	33.0
90	73036.	2540.	77419.	3.887E-02	6.188E-05	218.8	21.6	33.0
100	90572.	3219.	98115.	1.719E-02	2.672E-05	224.1	21.2	33.0
110	110372.	3978.	121249.	6.989E-03	1.046E-05	232.7	21.1	33.0
115	125290.	4322.	131735.	3.675E-03	5.218E-06	245.4	21.0	33.0
120	131743.	4501.	137190.	2.813E-03	3.907E-06	250.8	21.0	33.0
350	388000.	15000.	4.57+5	2.967E-08	3.011E-11	333.7	21.0	33.0
450	378000.	24000.	7.32+5	3.903E-08	4.488E-11	308.6	21.0	33.0

TABLE 3-3 DUMPING OF LOX TANK

TIME (S)	OUTFLOW VELOCITY (CM/S)	OUTFLOW MASS FLUX (G/CM ² .S)	HOLE AREA (FT ²)	OUTFLOW RATE (G/S)	LATERAL THRUST (DYNE)	MASS PER FT PATH (LB)	JET DIAMETER (CM)
10	1.590E+03	1.824E+03	145.0	1.524E+03	2.423E+11	1.825E+03	3.261E+02
20	1.589E+03	1.823E+03	145.0	1.523E+08	2.420E+11	7.807E+02	3.261E+02
30	1.589E+03	1.823E+03	145.0	1.522E+08	2.419E+11	4.958E+02	3.261E+02
40	1.590E+03	1.824E+03	145.0	1.524E+08	2.423E+11	3.787E+02	3.261E+02
50	1.590E+03	1.824E+03	145.0	1.523E+08	2.421E+11	3.129E+02	3.261E+02
60	1.587E+03	1.821E+03	145.0	1.521E+08	2.414E+11	2.625E+02	3.261E+02
70	1.591E+03	1.824E+03	145.0	1.524E+08	2.423E+11	2.129E+02	3.261E+02
80	1.590E+03	1.824E+03	145.0	1.524E+08	2.423E+11	1.682E+02	3.261E+02
90	1.590E+03	1.824E+03	145.0	1.523E+08	2.423E+11	1.322E+02	3.261E+02
100	1.587E+03	1.820E+03	145.0	1.520E+08	2.413E+11	1.041E+02	3.261E+02
110	1.589E+03	1.822E+03	145.0	1.522E+08	2.418E+11	8.436E+01	3.261E+02
115	1.587E+03	1.820E+03	145.0	1.520E+08	2.412E+11	7.755E+01	3.261E+02
120	1.587E+03	1.821E+03	145.0	1.521E+08	2.414E+11	7.448E+01	3.261E+02
350	1.589E+03	1.822E+03	145.0	1.522E+08	2.419E+11	2.237E+01	3.261E+02
450	1.589E+03	1.822E+03	145.0	1.522E+08	2.419E+11	1.398E+01	3.261E+02

DEFINITIONS OF TABLE COLUMNS--

- (1) FLIGHT TIME.
- (2) VELOCITY OF OUTFLOW FROM HOLE.
- (3) MASS FLUX FROM HOLE.
- (4) HOLE AREA.
- (5) RATE OF OUTFLOW FROM HOLE.
- (6) LATERAL THRUST ON EXTERNAL TANK DUE TO JET.
- (7) MASS OUTFLOW PER FOOT OF VEHICLE TRAVEL.
- (8) EQUIVALENT CIRCULAR DIAMETER OF JET.

TABLE 3-4 AERODYNAMIC STRIPPING OF LOX JET

TIME (S)	MAYER F	MAYER V	MAYER TAU (1/S)	D BAR (CM)	STRIP RATE M DOT (G/CM ² /S)
10	3.635E+03	5.989E-01	3.528E-05	1.818E-03	6.067E-01
20	1.818E+04	5.989E-01	4.126E-06	6.218E-04	1.774E+00
30	3.837E+04	5.989E-01	1.524E-06	3.779E-04	2.919E+00
40	4.778E+04	5.989E-01	1.137E-06	3.264E-04	3.379E+00
50	5.777E+04	5.989E-01	8.830E-07	2.876E-04	3.835E+00
60	5.793E+04	5.989E-01	8.797E-07	2.871E-04	3.842E+00
70	5.349E+04	5.989E-01	9.782E-07	3.028E-04	3.643E+00
80	4.608E+04	5.989E-01	1.194E-06	3.344E-04	3.298E+00
90	3.584E+04	5.989E-01	1.669E-06	3.954E-04	2.789E+00
100	2.486E+04	5.989E-01	2.718E-06	5.047E-04	2.186E+00
110	1.486E+04	5.989E-01	5.397E-06	7.112E-04	1.551E+00
115	8.750E+03	5.989E-01	1.094E-05	1.012E-03	1.090E+00
120	7.106E+03	5.989E-01	1.443E-05	1.163E-03	9.485E-01
350	6.080E-01	5.989E-01	3.828E+00	5.989E-01	1.842E-03
450	2.322E+00	5.989E-01	6.414E-01	2.452E-01	4.494E-03

DEFINITIONS OF TABLE COLUMNS--

- (1) FLIGHT TIME.
- (2) MAYER PARAMETER F.
- (3) MAYER PARAMETER V.
- (4) EXPONENTIAL GROWTH RATE OF FASTEST-GROWING WAVELENGTH.
- (5) MEAN DROPLET DIAMETER.
- (6) GRAMS STRIPPED PER SQUARE CM PER SECOND BY AIRFLOW.

TABLE 3-5 DUMPING OF LH₂ TANK

TIME (S)	OUTFLOW VELOCITY (CM/S)	OUTFLOW MASS FLUX (G/CM ² .S)	HOLE AREA (FT ²)	OUTFLOW RATE (G/S)	LATERAL THRUST (DYNE)	MASS PER FT PATH (LB)	JET DIAMETER (CM)
10	6.076E+03	4.253E+02	271.0	6.639E+07	4.033E+11	7.954E+02	4.458E+02
20	6.310E+03	4.417E+02	572.0	1.455E+08	9.183E+11	7.462E+02	6.477E+02
30	6.659E+03	4.661E+02	572.0	1.536E+08	1.023E+12	5.001E+02	6.477E+02
40	7.149E+03	5.004E+02	572.0	1.649E+08	1.179E+12	4.098E+02	6.477E+02
50	7.350E+03	5.145E+02	572.0	1.695E+08	1.246E+12	3.483E+02	6.477E+02
60	7.605E+03	5.324E+02	572.0	1.754E+08	1.334E+12	3.028E+02	6.477E+02
70	7.795E+03	5.456E+02	572.0	1.798E+08	1.401E+12	2.512E+02	6.477E+02
80	7.920E+03	5.544E+02	572.0	1.827E+08	1.447E+12	2.016E+02	6.477E+02
90	7.994E+03	5.595E+02	572.0	1.844E+08	1.474E+12	1.600E+02	6.477E+02
100	8.032E+03	5.623E+02	572.0	1.852E+08	1.488E+12	1.269E+02	6.477E+02
110	8.050E+03	5.635E+02	572.0	1.857E+08	1.495E+12	1.029E+02	6.477E+02
115	8.056E+03	5.639E+02	572.0	1.858E+08	1.497E+12	9.478E+01	6.477E+02
120	8.058E+03	5.640E+02	572.0	1.858E+08	1.497E+12	9.102E+01	6.477E+02
350	8.063E+03	5.644E+02	572.0	1.860E+08	1.499E+12	2.733E+01	6.477E+02
450	8.063E+03	5.644E+02	572.0	1.860E+08	1.499E+12	1.708E+01	6.477E+02

Definitions are same as for Table 3-3.

TABLE 3-6 AERODYNAMIC STRIPPING OF LH₂ JET

TIME (S)	MAYER F	MAYER V	MAYER TAU (1/S)	DROP DIAM D BAR (CM)	STRIP RATE M DOT (G/CM ² /S)
10	3.780E+04	2.707E-01	1.193E-06	2.248E-04	1.354E-01
20	1.890E+05	2.707E-01	1.395E-07	7.687E-05	3.959E-01
30	3.990E+05	2.707E-01	5.152E-08	4.671E-05	6.514E-01
40	4.969E+05	2.707E-01	3.845E-08	4.036E-05	7.540E-01
50	6.007E+05	2.707E-01	2.985E-08	3.556E-05	8.557E-01
60	6.024E+05	2.707E-01	2.974E-08	3.549E-05	8.573E-01
70	5.563E+05	2.707E-01	3.307E-08	3.743E-05	8.130E-01
80	4.792E+05	2.707E-01	4.036E-08	4.135E-05	7.360E-01
90	3.727E+05	2.707E-01	5.642E-08	4.888E-05	6.225E-01
100	2.585E+05	2.707E-01	9.190E-08	6.239E-05	4.877E-01
110	1.545E+05	2.707E-01	1.825E-07	8.792E-05	3.461E-01
115	9.100E+04	2.707E-01	3.697E-07	1.251E-04	2.432E-01
120	7.389E+04	2.707E-01	4.880E-07	1.438E-04	2.116E-01
350	6.323E+00	2.707E-01	1.294E-01	7.404E-02	4.110E-04
450	2.414E+01	2.707E-01	2.168E-02	3.031E-02	1.004E-03

Definitions are same as for Table 3-4.

TABLE 3-7 PROPERTIES OF PLUME FROM 1 CM SECTION OF LOX JET

TIME (S)	LIQ MASS (G/S)	AIR MASS (G/S)	VEL OUT (CM/S)	VEL LONG (CM/S)	V RATIO	LOX UNDER OV (G)	O2 UNDER OV (G)
10	2.184E+02	6.225E+03	5.391E+01	5.418E+03	9.950E-03	2.419E+04	1.827E+05
20	6.386E+02	1.332E+04	7.273E+01	1.251E+04	5.815E-03	3.064E+04	1.776E+05
30	1.051E+03	1.786E+04	8.833E+01	1.949E+04	4.533E-03	3.236E+04	1.588E+05
40	1.216E+03	1.697E+04	1.064E+02	2.523E+04	4.216E-03	2.893E+04	1.218E+05
50	1.381E+03	1.696E+04	1.197E+02	3.024E+04	3.956E-03	2.739E+04	1.048E+05
60	1.383E+03	1.429E+04	1.401E+02	3.549E+04	3.946E-03	2.338E+04	7.896E+04
70	1.312E+03	1.068E+04	1.739E+02	4.284E+04	4.061E-03	1.837E+04	5.278E+04
80	1.187E+03	7.270E+03	2.233E+02	5.232E+04	4.267E-03	1.362E+04	3.279E+04
90	1.004E+03	4.446E+03	2.930E+02	6.315E+04	4.640E-03	9.541E+03	1.926E+04
100	7.868E+02	2.433E+03	3.878E+02	7.414E+04	5.231E-03	6.368E+03	1.090E+04
110	5.584E+02	1.177E+03	5.112E+02	8.224E+04	6.217E-03	4.074E+03	6.049E+03
115	3.923E+02	6.379E+02	6.043E+02	8.157E+04	7.408E-03	2.885E+03	3.965E+03
120	3.414E+02	4.974E+02	6.461E+02	8.135E+04	7.943E-03	2.518E+03	3.362E+03
350	6.630E-01	1.277E-02	1.559E+03	8.640E+03	1.804E-01	4.604E+01	4.624E+01
450	1.620E+00	3.048E-02	1.560E+03	1.351E+04	1.154E-01	7.193E+01	7.224E+01

DEFINITIONS OF TABLE COLUMNS--

- (1) FLIGHT TIME.
 - (2) MASS OF LOX STRIPPED FROM JET PER SECOND PER CM OF JET.
 - (3) MASS OF AIR PER SECOND INVOLVED IN THE STRIPPING.
 - (4) RADIAL VELOCITY OF LOX-AIR MIXTURE IN PLUME.
 - (5) LONGITUDINAL VELOCITY OF LOX-AIR MIXTURE IN PLUME.
 - (6) RATIO OF RADIAL TO LONGITUDINAL VELOCITY.
 - (7) MASS OF LOX IN 2-M BY 30-M REGION UNDER ORBITER.
 - (8) MASS OF TOTAL OXYGEN IN 2-M BY 30-M REGION UNDER ORBITER.
- WIDTH OF LOX PLUME IS GIVEN BY LAST COLUMN OF TABLE VIII.

TABLE 3-8 COMPOSITION OF PLUME FROM 1 CM SECTION OF LOX JET

TIME (S)	PLUME TEMP(K)	MASS FRACTIONS OF SOLID, LIQUID, AND VAPOR						EXPANDED SIZE(CM)		
		LIQ H	VAP H	SOL O	LIQ O	VAP O	SOL A	LIQ A	VAP A	
10	280.50	0.000	0.000	0.000	0.000	1.000	0.000	0.000	1.000	9.746E+02
20	272.74	0.000	0.000	0.000	0.000	1.000	0.000	0.000	1.000	9.907E+02
30	261.26	0.000	0.000	0.000	0.000	1.000	0.000	0.000	1.000	1.005E+03
40	240.90	0.000	0.000	0.000	0.000	1.000	0.000	0.000	1.000	1.022E+03
50	229.53	0.000	0.000	0.000	0.000	1.000	0.000	0.000	1.000	1.036E+03
60	210.56	0.000	0.000	0.000	0.000	1.000	0.000	0.000	1.000	1.059E+03
70	204.07	0.000	0.000	0.000	0.000	1.000	0.000	0.000	1.000	1.095E+03
80	200.46	0.000	0.000	0.000	0.000	1.000	0.000	0.000	1.000	1.151E+03
90	197.15	0.000	0.000	0.000	0.000	1.000	0.000	0.000	1.000	1.239E+03
100	194.02	0.000	0.000	0.000	0.000	1.000	0.000	0.000	1.000	1.379E+03
110	190.20	0.000	0.000	0.000	0.000	1.000	0.000	0.000	1.000	1.603E+03
115	190.27	0.000	0.000	0.000	0.000	1.000	0.000	0.000	1.000	1.814E+03
120	189.65	0.000	0.000	0.000	0.000	1.000	0.000	0.000	1.000	1.924E+03
350	PLUME NEGLIGIBLE NEAR ET.									
450	PLUME NEGLIGIBLE NEAR ET.									

LOX PLUME WIDTH BEFORE P EQUILIBRATION WAS 2X589 = 1179 CM.

TABLE 3-9 AERODYNAMIC STRIPPING OF LH₂ BY LOX-AIR PLUME

TIME (S)	MAYER F	MAYER V	MAYER TAU	DROP (1/S)	STRIP DIAM (CM)	STRIP RATE 1 (G/CM ² /S)	STRIP RATE 2 (G/CM ² /S)	AIR-LOX DENSITY (G/CM ³)
10	3.599E+04	2.707E-01	1.273E-06	2.322E-04	1.310E-01	3.571E-01	1.220E-03	
20	1.770E+05	2.707E-01	1.522E-07	8.030E-05	3.789E-01	6.533E-01	1.126E-03	
30	3.686E+05	2.707E-01	5.727E-08	4.925E-05	6.178E-01	9.143E-01	9.657E-04	
40	4.511E+05	2.707E-01	4.373E-08	4.304E-05	7.070E-01	9.860E-01	7.054E-04	
50	5.379E+05	2.707E-01	3.459E-08	3.828E-05	7.950E-01	1.063E+00	5.853E-04	
60	5.279E+05	2.707E-01	3.547E-08	3.876E-05	7.851E-01	1.017E+00	4.171E-04	
70	4.715E+05	2.707E-01	4.123E-08	4.179E-05	7.281E-01	9.099E-01	2.557E-04	
80	3.863E+05	2.707E-01	5.378E-08	4.773E-05	6.375E-01	7.693E-01	1.404E-04	
90	2.792E+05	2.707E-01	8.293E-08	5.927E-05	5.134E-01	6.018E-01	6.966E-05	
100	1.739E+05	2.707E-01	1.558E-07	8.125E-05	3.745E-01	4.296E-01	3.149E-05	
110	8.946E+04	2.707E-01	3.782E-07	1.266E-04	2.404E-01	2.723E-01	1.316E-05	
115	4.655E+04	2.707E-01	9.037E-07	1.957E-04	1.555E-01	1.763E-01	6.961E-06	
120	3.565E+04	2.707E-01	1.290E-06	2.337E-04	1.302E-01	1.477E-01	5.361E-06	
350	6.323E-02	2.707E-01	6.008E+01	1.595E+00	NEGLIGIBLE			
450	2.414E-01	2.707E-01	1.006E+01	6.529E-01	NEGLIGIBLE			

Definitions are same as for Table 3-6.

TWO STRIPPING RATES ARE SHOWN.

RATE 1 IS FOR LH₂ AT REST WITH REFERENCE TO THE ET.

RATE 2 IS FOR LH₂ MOVING AT ITS EXIT VELOCITY TOWARD THE LOX JET.
COLUMN 8 GIVES THE DENSITY OF THE IMPINGING LOX-AIR PLUME.

TABLE 3-10 DETONATION PROPERTIES OF LOX+AIR FLOW ON LH₂ PANCAKE

TIME (S)	---NO FORWARD LH ₂ VELOC---			----FULL FORWARD LH ₂ VELOC--		
	BL VEL (CM/S)	DET H ₂ (G)	TNT EQUIV (G/CM ²)	BL VEL (CM/S)	DET H ₂ (G)	TNT EQUIV (G/CM ²)
10	2.709E+03	4.568E+03	4.218E-02	-3.287E+02	-3.765E+04	-3.477E-01
20	6.253E+03	4.440E+03	4.033E-02	3.098E+03	8.961E+03	8.140E-02
30	9.744E+03	3.970E+03	3.557E-02	6.415E+03	6.031E+03	5.403E-02
40	1.261E+04	3.044E+03	2.681E-02	9.040E+03	4.248E+03	3.741E-02
50	1.512E+04	2.620E+03	2.275E-02	1.145E+04	3.461E+03	3.006E-02
60	1.774E+04	1.974E+03	1.678E-02	1.394E+04	2.512E+03	2.136E-02
70	2.142E+04	1.319E+03	1.085E-02	1.752E+04	1.613E+03	1.326E-02
80	2.616E+04	8.197E+02	6.410E-03	2.220E+04	9.659E+02	7.553E-03
90	3.158E+04	4.814E+02	3.497E-03	2.758E+04	5.511E+02	4.004E-03
100	3.707E+04	2.724E+02	1.778E-03	3.305E+04	3.055E+02	1.994E-03
110	4.112E+04	1.512E+02	8.491E-04	3.709E+04	1.676E+02	9.413E-04
115	4.079E+04	9.911E+01	4.917E-04	3.676E+04	1.100E+02	5.456E-04
120	4.067E+04	8.405E+01	3.933E-04	3.665E+04	9.330E+01	4.365E-04
350	4.320E+03	1.156E+00	1.121E-07	2.888E+02	1.730E+01	1.677E-06
450	6.756E+03	1.806E+00	1.752E-07	2.724E+03	4.479E+00	4.344E-07

20 CM THICKNESS OF LOX-AIR PLUME MIXED WITH LH₂.

BL VEL = VELOCITY RELATIVE TO ET IN CENTER OF BOUNDARY LAYER.

DET H₂ = TOTAL STRIPPED LH₂ IN LOX-AIR SWATH ON LH₂ PANCAKE.

TNT EQUIV = EQUIVALENT TNT ENERGY OF STRIPPED LH₂.

TABLE 3-11 VENTING OF LOX TANK AT 10 SECONDS FLIGHT TIME

EFFECTIVE HOLE AREA = 145 SQ FT, VAPOR PRESSURE=15.7 PSIA

VENT T(S)	FLOW VEL(CM/S)	OUTFLOW (G/S)	SPEC VOL (CC/G)	JET THRUST	ULLAGE P(BAR)	VENTED FRAC
.0000	1.598E+03	2.439E+08	8.826E-01	2.417E+11	2.430	.0000
.0441	1.288E+03	1.966E+08	8.826E-01	1.569E+11	1.923	.0100
.0992	1.018E+03	1.554E+08	8.826E-01	9.804E+10	1.570	.0200
.1715	7.641E+02	1.166E+08	8.826E-01	5.525E+10	1.314	.0301
.2713	4.991E+02	7.618E+07	8.826E-01	2.358E+10	1.124	.0400
BEGIN SUBSONIC FLOW						
.3192	4.180E+02	6.381E+07	8.826E-01	1.654E+10	1.082	.0434
.4199	4.192E+02	6.346E+07	8.899E-01	1.649E+10	1.082	.0501
.5728	4.207E+02	6.296E+07	9.001E-01	1.642E+10	1.081	.0601
.7257	4.222E+02	6.247E+07	9.103E-01	1.635E+10	1.081	.0701
.8803	4.236E+02	6.197E+07	9.209E-01	1.628E+10	1.081	.0801
1.0367	4.251E+02	6.146E+07	9.316E-01	1.620E+10	1.080	.0901
1.1930	4.265E+02	6.095E+07	9.426E-01	1.612E+10	1.080	.1000
1.3511	4.279E+02	6.043E+07	9.538E-01	1.603E+10	1.079	.1100
1.5127	4.292E+02	5.990E+07	9.653E-01	1.594E+10	1.079	.1201
1.6726	4.306E+02	5.937E+07	9.770E-01	1.585E+10	1.078	.1300
1.8359	4.319E+02	5.883E+07	9.890E-01	1.575E+10	1.078	.1400
2.0009	4.332E+02	5.828E+07	1.001E+00	1.565E+10	1.077	.1501
2.1660	4.344E+02	5.772E+07	1.014E+00	1.555E+10	1.076	.1600
2.3345	4.356E+02	5.716E+07	1.027E+00	1.544E+10	1.076	.1701
2.5031	4.368E+02	5.659E+07	1.040E+00	1.532E+10	1.075	.1800
2.6751	4.379E+02	5.601E+07	1.053E+00	1.520E+10	1.074	.1901
2.8471	4.389E+02	5.542E+07	1.067E+00	1.508E+10	1.074	.2000
3.0243	4.400E+02	5.483E+07	1.081E+00	1.496E+10	1.073	.2102
3.1980	4.409E+02	5.423E+07	1.095E+00	1.483E+10	1.072	.2200
3.3787	4.418E+02	5.361E+07	1.110E+00	1.469E+10	1.071	.2302
3.5594	4.427E+02	5.299E+07	1.125E+00	1.454E+10	1.071	.2402
3.7401	4.434E+02	5.237E+07	1.141E+00	1.440E+10	1.070	.2500
3.9243	4.441E+02	5.173E+07	1.157E+00	1.424E+10	1.069	.2600
4.1119	4.447E+02	5.108E+07	1.173E+00	1.408E+10	1.068	.2700
4.3030	4.453E+02	5.041E+07	1.190E+00	1.392E+10	1.067	.2801
4.4942	4.457E+02	4.975E+07	1.207E+00	1.375E+10	1.066	.2900
4.6888	4.460E+02	4.907E+07	1.225E+00	1.357E+10	1.065	.3000
5.0884	4.463E+02	4.767E+07	1.261E+00	1.319E+10	1.063	.3201
5.4984	4.461E+02	4.622E+07	1.300E+00	1.279E+10	1.060	.3401
5.9223	4.453E+02	4.472E+07	1.341E+00	1.235E+10	1.058	.3601
6.3602	4.438E+02	4.317E+07	1.385E+00	1.188E+10	1.055	.3801
6.8154	4.414E+02	4.155E+07	1.431E+00	1.137E+10	1.052	.4001
7.7814	4.334E+02	3.809E+07	1.533E+00	1.024E+10	1.045	.4401
8.8447	4.195E+02	3.428E+07	1.648E+00	8.917E+09	1.037	.4801
10.0436	3.965E+02	2.998E+07	1.782E+00	7.370E+09	1.027	.5201
11.4439	3.590E+02	2.498E+07	1.936E+00	5.559E+09	1.017	.5600
13.2092	2.938E+02	1.868E+07	2.118E+00	3.403E+09	1.003	.6000
13.7513	2.698E+02	1.676E+07	2.169E+00	2.804E+09	1.000	.6100
14.3698	2.403E+02	1.457E+07	2.222E+00	2.171E+09	.996	.6201
15.0926	2.036E+02	1.204E+07	2.277E+00	1.521E+09	.992	.6301
16.0238	1.519E+02	8.757E+06	2.336E+00	8.245E+08	.988	.6401
17.6640	5.556E+01	3.122E+06	2.397E+00	1.076E+08	.984	.6501
18.3868	8.615E+00	4.824E+05	2.406E+00	2.576E+06	.983	.6514

TABLE 3-12 VENTING OF LOX TANK AT 20 SECONDS FLIGHT TIME

EFFECTIVE HOLE AREA = 145 SQ FT, VAPOR PRESSURE=15.7 PSIA

VENT T(S)	FLOW VEL(CM/S)	OUTFLOW (G/S)	SPEC VOL (CC/G)	JET THRUST	ULLAGE P(BAR)	VENTED FRAC
.0000	1.599E+03	2.440E+08	8.826E-01	2.419E+11	2.330	.0000
.0896	1.197E+03	1.828E+08	8.826E-01	1.357E+11	1.694	.0200
.2112	8.650E+02	1.320E+08	8.826E-01	7.080E+10	1.306	.0401
BEGIN SUBSONIC FLOW						
.3633	5.944E+02	9.065E+07	8.833E-01	3.341E+10	1.082	.0577
.3873	5.951E+02	9.049E+07	8.858E-01	3.338E+10	1.082	.0600
.5970	6.008E+02	8.913E+07	9.080E-01	3.320E+10	1.081	.0800
.8101	6.066E+02	8.775E+07	9.312E-01	3.300E+10	1.080	.1000
1.0266	6.124E+02	8.635E+07	9.554E-01	3.279E+10	1.079	.1201
1.2466	6.184E+02	8.494E+07	9.807E-01	3.256E+10	1.078	.1401
1.4700	6.243E+02	8.351E+07	1.007E+00	3.233E+10	1.077	.1601
1.6980	6.303E+02	8.207E+07	1.035E+00	3.207E+10	1.076	.1801
1.9294	6.363E+02	8.060E+07	1.063E+00	3.180E+10	1.075	.2001
2.1654	6.424E+02	7.912E+07	1.094E+00	3.151E+10	1.073	.2201
2.4060	6.485E+02	7.761E+07	1.126E+00	3.120E+10	1.072	.2401
2.6512	6.546E+02	7.607E+07	1.159E+00	3.088E+10	1.070	.2601
2.9010	6.607E+02	7.452E+07	1.194E+00	3.053E+10	1.068	.2801
3.1553	6.668E+02	7.295E+07	1.231E+00	3.016E+10	1.066	.3000
3.4165	6.729E+02	7.134E+07	1.270E+00	2.976E+10	1.064	.3200
3.6846	6.789E+02	6.970E+07	1.312E+00	2.934E+10	1.061	.3401
3.9573	6.848E+02	6.805E+07	1.356E+00	2.889E+10	1.059	.3601
4.2368	6.905E+02	6.636E+07	1.402E+00	2.841E+10	1.056	.3800
4.5255	6.962E+02	6.462E+07	1.451E+00	2.789E+10	1.053	.4001
4.8211	7.016E+02	6.286E+07	1.504E+00	2.734E+10	1.050	.4201
5.1236	7.067E+02	6.107E+07	1.559E+00	2.676E+10	1.047	.4400
5.4375	7.116E+02	5.922E+07	1.619E+00	2.613E+10	1.043	.4601
5.7606	7.160E+02	5.733E+07	1.682E+00	2.545E+10	1.039	.4801
6.0951	7.198E+02	5.539E+07	1.750E+00	2.472E+10	1.034	.5001
6.4411	7.230E+02	5.340E+07	1.824E+00	2.394E+10	1.029	.5201
6.8009	7.253E+02	5.135E+07	1.903E+00	2.309E+10	1.024	.5401
7.1744	7.266E+02	4.924E+07	1.988E+00	2.218E+10	1.019	.5600
7.5662	7.266E+02	4.704E+07	2.081E+00	2.119E+10	1.013	.5801
7.9763	7.249E+02	4.476E+07	2.182E+00	2.012E+10	1.006	.6001
8.4094	7.211E+02	4.238E+07	2.292E+00	1.895E+10	.999	.6201
8.8677	7.145E+02	3.990E+07	2.412E+00	1.768E+10	.991	.6401
9.3534	7.044E+02	3.729E+07	2.545E+00	1.628E+10	.982	.6600
9.8804	6.894E+02	3.448E+07	2.693E+00	1.474E+10	.972	.6801
10.4533	6.679E+02	3.148E+07	2.858E+00	1.303E+10	.962	.7001
11.0811	6.374E+02	2.823E+07	3.042E+00	1.115E+10	.950	.7200
11.7960	5.934E+02	2.458E+07	3.252E+00	9.043E+09	.937	.7401
12.6392	5.282E+02	2.039E+07	3.490E+00	6.677E+09	.922	.7602
13.6933	4.248E+02	1.521E+07	3.764E+00	4.005E+09	.906	.7801
15.3980	2.138E+02	7.051E+06	4.085E+00	9.348E+08	.888	.8001
16.7366	2.357E+01	7.590E+05	4.183E+00	1.109E+07	.882	.8056

TABLE 3-13 VENTING OF LOX TANK AT 50 SECONDS FLIGHT TIME

EFFECTIVE HOLE AREA = 145 SQ FT, VAPOR PRESSURE=15.7 PSIA

VENT T(S)	FLOW VEL(CM/S)	OUTFLOW (G/S)	SPEC VOL (CC/G)	JET THRUST	ULLAGE P(BAR)	VENTED FRAC
.0000	1.598E+03	2.439E+08	8.826E-01	2.415E+11	1.830	.0000
.0768	1.426E+03	2.177E+08	8.826E-01	1.924E+11	1.536	.0200
.1625	1.281E+03	1.955E+08	8.826E-01	1.552E+11	1.313	.0400
.2579	1.155E+03	1.763E+08	8.826E-01	1.263E+11	1.140	.0600
BEGIN SUBSONIC FLOW						
.3024	1.111E+03	1.692E+08	8.839E-01	1.165E+11	1.082	.0687
.3623	1.120E+03	1.663E+08	9.068E-01	1.155E+11	1.082	.0801
.4706	1.136E+03	1.614E+08	9.482E-01	1.137E+11	1.081	.1002
.5816	1.153E+03	1.566E+08	9.914E-01	1.119E+11	1.080	.1201
.6959	1.170E+03	1.520E+08	1.037E+00	1.103E+11	1.079	.1401
.8135	1.187E+03	1.476E+08	1.084E+00	1.087E+11	1.078	.1600
.9354	1.205E+03	1.433E+08	1.133E+00	1.071E+11	1.077	.1801
1.0606	1.224E+03	1.391E+08	1.185E+00	1.056E+11	1.075	.2001
1.1890	1.243E+03	1.351E+08	1.239E+00	1.041E+11	1.074	.2201
1.3218	1.262E+03	1.312E+08	1.296E+00	1.027E+11	1.072	.2401
1.4590	1.283E+03	1.274E+08	1.356E+00	1.013E+11	1.071	.2601
1.5994	1.303E+03	1.237E+08	1.419E+00	9.995E+10	1.069	.2801
1.7442	1.324E+03	1.201E+08	1.485E+00	9.863E+10	1.067	.3001
1.8933	1.346E+03	1.166E+08	1.555E+00	9.734E+10	1.065	.3200
2.0468	1.369E+03	1.132E+08	1.629E+00	9.608E+10	1.063	.3400
BEGIN SONIC FLOW						
2.1088	1.379E+03	1.119E+08	1.659E+00	9.566E+10	1.062	.3479
2.2057	1.306E+03	1.099E+08	1.699E+00	9.445E+10	1.060	.3601
2.3690	1.400E+03	1.067E+08	1.768E+00	9.256E+10	1.057	.3801
2.5366	1.414E+03	1.035E+08	1.840E+00	9.076E+10	1.054	.4000
2.8893	1.446E+03	9.743E+07	2.000E+00	8.736E+10	1.048	.4401
3.2627	1.483E+03	9.160E+07	2.180E+00	8.420E+10	1.040	.4800
3.6611	1.524E+03	8.593E+07	2.389E+00	8.121E+10	1.031	.5200
4.0867	1.572E+03	8.039E+07	2.633E+00	7.833E+10	1.021	.5601
4.5417	1.626E+03	7.491E+07	2.924E+00	7.550E+10	1.008	.6001
5.0316	1.688E+03	6.944E+07	3.276E+00	7.269E+10	.993	.6401
5.5628	1.762E+03	6.393E+07	3.712E+00	6.982E+10	.975	.6801
6.1397	1.848E+03	5.835E+07	4.266E+00	6.685E+10	.954	.7200
6.7776	1.952E+03	5.261E+07	4.998E+00	6.368E+10	.927	.7601
7.4895	2.081E+03	4.665E+07	6.008E+00	6.018E+10	.893	.8000
7.8814	2.158E+03	4.356E+07	6.672E+00	5.828E+10	.872	.8201
8.3038	2.245E+03	4.037E+07	7.493E+00	5.619E+10	.849	.8401
8.7610	2.348E+03	3.702E+07	8.543E+00	5.388E+10	.821	.8601
9.2617	2.468E+03	3.352E+07	9.920E+00	5.129E+10	.788	.8801
BEGIN SUBSONIC FLOW						
9.8060	2.610E+03	2.989E+07	1.176E+01	4.836E+10	.750	.8996
9.8190	2.611E+03	2.980E+07	1.180E+01	4.825E+10	.749	.9001
10.4548	2.678E+03	2.577E+07	1.400E+01	4.278E+10	.701	.9200
11.2080	2.707E+03	2.116E+07	1.723E+01	3.551E+10	.639	.9400
12.1747	2.597E+03	1.548E+07	2.259E+01	2.492E+10	.554	.9600
13.8119	1.595E+03	6.302E+06	3.409E+01	6.231E+09	.423	.9801
14.8685	1.336E+02	4.672E+05	3.852E+01	3.870E+07	.384	.9841

TABLE 3-14 VENTING OF LOX TANK AT 65 SECONDS FLIGHT TIME

EFFECTIVE HOLE AREA = 145 SQ FT, VAPOR PRESSURE=15.7 PSIA

VENT T(S)	FLOW VEL(CM/S)	OUTFLOW (G/S)	SPEC VOL (CC/G)	JET THRUST	ULLAGE P(BAR)	VENTED FRAC
.0000	1.597E+03	2.437E+08	8.826E-01	2.413E+11	1.640	.0000
.0729	1.476E+03	2.253E+08	8.826E-01	2.061E+11	1.430	.0201
.1510	1.372E+03	2.094E+08	8.826E-01	1.781E+11	1.262	.0400
.2355	1.280E+03	1.954E+08	8.826E-01	1.550E+11	1.124	.0601
BEGIN SUBSONIC FLOW						
.2692	1.252E+03	1.906E+08	8.848E-01	1.479E+11	1.082	.0677
.3250	1.265E+03	1.843E+08	9.245E-01	1.445E+11	1.082	.0800
.4205	1.287E+03	1.748E+08	9.922E-01	1.395E+11	1.081	.1002
.5201	1.310E+03	1.661E+08	1.062E+00	1.349E+11	1.080	.1201
BEGIN SONIC FLOW						
.5209	1.310E+03	1.661E+08	1.063E+00	1.349E+11	1.080	.1202
.6253	1.307E+03	1.586E+08	1.111E+00	1.285E+11	1.079	.1402
.7346	1.307E+03	1.521E+08	1.158E+00	1.233E+11	1.078	.1601
.8487	1.310E+03	1.464E+08	1.205E+00	1.188E+11	1.077	.1801
.9668	1.314E+03	1.412E+08	1.253E+00	1.150E+11	1.075	.2001
1.0891	1.319E+03	1.364E+08	1.302E+00	1.116E+11	1.074	.2200
1.2161	1.325E+03	1.320E+08	1.353E+00	1.085E+11	1.072	.2400
1.3473	1.333E+03	1.278E+08	1.405E+00	1.057E+11	1.071	.2601
1.4824	1.342E+03	1.239E+08	1.459E+00	1.031E+11	1.069	.2801
1.6216	1.352E+03	1.202E+08	1.515E+00	1.007E+11	1.067	.3001
1.7657	1.362E+03	1.166E+08	1.574E+00	9.849E+10	1.065	.3201
1.9138	1.374E+03	1.132E+08	1.636E+00	9.639E+10	1.062	.3401
2.0660	1.386E+03	1.098E+08	1.700E+00	9.441E+10	1.060	.3600
2.2230	1.400E+03	1.066E+08	1.769E+00	9.253E+10	1.057	.3800
2.3857	1.414E+03	1.035E+08	1.841E+00	9.073E+10	1.054	.4001
2.5524	1.430E+03	1.004E+08	1.918E+00	8.901E+10	1.051	.4201
2.9021	1.464E+03	9.449E+07	2.087E+00	8.576E+10	1.044	.4601
3.2728	1.502E+03	8.878E+07	2.280E+00	8.270E+10	1.036	.5001
3.6694	1.547E+03	8.319E+07	2.505E+00	7.977E+10	1.026	.5401
4.0919	1.597E+03	7.770E+07	2.769E+00	7.694E+10	1.015	.5801
4.5467	1.655E+03	7.224E+07	3.087E+00	7.413E+10	1.001	.6201
5.0356	1.722E+03	6.679E+07	3.474E+00	7.131E+10	.985	.6601
5.5665	1.801E+03	6.131E+07	3.958E+00	6.846E+10	.965	.7000
6.1493	1.895E+03	5.567E+07	4.586E+00	6.540E+10	.941	.7401
6.7952	2.009E+03	4.986E+07	5.428E+00	6.211E+10	.912	.7801
7.1481	2.077E+03	4.685E+07	5.971E+00	6.031E+10	.894	.8002
7.9251	2.239E+03	4.057E+07	7.434E+00	5.633E+10	.850	.8400
8.3621	2.340E+03	3.725E+07	8.461E+00	5.404E+10	.823	.8600
8.8413	2.459E+03	3.377E+07	9.808E+00	5.148E+10	.791	.8800
9.3755	2.603E+03	3.008E+07	1.166E+01	4.854E+10	.752	.9000
9.9841	2.784E+03	2.612E+07	1.436E+01	4.509E+10	.705	.9201
10.6964	3.022E+03	2.178E+07	1.869E+01	4.082E+10	.643	.9401
11.5770	3.362E+03	1.691E+07	2.679E+01	3.523E+10	.560	.9601
12.8072	3.931E+03	1.105E+07	4.791E+01	2.694E+10	.432	.9802
BEGIN SUBSONIC FLOW						
13.3511	4.221E+03	8.819E+06	6.448E+01	2.308E+10	.372	.9865
ULLAGE GASES HAVE REACHED VENT						
14.2188	3.571E+03	5.426E+06	8.867E+01	1.201E+10	.277	.9937

TABLE 3-15 VENTING OF LOX TANK AT 100 SECONDS FLIGHT TIME

EFFECTIVE HOLE AREA = 145 SQ FT, VAPOR PRESSURE=15.7 PSIA

VENT T(S)	FLOW VEL(CM/S)	OUTFLOW (G/S)	SPEC VOL (CC/G)	JET THRUST	ULLAGE P(BAR)	VENTED FRAC
.0000	1.601E+03	2.444E+08	8.826E-01	2.427E+11	1.470	.0000
.0656	1.530E+03	2.335E+08	8.826E-01	2.215E+11	1.343	.0200
.1341	1.465E+03	2.236E+08	8.826E-01	2.032E+11	1.233	.0401
.2057	1.406E+03	2.147E+08	8.826E-01	1.872E+11	1.138	.0602
BEGIN SONIC FLOW						
.2569	1.371E+03	2.064E+08	8.946E-01	1.754E+11	1.082	.0740
.2803	1.347E+03	1.954E+08	9.286E-01	1.632E+11	1.082	.0800
.3648	1.322E+03	1.790E+08	9.943E-01	1.467E+11	1.081	.1001
.4545	1.312E+03	1.688E+08	1.047E+00	1.373E+11	1.080	.1200
.5501	1.308E+03	1.607E+08	1.096E+00	1.303E+11	1.079	.1402
.6489	1.307E+03	1.539E+08	1.144E+00	1.247E+11	1.078	.1600
.7526	1.309E+03	1.480E+08	1.191E+00	1.201E+11	1.077	.1801
.8605	1.312E+03	1.426E+08	1.239E+00	1.160E+11	1.076	.2001
.9717	1.317E+03	1.377E+08	1.288E+00	1.125E+11	1.074	.2201
1.0870	1.324E+03	1.333E+08	1.338E+00	1.094E+11	1.073	.2400
1.2064	1.331E+03	1.290E+08	1.390E+00	1.065E+11	1.071	.2601
1.3291	1.339E+03	1.250E+08	1.443E+00	1.038E+11	1.069	.2800
1.4568	1.349E+03	1.212E+08	1.499E+00	1.014E+11	1.067	.3001
1.5877	1.359E+03	1.176E+08	1.557E+00	9.907E+10	1.065	.3201
1.7220	1.371E+03	1.141E+08	1.618E+00	9.695E+10	1.063	.3400
1.8612	1.383E+03	1.107E+08	1.682E+00	9.493E+10	1.061	.3600
2.0045	1.396E+03	1.075E+08	1.750E+00	9.302E+10	1.058	.3800
2.1527	1.410E+03	1.043E+08	1.821E+00	9.119E+10	1.055	.4001
2.4615	1.442E+03	9.820E+07	1.978E+00	8.777E+10	1.049	.4401
2.7893	1.477E+03	9.238E+07	2.154E+00	8.461E+10	1.041	.4800
3.1385	1.518E+03	8.674E+07	2.358E+00	8.165E+10	1.033	.5200
3.5107	1.565E+03	8.119E+07	2.596E+00	7.876E+10	1.022	.5600
3.9093	1.618E+03	7.571E+07	2.878E+00	7.593E+10	1.010	.6000
4.3392	1.679E+03	7.024E+07	3.220E+00	7.311E+10	.996	.6401
4.8021	1.750E+03	6.477E+07	3.640E+00	7.027E+10	.978	.6801
5.3061	1.834E+03	5.922E+07	4.172E+00	6.732E+10	.957	.7200
5.8611	1.934E+03	5.352E+07	4.869E+00	6.419E+10	.931	.7600
6.4805	2.059E+03	4.760E+07	5.827E+00	6.075E+10	.898	.8001
6.8198	2.132E+03	4.456E+07	6.446E+00	5.890E+10	.879	.8201
7.1854	2.217E+03	4.136E+07	7.220E+00	5.684E+10	.856	.8402
7.5774	2.314E+03	3.807E+07	8.188E+00	5.461E+10	.830	.8601
8.0090	2.429E+03	3.459E+07	9.458E+00	5.210E+10	.799	.8801
8.4866	2.568E+03	3.093E+07	1.118E+01	4.924E+10	.762	.9001
9.0236	2.739E+03	2.701E+07	1.366E+01	4.587E+10	.716	.9200
9.6561	2.965E+03	2.274E+07	1.757E+01	4.179E+10	.658	.9401
10.4269	3.283E+03	1.790E+07	2.470E+01	3.645E+10	.579	.9601
11.4745	3.808E+03	1.212E+07	4.234E+01	2.861E+10	.458	.9801
ULLAGE GASES HAVE REACHED VENT						
11.8830	4.044E+03	1.015E+07	5.369E+01	2.544E+10	.408	.9859
13.5169	5.254E+03	3.711E+06	1.907E+02	1.209E+10	.195	.9999

TABLE 3-16 VENTING OF LOX TANK AT 115 SECONDS FLIGHT TIME

EFFECTIVE HOLE AREA = 145 SQ FT, VAPOR PRESSURE=15.7 PSIA

VENT T(S)	FLOW VEL (CM/S)	OUTFLOW (G/S)	SPEC VOL (CC/G)	JET THRUST	ULLAGE P(BAR)	VENTED FRAC
.0000	1.598E+03	2.439E+08	8.826E-01	2.416E+11	1.450	.0000
.0630	1.537E+03	2.346E+08	8.826E-01	2.236E+11	1.342	.0201
.1283	1.482E+03	2.261E+08	8.826E-01	2.077E+11	1.247	.0401
.1961	1.430E+03	2.183E+08	8.826E-01	1.936E+11	1.163	.0601
.2659	1.384E+03	2.112E+08	8.826E-01	1.812E+11	1.088	.0801
BEGIN SONIC FLOW						
.2744	1.371E+03	2.065E+08	8.943E-01	1.755E+11	1.082	.0825
.3428	1.329E+03	1.847E+08	9.693E-01	1.522E+11	1.081	.1000
.4275	1.315E+03	1.726E+08	1.026E+00	1.407E+11	1.080	.1201
.5167	1.309E+03	1.638E+08	1.077E+00	1.329E+11	1.080	.1401
.6107	1.307E+03	1.565E+08	1.125E+00	1.268E+11	1.079	.1601
.7085	1.308E+03	1.502E+08	1.173E+00	1.218E+11	1.077	.1801
.8106	1.311E+03	1.446E+08	1.221E+00	1.175E+11	1.076	.2001
.9164	1.315E+03	1.395E+08	1.270E+00	1.138E+11	1.075	.2201
1.0260	1.321E+03	1.349E+08	1.320E+00	1.105E+11	1.073	.2401
1.1392	1.328E+03	1.305E+08	1.371E+00	1.075E+11	1.072	.2601
1.2562	1.336E+03	1.264E+08	1.424E+00	1.047E+11	1.070	.2801
1.3769	1.345E+03	1.225E+08	1.479E+00	1.022E+11	1.068	.3001
1.5019	1.356E+03	1.188E+08	1.537E+00	9.985E+10	1.066	.3202
1.6294	1.367E+03	1.153E+08	1.597E+00	9.766E+10	1.064	.3400
1.7618	1.379E+03	1.118E+08	1.660E+00	9.559E+10	1.062	.3600
1.8992	1.392E+03	1.085E+08	1.728E+00	9.362E+10	1.059	.3802
2.0390	1.406E+03	1.053E+08	1.798E+00	9.177E+10	1.056	.4001
2.1839	1.420E+03	1.022E+08	1.873E+00	8.999E+10	1.053	.4201
2.4871	1.454E+03	9.614E+07	2.037E+00	8.665E+10	1.046	.4601
2.8089	1.492E+03	9.038E+07	2.223E+00	8.357E+10	1.038	.5000
3.1530	1.534E+03	8.470E+07	2.440E+00	8.058E+10	1.029	.5401
3.5193	1.583E+03	7.916E+07	2.694E+00	7.770E+10	1.018	.5800
3.9129	1.639E+03	7.366E+07	2.998E+00	7.487E+10	1.005	.6200
4.3375	1.705E+03	6.816E+07	3.369E+00	7.203E+10	.989	.6601
4.7967	1.781E+03	6.263E+07	3.830E+00	6.914E+10	.971	.7000
5.2992	1.871E+03	5.702E+07	4.420E+00	6.613E+10	.948	.7400
5.8561	1.981E+03	5.122E+07	5.210E+00	6.290E+10	.919	.7801
6.1581	2.045E+03	4.821E+07	5.714E+00	6.113E+10	.902	.8001
6.8240	2.200E+03	4.196E+07	7.063E+00	5.723E+10	.861	.8400
7.1978	2.295E+03	3.864E+07	8.003E+00	5.499E+10	.835	.8601
7.6038	2.408E+03	3.519E+07	9.216E+00	5.253E+10	.805	.8800
8.0543	2.543E+03	3.153E+07	1.086E+01	4.971E+10	.768	.9000
8.5642	2.710E+03	2.762E+07	1.322E+01	4.642E+10	.724	.9201
9.1534	2.929E+03	2.336E+07	1.689E+01	4.243E+10	.667	.9400
9.8713	3.236E+03	1.855E+07	2.350E+01	3.722E+10	.590	.9600
ULLAGE GASES HAVE REACHED VENT						
10.7971	3.711E+03	1.303E+07	3.838E+01	2.997E+10	.479	.9794
10.8367	3.734E+03	1.281E+07	3.928E+01	2.965E+10	.474	.9800
12.6091	5.039E+03	4.520E+06	1.502E+02	1.412E+10	.228	.9998

TABLE 3-17 VENTING OF LOX TANK AT 350 SECONDS FLIGHT TIME

EFFECTIVE HOLE AREA = 145 SQ FT, VAPOR PRESSURE=15.7 PSIA

VENT T(S)	FLOW VEL(CM/S)	OUTFLOW (G/S)	SPEC VOL (CC/G)	JET THRUST	ULLAGE P(BAR)	VENTED FRAC
BEGIN SONIC FLOW						
.0000	2.247E+03	4.027E+07	7.516E+00	5.609E+10	.848	.0000
.0883	2.263E+03	3.972E+07	7.673E+00	5.572E+10	.844	.0200
.1779	2.279E+03	3.918E+07	7.836E+00	5.536E+10	.839	.0401
.2668	2.296E+03	3.862E+07	8.008E+00	5.498E+10	.835	.0601
.3609	2.313E+03	3.806E+07	8.188E+00	5.459E+10	.830	.0801
.4544	2.331E+03	3.750E+07	8.375E+00	5.419E+10	.825	.1001
.5491	2.349E+03	3.693E+07	8.570E+00	5.379E+10	.820	.1201
.6451	2.368E+03	3.636E+07	8.773E+00	5.338E+10	.815	.1401
.7430	2.387E+03	3.578E+07	8.988E+00	5.296E+10	.810	.1601
.8422	2.407E+03	3.520E+07	9.211E+00	5.253E+10	.805	.1800
.9433	2.428E+03	3.461E+07	9.447E+00	5.210E+10	.799	.2000
1.0464	2.449E+03	3.402E+07	9.695E+00	5.165E+10	.794	.2201
1.1507	2.470E+03	3.343E+07	9.955E+00	5.120E+10	.788	.2400
1.2576	2.493E+03	3.282E+07	1.023E+01	5.073E+10	.782	.2601
1.3657	2.516E+03	3.222E+07	1.052E+01	5.026E+10	.776	.2800
1.4765	2.540E+03	3.161E+07	1.083E+01	4.977E+10	.769	.3001
1.5891	2.564E+03	3.099E+07	1.115E+01	4.927E+10	.763	.3200
1.7043	2.590E+03	3.036E+07	1.149E+01	4.876E+10	.756	.3401
1.8214	2.617E+03	2.973E+07	1.186E+01	4.823E+10	.749	.3600
1.9417	2.644E+03	2.909E+07	1.225E+01	4.769E+10	.741	.3801
2.0646	2.673E+03	2.844E+07	1.266E+01	4.713E+10	.734	.4001
2.1901	2.703E+03	2.779E+07	1.310E+01	4.656E+10	.726	.4201
2.3181	2.733E+03	2.713E+07	1.357E+01	4.598E+10	.718	.4400
2.4499	2.766E+03	2.647E+07	1.407E+01	4.540E+10	.709	.4600
2.5856	2.800E+03	2.579E+07	1.462E+01	4.477E+10	.701	.4801
2.7238	2.835E+03	2.511E+07	1.521E+01	4.412E+10	.691	.5001
3.0131	2.910E+03	2.370E+07	1.654E+01	4.276E+10	.672	.5401
3.3203	2.994E+03	2.225E+07	1.813E+01	4.129E+10	.651	.5801
3.6493	3.086E+03	2.074E+07	2.004E+01	3.970E+10	.627	.6201
4.0025	3.191E+03	1.919E+07	2.240E+01	3.796E+10	.601	.6601
4.3865	3.309E+03	1.756E+07	2.538E+01	3.603E+10	.572	.7001
4.8089	3.447E+03	1.586E+07	2.927E+01	3.389E+10	.540	.7401
5.2800	3.608E+03	1.407E+07	3.455E+01	3.147E+10	.503	.7800
5.8189	3.803E+03	1.216E+07	4.213E+01	2.868E+10	.459	.8200
6.4537	4.049E+03	1.010E+07	5.398E+01	2.537E+10	.407	.8600
7.2448	4.377E+03	7.842E+06	7.519E+01	2.128E+10	.343	.9001
7.7363	4.591E+03	6.612E+06	9.353E+01	1.882E+10	.303	.9202
8.3251	4.857E+03	5.301E+06	1.234E+02	1.596E+10	.258	.9400
9.1033	5.216E+03	3.847E+06	1.826E+02	1.244E+10	.201	.9600
10.2963	5.750E+03	2.200E+06	3.522E+02	7.842E+09	.127	.9801
14.1875	6.475E+03	2.018E+05	4.323E+03	8.102E+08	.013	.9994

TABLE 3-18 VENTING OF LOX TANK AT 450 SECONDS FLIGHT TIME

EFFECTIVE HOLE AREA = 145 SQ FT, VAPOR PRESSURE=15.7 PSIA

VENT T(S)	FLOW VEL(CM/S)	OUTFLOW (G/S)	SPEC VOL (CC/G)	JET THRUST	ULLAGE P(BAR)	VENTED FRAC
BEGIN SONIC FLOW						
.0000	3.580E+03	1.437E+07	3.356E+01	3.189E+10	.509	.0000
.0569	3.599E+03	1.416E+07	3.424E+01	3.160E+10	.505	.0200
.1145	3.619E+03	1.395E+07	3.495E+01	3.130E+10	.500	.0400
.1734	3.640E+03	1.374E+07	3.570E+01	3.100E+10	.495	.0601
.2326	3.661E+03	1.352E+07	3.647E+01	3.070E+10	.491	.0800
.2931	3.683E+03	1.331E+07	3.727E+01	3.039E+10	.486	.1000
.3545	3.705E+03	1.309E+07	3.812E+01	3.007E+10	.481	.1200
.4169	3.727E+03	1.287E+07	3.900E+01	2.975E+10	.476	.1400
.4806	3.750E+03	1.265E+07	3.992E+01	2.942E+10	.471	.1601
.5453	3.774E+03	1.243E+07	4.089E+01	2.909E+10	.466	.1801
.6112	3.798E+03	1.221E+07	4.191E+01	2.875E+10	.460	.2001
.6784	3.823E+03	1.198E+07	4.298E+01	2.840E+10	.455	.2201
.7469	3.849E+03	1.176E+07	4.410E+01	2.805E+10	.449	.2402
.8160	3.875E+03	1.153E+07	4.528E+01	2.769E+10	.444	.2600
.8870	3.902E+03	1.130E+07	4.653E+01	2.733E+10	.438	.2800
.9600	3.930E+03	1.106E+07	4.786E+01	2.695E+10	.432	.3001
1.0342	3.958E+03	1.083E+07	4.926E+01	2.657E+10	.426	.3202
1.1097	3.987E+03	1.059E+07	5.073E+01	2.618E+10	.420	.3401
1.1872	4.018E+03	1.035E+07	5.230E+01	2.578E+10	.414	.3601
1.2665	4.049E+03	1.011E+07	5.398E+01	2.537E+10	.407	.3801
1.3478	4.081E+03	9.860E+06	5.576E+01	2.495E+10	.401	.4001
1.4310	4.115E+03	9.612E+06	5.766E+01	2.452E+10	.394	.4201
1.5161	4.149E+03	9.363E+06	5.969E+01	2.408E+10	.387	.4400
1.6045	4.185E+03	9.108E+06	6.189E+01	2.363E+10	.380	.4601
1.6947	4.222E+03	8.852E+06	6.425E+01	2.317E+10	.372	.4801
1.7875	4.260E+03	8.593E+06	6.678E+01	2.270E+10	.365	.5001
1.8835	4.300E+03	8.330E+06	6.954E+01	2.221E+10	.357	.5201
1.9821	4.342E+03	8.065E+06	7.251E+01	2.171E+10	.349	.5400
2.0845	4.385E+03	7.796E+06	7.577E+01	2.119E+10	.341	.5601
2.1901	4.430E+03	7.523E+06	7.932E+01	2.066E+10	.333	.5800
2.3001	4.477E+03	7.246E+06	8.324E+01	2.011E+10	.324	.6001
2.4141	4.526E+03	6.965E+06	8.754E+01	1.955E+10	.315	.6200
2.5331	4.578E+03	6.680E+06	9.233E+01	1.896E+10	.306	.6401
2.6573	4.633E+03	6.389E+06	9.768E+01	1.835E+10	.296	.6601
2.7878	4.690E+03	6.095E+06	1.037E+02	1.772E+10	.286	.6802
2.9235	4.751E+03	5.796E+06	1.104E+02	1.707E+10	.275	.7001
3.2192	4.884E+03	5.179E+06	1.270E+02	1.568E+10	.253	.7400
3.5533	5.035E+03	4.535E+06	1.496E+02	1.416E+10	.229	.7800
3.9411	5.212E+03	3.859E+06	1.819E+02	1.247E+10	.201	.8201
4.4045	5.421E+03	3.149E+06	2.319E+02	1.058E+10	.171	.8600
4.9933	5.680E+03	2.387E+06	3.206E+02	8.406E+09	.136	.9000
5.3670	5.837E+03	1.980E+06	3.970E+02	7.166E+09	.116	.9201
5.8304	6.016E+03	1.555E+06	5.213E+02	5.799E+09	.094	.9402
6.4448	6.225E+03	1.103E+06	7.603E+02	4.258E+09	.069	.9601
7.4073	6.455E+03	6.175E+05	1.408E+03	2.471E+09	.040	.9801
9.6909	6.351E+03	1.304E+05	6.560E+03	5.135E+08	.008	.9979

TABLE 3-19 VENTING OF LH₂ TANK AT 10 SECONDS FLIGHT TIME

EFFECTIVE HOLE AREA = 271 SQ FT

VENT T(S)	FLOW VEL(CM/S)	OUTFLOW (G/S)	SPEC VOL (CC/G)	JET THRUST	ULLAGE P(BAR)	VENTED FRAC
.0000	6.088E+03	1.073E+08	1.429E+01	4.049E+11	2.280	.0000
.0165	5.043E+03	8.886E+07	1.429E+01	2.778E+11	1.873	.0100
.0366	4.095E+03	7.217E+07	1.429E+01	1.832E+11	1.570	.0200
.0619	3.203E+03	5.644E+07	1.429E+01	1.121E+11	1.342	.0301
.0952	2.300E+03	4.053E+07	1.429E+01	5.779E+10	1.168	.0401
BEGIN SUBSONIC FLOW						
.1406	1.683E+03	2.966E+07	1.429E+01	3.095E+10	1.082	.0493
.1452	1.685E+03	2.955E+07	1.435E+01	3.087E+10	1.082	.0502
.1996	1.668E+03	2.893E+07	1.451E+01	2.991E+10	1.079	.0601
.2559	1.649E+03	2.830E+07	1.467E+01	2.893E+10	1.076	.0701
.3130	1.630E+03	2.766E+07	1.484E+01	2.795E+10	1.073	.0800
.3721	1.609E+03	2.700E+07	1.501E+01	2.694E+10	1.069	.0901
.4320	1.588E+03	2.634E+07	1.518E+01	2.593E+10	1.066	.1000
.4938	1.565E+03	2.566E+07	1.535E+01	2.490E+10	1.063	.1100
.5575	1.540E+03	2.497E+07	1.553E+01	2.384E+10	1.060	.1201
.6229	1.514E+03	2.426E+07	1.571E+01	2.278E+10	1.056	.1301
.6903	1.486E+03	2.354E+07	1.589E+01	2.169E+10	1.053	.1401
.7594	1.457E+03	2.281E+07	1.608E+01	2.060E+10	1.049	.1501
.8305	1.425E+03	2.206E+07	1.627E+01	1.950E+10	1.046	.1600
.9052	1.391E+03	2.128E+07	1.646E+01	1.836E+10	1.042	.1701
.9817	1.355E+03	2.048E+07	1.666E+01	1.721E+10	1.038	.1801
1.0620	1.316E+03	1.966E+07	1.686E+01	1.604E+10	1.035	.1901
1.1450	1.275E+03	1.881E+07	1.706E+01	1.487E+10	1.031	.2000
1.2326	1.229E+03	1.792E+07	1.727E+01	1.366E+10	1.027	.2100
1.3257	1.180E+03	1.699E+07	1.749E+01	1.243E+10	1.023	.2202
1.4217	1.127E+03	1.603E+07	1.770E+01	1.120E+10	1.019	.2300
1.5268	1.067E+03	1.499E+07	1.792E+01	9.916E+09	1.015	.2402
1.6375	1.002E+03	1.390E+07	1.815E+01	8.632E+09	1.011	.2501
1.7574	9.287E+02	1.272E+07	1.838E+01	7.327E+09	1.007	.2600
1.8902	8.452E+02	1.143E+07	1.861E+01	5.992E+09	1.002	.2700
2.0414	7.469E+02	9.976E+06	1.885E+01	4.620E+09	.998	.2801
2.2185	6.297E+02	8.302E+06	1.909E+01	3.241E+09	.993	.2902
2.4399	4.759E+02	6.193E+06	1.935E+01	1.827E+09	.989	.3001
2.7977	2.207E+02	2.835E+06	1.960E+01	3.881E+08	.984	.3101
3.0486	4.505E+01	5.767E+05	1.967E+01	1.611E+07	.983	.3127

TABLE 3-20 VENTING OF LH₂ TANK AT 20 SECONDS FLIGHT TIME
EFFECTIVE HOLE AREA = 572 SQ FT, VAPOR PRESSURE=15.7 PSIA

VENT T(S)	FLOW VEL(CM/S)	OUTFLOW G/S	SPEC VOL CC/G	JET THRUST	ULLAGE P(BAR)	VENTED FRAC
.0001	6.320E+03	2.351E+08	1.429E+01	9.212E+11	2.280	.0001
.0072	5.561E+03	2.068E+08	1.429E+01	7.132E+11	1.964	.0101
.0153	4.882E+03	1.816E+08	1.429E+01	5.497E+11	1.716	.0201
.0245	4.264E+03	1.586E+08	1.429E+01	4.193E+11	1.518	.0300
.0352	3.681E+03	1.369E+08	1.429E+01	3.125E+11	1.356	.0400
.0478	3.107E+03	1.156E+08	1.429E+01	2.227E+11	1.220	.0501
.0628	2.533E+03	9.423E+07	1.429E+01	1.480E+11	1.107	.0601
BEGIN SUBSONIC FLOW						
.0728	2.396E+03	8.874E+07	1.435E+01	1.318E+11	1.082	.0658
.0805	2.394E+03	8.822E+07	1.442E+01	1.309E+11	1.081	.0701
.0984	2.388E+03	8.696E+07	1.460E+01	1.288E+11	1.078	.0802
.1164	2.383E+03	8.572E+07	1.477E+01	1.266E+11	1.075	.0900
.1350	2.376E+03	8.445E+07	1.495E+01	1.244E+11	1.071	.1001
.1538	2.370E+03	8.317E+07	1.514E+01	1.222E+11	1.068	.1101
.1727	2.362E+03	8.191E+07	1.533E+01	1.200E+11	1.065	.1200
.1921	2.354E+03	8.062E+07	1.552E+01	1.177E+11	1.062	.1301
.2118	2.346E+03	7.932E+07	1.571E+01	1.154E+11	1.058	.1401
.2316	2.337E+03	7.804E+07	1.591E+01	1.131E+11	1.055	.1500
.2519	2.327E+03	7.673E+07	1.611E+01	1.107E+11	1.051	.1600
.2725	2.316E+03	7.542E+07	1.632E+01	1.083E+11	1.048	.1700
.2937	2.304E+03	7.409E+07	1.653E+01	1.058E+11	1.044	.1801
.3149	2.292E+03	7.277E+07	1.674E+01	1.034E+11	1.040	.1900
.3367	2.279E+03	7.142E+07	1.696E+01	1.009E+11	1.037	.2000
.3591	2.265E+03	7.005E+07	1.718E+01	9.837E+10	1.033	.2101
.3818	2.250E+03	6.868E+07	1.741E+01	9.580E+10	1.029	.2201
.4048	2.234E+03	6.731E+07	1.763E+01	9.321E+10	1.025	.2300
.4283	2.216E+03	6.591E+07	1.787E+01	9.057E+10	1.021	.2400
.4525	2.198E+03	6.450E+07	1.811E+01	8.788E+10	1.017	.2500
.4772	2.178E+03	6.306E+07	1.835E+01	8.515E+10	1.013	.2601
.5023	2.157E+03	6.162E+07	1.860E+01	8.240E+10	1.008	.2700
.5282	2.134E+03	6.015E+07	1.885E+01	7.958E+10	1.004	.2801
.5547	2.110E+03	5.865E+07	1.911E+01	7.672E+10	1.000	.2901
.5818	2.084E+03	5.714E+07	1.938E+01	7.382E+10	.995	.3001
.6383	2.026E+03	5.403E+07	1.993E+01	6.786E+10	.986	.3201
.6981	1.960E+03	5.082E+07	2.049E+01	6.175E+10	.977	.3400
.7623	1.882E+03	4.743E+07	2.109E+01	5.534E+10	.967	.3601
.8313	1.792E+03	4.385E+07	2.171E+01	4.871E+10	.957	.3801
.9061	1.685E+03	4.004E+07	2.237E+01	4.183E+10	.946	.4001
.9461	1.625E+03	3.803E+07	2.270E+01	3.630E+10	.941	.4100
.9891	1.557E+03	3.589E+07	2.305E+01	3.464E+10	.935	.4201
1.0339	1.483E+03	3.368E+07	2.340E+01	3.098E+10	.929	.4300
1.0822	1.401E+03	3.132E+07	2.377E+01	2.721E+10	.924	.4400
1.1347	1.308E+03	2.878E+07	2.414E+01	2.334E+10	.918	.4500
1.1930	1.201E+03	2.602E+07	2.453E+01	1.938E+10	.912	.4602
1.2566	1.079E+03	2.300E+07	2.492E+01	1.538E+10	.905	.4701
1.3308	9.293E+02	1.950E+07	2.533E+01	1.124E+10	.899	.4801
1.4204	7.418E+02	1.532E+07	2.574E+01	7.045E+09	.893	.4900
1.5488	4.639E+02	9.421E+06	2.617E+01	2.709E+09	.886	.5001
1.7345	4.469E+01	8.985E+05	2.643E+01	2.489E+07	.882	.5061

TABLE 3-21 VENTING OF LH₂ TANK AT 50 SECONDS FLIGHT TIME

EFFECTIVE HOLE AREA = 572 SQ FT

VENT T(S)	FLOW VEL(CM/S)	OUTFLOW (G/S)	SPEC VOL (CC/G)	JET THRUST	ULLAGE P(BAR)	VENTED FRAC
.0000	7.360E+03	2.738E+08	1.429E+01	1.249E+12	2.280	.0000
.0114	6.653E+03	2.474E+08	1.429E+01	1.021E+12	1.933	.0201
.0239	6.059E+03	2.254E+08	1.429E+01	8.465E+11	1.669	.0400
.0376	5.544E+03	2.062E+08	1.429E+01	7.087E+11	1.460	.0600
.0525	5.091E+03	1.894E+08	1.429E+01	5.978E+11	1.291	.0801
.0688	4.690E+03	1.745E+08	1.429E+01	5.073E+11	1.154	.1001
BEGIN SUBSONIC FLOW						
.0821	4.477E+03	1.653E+08	1.440E+01	4.588E+11	1.082	.1153
.0863	4.488E+03	1.639E+08	1.455E+01	4.562E+11	1.081	.1201
.1046	4.535E+03	1.584E+08	1.522E+01	4.454E+11	1.074	.1400
.1236	4.583E+03	1.531E+08	1.591E+01	4.349E+11	1.068	.1600
.1432	4.630E+03	1.480E+08	1.663E+01	4.248E+11	1.061	.1800
.1635	4.678E+03	1.431E+08	1.737E+01	4.151E+11	1.054	.2000
.1844	4.726E+03	1.384E+08	1.814E+01	4.057E+11	1.046	.2200
.2062	4.775E+03	1.339E+08	1.895E+01	3.964E+11	1.039	.2402
.2287	4.823E+03	1.296E+08	1.978E+01	3.875E+11	1.031	.2602
.2517	4.872E+03	1.254E+08	2.065E+01	3.788E+11	1.023	.2800
.2757	4.921E+03	1.213E+08	2.155E+01	3.702E+11	1.014	.3001
.3003	4.970E+03	1.174E+08	2.249E+01	3.618E+11	1.006	.3200
.3259	5.019E+03	1.136E+08	2.348E+01	3.535E+11	.997	.3401
.3524	5.068E+03	1.099E+08	2.450E+01	3.454E+11	.987	.3601
.3796	5.117E+03	1.063E+08	2.557E+01	3.373E+11	.978	.3801
.4079	5.166E+03	1.028E+08	2.669E+01	3.293E+11	.968	.4001
.4370	5.214E+03	9.943E+07	2.786E+01	3.214E+11	.957	.4200
.4672	5.262E+03	9.608E+07	2.910E+01	3.135E+11	.946	.4401
.4985	5.309E+03	9.282E+07	3.040E+01	3.055E+11	.935	.4601
.5308	5.356E+03	8.962E+07	3.176E+01	2.976E+11	.923	.4801
.5643	5.401E+03	8.648E+07	3.319E+01	2.896E+11	.911	.5001
.5991	5.446E+03	8.339E+07	3.470E+01	2.815E+11	.898	.5200
.6352	5.489E+03	8.033E+07	3.631E+01	2.734E+11	.884	.5401
.6725	5.530E+03	7.733E+07	3.800E+01	2.651E+11	.870	.5600
.7115	5.568E+03	7.434E+07	3.980E+01	2.566E+11	.855	.5801
.7523	5.604E+03	7.138E+07	4.172E+01	2.480E+11	.840	.6002
.7943	5.636E+03	6.845E+07	4.375E+01	2.392E+11	.824	.6201
.8383	5.663E+03	6.552E+07	4.594E+01	2.300E+11	.807	.6400
.8843	5.685E+03	6.258E+07	4.828E+01	2.206E+11	.789	.6600
.9327	5.701E+03	5.962E+07	5.081E+01	2.107E+11	.770	.6801
.9836	5.707E+03	5.664E+07	5.354E+01	2.004E+11	.750	.7001
1.0369	5.702E+03	5.365E+07	5.649E+01	1.897E+11	.728	.7200
1.0938	5.684E+03	5.057E+07	5.973E+01	1.782E+11	.706	.7401
1.1540	5.647E+03	4.744E+07	6.325E+01	1.661E+11	.682	.7601
1.2182	5.586E+03	4.422E+07	6.713E+01	1.532E+11	.656	.7800
1.2876	5.493E+03	4.086E+07	7.144E+01	1.392E+11	.629	.8000
1.3631	5.356E+03	3.732E+07	7.627E+01	1.239E+11	.599	.8200
1.4471	5.156E+03	3.352E+07	8.173E+01	1.072E+11	.567	.8402
1.5407	4.862E+03	2.938E+07	8.793E+01	8.857E+10	.533	.8601
1.6497	4.417E+03	2.468E+07	9.510E+01	6.760E+10	.495	.8801
1.7846	3.698E+03	1.898E+07	1.035E+02	4.353E+10	.454	.9000
1.9840	2.288E+03	1.069E+07	1.137E+02	1.517E+10	.407	.9200
2.2266	1.033E+02	4.604E+05	1.192E+02	2.949E+07	.384	.9293

TABLE 3-22 VENTING OF LH₂ TANK AT 65 SECONDS FLIGHT TIME
EFFECTIVE HOLE AREA = 572 SQ FT, VAPOR PRESSURE=15.7 PSIA

VENT T(S)	FLOW VEL(CM/S)	OUTFLOW (G/S)	SPEC VOL (CC/G)	JET THRUST	ULLAGE P(BAR)	VENTED FRAC
.0001	7.717E+03	2.870E+08	1.429E+01	1.373E+12	2.280	.0002
.0104	7.165E+03	2.665E+08	1.429E+01	1.184E+12	1.992	.0201
.0215	6.688E+03	2.488E+08	1.429E+01	1.031E+12	1.761	.0401
.0334	6.270E+03	2.332E+08	1.429E+01	9.067E+11	1.572	.0601
.0460	5.904E+03	2.196E+08	1.429E+01	8.038E+11	1.416	.0801
.0594	5.576E+03	2.074E+08	1.429E+01	7.170E+11	1.284	.1001
.0736	5.281E+03	1.964E+08	1.429E+01	6.431E+11	1.172	.1201
.0885	5.033E+03	1.872E+08	1.429E+01	5.843E+11	1.083	.1401
BEGIN SUBSONIC FLOW						
.0898	5.047E+03	1.855E+08	1.446E+01	5.803E+11	1.082	.1418
.1043	5.114E+03	1.757E+08	1.546E+01	5.572E+11	1.076	.1601
.1210	5.188E+03	1.661E+08	1.660E+01	5.344E+11	1.070	.1801
BEGIN SONIC FLOW						
.1307	5.230E+03	1.612E+08	1.724E+01	5.227E+11	1.066	.1912
.1387	5.218E+03	1.575E+08	1.760E+01	5.097E+11	1.063	.2001
.1572	5.196E+03	1.502E+08	1.839E+01	4.838E+11	1.056	.2200
.1767	5.185E+03	1.437E+08	1.917E+01	4.620E+11	1.048	.2400
.1971	5.182E+03	1.379E+08	1.996E+01	4.431E+11	1.041	.2601
.2182	5.184E+03	1.327E+08	2.076E+01	4.264E+11	1.033	.2800
.2401	5.190E+03	1.278E+08	2.158E+01	4.112E+11	1.025	.3000
.2629	5.201E+03	1.232E+08	2.243E+01	3.973E+11	1.016	.3200
.2865	5.217E+03	1.189E+08	2.331E+01	3.846E+11	1.007	.3401
.3110	5.235E+03	1.148E+08	2.423E+01	3.725E+11	.998	.3601
.3364	5.255E+03	1.108E+08	2.519E+01	3.611E+11	.989	.3801
.3626	5.278E+03	1.071E+08	2.620E+01	3.504E+11	.979	.4001
.3897	5.304E+03	1.034E+08	2.725E+01	3.401E+11	.969	.4200
.4470	5.365E+03	9.644E+07	2.956E+01	3.208E+11	.947	.4601
.5083	5.435E+03	8.982E+07	3.216E+01	3.027E+11	.924	.5000
.5744	5.517E+03	8.346E+07	3.513E+01	2.855E+11	.898	.5400
.6455	5.610E+03	7.729E+07	3.857E+01	2.688E+11	.870	.5800
.7226	5.715E+03	7.126E+07	4.262E+01	2.525E+11	.839	.6201
.8064	5.834E+03	6.533E+07	4.745E+01	2.363E+11	.805	.6601
.8980	5.968E+03	5.943E+07	5.336E+01	2.199E+11	.767	.7000
.9474	6.043E+03	5.648E+07	5.686E+01	2.116E+11	.747	.7200
.9994	6.122E+03	5.351E+07	6.080E+01	2.031E+11	.725	.7400
1.0543	6.207E+03	5.054E+07	6.527E+01	1.945E+11	.701	.7600
1.1127	6.299E+03	4.753E+07	7.042E+01	1.856E+11	.677	.7801
1.1749	6.397E+03	4.450E+07	7.639E+01	1.765E+11	.650	.8001
1.2414	6.504E+03	4.145E+07	8.337E+01	1.671E+11	.621	.8201
1.3130	6.618E+03	3.834E+07	9.174E+01	1.573E+11	.591	.8400
1.3909	6.743E+03	3.515E+07	1.019E+02	1.470E+11	.557	.8601
1.4762	6.879E+03	3.191E+07	1.145E+02	1.361E+11	.521	.8801
1.5708	7.029E+03	2.856E+07	1.308E+02	1.245E+11	.481	.9001
1.6773	7.194E+03	2.510E+07	1.523E+02	1.119E+11	.437	.9200
ULLAGE GASES HAVE REACHED VENT						
1.6918	7.216E+03	2.465E+07	1.556E+02	1.103E+11	.431	.9225
1.8008	7.380E+03	2.146E+07	1.828E+02	9.818E+10	.386	.9401
BEGIN SUBSONIC FLOW						
1.8111	7.390E+03	2.117E+07	1.855E+02	9.699E+10	.382	.9416
1.9474	6.796E+03	1.741E+07	2.074E+02	7.335E+10	.330	.9600
2.1417	5.395E+03	1.199E+07	2.392E+02	4.010E+10	.263	.9800
2.5184	4.352E+02	8.320E+05	2.779E+02	2.245E+08	.196	.9969

TABLE 3-23 VENTING OF LH₂ TANK AT 100 SECONDS FLIGHT TIME

EFFECTIVE HOLE AREA = 572 SQ FT

VENT T(S)	FLOW VEL(CM/S)	OUTFLOW (G/S)	SPEC VOL (CC/G)	JET THRUST	ULLAGE P(BAR)	VENTED FRAC
.0000	8.041E+03	2.991E+08	1.429E+01	1.491E+12	2.280	.0000
.0090	7.695E+03	2.862E+08	1.429E+01	1.365E+12	2.089	.0201
.0183	7.380E+03	2.745E+08	1.429E+01	1.256E+12	1.923	.0401
.0280	7.095E+03	2.639E+08	1.429E+01	1.161E+12	1.779	.0601
.0381	6.836E+03	2.543E+08	1.429E+01	1.078E+12	1.653	.0800
.0486	6.597E+03	2.454E+08	1.429E+01	1.004E+12	1.540	.1001
.0594	6.378E+03	2.372E+08	1.429E+01	9.382E+11	1.441	.1201
.0706	6.176E+03	2.297E+08	1.429E+01	8.795E+11	1.352	.1401
.0821	5.988E+03	2.227E+08	1.429E+01	8.270E+11	1.272	.1600
.0940	5.814E+03	2.162E+08	1.429E+01	7.794E+11	1.200	.1800
.1063	5.650E+03	2.102E+08	1.429E+01	7.362E+11	1.134	.2001
.1189	5.516E+03	2.052E+08	1.429E+01	7.018E+11	1.082	.2201
BEGIN SUBSONIC FLOW						
.1191	5.516E+03	2.052E+08	1.429E+01	7.017E+11	1.082	.2203
BEGIN SONIC FLOW						
.1191	5.458E+03	1.962E+08	1.478E+01	6.639E+11	1.082	.2203
.1330	5.308E+03	1.764E+08	1.599E+01	5.803E+11	1.075	.2401
.1484	5.247E+03	1.648E+08	1.692E+01	5.360E+11	1.068	.2601
.1647	5.212E+03	1.559E+08	1.777E+01	5.036E+11	1.061	.2801
.1819	5.192E+03	1.484E+08	1.859E+01	4.777E+11	1.054	.3000
.2000	5.183E+03	1.418E+08	1.942E+01	4.558E+11	1.046	.3201
.2187	5.181E+03	1.360E+08	2.024E+01	4.369E+11	1.038	.3400
.2383	5.187E+03	1.307E+08	2.109E+01	4.203E+11	1.029	.3600
.2587	5.196E+03	1.257E+08	2.197E+01	4.049E+11	1.021	.3800
.2800	5.209E+03	1.210E+08	2.288E+01	3.908E+11	1.012	.4001
.3019	5.226E+03	1.166E+08	2.381E+01	3.778E+11	1.002	.4200
.3247	5.246E+03	1.124E+08	2.480E+01	3.656E+11	.993	.4400
.3731	5.296E+03	1.045E+08	2.693E+01	3.431E+11	.972	.4801
.4249	5.358E+03	9.713E+07	2.931E+01	3.226E+11	.949	.5201
.4808	5.431E+03	9.014E+07	3.202E+01	3.035E+11	.925	.5601
.5411	5.517E+03	8.345E+07	3.513E+01	2.854E+11	.898	.6001
.6062	5.616E+03	7.699E+07	3.876E+01	2.681E+11	.868	.6401
.6771	5.728E+03	7.063E+07	4.309E+01	2.508E+11	.835	.6801
.7545	5.855E+03	6.437E+07	4.834E+01	2.337E+11	.799	.7200
.8400	6.001E+03	5.812E+07	5.487E+01	2.163E+11	.758	.7601
.8861	6.083E+03	5.499E+07	5.878E+01	2.074E+11	.736	.7800
ULLAGE GASES HAVE REACHED VENT						
.9314	6.163E+03	5.207E+07	6.290E+01	1.990E+11	.714	.7985
.9353	6.170E+03	5.182E+07	6.328E+01	1.982E+11	.712	.8001
.9872	6.264E+03	4.864E+07	6.844E+01	1.889E+11	.686	.8201
1.0431	6.367E+03	4.541E+07	7.452E+01	1.792E+11	.658	.8401
1.1025	6.478E+03	4.215E+07	8.166E+01	1.693E+11	.628	.8600
1.1672	6.599E+03	3.881E+07	9.035E+01	1.588E+11	.596	.8801
1.2377	6.732E+03	3.539E+07	1.011E+02	1.477E+11	.560	.9001
1.3152	6.879E+03	3.188E+07	1.147E+02	1.360E+11	.521	.9200
1.4026	7.044E+03	2.824E+07	1.325E+02	1.233E+11	.477	.9401
1.5018	7.228E+03	2.442E+07	1.573E+02	1.094E+11	.427	.9601
1.6189	7.438E+03	2.035E+07	1.942E+02	9.385E+10	.370	.9801
1.7315	7.629E+03	1.686E+07	2.404E+02	7.976E+10	.317	.9901

TABLE 3-25 VENTING OF LH₂ TANK AT 350 SECONDS FLIGHT TIME

EFFECTIVE HOLE AREA = 572 SQ FT
 ULLAGE GAS ESCAPES IMMEDIATELY.

VENT T(S)	FLOW VEL(CM/S)	OUTFLOW (G/S)	SPEC VOL (CC/G)	JET THRUST	ULLAGE P(BAR)	VENTED FRAC
BEGIN SONIC FLOW						
.0000	6.531E+03	4.067E+07	8.533E+01	1.647E+11	.614	.0000
.0212	6.556E+03	3.998E+07	8.715E+01	1.625E+11	.607	.0201
.0428	6.582E+03	3.928E+07	8.905E+01	1.603E+11	.600	.0400
.0646	6.608E+03	3.858E+07	9.103E+01	1.581E+11	.593	.0600
.0870	6.635E+03	3.787E+07	9.310E+01	1.558E+11	.586	.0801
.1098	6.662E+03	3.716E+07	9.527E+01	1.535E+11	.579	.1001
.1330	6.690E+03	3.645E+07	9.752E+01	1.512E+11	.571	.1201
.1567	6.718E+03	3.574E+07	9.988E+01	1.489E+11	.564	.1401
.1807	6.747E+03	3.503E+07	1.024E+02	1.465E+11	.556	.1601
.2053	6.777E+03	3.433E+07	1.049E+02	1.442E+11	.548	.1800
.2305	6.806E+03	3.360E+07	1.075E+02	1.418E+11	.540	.2001
.2563	6.837E+03	3.288E+07	1.105E+02	1.394E+11	.532	.2201
.2824	6.867E+03	3.215E+07	1.135E+02	1.369E+11	.524	.2400
.3092	6.898E+03	3.141E+07	1.167E+02	1.343E+11	.515	.2600
.3369	6.931E+03	3.068E+07	1.200E+02	1.319E+11	.507	.2801
.3651	6.964E+03	2.995E+07	1.236E+02	1.293E+11	.498	.3001
.3937	6.997E+03	2.921E+07	1.273E+02	1.267E+11	.489	.3200
.4234	7.031E+03	2.847E+07	1.313E+02	1.241E+11	.480	.3401
.4539	7.066E+03	2.772E+07	1.355E+02	1.214E+11	.471	.3601
.4851	7.102E+03	2.696E+07	1.400E+02	1.187E+11	.461	.3801
.5171	7.138E+03	2.621E+07	1.447E+02	1.160E+11	.451	.4001
.5501	7.175E+03	2.545E+07	1.498E+02	1.132E+11	.441	.4200
.5842	7.213E+03	2.468E+07	1.553E+02	1.104E+11	.431	.4400
.6193	7.251E+03	2.391E+07	1.611E+02	1.075E+11	.421	.4600
.6556	7.291E+03	2.314E+07	1.674E+02	1.046E+11	.410	.4800
.6932	7.331E+03	2.235E+07	1.743E+02	1.016E+11	.399	.5001
.7322	7.372E+03	2.157E+07	1.817E+02	9.857E+10	.388	.5201
.7724	7.414E+03	2.077E+07	1.896E+02	9.549E+10	.377	.5400
.8143	7.456E+03	1.997E+07	1.984E+02	9.233E+10	.365	.5601
.8579	7.501E+03	1.918E+07	2.079E+02	8.918E+10	.353	.5800
.9034	7.545E+03	1.836E+07	2.184E+02	8.589E+10	.341	.6001
.9510	7.590E+03	1.754E+07	2.300E+02	8.254E+10	.328	.6201
1.0007	7.636E+03	1.671E+07	2.428E+02	7.913E+10	.315	.6400
1.0532	7.682E+03	1.588E+07	2.571E+02	7.563E+10	.302	.6601
1.1085	7.730E+03	1.503E+07	2.732E+02	7.204E+10	.288	.6801
1.1668	7.777E+03	1.418E+07	2.915E+02	6.837E+10	.274	.7000
1.2293	7.825E+03	1.331E+07	3.124E+02	6.457E+10	.259	.7201
1.3665	7.920E+03	1.155E+07	3.643E+02	5.674E+10	.228	.7600
1.5273	8.011E+03	9.747E+06	4.367E+02	4.841E+10	.195	.8101
1.6189	8.052E+03	8.829E+06	4.846E+02	4.408E+10	.178	.8200
1.7213	8.088E+03	7.897E+06	5.443E+02	3.960E+10	.160	.8400
1.8371	8.116E+03	6.943E+06	6.212E+02	3.494E+10	.142	.8601
1.9692	8.132E+03	5.981E+06	7.225E+02	3.015E+10	.123	.8801
2.1248	8.126E+03	5.002E+06	8.633E+02	2.520E+10	.103	.9001
2.3153	8.086E+03	4.011E+06	1.071E+03	2.011E+10	.082	.9201
2.4405	8.038E+03	3.454E+06	1.237E+03	1.721E+10	.070	.9310

TABLE 3-25 VENTING OF LH₂ TANK AT 350 SECONDS FLIGHT TIME

EFFECTIVE HOLE AREA = 572 SQ FT
 ULLAGE GAS ESCAPES IMMEDIATELY.

VENT T(S)	FLOW VEL(CM/S)	OUTFLOW (G/S)	SPEC VOL (CC/G)	JET THRUST	ULLAGE P(BAR)	VENTED FRAC
BEGIN SONIC FLOW						
.0000	6.531E+03	4.067E+07	8.533E+01	1.647E+11	.614	.0000
.0212	6.556E+03	3.998E+07	8.715E+01	1.625E+11	.607	.0201
.0428	6.582E+03	3.928E+07	8.905E+01	1.603E+11	.600	.0400
.0646	6.608E+03	3.858E+07	9.103E+01	1.581E+11	.593	.0600
.0870	6.635E+03	3.787E+07	9.310E+01	1.558E+11	.586	.0801
.1098	6.662E+03	3.716E+07	9.527E+01	1.535E+11	.579	.1001
.1330	6.690E+03	3.645E+07	9.752E+01	1.512E+11	.571	.1201
.1567	6.718E+03	3.574E+07	9.988E+01	1.489E+11	.564	.1401
.1807	6.747E+03	3.503E+07	1.024E+02	1.465E+11	.556	.1601
.2053	6.777E+03	3.433E+07	1.049E+02	1.442E+11	.548	.1800
.2305	6.806E+03	3.360E+07	1.075E+02	1.418E+11	.540	.2001
.2563	6.837E+03	3.288E+07	1.105E+02	1.394E+11	.532	.2201
.2824	6.867E+03	3.215E+07	1.135E+02	1.369E+11	.524	.2400
.3092	6.898E+03	3.141E+07	1.167E+02	1.343E+11	.515	.2600
.3369	6.931E+03	3.068E+07	1.200E+02	1.319E+11	.507	.2801
.3651	6.964E+03	2.995E+07	1.236E+02	1.293E+11	.498	.3001
.3937	6.997E+03	2.921E+07	1.273E+02	1.267E+11	.489	.3200
.4234	7.031E+03	2.847E+07	1.313E+02	1.241E+11	.480	.3401
.4539	7.066E+03	2.772E+07	1.355E+02	1.214E+11	.471	.3601
.4851	7.102E+03	2.696E+07	1.400E+02	1.187E+11	.461	.3801
.5171	7.138E+03	2.621E+07	1.447E+02	1.160E+11	.451	.4001
.5501	7.175E+03	2.545E+07	1.498E+02	1.132E+11	.441	.4200
.5842	7.213E+03	2.468E+07	1.553E+02	1.104E+11	.431	.4400
.6193	7.251E+03	2.391E+07	1.611E+02	1.075E+11	.421	.4600
.6556	7.291E+03	2.314E+07	1.674E+02	1.046E+11	.410	.4800
.6932	7.331E+03	2.235E+07	1.743E+02	1.016E+11	.399	.5001
.7322	7.372E+03	2.157E+07	1.817E+02	9.857E+10	.388	.5201
.7724	7.414E+03	2.077E+07	1.896E+02	9.549E+10	.377	.5400
.8143	7.456E+03	1.997E+07	1.984E+02	9.233E+10	.365	.5601
.8579	7.501E+03	1.918E+07	2.079E+02	8.918E+10	.353	.5800
.9034	7.545E+03	1.836E+07	2.184E+02	8.589E+10	.341	.6001
.9510	7.590E+03	1.754E+07	2.300E+02	8.254E+10	.328	.6201
1.0007	7.636E+03	1.671E+07	2.428E+02	7.913E+10	.315	.6400
1.0532	7.682E+03	1.588E+07	2.571E+02	7.563E+10	.302	.6601
1.1085	7.730E+03	1.503E+07	2.732E+02	7.204E+10	.288	.6801
1.1668	7.777E+03	1.418E+07	2.915E+02	6.837E+10	.274	.7000
1.2293	7.825E+03	1.331E+07	3.124E+02	6.457E+10	.259	.7201
1.3665	7.920E+03	1.155E+07	3.643E+02	5.674E+10	.228	.7600
1.5273	8.011E+03	9.747E+06	4.367E+02	4.841E+10	.195	.8101
1.6189	8.052E+03	8.829E+06	4.846E+02	4.408E+10	.178	.8200
1.7213	8.088E+03	7.897E+06	5.443E+02	3.960E+10	.160	.8400
1.8371	8.116E+03	6.943E+06	6.212E+02	3.494E+10	.142	.8601
1.9692	8.132E+03	5.981E+06	7.225E+02	3.015E+10	.123	.8801
2.1248	8.126E+03	5.002E+06	8.633E+02	2.520E+10	.103	.9001
2.3153	8.086E+03	4.011E+06	1.071E+03	2.011E+10	.082	.9201
2.4405	8.038E+03	3.454E+06	1.237E+03	1.721E+10	.070	.9310

TABLE 3-26 VENTING OF LH₂ TANK AT 450 SECONDS FLIGHT TIME

EFFECTIVE HOLE AREA = 572 SQ FT
 ULLAGE GAS ESCAPES IMMEDIATELY.

VENT T(S)	FLOW VEL(CM/S)	OUTFLOW (G/S)	SPEC VOL (CC/G)	JET THRUST	ULLAGE P(BAR)	VENTED FRAC
BEGIN SONIC FLOW						
.0000	7.978E+03	1.043E+07	4.065E+02	5.158E+10	.208	.0000
.0180	7.987E+03	1.023E+07	4.148E+02	5.068E+10	.204	.0200
.0365	7.997E+03	1.003E+07	4.235E+02	4.976E+10	.201	.0401
.0552	8.007E+03	9.838E+06	4.325E+02	4.883E+10	.197	.0601
.0742	8.016E+03	9.640E+06	4.419E+02	4.791E+10	.193	.0801
.0937	8.025E+03	9.441E+06	4.517E+02	4.697E+10	.190	.1000
.1137	8.034E+03	9.241E+06	4.620E+02	4.603E+10	.186	.1201
.1340	8.043E+03	9.041E+06	4.727E+02	4.508E+10	.182	.1401
.1548	8.051E+03	8.841E+06	4.840E+02	4.413E+10	.178	.1600
.1761	8.060E+03	8.639E+06	4.958E+02	4.317E+10	.175	.1801
.1979	8.068E+03	8.437E+06	5.082E+02	4.220E+10	.171	.2001
.2202	8.076E+03	8.235E+06	5.212E+02	4.123E+10	.167	.2201
.2431	8.083E+03	8.031E+06	5.349E+02	4.025E+10	.163	.2401
.2665	8.090E+03	7.827E+06	5.493E+02	3.926E+10	.159	.2601
.2906	8.097E+03	7.623E+06	5.645E+02	3.827E+10	.155	.2800
.3153	8.104E+03	7.418E+06	5.805E+02	3.727E+10	.151	.3000
.3409	8.109E+03	7.212E+06	5.975E+02	3.626E+10	.147	.3202
.3670	8.115E+03	7.006E+06	6.155E+02	3.525E+10	.143	.3401
.3939	8.120E+03	6.799E+06	6.346E+02	3.423E+10	.139	.3601
.4218	8.124E+03	6.590E+06	6.551E+02	3.319E+10	.135	.3801
.4504	8.127E+03	6.381E+06	6.768E+02	3.215E+10	.131	.4001
.4799	8.130E+03	6.173E+06	6.999E+02	3.112E+10	.126	.4200
.5106	8.132E+03	5.963E+06	7.247E+02	3.006E+10	.122	.4400
.5423	8.133E+03	5.752E+06	7.514E+02	2.900E+10	.118	.4600
.5754	8.133E+03	5.540E+06	7.801E+02	2.793E+10	.114	.4801
.6097	8.131E+03	5.327E+06	8.111E+02	2.686E+10	.109	.5001
.6452	8.128E+03	5.114E+06	8.446E+02	2.577E+10	.105	.5201
.6824	8.124E+03	4.901E+06	8.809E+02	2.469E+10	.101	.5401
.7210	8.118E+03	4.687E+06	9.204E+02	2.359E+10	.096	.5600
.7617	8.110E+03	4.472E+06	9.638E+02	2.249E+10	.092	.5800
.8045	8.100E+03	4.255E+06	1.012E+03	2.137E+10	.087	.6001
.8493	8.087E+03	4.039E+06	1.064E+03	2.025E+10	.083	.6201
.8966	8.072E+03	3.822E+06	1.122E+03	1.913E+10	.078	.6401
.9468	8.053E+03	3.605E+06	1.187E+03	1.800E+10	.073	.6601
.9816	8.038E+03	3.461E+06	1.234E+03	1.725E+10	.070	.6733

TABLE 3-27 VENTING TIMES FOR LOX AND LH₂ TANKS

FLIGHT TIME(S)	LOX TANK-----			
	T(0.9)	T(STOP)	F(STOP)	T(ULL)
10	12.6	18.4	.65	NONE
20	11.3	16.7	.81	NONE
30	-	-	-	NONE
40	-	-	-	NONE
50	9.4	14.9	.98	NONE
60	>9.6	>15.2	.99	15.2
70	-	-	.99	-
80	-	-	>.99	-
90	-	-	>.99	-
100	>8.5	>13.5	>.99	11.9
350	7.2	14.2	>.99	0
450	5.0	9.7	>.99	0

FLIGHT TIME(S)	LH ₂ TANK-----			
	T(0.9)	T(STOP)	F(STOP)	T(ULL)
10	1.03	3.05	.31	NONE
20	1.13	1.73	.51	NONE
30	1.28	1.93	.70	NONE
40	1.39	2.14	.88	NONE
50	1.43	2.23	.93	NONE
60	>1.62	>2.43	.98	1.81
70	-	-	>.99	-
80	-	-	>.99	-
90	-	-	>.99	-
100	1.24	1.73	>.99	0.93
350	1.71	2.44	.93	0
450	.82	.98	.67	0

T(0.9) = TIME NEEDED TO VENT 90 PERCENT OF WHAT WILL EVENTUALLY VENT.

T(STOP) = TIME WHEN FLOW STOPS (PRESSURES BECOME EQUALIZED).

F(STOP) = FRACTION VENTED WHEN FLOW STOPS.

T(ULL) = TIME WHEN ULLAGE GASES REACH VENT AND ESCAPE.
ULLAGE ESCAPES IMMEDIATELY AT T=350 AND 450.

RATE OF BUBBLE GROWTH

In the following, the rate of bubble growth in the cryogens is considered. The growth of a vapor bubble may be written as follows:¹

$$R = 2A \frac{\rho_L^c}{\rho_v^L} D \frac{3}{\pi} t (T_L - T_B)$$

where

R	= bubble radius (cm)	LH ₂	LOX
A	= proportionality constant	0.070	1.147
L	= liquid density (g/cc)	1.314-3	4.43-3
v	= vapor density (g/cc)	2.0	0.398
c	= liquid specific heat (cal/g/deg)	108.0	50.9
L	= latent heat of evaporation (cal/g)	2.01-3	7.85-4
D	= liquid thermal diffusivity (cm ² /s)	20.47	90.81
t	= time since beginning of bubble growth (s)		
T _L	= liquid temperature (K)		
T _B	= boiling temperature (K) at desired pressure		
T _L - T _B	= degrees of superheat		

The factor in brackets may be compared with other liquids:

water	0.121
LOX	0.0567
LH ₂	0.0442
ethanol	0.044

From experiments on water², the constant A is about 0.216 (see Figs. 4 and 9 in footnote 2 below). The bubble growth rates are then

$$\text{for LH}_2 \quad R = 0.080 (T_L - T_B) \quad \sqrt{t}$$

$$\text{for LOX} \quad R = 0.102 (T_L - T_B) \quad \sqrt{t}$$

with R in cm, T_L - T_B in °K, and t in seconds.

The superheats are as follows, where T_B is the boiling point at ambient pressure:

¹Dergarabedian, P., "Observations on Bubble Growths in Various Superheated Liquids," Journal of Fluid Mechanics Vol. 9, 1960, p. 39.

²Dergarabedian, P., "The Rate of Growth of Vapor Bubbles in Superheated Water," Journal of Applied Mechanics Vol. 20, 1953, P. 537.

Flight time (sec)	LH ₂			LOX		
	T _L	T _B	T _L - T _B	T _L	T _B	T _L - T _B
0	20.47	20.25	0.22	90.81	90.18	0.63
10	20.47	20.16	0.31	90.81	89.89	0.92
50	20.47	17.36	3.11	90.81	81.85	8.96
100	20.47	Freezes		90.81	63.58	27.2

T_L is the boiling point at 15.7 psia (1.0822 bar).

The nucleation rate is estimated by Boggs at 10⁶ nuclei/sec/m³ (1 nucleus/sec/cm³).³ If one nucleus per cm³ were present at time zero, the volume of the bubble would be

$$V_{bub} = \frac{4}{3} \pi R^3$$

where R is as above.

Some times for bubble growth at a flight time of 50 seconds are shown below:

<u>V_L + V_{bub}</u> (cm ³)	<u>V_{bub}</u> (cm ³)	<u>R_{bub}</u> (cm)	Time (sec) to grow to radius R _{bub}	
			LH ₂	LOX
1.0	0.0	0.0	0.0	0.0
1.1	0.1	0.29	1.34	0.00013
1.5	0.5	0.49	3.92	0.29
2.0	1.0	0.62	6.22	0.46

The LOX bubbles grow about ten times faster than the LH₂ bubbles.

The growth in volume of a large mass of superheated liquid is much slower than indicated in this table, because the inner part of the mass continues to feel its vapor pressure until the outer part moves out. The full superheat is felt only on the outside of the mass at first, and gradually moves in as the outer layers expand. There is also a lag of about 0.1 seconds (see footnote 2, p. 3-28) between a drop in pressure and the beginning of rapid bubble growth. This means that while the jet is being pushed by ullage pressure and there is no boiling in the tank, there is little boiling in the first few meters of jet. After the liquid in the tank has begun to boil, the jet already has bubbles in it when it exists, and bubbles will grow as described here.

Thus, the critical part of the LOX jet (within the first few meters of the ET), from which the part of the LOX plume passing under the orbiter originates, will not be expanded much by boiling. The expansion by boiling of the pancake of LH₂ covering the bottom of the orbiter will also be small until the bulk of the LH₂ has moved out clear of the orbiter.

³Boggs, W. H., "Physical Processes Causing LOX/LH₂ Autoignition," Minutes of the Seventeenth Explosives Safety Seminar, Denver, Colo., Vol. 1, Sep 1976, p. 135.

STRIPPING OF LIQUID JET. The stripping analysis of Mayer was followed herein.⁴ Assume that the airflow raises those capillary waves of wavelength $\bar{\lambda}$ of maximum growth rate and these waves crest, forming a ligament that breaks into droplets. Let each element of liquid area $\bar{\lambda}^2$ produce one droplet of mean diameter $D = 0.14 \bar{\lambda}$ every τ seconds. Then the droplet formation rate per cm^2 of surface exposed to the airflow is

$$\dot{n} = 1/(\bar{\lambda}^2 \tau) = (0.14)^2/(\bar{D}^2 \tau) \quad (3-1)$$

where τ is the time modulus calculated from

$$1/\tau = f/\bar{\lambda}^{1/2} - v/\bar{\lambda}^2$$

with

$$f = \sqrt{\pi/2} \beta \rho_g v_g^2 / \sqrt{\sigma \rho_L} \quad (\text{forcing parameter})$$

$$v = 8\pi^2 \mu_L / \rho_L \quad (\text{viscous damping parameter})$$

$$\beta = \text{sheltering parameter} = 0.3$$

$$\rho_g = \text{density of gas flow } (\text{g/cm}^3)$$

$$v_g = \text{velocity of gas flow } (\text{cm/s})$$

$$\sigma = \text{surface tension of liquid } (\text{dyne/cm})$$

$$\rho_L = \text{density of liquid } (\text{g/cm}^3)$$

$$\mu_L = \text{dynamic viscosity of liquid } (\text{g/cm/s})$$

The mean droplet diameter \bar{D} is given by

$$\bar{D} = 9\pi 16^{1/3} B \left[\mu_L \sqrt{\sigma/\rho_L} / \left(\rho_g v_g^2 \right) \right]^{2/3} \quad (3-2)$$

where

$$B = 0.3$$

The mass per droplet is

$$m_d = \pi \bar{D}^3 \rho_L / 6$$

The mass loss rate per cm^2 of liquid surface is then

$$\dot{m} = (0.14)^2 \pi/6 \cdot \bar{D} \rho_L / \tau$$

⁴Mayer, E., "Theory of Liquid Atomization in High Velocity Gas Streams," American Rocket Society Journal, Dec 1961, p. 1783.

The sides of the approximately rectangular LOX jet are subject to stripping. The stripped area per cm of jet length is about twice the hole length, or $A_s = 2 \times 229 \text{ cm}$. The mass loss rate per centimeter of jet length is then m_s .

The wake of the LOX plume when it reaches the orbiter is roughly four times the diameter of an equivalent circular jet, or $4 \times 326.1 = 1304 \text{ cm}$. The amount of air involved in the wake (per cm of jet) is $m_a = 1304 \rho_a$. A momentum balance gives the direction and speed of the wake relative to the orbiter.

The outward velocity component of the air-oxygen mixture is

$$v_{out} = v_L m_L / (m_L + m_a)$$

The longitudinal component (parallel to the ET axis) is

$$v_{long} = v_a m_a / (m_L + m_a)$$

DROPLET EVAPORATION TIME. Next, available time for the stripped LOX droplets to evaporate before they reach the LH₂ was considered.

The time required to evaporate a droplet in a still gas was estimated as follows:⁵

$$\theta = \frac{\rho_l r_o^2 RT}{2M \delta P (y_i - y_\infty)} \quad (3-3)$$

where

ρ_l = drop density

r_o = initial drop radius

y_i = mole fraction in interface gas

y_∞ = mole fraction at infinity

R = gas constant

T = temperature

M = molecular weight of liquid

δ = diffusion coefficient

P = pressure

⁵Perry, J. H., Ed., Chemical Engineer's Handbook, 3rd ed. (New York: McGraw-Hill 1950.)

The diffusion coefficient is obtained from

$$\delta = 0.0043 \frac{T^{3/2}}{P \left(V_1^{1/3} + V_2^{1/3} \right)^2} \sqrt{\frac{1}{M_1} + \frac{1}{M_2}} \quad (3-4)$$

where

- δ = diffusivity (cm^2/s)
- T = temperature (K)
- P = pressure (atm)
- M_1, M_2 = molecular weights of materials 1 and 2
- V_1, V_2 = molecular volumes at normal boiling points (cm^3/mole)
 - = 13.0 for air, 7.15 for hydrogen, 7.4 for oxygen

For the conditions of interest here, Equation 3-3 may be written

$$\theta = C_t d_o^2 \quad (C_t \text{ in } \text{s}/\text{cm}^2) \quad (3-5)$$

The C_t values and times to evaporate a 0.001 cm droplet are as follows:

Flight Time (sec)			Time to Evaporate 0.001 cm drop (sec)	
	C_t LOX	C_t LH_2	LOX	LH_2
10	665.0	224.0	0.000665	0.000244
50	700.0	256.0	0.000700	0.000256
100	802.0	269.0	0.000802	0.000269

The evaporation times for the drops of 0.001 cm diameter expected from stripping of the jet are short enough to make thermodynamic equilibrium in the plume a reasonable assumption.

CLUSTER WITH ORBITER

If the orbiter is still attached to the ET at destruct time, the LH_2 jet will impact the bottom of the orbiter and will spread out laterally in all directions as an expanding sheet that covers the bottom of the wings before any LOX arrives.

The orbiter tends to separate the stripped LOX from the LH_2 . The LOX is carried out beyond the orbiter, but the LH_2 spreads out under the orbiter. However, this spreading caused by the orbiter allows the LH_2 stream to impact the LOX jet and cause an explosion. Figure 3-3 shows the shape of the LOX plume under the orbiter. Figure 3-4 shows the shape of the LH_2 jet deflected by the orbiter.

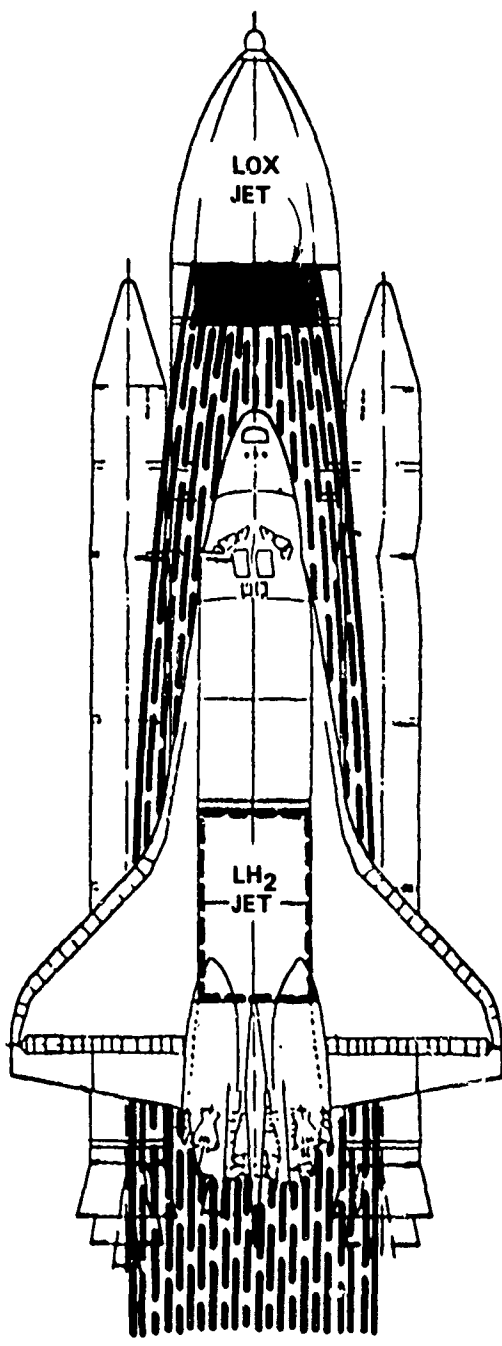
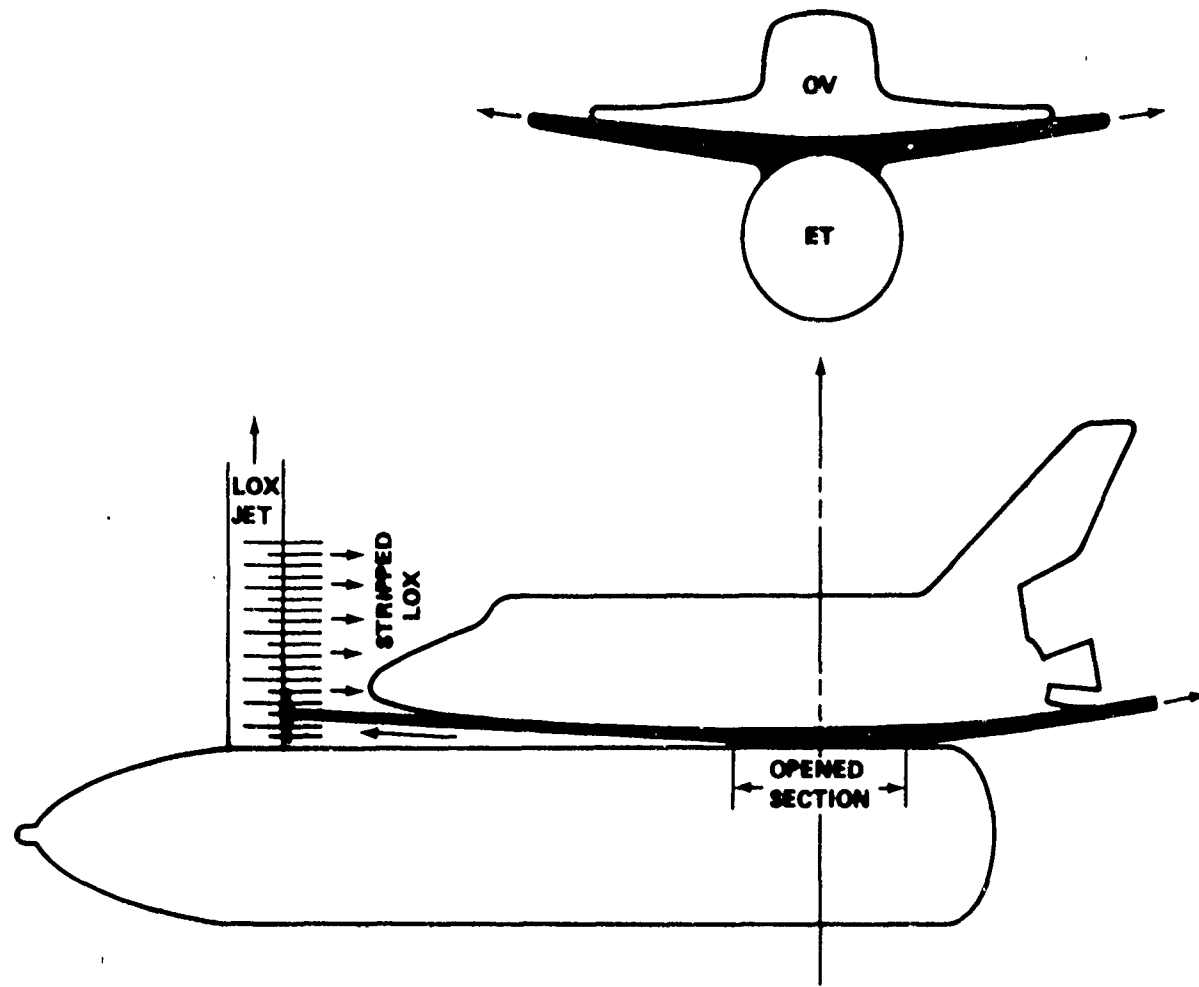


FIGURE 3-3 PORTION OF LOX PLUME PASSING UNDER ORBITER

FIGURE 3-4 SHAPE OF LH₂ JET UNDER ORBITER

MIXING UNDER ORBITER. The boundary layer thickness of a sheet at zero angle of attack may be estimated as follows:⁶

$$\delta^* = 1.729 \sqrt{v/u_g} \sqrt{x}$$

where

δ^* = effective boundary layer thickness at distance x

v = kinematic viscosity of the gas (oxygen-air mixture)

⁶Schlichting, H., Boundary Layer Theory, 4th ed. (New York: McGraw-Hill, 1960).

u_g = velocity of gas relative to sheet

x = distance back from leading edge of sheet

Some results from this equation are:

<u>T (sec)</u>	<u>v (cm²/s)</u>	<u>u_g (cm/s)</u>	<u>δ^* (cm) at $x = 10^3$ cm</u>
10	0.21	4000.0	0.40
50	0.33	21000.0	0.22
100	1.0	28000.0	0.33

The boundary layer is only 2 to 4 millimeters thick at 10 meters away from the leading edge of the sheet.

However, this does not include the effects of roughness due to capillary waves or stripped droplets. The roughness due to capillary waves is small because of their short wavelengths (about 0.001 centimeter). The distance to which droplets are thrown by wave breakup depends on the scale of the waves, not on the scale of the jet. Therefore, from experiments on breakup of water droplets, the LH₂ droplets move out only a few millimeters due to wave breakup. This keeps down the amount of the mixing with the oxygen and air by keeping the mixing layer thin and by loading the airflow. This reduces its velocity so the stripping is less as one moves downstream along the LH₂ pancake. Because this shielding of the LH₂ by its own droplets (and own gaseous hydrogen) is rejected, the amount of mixing calculated is an overestimate. It is assumed that the mixing thickness is 10 centimeters. The TNT equivalence of the mixture is insignificant (Table 3-10, last column).

IMPACT OF LH₂ PANCAKE ON LOX JET. If the LH₂ spreads out uniformly in all lateral directions after impacting the orbiter, part of it will move toward the LOX jet. If there were no air resistance or LH₂ removal by stripping, the fraction of the total existing LH₂ impacting the LOX jet 25 meters away would be

$$f_i = (\text{LOX jet width}) / (\text{pancake perimeter at } 25 \text{ m}) = 5.89 / (2\pi(25)) = 0.037$$

Thus, a maximum of 3.7 percent of the existing LH₂ could impact the LOX jet. The leading edge of the LH₂ pancake is about 20 centimeters thick when it reaches the LOX jet; less than 1 centimeter has been stripped from it by the airflow.

The effects of air resistance can be estimated by calculating what minimum size sphere of LH₂ can travel 25 meters upstream against the drag of the airflow. The results are shown in Table 3-28. It can be concluded that since the pancake has a smaller ballistic coefficient than a sphere, it will not be stopped from reaching the LOX jet by airflow drag.

Since neither stripping nor air drag can significantly reduce the amount of LH₂ reaching the LOX jet, we may use the 3.7-percent figure; the resulting mixing parameters are given in Table 3-28.

TABLE 3-28 IMPACT OF LH₂ ON LOX JET

FLIGHT TIME(S)	10	20	50	65	100	115
TOTAL LH ₂ EXITING (MEGAGRAMS)	31.1	49.3	85.0	88.3	81.0	77.6
MAX LH ₂ HITTING LOX JET(LB)	2535.	4020.	6930.	7200.	6600.	6330.
THICKNESS OF LH ₂ SHEET (CM)	10.	22.	22.	22.	22.	22.
TIME WHEN LH ₂ FIRST HITS LOX(S)	0.39	0.38	0.33	0.32	0.31	0.31
MINIMUM DIAM SPHERE OF LH ₂ ABLE TO REACH LOX (CM)	1.8	8.4	18.6	15.1	5.0	1.3
LOX JET VELOC (M/S) AT 1 SEC	4.2	6.1	12.1	13.2	13.2	13.2
LOX JET TRAVEL (M) WHILE 256 LB OF LH ₂ MIXES WITH LOX	3.7	3.1	4.6	4.9	4.8	4.5
TIME INTERVAL(S) NEEDED TO MIX 256 LB LH ₂ WITH LOX	0.87	0.51	0.38	0.37	0.36	0.34
TIME(S) WHEN 256 LB LH ₂ HAS MIXED (AUTOIGNITION OCCURS)	1.26	0.89	0.71	0.69	0.66	0.65
DISTANCE (M) OF CENTER OF EXPLSION FROM ET	3.9	3.9	4.6	4.5	4.4	4.3

TABLE 3-29 MIXING OF JETS WITH ORBITER SEPARATED

FLIGHT TIME(S)	20	65	115	350	450
TIME (S) WHEN ONE OF THE TANKS BREAKS AND ITS FLOW STOPS	1.58	0.94	0.96	1.36	1.02
MAX ANGLE BETWEEN JETS (DEG)	7.79	10.4	19.2	22.1	26.2
DISTANCE (M) FROM ET TO JET INTERSECTION	176	131	71	61	52
SHOCK PROPERTIES AT ET FOR 7400 LB TNT CHARGE AT JET INTERSECTION--					
PEAK INCID OVERPRESSURE(PSI)	1.2	0.83	1.0	NEGLIGIBLE	
POS OVERPR IMPULSE (PSI.S)	0.070	0.062	0.050	NEGLIGIBLE	

Autoignition occurs with 100 percent probability when 256 pounds of LH₂ mix with 2,044 pounds of LOX. Since the amount of the LH₂ impacting the LOX jet is considerably above 256 pounds, an explosion with a maximum energy equivalent of 7,400 pounds TNT is expected. This is an upper limit; smaller explosions are possible by earlier autoignition or ignition by flame. More than one explosion is possible since an explosion will not necessarily stop the jets.

CLUSTER WITHOUT ORBITER

Mixing of the liquid cryogens can occur if the ET deforms so that the LOX and LH₂ jets intersect. Table 3-29 lists the blast effects, assuming that autoignition occurs when 2,300 pounds (equivalent in energy to 7,400 pounds TNT) are mixed. This is an upper limit because autoignition or ignition by propellant fragments can occur before 2,300 pounds are mixed. The loading of the ET is not enough to cause significant damage to the ET or significant effect on the fragment trajectories.

TURBULENT MIXING IN WAKE OR CLUSTER

The plume formed from the LH₂ jet is assumed to be jet moving into a coaxial secondary stream of air. Forstall and Shapiro developed empirical relations for a jet faster than the secondary stream.⁷ No one seems to have considered the case wanted here: a jet slower than the secondary stream. However, it is plausible to assume that the velocity ratio is the important quantity, regardless of which velocity is larger. Following Forstall and Shapiro with this change and writing in a factor of 0.7 because convection rather than stream velocity is wanted yields:

$$L/D = 0.7 (4 + 12\lambda)$$

$$C_c = L/x \text{ for } x \geq L$$

$$r_h/a = (x/L)^{1-\lambda}$$

$$C/C_c = \frac{1}{2} \left(1 + \cos \left(\frac{\pi}{2} r/r_h \right) \right)$$

where

λ = $u_{\text{plume}}/u_{\text{air}}$ = ratio of velocities relative to ET

u_{plume} = mixed plume velocity (from conservation of momentum)

u_{air} = airstream velocity

D = diameter at breakup

a = $D/2$ = plume radius

L = length of potential core

⁷Forstall, W., Jr., and Shapiro, A. H., "Momentum and Mass Transfer in Coaxial Gas Jets," Journal of Applied Mechanics, Vol. 17, 1950, p. 399.

- x = downstream distance
 C_c = mole concentration of jet matter on axis ($r = 0$) at x
 C = mole concentration of jet matter at radius r at x
 r_h = radius at which mole concentration is half of C_c

The fraction of the jet material lying between concentrations C_U and C_L (which may be the upper and lower detonation or burn limits) is obtained from

$$r_H/r_h = \text{arc cos } (C_H/C_c/\text{arc cos } (0.5))$$

$$r_L/r_h = \text{arc cos } (C_L/C_c/\text{arc cos } (0.5))$$

$$f_{HL} = \left[f(r_H/r_h) - f(r_L/r_h) \right] / f(0)$$

where

$$f(y) = \frac{1}{2} \pi y^2 + \frac{4}{\pi} \left[\cos \left(\frac{1}{2} \pi y \right) - 1 \right] + 2y \sin \left(\frac{1}{2} \pi y \right)$$

Next, detonable concentrations will be considered.

DETONABILITY OF HYDROGEN-OXYGEN-AIR MIXTURES

The deontion limits for gaseous mixtures were worked out using the theory of Belles.⁸ For liquids and solids, experimental data were used.

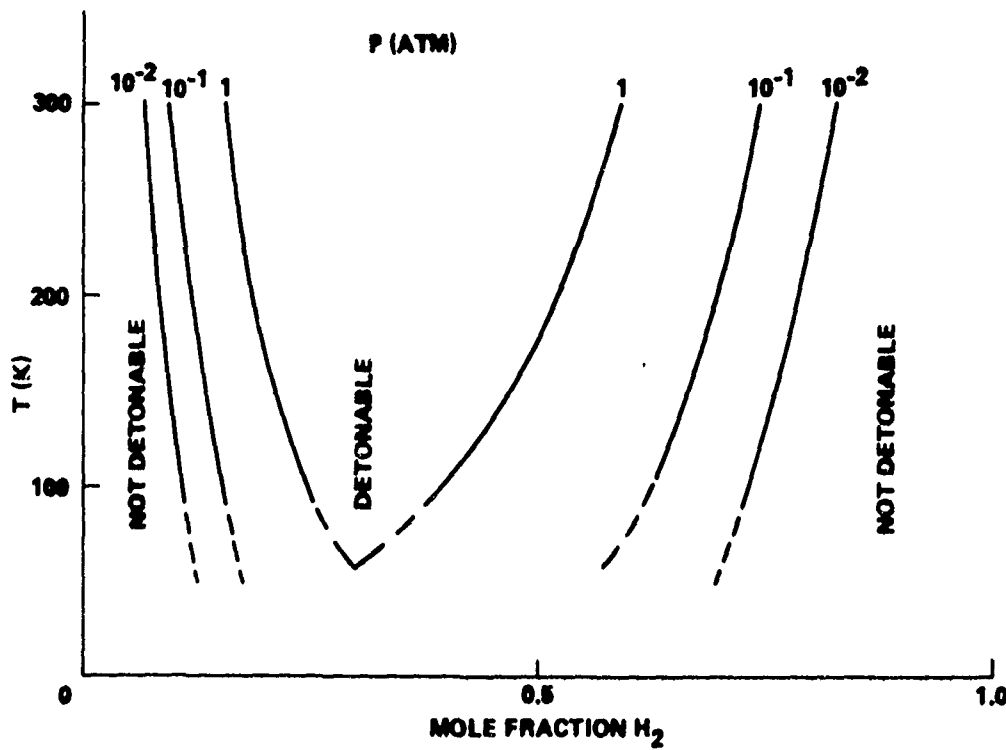
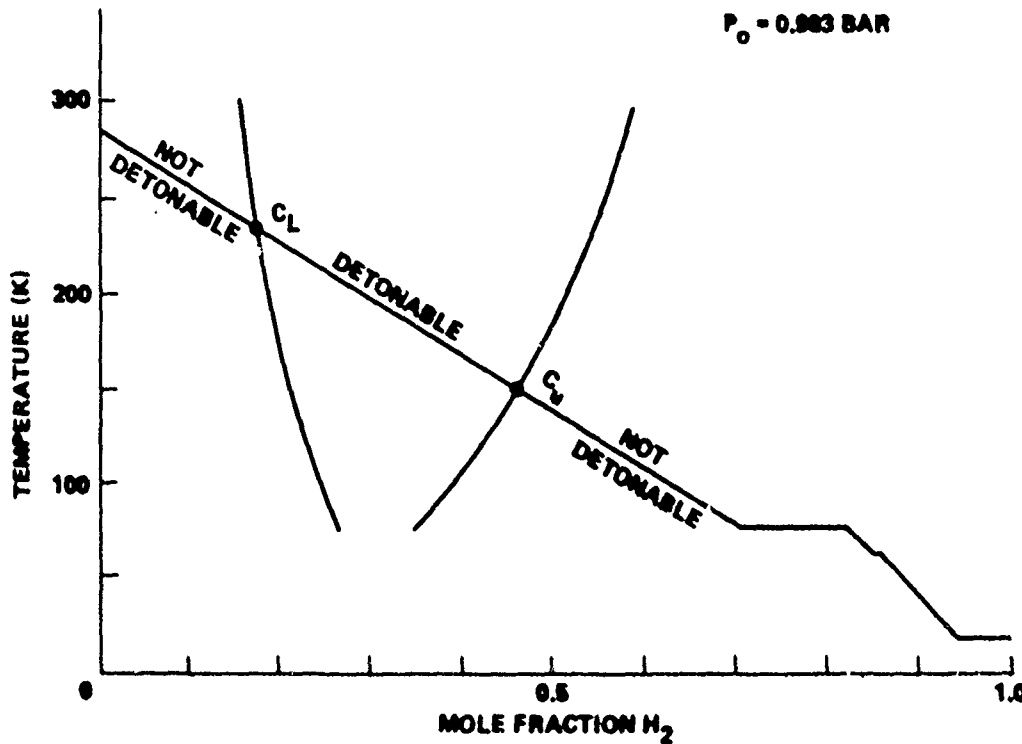
HYDROGEN-AIR MIXTURES. Figure 3-5 shows the theoretical results for gaseous hydrogen air mixtures. The effect of the low temperature in the plume is to reduce the range of composition that can detonate. In Figures 3-6 through 3-8, the theory is applied to the H₂ air mixtures encountered for the flight conditions at 10, 50, and 100 seconds, respectively. These figures (while intended for gases) suggest that mixtures of LH₂ with liquid air or solid air might not detonate. Indeed, Cassutt, et al were unable to detonate LH₂-solid air (at 1 atm pressure) by impact or by hot wire.⁹ If the mixture is allowed to stand for a while, however, it becomes oxygen-enriched by boiling off nitrogen and thus becomes detonable.

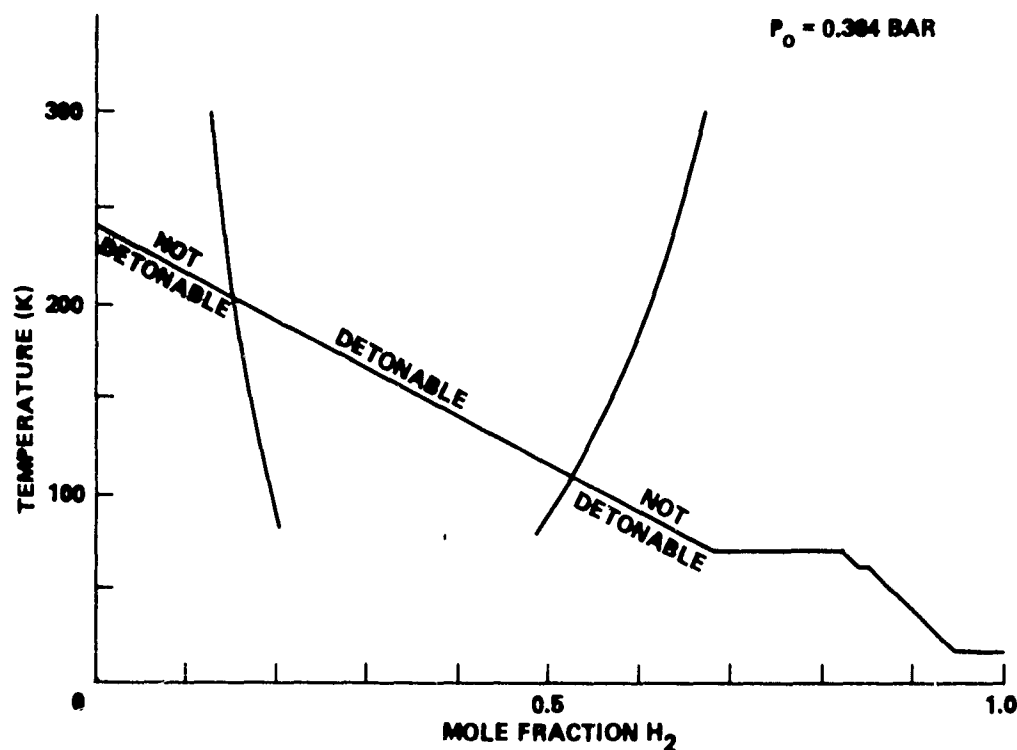
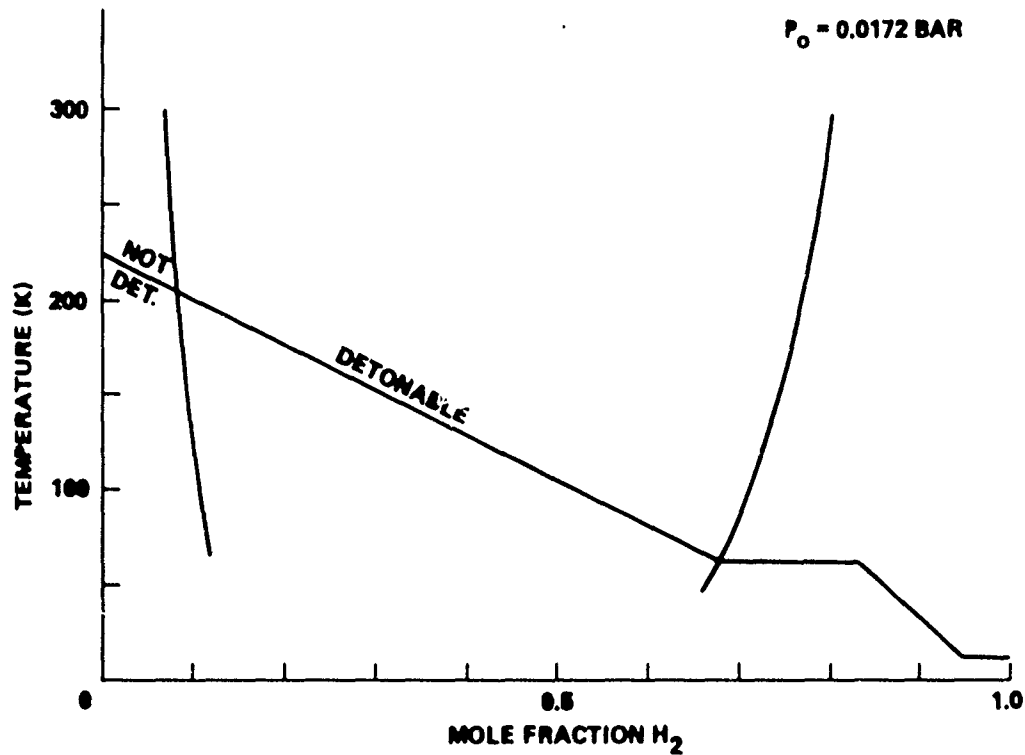
Applying these detonability criteria to the turbulent plume gives the fraction of the H₂ that is detonable within a cross section of the plume at any desired downstream distance (i.e., any chosen C_c value). The results are shown in Figure 3-7.

If a mixture is detonable, this simply means that there are conditions under which it can be made to detonate by a sufficiently strong initiator. It

⁸Belles, F. E., "Detonability and Chemical Kinetics: Prediction of Limits of Detonability of Hydrogen," Combustion Symposium, Vol. 7, 1962, p. 745.

⁹Cassutt, L. H., Maddocks, F. E., and Sawyer, W. A., "A Study of the Hazards in the Storage and Handling of Liquid Hydrogen," Advances in Cryogenic Engineering, Vol. 5, 1960, p. 55.

FIGURE 3-5 DETONATION LIMITS OF H_2 AIR MIXTURESFIGURE 3-6 DETONABILITY OF H_2 AIR MIXTURE AT ALTITUDE OF 831 FT (10 SEC)

FIGURE 3-7 DETONABILITY OF H₂ AIR MIXTURE AT ALTITUDE OF 24.49 KFT (50 SEC)FIGURE 3-8 DETONABILITY OF H₂ AIR MIXTURE AT ALTITUDE OF 90.57 KFT (T = 100 SEC)

may burn or not react at all under other initiation conditions. As shown in footnote 9, on page 3-37, 5-foot and 8-foot diameter balloons of H₂ air mixtures were initiated with flames, sparks, hot wires, and blasting caps. In all cases, there was burning rather than detonation. A 2-gram HE charge was needed to cause detonation. This means that the H₂ air plume can be ignited but not detonated by burning SRB propellants, hot gases, or hot pieces of metal. The shock waves from the SRB explosion are long gone by the time the plume forms. There is every indication that the plume will burn rather than detonate.

HYDROGEN-OXYGEN MIXTURES. Figure 3-9 shows the theoretical detonation limits for gaseous H₂-O₂ mixtures. The theory agrees well with experiments at 1 atm pressure and temperatures near 300 K. Cassutt, et al (see footnote 9, p. 3-38) were able to detonate an LH₂-solid O₂ mixture with a hot wire and found an impact sensitivity like RDX. Kaye was able to detonate confined dumped mixtures of LH₂ and LOX with hot surfaces, hot wires, spark, and flame, but got burning rather than detonation for unconfined mixtures.¹⁰ He was unable to detonate mixtures of solid hydrogen with solid oxygen or liquid oxygen when the pressure was below 0.013 bar (10 mm Hg).

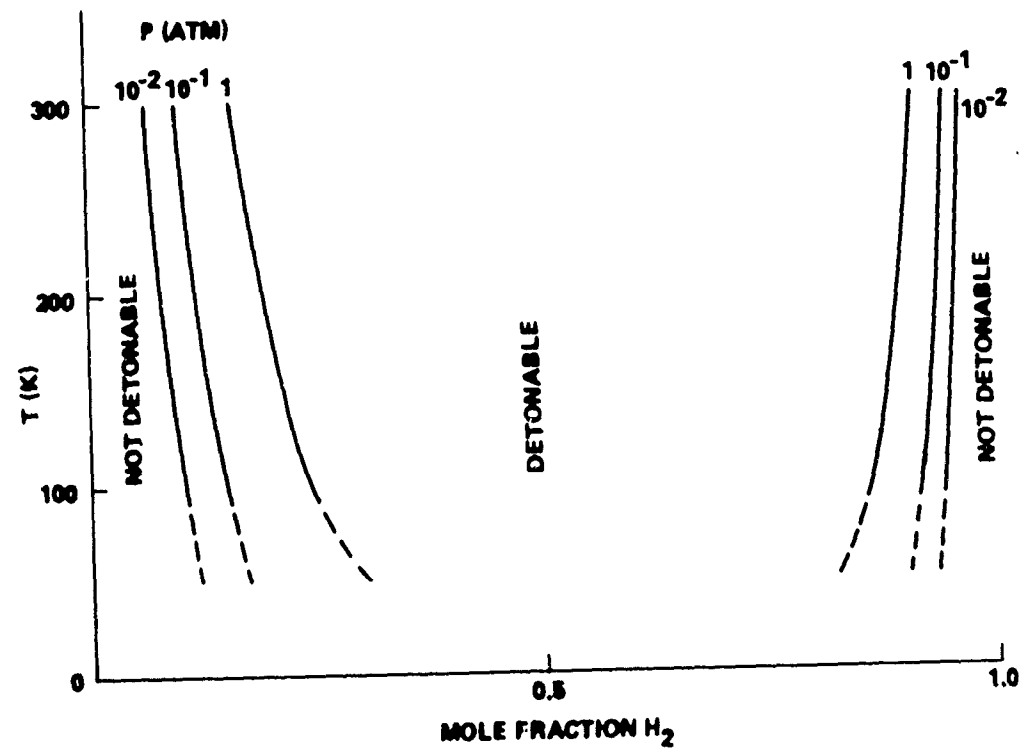


FIGURE 3-9 DEONTATION LIMITS OF H₂-O₂ MIXTURES

¹⁰Kaye, S., "Hazard Studies with Hydrogen and Oxygen in the Liquid and Solid Phases," Advances in Cryogenic Engineering, Vol. 11, 1966, p. 277.

The large-scale PYRO tests showed spontaneous detonation when large quantities of LH₂ and LOX were dumped together. The "critical mass" above which detonation is inevitable is about 2,300 pounds of mixture.¹¹ It is not clear how the PYRO experience can be applied to the situation where a fine mist of LOX impacts an LH₂ jet and an LH₂ mist at low ambient pressure. The arguments leading to the 2,300-pound critical mass should apply, however, to the mixing of LH₂ and LOX jets.

LH₂-LOX MIXTURES. The next point of consideration is gross mixing of liquid hydrogen with liquid oxygen.

The size of the possible explosion is self-limited by spontaneous spark ignition which occurs when (or before) about 2,300 pounds of LOX and LH₂ have been mixed (see footnote 11). This figure is based on mixing energized by the pdV work of boiling the LH₂. If additional energy such as that of ground impact were present, this would increase the amount of mixing before spontaneous spark ignition and the 2,300-pound figure would increase. Farber, et al (see footnote 11) find for LOX-LH₂ or LOX-RP1,

$$M_{crit}(lb) = 1870/(E/E_b) + 940 (E/E_b)^2$$

where E_b is the boiling energy and E is the total mixing energy. (This equation gives 2,810 rather than 2,300 for E/E_b = 1 because it includes LOX-RP1 mixtures.) The kinetic energy of the jets is small compared to E_b. Thus, the maximum amount of the LOX-LH₂ mixture that can detonate is 2,300 pounds (256 pounds LH₂ and 2,044 pounds LOX). Using an energy equivalence of 3.2 pounds TNT per pound of LOX-LH₂ mixture gives an upper-limit explosion energy of 7,400 pounds TNT.

PROPAGATION OF BURNING. The burning velocity of H₂-O₂-N₂ mixtures is less than 10 m/s at room temperature and atmospheric pressure, and decreases with decreasing pressure.¹² Because the airflow velocity considerably exceeds 10 m/s, as does the LH₂ exit velocity during most of the outflow, a flame cannot work its way upstream and spread radially, but is swept downstream from each point of ignition. (The ignition sources are the burning propellant pieces from the SRB's, the rocket engine exhausts, and the LSC.)

For destruct with the orbiter attached, there is a thin region in the boundary layer on the LH₂ pancake below the orbiter that has a low enough velocity to hold a flame steady relative to the orbiter. However, this region is probably too thin to sustain a flame.

Although flame propagation speeds are small, any object in a high-speed combustible flow can act as a "flameholder" because of the low velocities in its near wake. Because of the large number of ignition sources, the hydrogen plume is expected to ignite, and the flame will be held by the cluster and by the

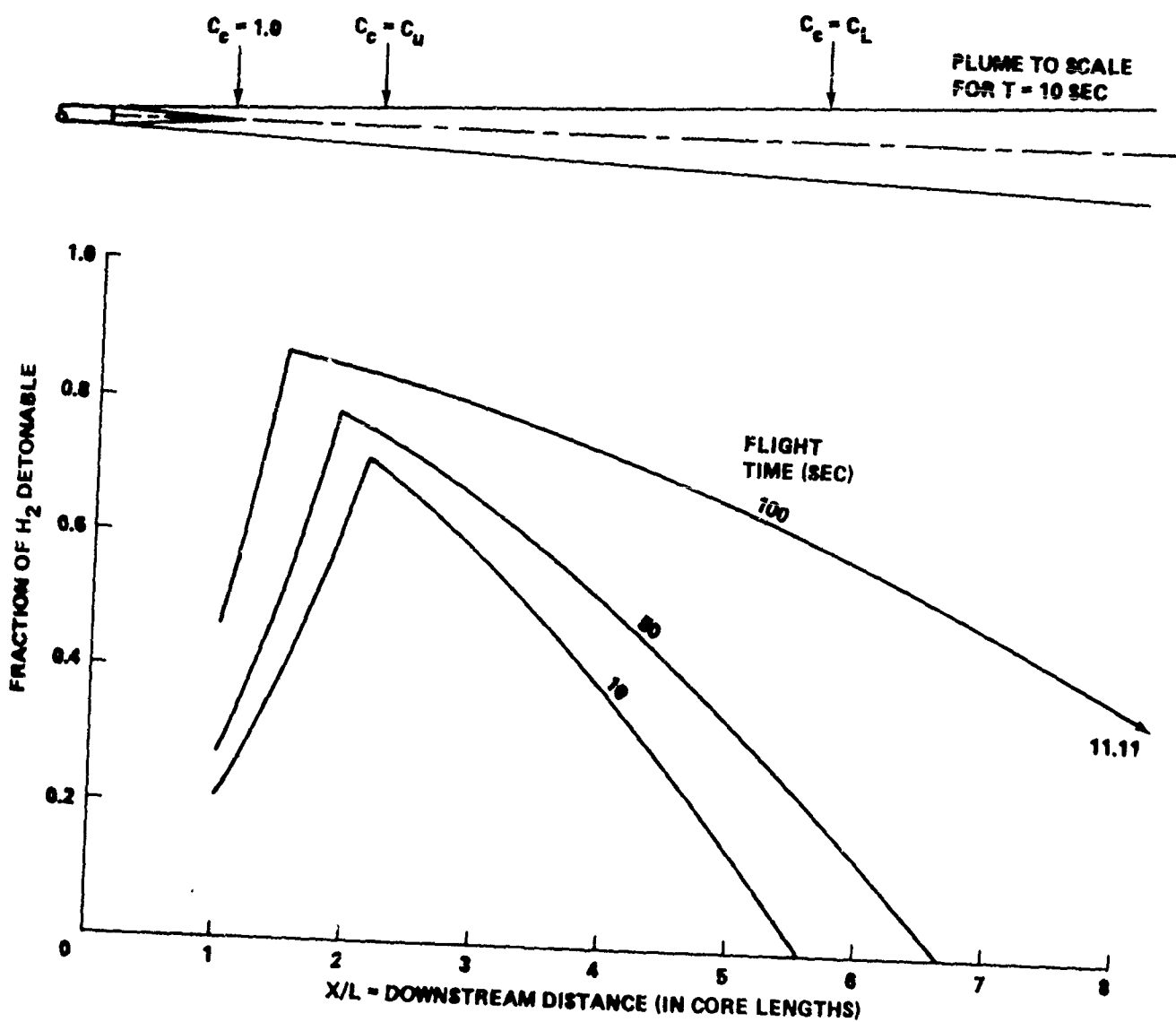
¹¹Farber, E. A., Smith, J. H., and Watts, E. H., "Prediction of Explosive Yield and Other Characteristics of Liquid Rocket Propellant Explosions, Final Report," University of Florida, N74-20589, Jun 30, 1973.

¹²Lewis, B., and von Elbe, G., Combustion, Flames and Explosions of Gases, 2nd ed. (New York: Academic Press, 1961), pp. 382, 399.

hydrogen jet. An illustration of a fraction of H₂ detonable in a turbulent plume is presented in Figure 3-10.

BLAST

Because the upper-limit explosion for LH₂-LOX mixing has the energy equivalent of 7,400 pounds TNT, the shock pressure and impulse versus distance are given for this charge in Figures 3-11 and 3-12. It is recognized that this equivalence applies strictly only at large distances from the explosion. However, the exploding mixture is far from spherical; e.g., the LH₂ impacting the LOX jet is spread out nonuniformly along the aft side of the LOX jet. Furthermore, the actual yield will be some unpredictable number less than 7,400 pounds. Therefore, there is no point in trying to fine-tune the blast parameters to account for the type of energy source.

FIGURE 3-10 FRACTION OF H_2 DETONABLE IN TURBULENT PLUME

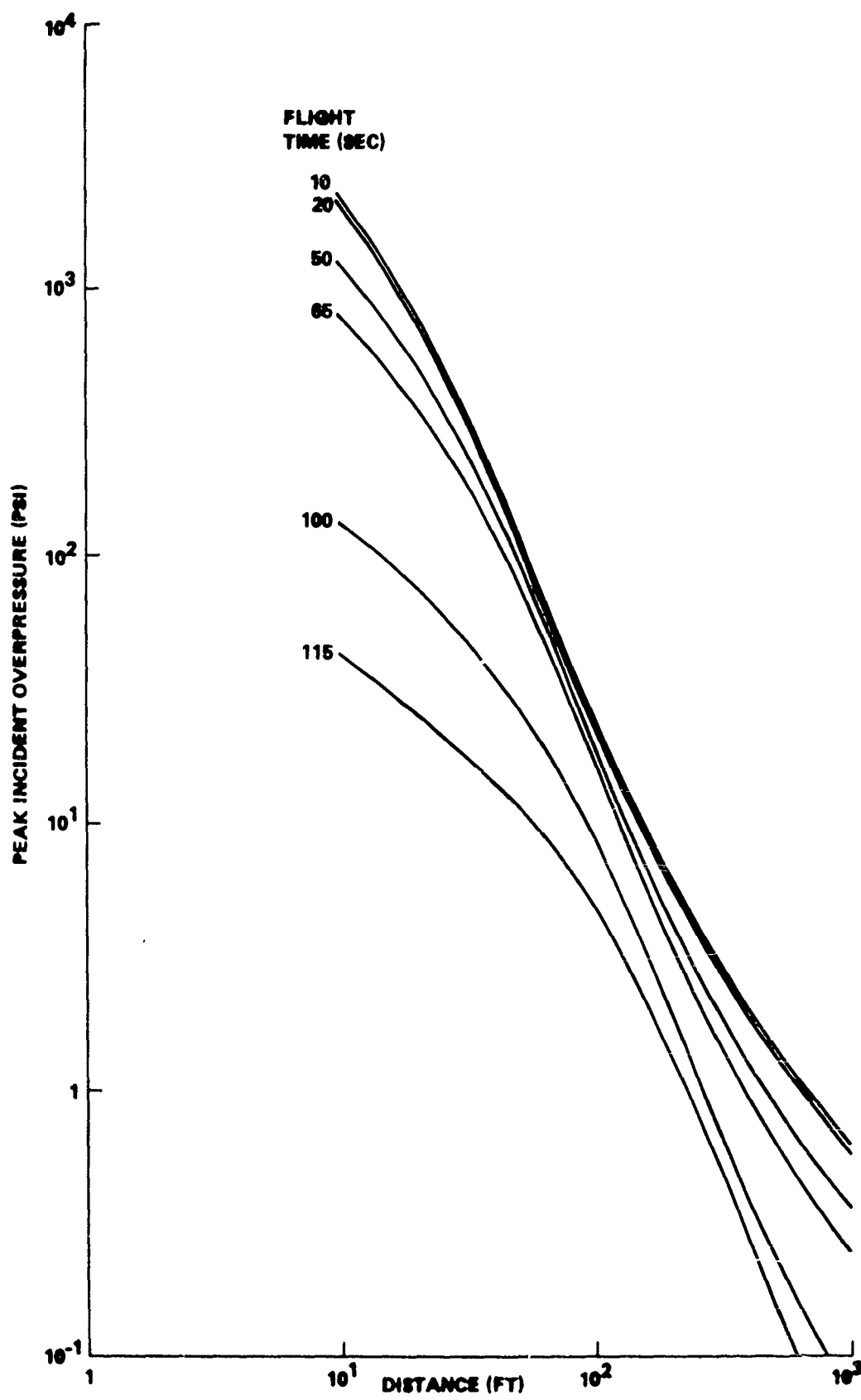


FIGURE 3-11 PRESSURE VS. DISTANCE FOR 7,400-LB TNT CHARGE

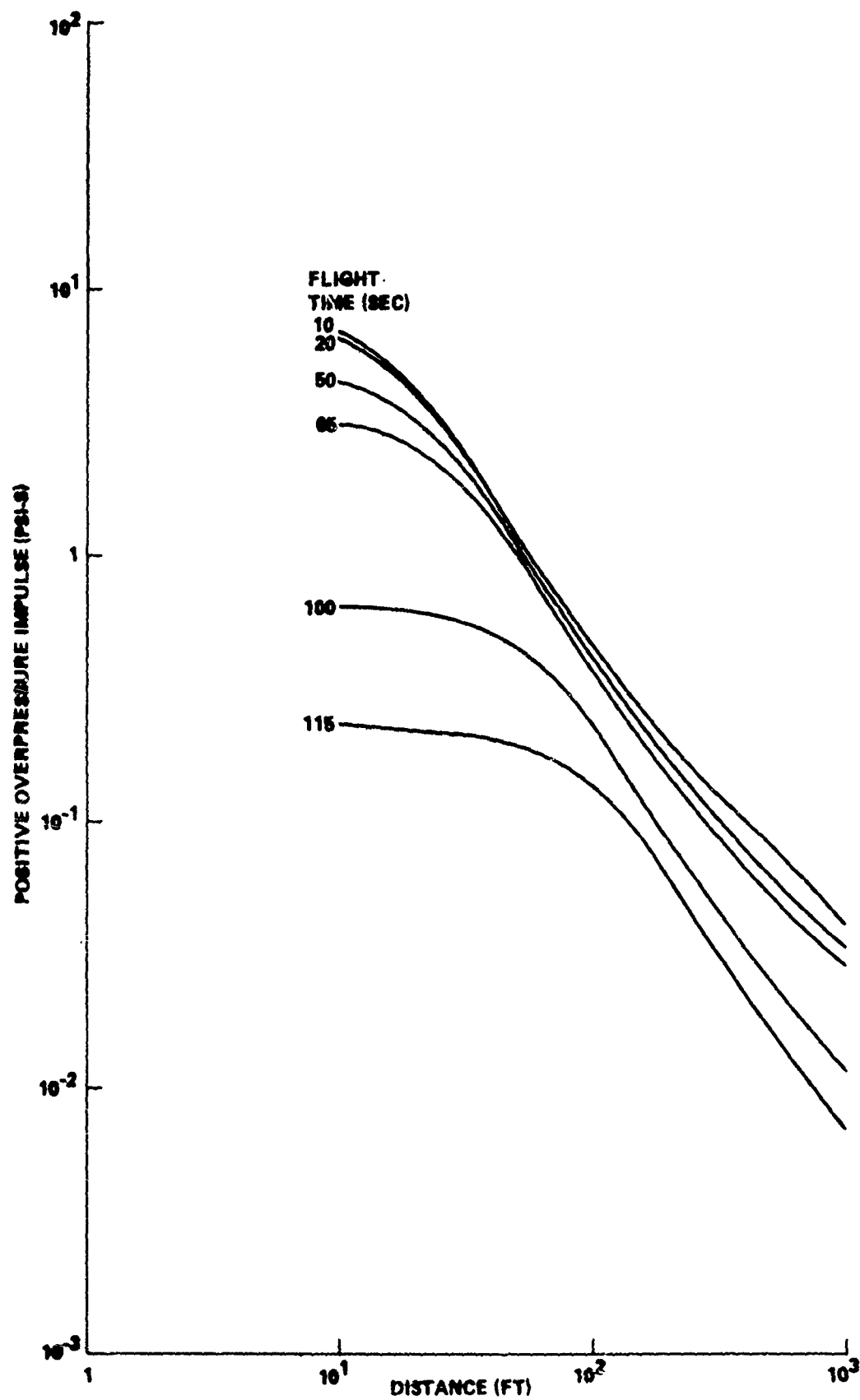


FIGURE 3-12 IMPULSE VS. DISTANCE FOR 7,400-LB TNT CHARGE

3-45/3-46

CHAPTER 4

SRB, ET, AND ORBITER BREAKUP

INTRODUCTION

The physical breakup of the shuttle ascent vehicle logically divides into three segments associated with the three major components; the solid rocket boosters (SRB's), external tank (ET), and orbiter. While coupling does exist, it does not materially alter the general fragmentation pattern and allows for one basic breakup analysis for each component. Interactions are then considered as perturbations to the basic breakup pattern. The rationale for the breakup analysis is presented in the following sections with the detail calculations attached as appendices.

SRB BREAKUP

The SRB consists of the solid rocket motor (SRM), a forward frustum and skirt, an aft skirt, and SRB/ET attach hardware. The Command Destruct System (Fig. 4-1), intended to terminate the thrust of the rocket, is applied solely to the SRM. It consists of a dual linear-shaped charge (LSC) running longitudinally along the outboard side of the cylindrical case from the intersection with the forward dome (X_B 531) to the ET attach ring (X_B 1491). The LSC's are housed in the equipment tunnel which is fragmented by the cutting action of the backside LSC sheath (Fig. 4-2). The sheath segments are accelerated to a velocity of about 2,300 ft/sec by the charge and lose little velocity in penetrating the tunnel wall. The tunnel fragments in turn, are accelerated by the pressure generated by the explosive charge but attain a much lower velocity due to the reduction in delivered impulse with distance. However, those fragments caught in the flow of the propellant gas vented through the LSC cut will achieve a velocity comparable to the LSC sheath segments.

The LSC (750 gr/ft HMX/aluminum) is sufficiently energetic to cut the SRM wall, except at the clevis joints connecting the individual case segments. This initial perforation pattern is shown in Figure 4-3. The internal pressure in the rocket produces a hoop load which is now reacted by the remaining ligaments at the joints. The load exceeds the ultimate capability of the case material (D6AC), and the ligaments fail in the hoop direction allowing the case to clamshell open. Simultaneously, the perforation pattern produces extremely high local axial loads at the tips of the cuts causing local axial clevis joint failures. As each individual pin fails, the adjacent pin becomes overloaded and the failure propagates from the LSC cut to the opposite side of the case, separating the segments.

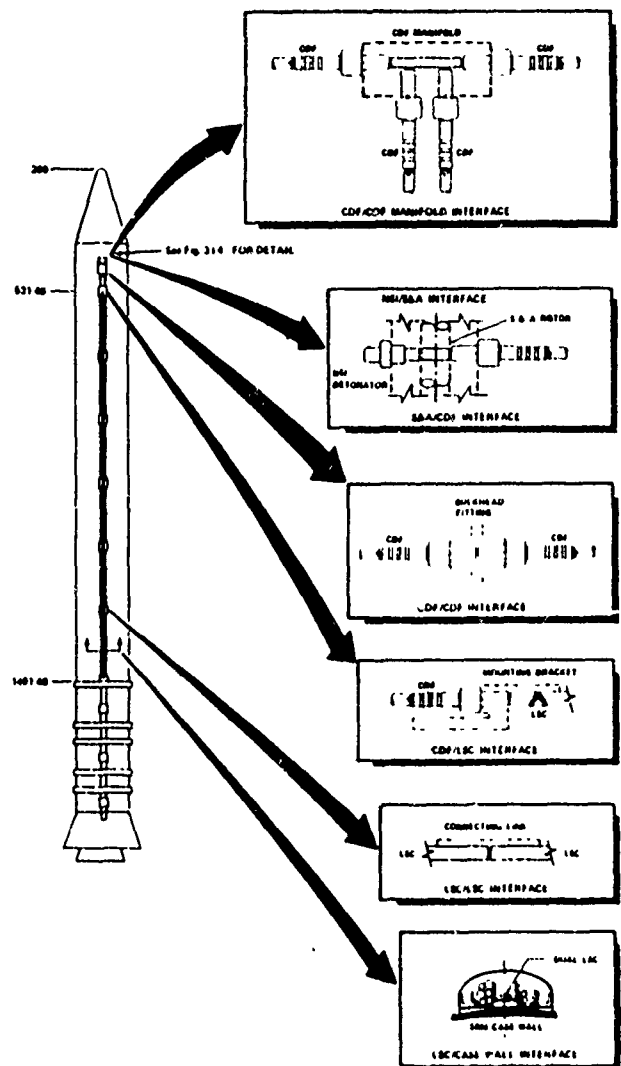


FIGURE 4-1 SRB COMMAND DESTRUCT SYSTEM

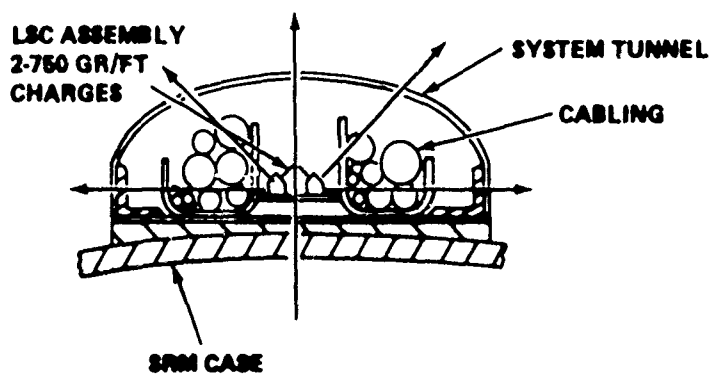


FIGURE 4-2 FRAGMENTATION OF SYSTEM TUNNEL BY LSC'S

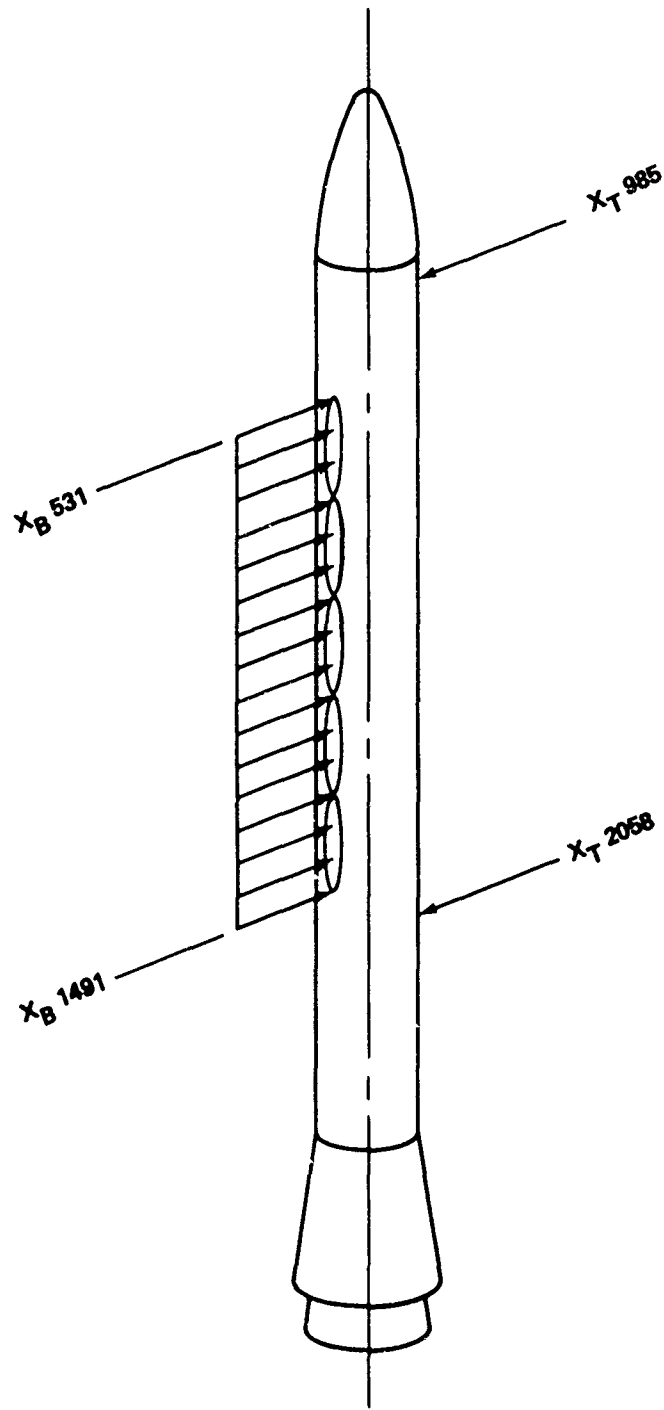


FIGURE 4-3 INITIAL SRB PERFORATION PATTERN

As the case opens, the propellant begins to develop cracks and breaks up. An exponential distribution has been found to fit test data reasonably well. Therefore, the size distributions given in Figure 4-4 are assumed to characterize the fragmentation of the propellant at the times given in the analysis matrix. The largest fragment allowed at any time is limited to a cube having one side equal to the radial thickness of the propellant at that time. The smallest fragment dimension is chosen as 1 inch, consistent with experimental observations. The equation plotted on Figure 4-4

$$N_L = N_o e^{-\frac{(L - L_{MIN})}{(L_o - L_{MIN})}}$$

where N_o is the total number of fragments, L_{MIN} is the minimum fragment dimension (1 inch) and L_o is a characteristic dimension dependent upon the maximum fragment dimension and the number of fragments. N_o is selected such that the total mass of fragments equals the total mass of fragmenting propellant. N_L is then interpreted as the number of cubic fragments having a side dimension of L or greater, up to the maximum dimension for which the distribution predicts only one fragment. No appreciable consumption of the propellant occurs during the duration of SRB breakup, but burnup of the small firebrands could occur before ground impact.

Note that no fragment distribution is presented for a destruct action at 115 seconds into flight. At this time, the radial thickness of the propellant has been reduced to the order of 1 inch and no fragmentation is predicted. It is reasonable to assume that in this situation the propellant remains adhered to the motor case and adds to the mass of the case fragments.

As the propellant fractures and new burning surfaces develop, the flame spreads to these surfaces producing additional combustion products. Initially the pressure in the motor increases. However, as the case opens, venting overtakes the increase in combustion rate. The pressure curve peaks and then falls to ambient pressure. The peak pressure is dependent upon the venting process and the generation of new burning surfaces. Figure 4-5 illustrates the sensitivity of the pressure to the rate of increase in burning surface. The prediction of new burning surfaces requires knowledge of the flame spread rate into the cracks. Lacking this information, the assumption is made that the flame spread rate equals the crack velocity. The crack velocity is on the order of 2,000 in/sec for PBAN propellants when loaded dynamically. Hence, the upper bound on the flame spread rate is taken as 2,000 in/sec yielding the pressure-time curves given in Figure 4-6 for the selected times.

During the venting process, cracked propellant (inert chunks and firebrands) is ejected from the SRB through the clamshell slit. The resulting velocities of the fragments are imparted by the gas flow in a direction normal to the SRM centerline. The smaller fragments, having lower ballistic coefficients, attain higher velocities. The maximum relative velocity imparted to a fragment of a given size is attained by that fragment which is ejected when the slit width just equals the fragment dimension (Fig. 4-7). A normal distribution is then assumed for the velocity distribution.

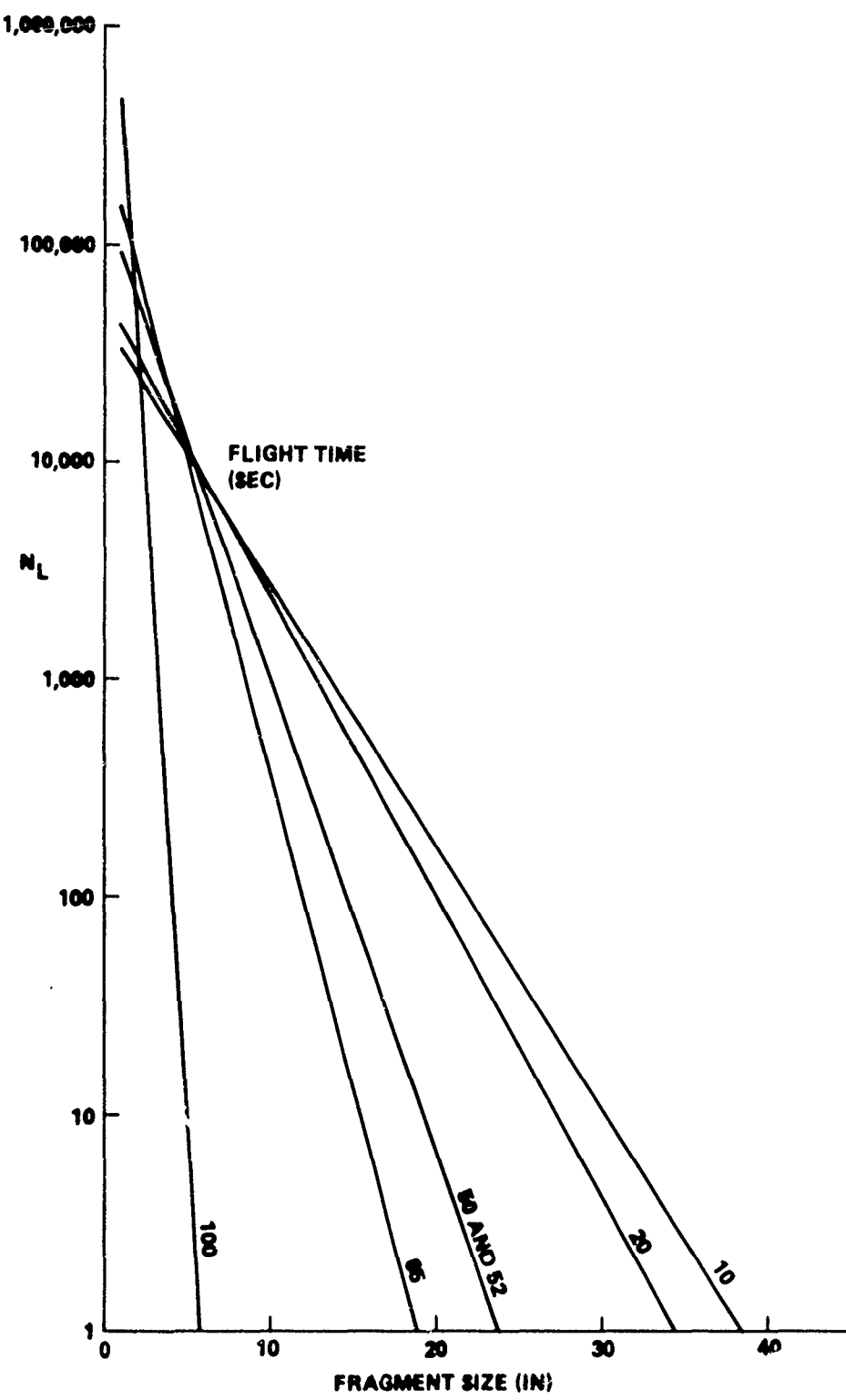


FIGURE 4-4 PROPELLANT FRAGMENT SIZE DISTRIBUTIONS

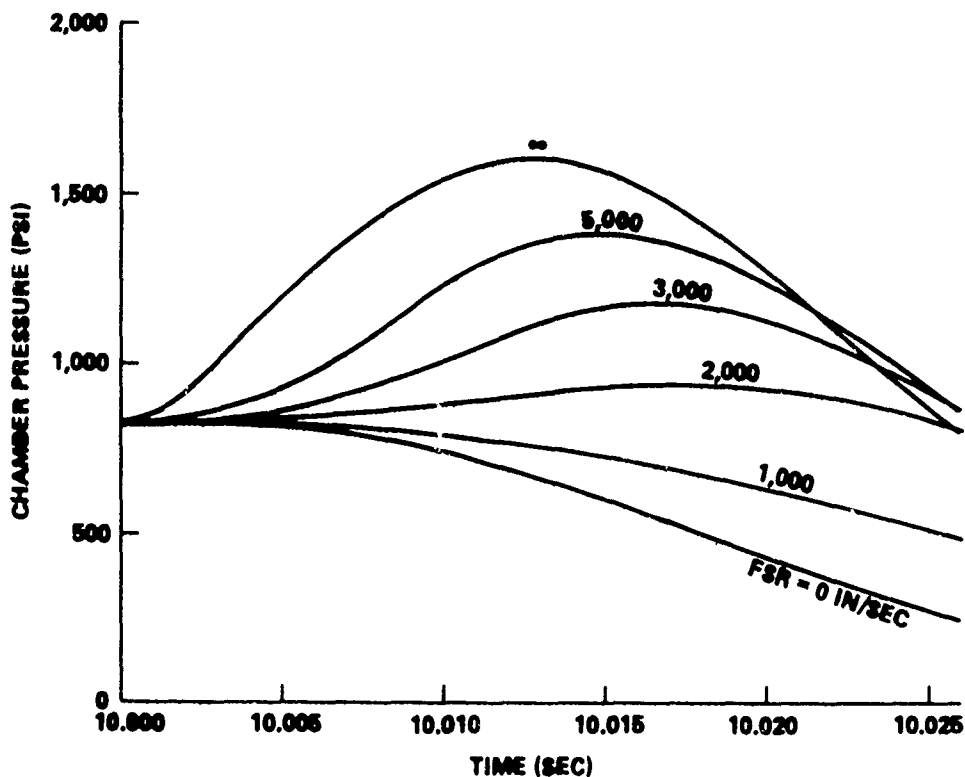


FIGURE 4-5 EFFECT OF FLAME SPREAD RATE ON CHAMBER PRESSURE DURING PROPELLANT BREAKUP

As the case opens, the shell flattens and begins to hinge about a line diametrically opposite to the cut. The hinge eventually becomes fully plastic and ruptures producing two large flattened plate fragments from each case segment. The velocity imparted to the case fragments is derived from the lateral thrust on the SRB and the momentum transfer from the propellant ejected in the outboard direction. This velocity is normal to the SRM axis.

The forward frustum, skirt, and forward dome of the motor (Fig. 4-8) remain as one large fragment propelled forward by the pressure in the SRB following clevis joint failure at the SRM dome-cylinder interface. In most instances considered, the SRB is attached to the ET at the time of destruct system initiation. Since the forward skirt contains the forward SRB/ET attach fitting, the fragment is constrained by the ET until the attach fitting breaks. The design of the fitting only allows a 3-degree rotation before failing the separation bolt. Therefore, failure of the fitting occurs very quickly, and the only major difference between response of a separated SRB and that of an attached SRB is the addition of a rotational velocity to the fragment in the latter case.

FSR = 2,000 IN/SEC

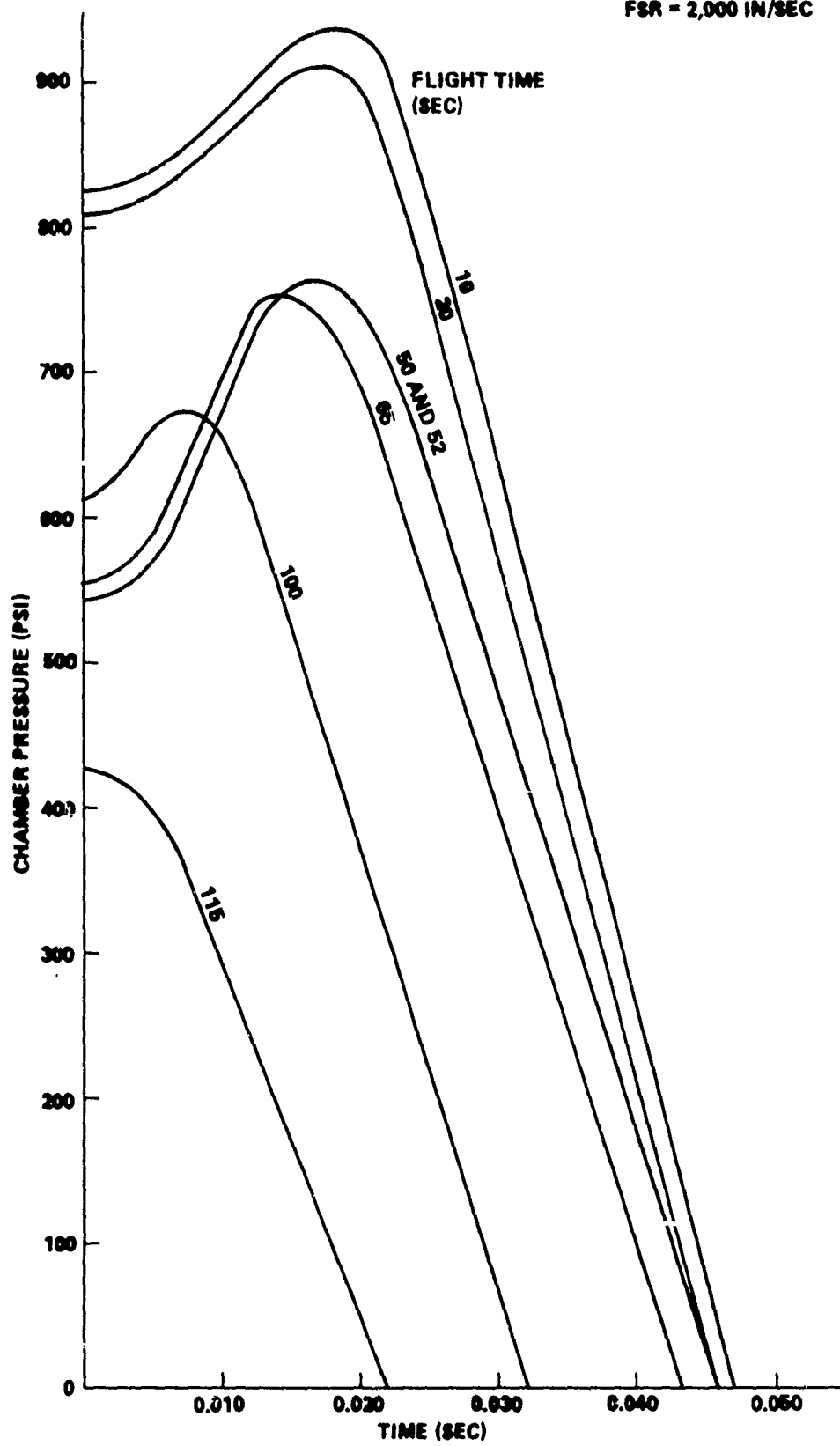


FIGURE 4-6 CHAMBER PRESSURE VS. TIME AFTER DESTRUCT ACTION

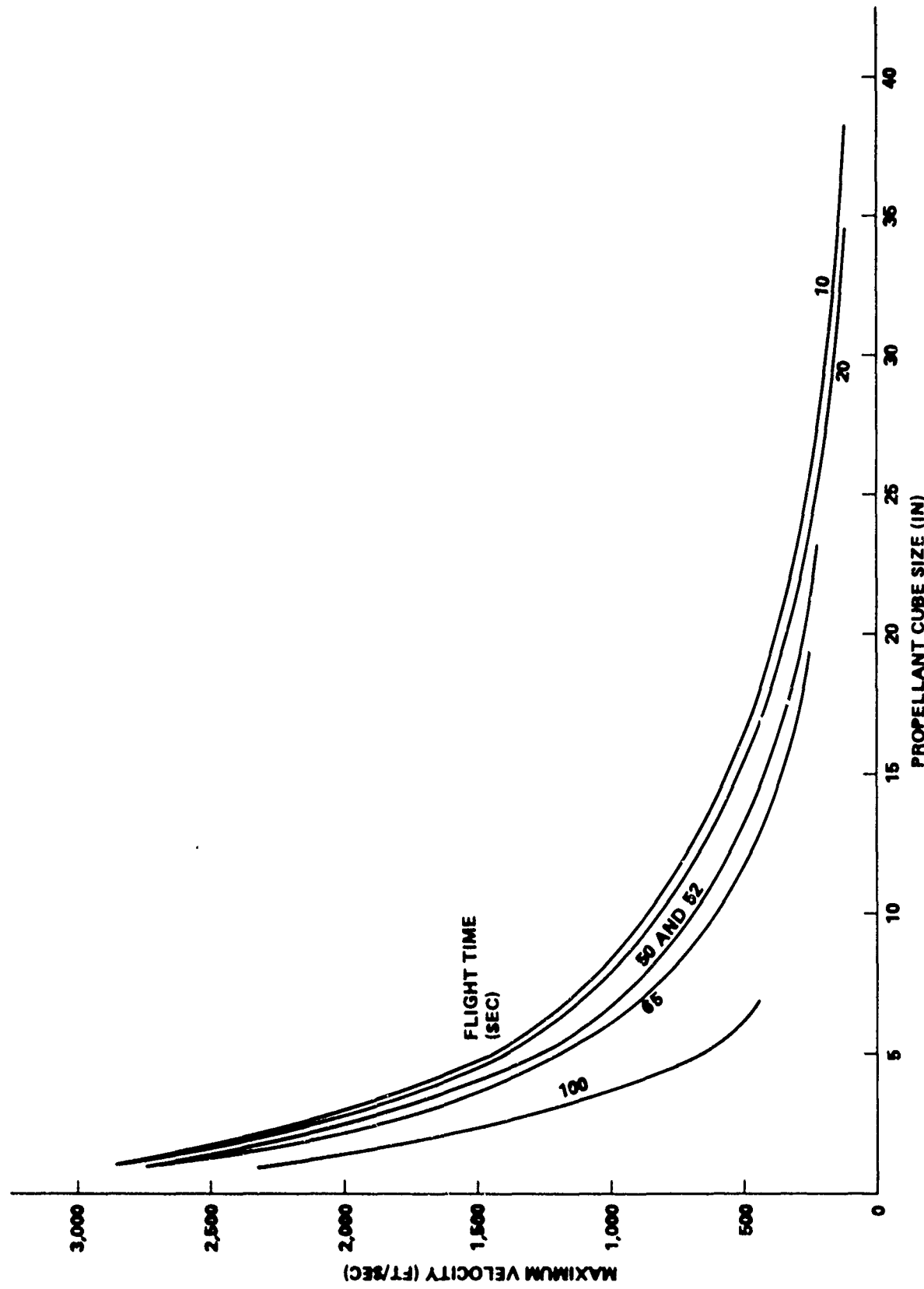


FIGURE 4-7 MAXIMUM RELATIVE VELOCITY OF PROPELLANT FRAGMENTS

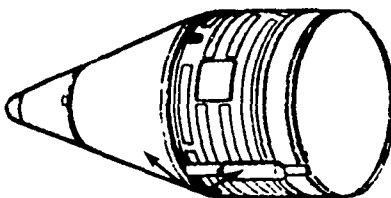


FIGURE 4-8 FORWARD FRUSTUM AND SKIRT

The aft motor case segment, aft skirt, and nozzle (Fig. 4-9) remain as one large fragment. The aft case is not cut by the LSC's and is strengthened for SRB/ET attach loads and water recovery loads. Therefore, propagation of the damage inflicted upon the other sections of the SRB into the aft section is not predicted. Similarly, the propellant in the aft case is cast as one section, independent of the propellant castings of the forward and mid-sections and, hence, fragmentation is not expected. The result is one large, heavy fragment which is accelerated in the aft direction by the internal motor pressure but resisted by the nozzle thrust. The aft SRB/ET attach struts are free to rotate at the ends and will not retard the motion of the fragment. The struts will fail at the monoball joints after a rotation of 8 degrees, creating three strut fragments (Fig. 4-10).

Explosion damage, created by any of the postulated sources presented in Chapter 3, will be minor due to the physical distance between the susceptible SRB fragments (forward frustum and aft case) and the source. The delay between the time of destruct initiation and the time of explosion is sufficient to allow the SRB fragments to move out of the severe damage region.

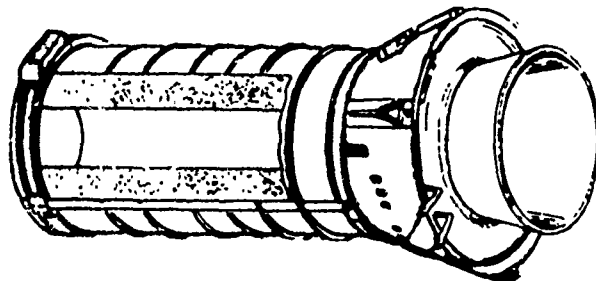


FIGURE 4-9 AFT CASE, AFT SKIRT AND NOZZLE



FIGURE 4-10 AFT SRB/ET ATTACH STRUT

ET BREAKUP

The purpose of the ET destruct system is to provide maximum dispersal of the fuel and oxidizer in the LH₂ and LOX tanks before ground impact. The ET system contains two simplex LSC's, each redundantly initiated. The LSC's are placed in the OFI cable trays along the barrel section of the LOX tank and the aft two bays of the LH₂ tank (Fig. 4-11). Upon initiation, the LSC jets cut the bottom of the cable trays and the majority of the length of the tank skin directly beneath the LSC's.

The cable tray support brackets and skin pads of the LOX tank will probably not be completely severed. However, analysis shows that the brackets and pads will fail by gross tension or crack propagation depending upon the hoop load generated by the tank pressure at any particular time. Experimental evidence suggests that the cut will not propagate through the fore and aft integral ring frames of the barrel section but will either turn or branch from the longitudinal to the circumferential direction. The crack propagates around the tank until arresting or again turning to the longitudinal direction upon encountering the superior strength of the barrel section forward of the SRB beam. The result is a hole in the LOX tank of about one quarter the circumference of the tank by the length of the barrel sections 160 ft² of skin area.

The skin is removed in two unequal sections (Fig. 4-12), due to the location of the cable tray, but the hole is centered on the +Z-axis. The skin sections are rapidly accelerated to the exit velocity of the LOX along with fragmented sections of the cable tray (Fig. 4-13), a broken length of the GO₂ pressurization line, lengths of vent valve actuation line and nose cap purge duct line, electrical wiring, brackets, slosh baffle debris, etc.

Similar response to the LSC cuts in the LH₂ tank will result in a hole in the aft bay of that tank confined by the ring frames at X_T 1871 and X_T 2058 and the longerons spanning the aft bay (Fig. 4-14). The resulting hole has a surface area of 300 ft². The extent of holing of the bay between X_T 1624 and X_T 1871 is unclear. The hoop load will propagate the cut forward to the ring frame at X_T 1624 where the crack will either turn or arrest. At early times into flight (around 10 seconds), the orbiter thrust load offsets the axial tension in the tank skin in the location of the LSC cut. No axial stress is present to propagate the crack in the circumferential direction. However, as the orbiter thrust is terminated due to the loss of oxidizer or at later times into the flight when the orbiter thrust is throttled, the bay does experience axial tension around the full circumference. While initially at 10 seconds no substantial holing is predicted, crack propagation is expected at later times. In this case, the extent of circumferential damage is difficult to predict. The forward end of the bay is of nearly uniform thickness. This presents no major obstructions to the crack movement. However, at 10-inch intervals the entire skin is longitudinally stiffened with integral T-stiffeners. It is probable that the crack, following paths of least resistance, will be caught between stiffeners and again turned to the longitudinal direction. The hole is then assumed to be on the order of the other LH₂ tank hole size or about 320 ft². Thus, sometime after 10 seconds, a total of 620 ft² of LH₂ tank skin is removed. Complete severing of this bay will not alter the fragment predictions for the ET but will influence the predictions for the orbiter.

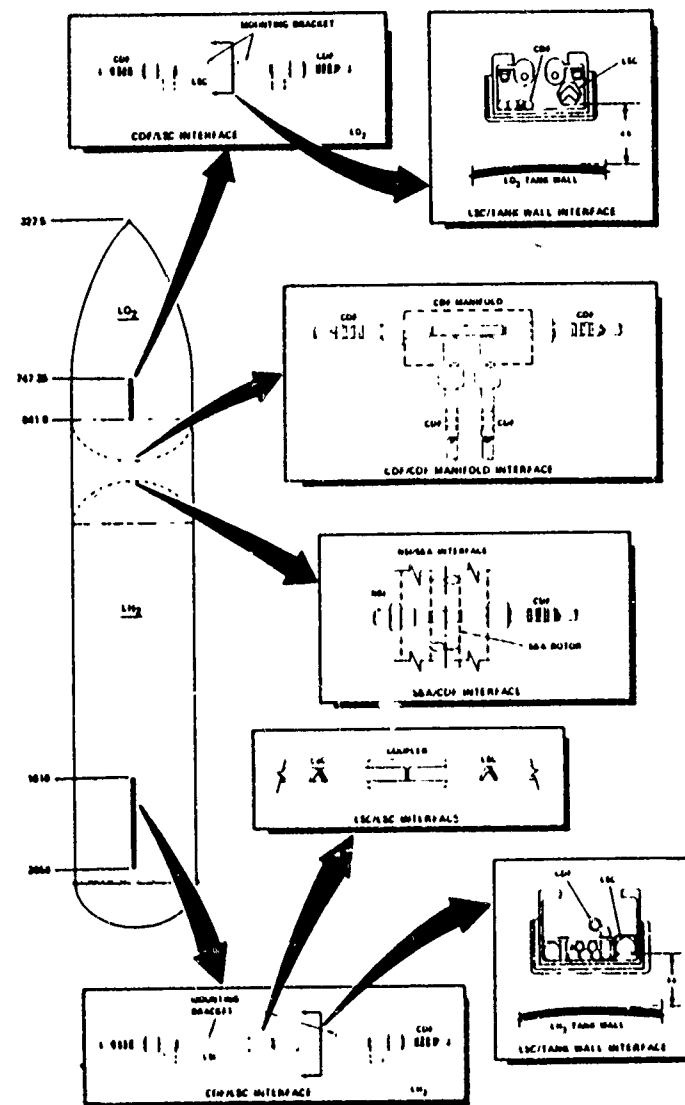


FIGURE 4-11 ET COMMAND DESTRUCT SYSTEM

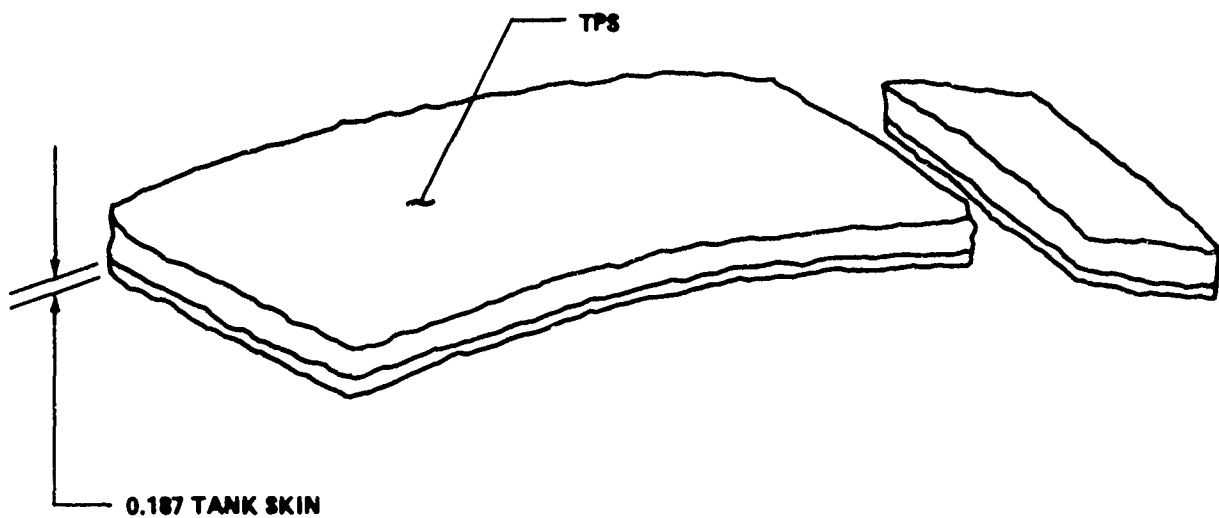


FIGURE 4-12 ET SKIN FRAGMENTS

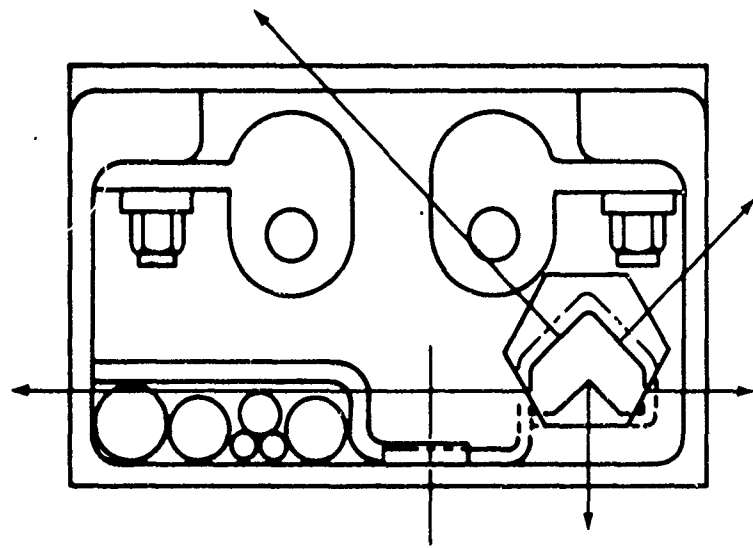
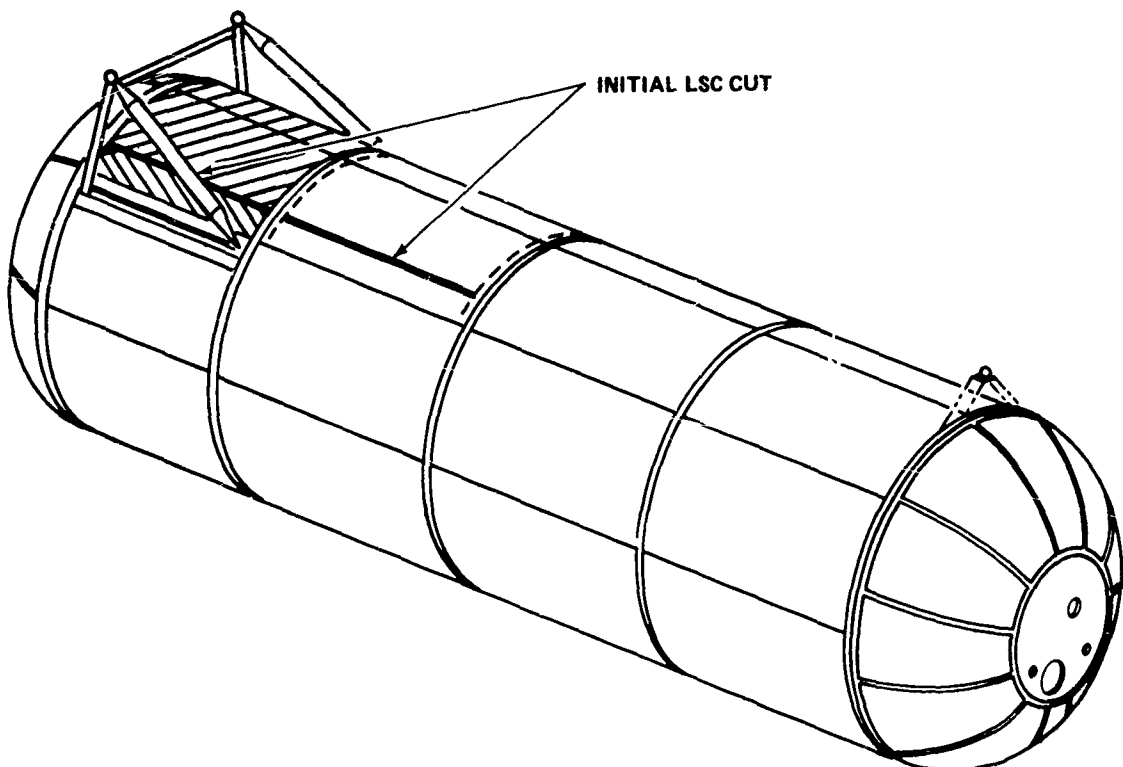


FIGURE 4-13 FRAGMENTATION OF CABLE TRAY

FIGURE 4-14 INITIAL HOLING OF LH₂ TANK

The outflow of LH₂ will break off sections of the LOX feed line, LOX pressurization line, LH₂ pressurization line, and additional sections of the cable tray. All of the structural fragments from the LH₂ tank will be caught in the flow and rapidly accelerated to the velocity of the LH₂ jet.

High lateral thrust loads are created by the LOX and LH₂ jets. These loads do not induce bending moments in the ET structure of sufficient magnitude to fail the undamaged portions. However, the barrel section of the LOX tank and the 3rd bay of the LH₂ tank, weakened by the loss of skin, are hinged. The lateral thrust, inertia, and aero loads eventually cause separation of the ET into three major segments (Fig. 4-15). As the LOX tank barrel section separates, additional debris fragments are produced from further breakage of the slosh baffles.

SRB breakup will not materially affect breaking of the ET. SRB clevis joint failures will relieve the transfer of thrust loads to the fore and aft attach points and preclude SRB beam or ring frame X_T 2058 failures. Venting of the SRB is directed outboard by the clamshell and eliminates any substantial overpressure on the ET. Impact of the SRM case segments on the LH₂ tank will be the primary interactive mechanism. However, holing is not expected since the contact area is large and the impact will be oblique.

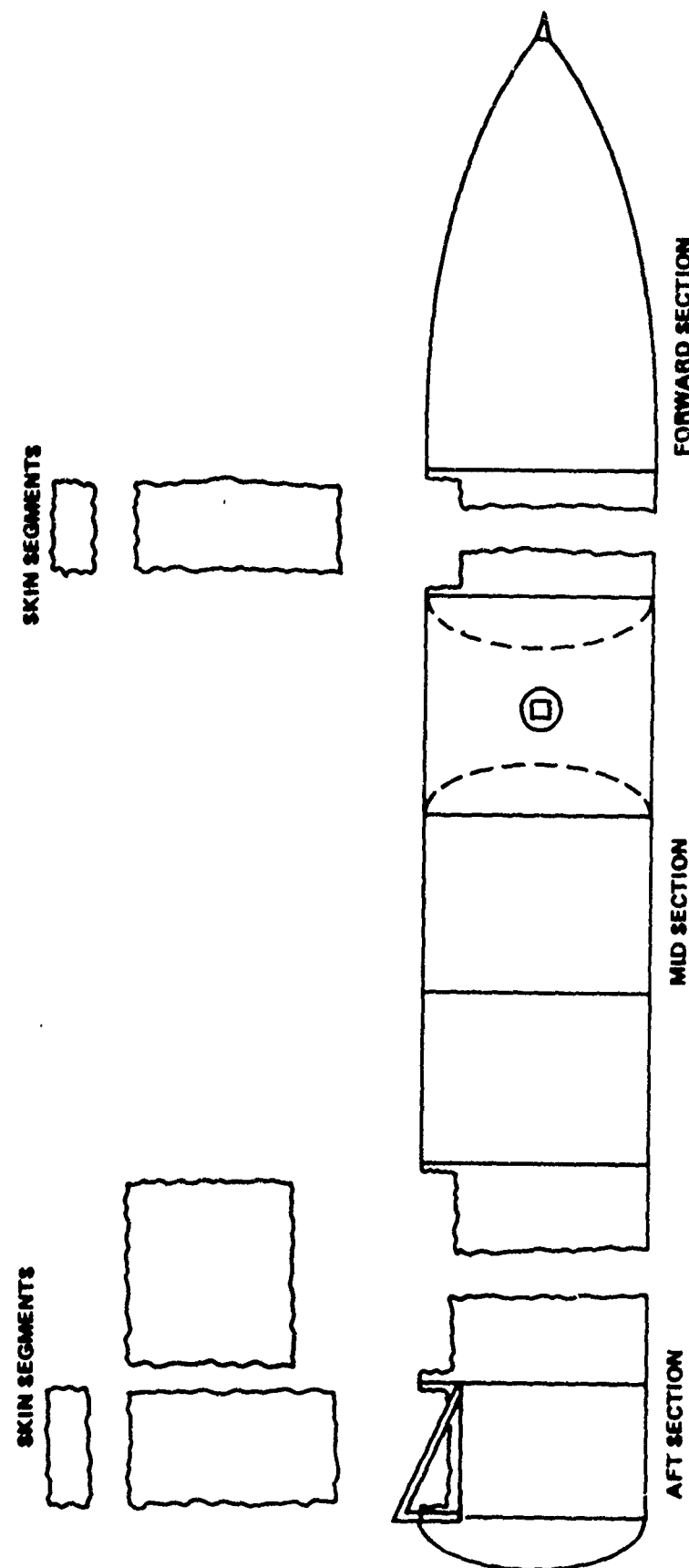


FIGURE 4-15 MAJOR ET FRAGMENTS

Blast effects on the ET are modest when the orbiter is not attached to the tank. The LOX and LH₂ jets propagate large distances before mixing. The resulting explosion, created by auto-ignition or firebrands, is sufficiently distant to preclude further break up. However, when present, the orbiter blocks the LH₂ jet, spreading it in all lateral directions. The aerodynamic flow is not sufficient to prevent the LH₂ from moving forward under the orbiter and mixing with the LOX jet. Auto-ignition occurs when enough fluids have mixed to create an explosion equivalent to 7,400 pounds of TNT. Because of proximity to the ET, the resulting pressure on the LOX tank and the intertank (IT) is extremely high. The structure, however, can absorb the energy of an external explosion through compaction of the TPS foam and large plastic deformation of the aluminum. Substantial damage may be incurred, but no major additional breakup will evolve.

ORBITER BREAKUP

Breakup of the orbiter occurs from two sources, the LH₂ jet impact on the underside of the fuselage and the LOX/LH₂ explosion just forward of the orbiter nose (Fig. 4-16).

The LH₂ jet impacts with a velocity that produces a total pressure of from 18 to 33 psi. This pressure will not catastrophically hole the underside of the fuselage but will result in plastic deformation of the skin panels, loss of some bending moment capability, and removal of thermal protection tiles. The total load will cause breaking of the orbiter/ET attach joints, hinging of the fuselage in the mid-cargo bay area, cargo bay door separation, and TPS tile removal.

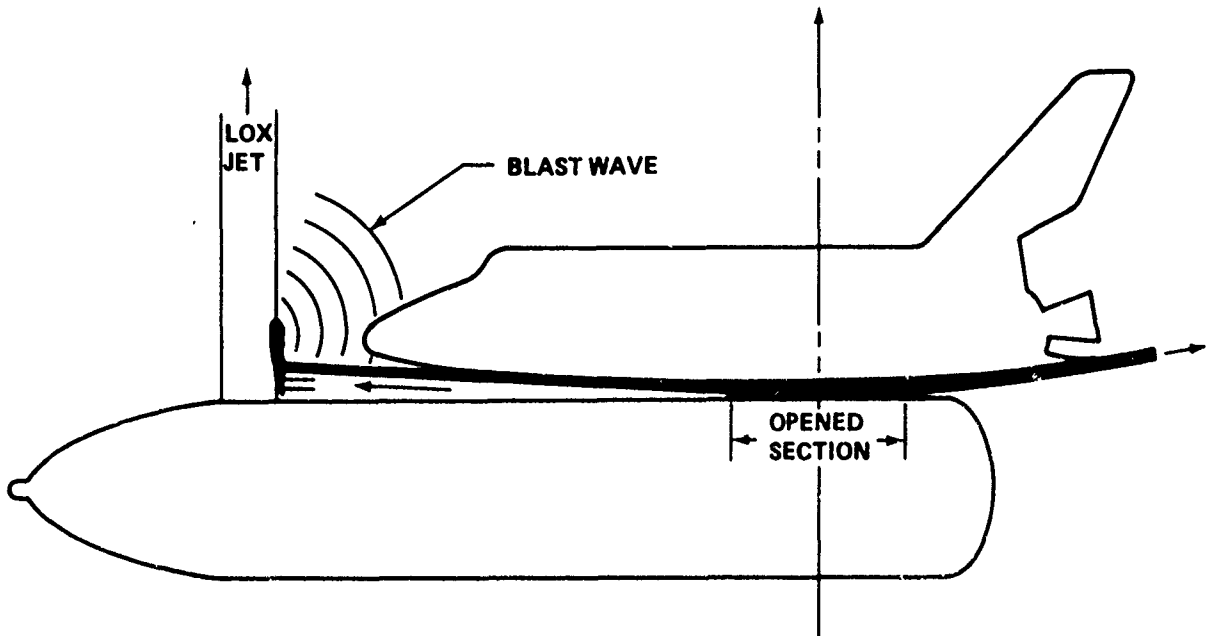


FIGURE 4-16 BLAST LOADING ON ORBITER

The explosion will precipitate extensive breakup of the nose portion of the orbiter ahead of the crew module (Fig. 4-17). The resulting debris consists of skin segments, thermal protection tiles, structural beams, frames, and trusses; reaction control system (RCS) nozzles, pressure tanks, fuel tanks, and piping; and landing gear structure, operating equipment and doors. The remaining forward fuselage will collapse on the crew module, absorbing the blast energy in so doing. Windows will be blown in, but the crew section will remain essentially intact.

Orbiter response to SRB breakup will be modest. The venting of the SRB is directed outboard, precluding high-pressure loads on the undersides of the wings. Impacting propellant and SRM case fragments will cause only local damage.

DEBRIS FRAGMENTS

Listings of the debris fragments are presented in table and chart form in Appendices A through C. These tables and charts were grouped separately for the SRB's, and ET, and the orbiter, with Appendix A covering the SRB's, Appendix B the ET, and Appendix C the orbiter.

In most cases, the fragments will tumble and no lift coefficient is presented. However, two SRB fragments and one orbiter fragment assume trim attitudes that produce negligible lift. Three ET fragments develop lift over some range of Mach number. The C_D and C_L are defined as

$$C_D = F / \left(\frac{1}{2} \rho V^2 A \right)$$

$$C_L = F / \left(\frac{1}{2} \rho V^2 A \right)$$

where F_D and F_L are the drag and lift forces respectively, ρ is the ambient atmospheric density, A is the fragment reference area, and V is the fragment velocity.

The range of ballistic coefficient ($W/C_D A$) given for each fragment in the tables is a result of the variation of drag coefficient with Mach number. For those fragments having a range of sizes and weights (i.e., SRB propellant cubes), the range of ballistic coefficient also reflects a variation of weight/area.

Since the scope of the work presented here does not include predicting the trajectories of the fragments, no attempt has been made to ascertain the terminal velocities. Therefore, the full range of ballistic coefficient is given in each table for destruct at any time. However, the actual range of ballistic coefficient for any particular fragment produced at any given destruct time may be considerably reduced for limited variations in Mach number as evidenced in the plots of drag coefficient.

Note that the lists of debris fragments are essentially the same for both nominal and aberrant flight conditions at all times during the ascent phase. The main exception lies in the number, size and weight of SRM propellant fragments. This commonality exists because the breakup mechanisms are dominated by the internal pressures and lateral thrust loads imposed by the venting of the SRM, LOX tank, and LH₂ tank. The effects of aerodynamic, inertia, and body forces are seen predominantly in the velocities (ΔV) imparted to the fragments.

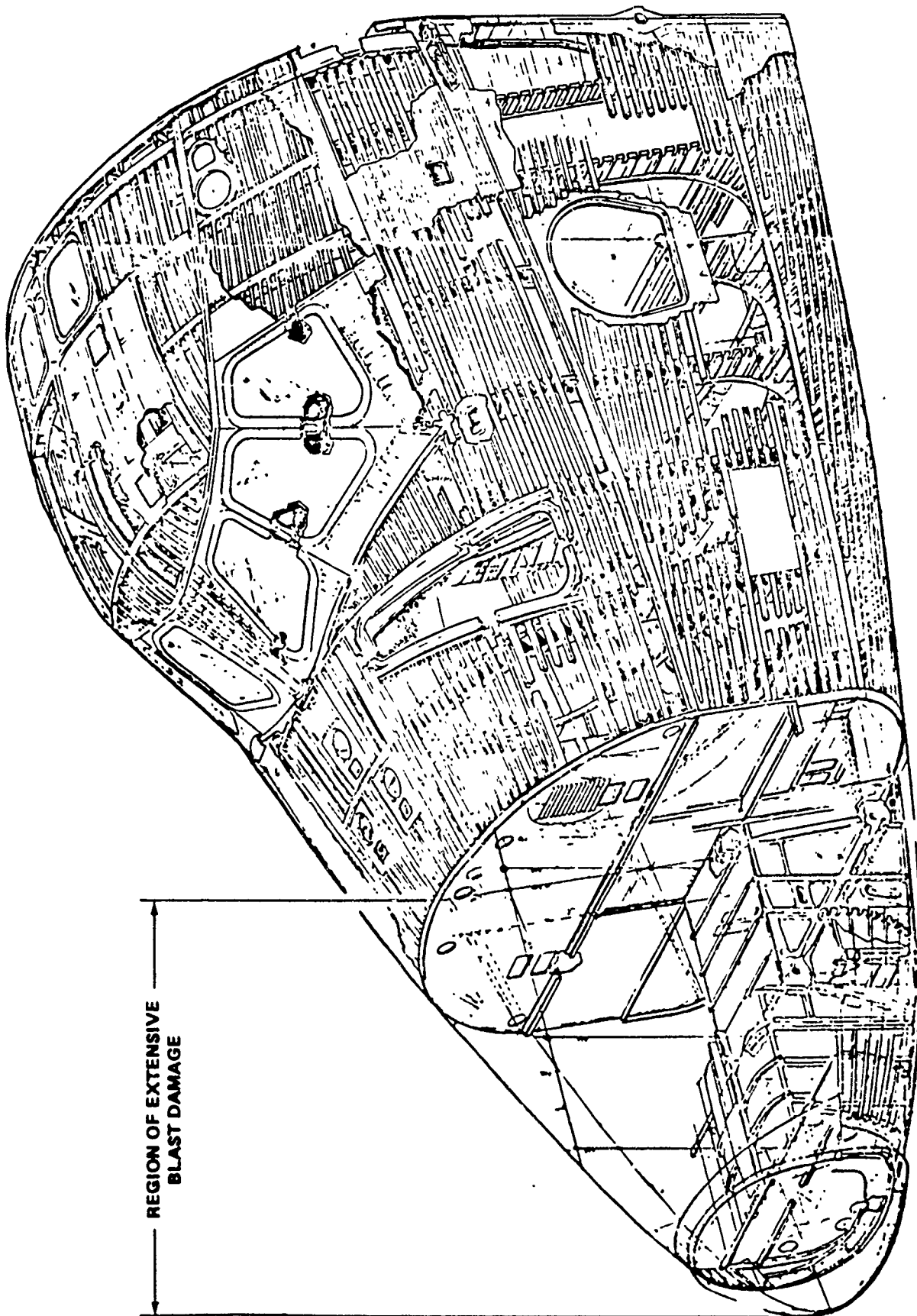


FIGURE 4-17 FORWARD FUSELAGE STRUCTURE

The velocity ΔV is defined here as the vector change in velocity due to the destruct action. The total velocity is the vector sum of the velocity V existing prior to destruct action and ΔV . The velocity V , angle of attack, and angle of sideslip are given in Table 4-1 for both nominal and aberrant flight. In some instances, particularly during the high-Q boost period of aberrant flight, these parameters change rapidly with time (Figs. 4-18 to 4-24). In such cases, those fragments achieving ΔV 's of significant magnitude compared to V will experience changes in their total velocity vectors with small changes in Δt , the time interval between inadvertent separation of the SRB or orbiter and initiation of destruct action. The Δt 's used here were selected by the criteria presented in Chapter 1 and do not necessarily maximize velocities or footprints.

The ΔV 's of a number of selected fragments are plotted in Figure 4-25 with respect to destruct action time. For most fragments the ΔV 's can be interpolated between successive times with reasonable confidence, regardless of nominal or aberrant conditions. Exceptions include, for example, the major ET tank fragments for which aerodynamic forces due to pitch and sideslip play a significant role.

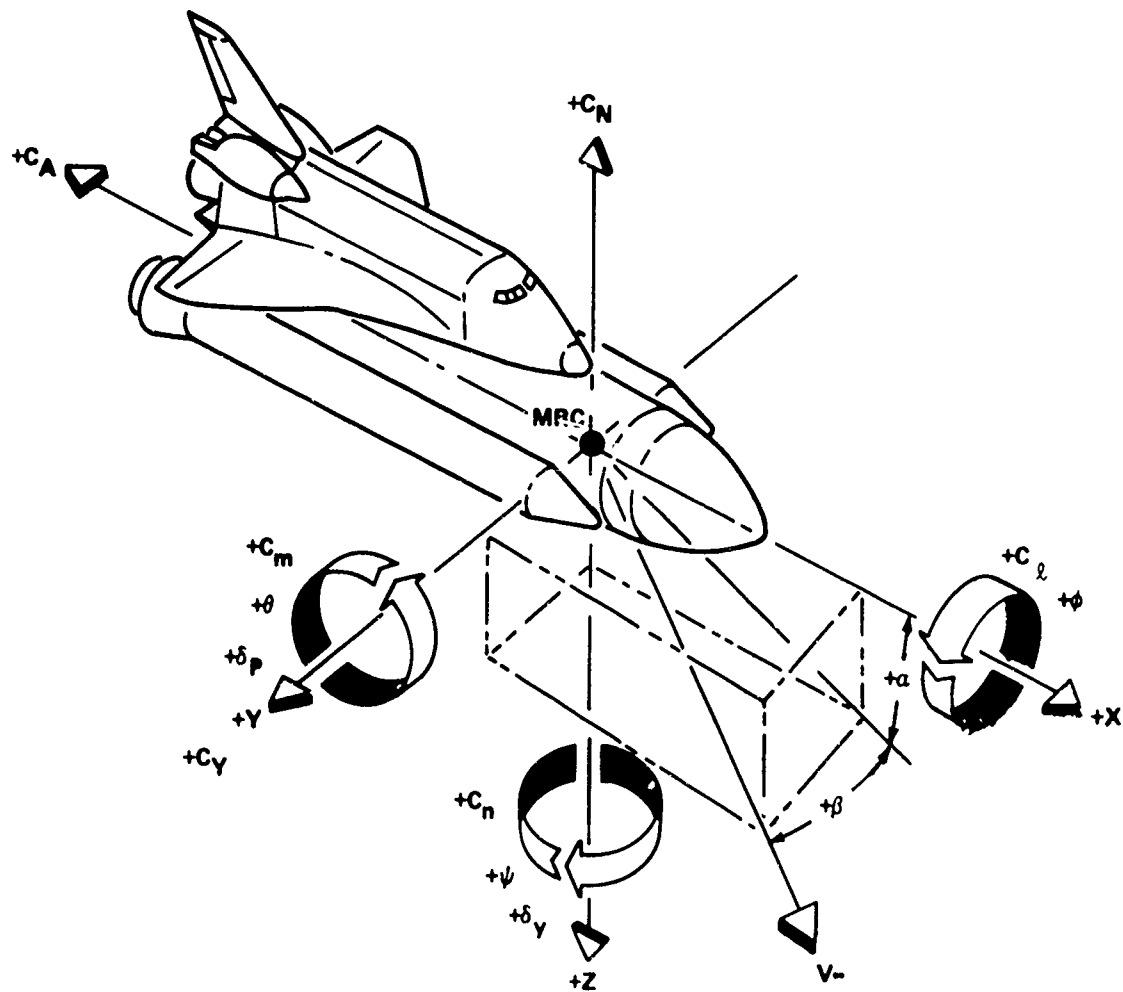
TABLE 4-1 VELOCITY, ANGLE OF ATTACK, AND ANGLE OF SIDESLIP AT DESTRUCT ACTION TIME FOR SELECTED TIMES

Case	Time (sec)	Velocity (fps)	Angle of Attack (deg)	Angle of Slip (deg)
Nominal	10	180	6.5	0
	50	1,070	-3.5	0
	100	3,200	0.5	0
	350	13,800	0.0	0
	450	22,100	0.0	0
One SRB Lost	20	300/710*	10.0	-10
	52	1,070/1,160*	9.0	-7
	115	3,700/4,900*	30.0	-11
Orbiter Lost	20	360	4.0	11
	65	1,300	28.0	54
	115	4,000	-10.0	-18

*Free SRB Velocity.

RELOCATION OF LH₂ TANK LSC

The original destruct system chosen for the LH₂ tank and analyzed by NSWC/WOL consisted of a 20-foot linear-shaped charge (LSC) placed in the cable tray and centered at the XT 1871 ring frame. This system produces 10-foot longitudinal cuts in the 3rd and 4th bays of the LH₂ tank which propagate axially and circumferentially under a combined hoop and axial tensile stress state to form vent holes for the LH₂. However, at early times during ascent,



NOTE: VEHICLE ATTITUDE IS "TAIL-DOWN"
DURING ASCENT.

FIGURE 4-18 ASCENT VEHICLE AXIS SYSTEM

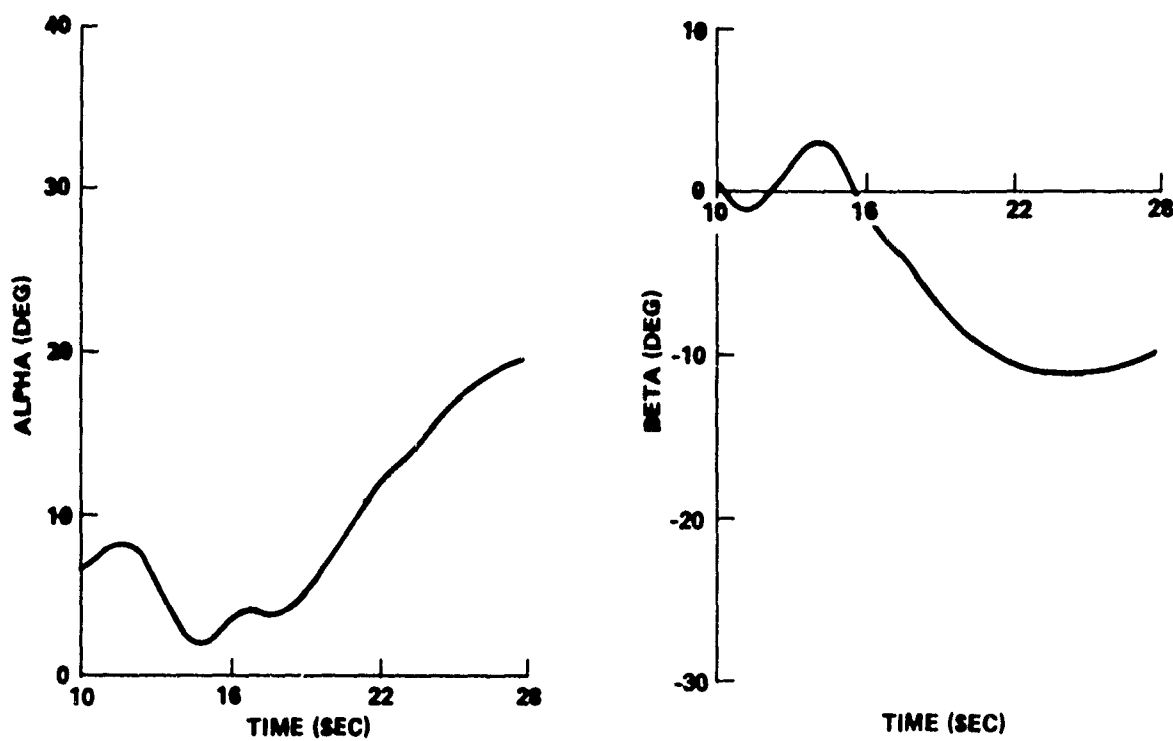


FIGURE 4-19 ASCENT TRAJECTORY PARAMETERS FOR INTEGRATED VEHICLE WITH INADVERTENT RIGHT SRB SEPARATION 10 SECONDS AFTER LIFT-OFF

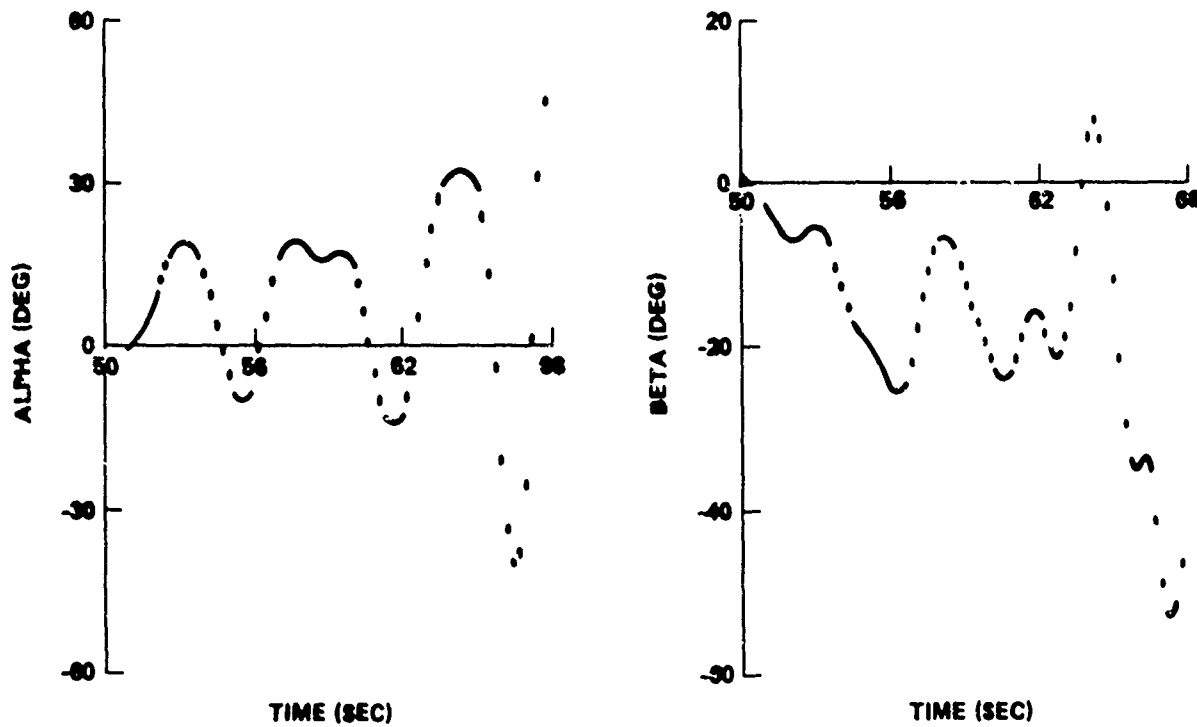


FIGURE 4-20 ASCENT TRAJECTORY PARAMETERS FOR INTEGRATED VEHICLE WITH INADVERTENT RIGHT SRB SEPARATION 50 SECONDS AFTER LIFT-OFF

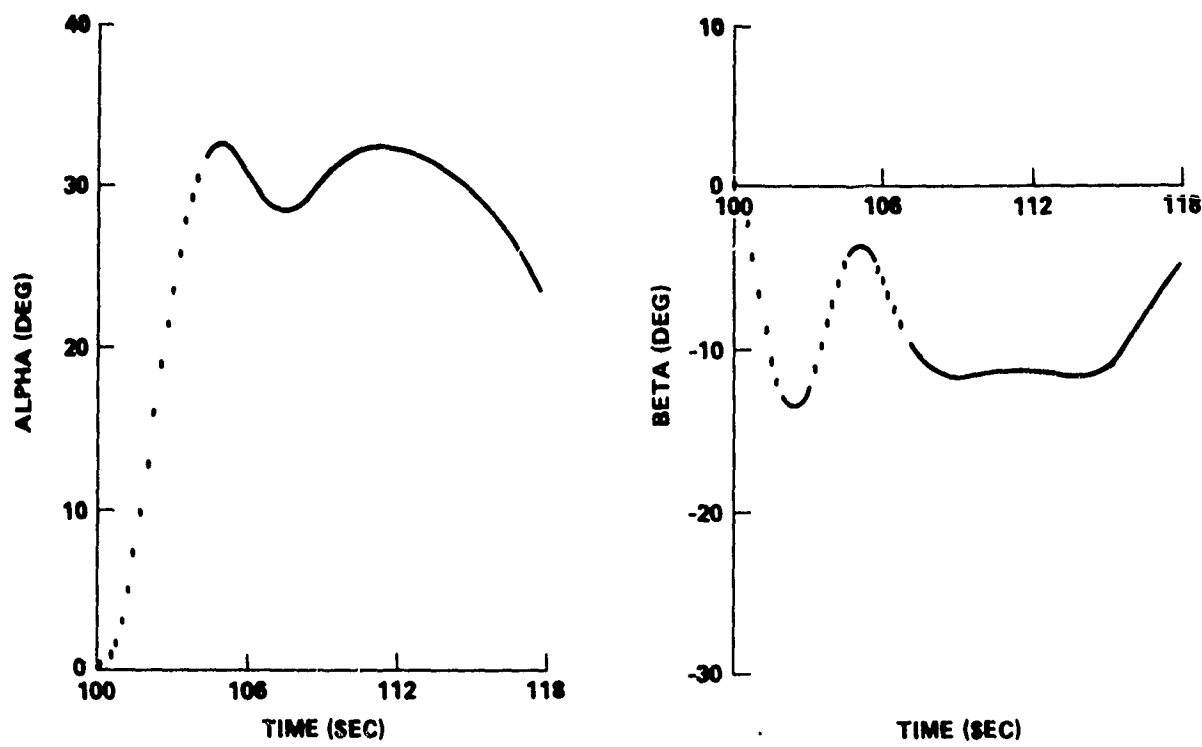


FIGURE 4-21 ASCENT TRAJECTORY PARAMETERS FOR INTEGRATED VEHICLE WITH INADVERTENT
RIGHT SRB SEPARATION 100 SECONDS AFTER LIFT-OFF

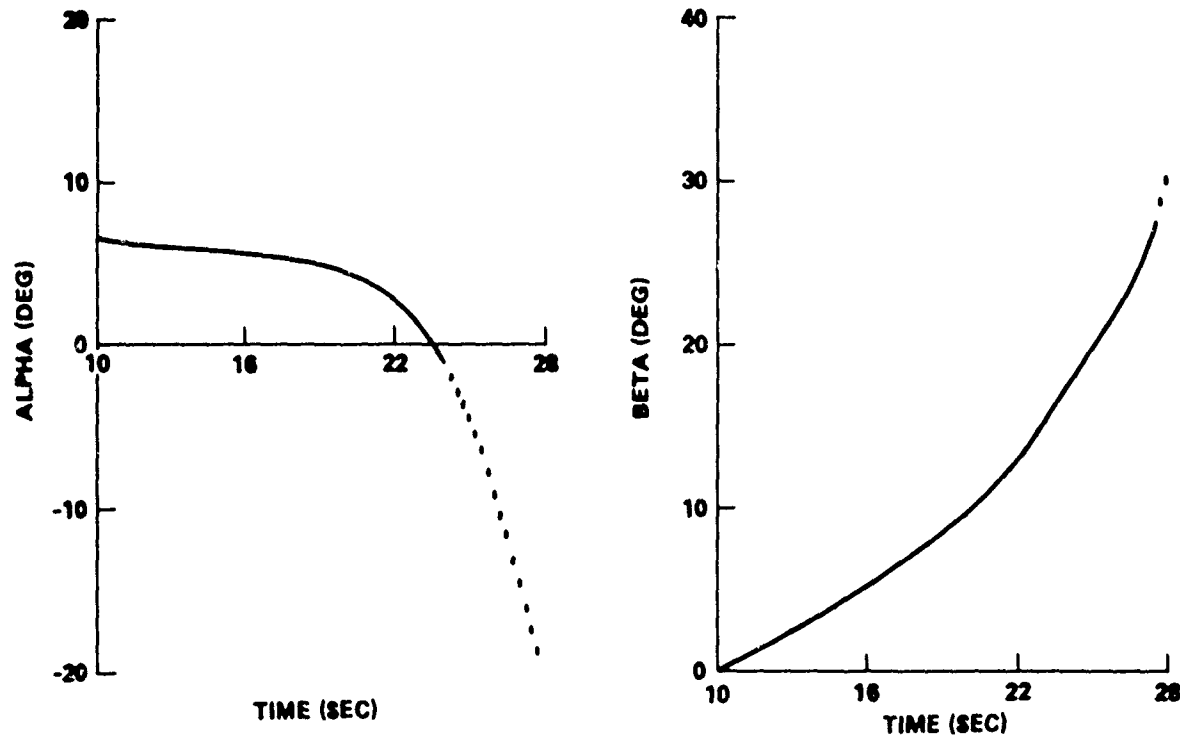


FIGURE 4-22 ASCENT TRAJECTORY PARAMETERS FOR INTEGRATED VEHICLE WITH INADVERTENT
ORBITER SEPARATION 10 SECONDS AFTER LIFT-OFF

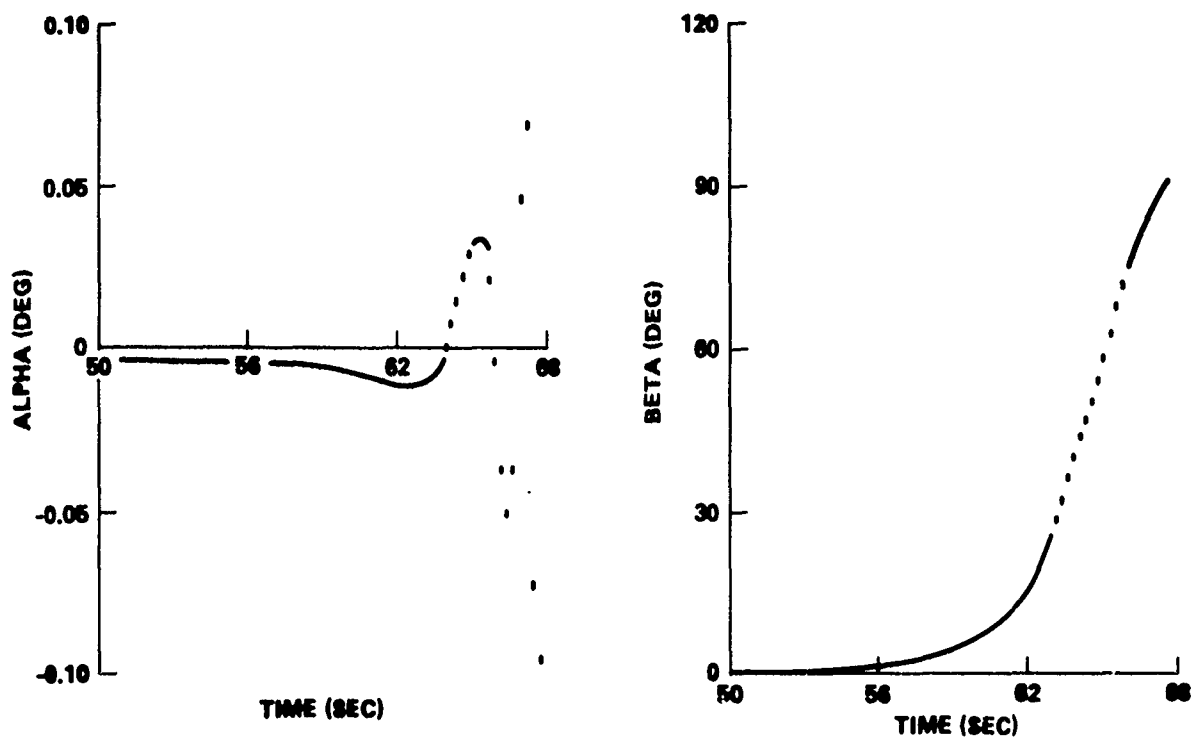


FIGURE 4-23 ASCENT TRAJECTORY PARAMETERS FOR INTEGRATED VEHICLE WITH INADVERTENT ORBITER SEPARATION 50 SECONDS AFTER LIFT-OFF

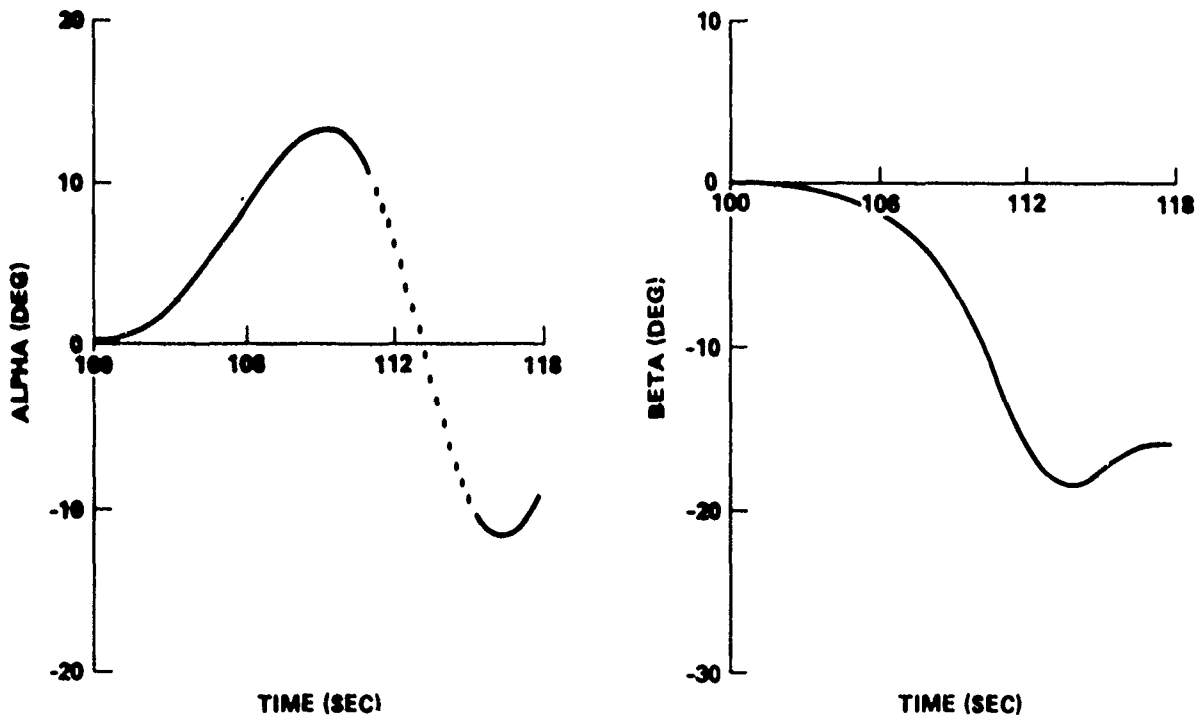


FIGURE 4-24 ASCENT TRAJECTORY PARAMETERS FOR INTEGRATED VEHICLE WITH INADVERTENT ORBITER SEPARATION 100 SECONDS AFTER LIFT-OFF

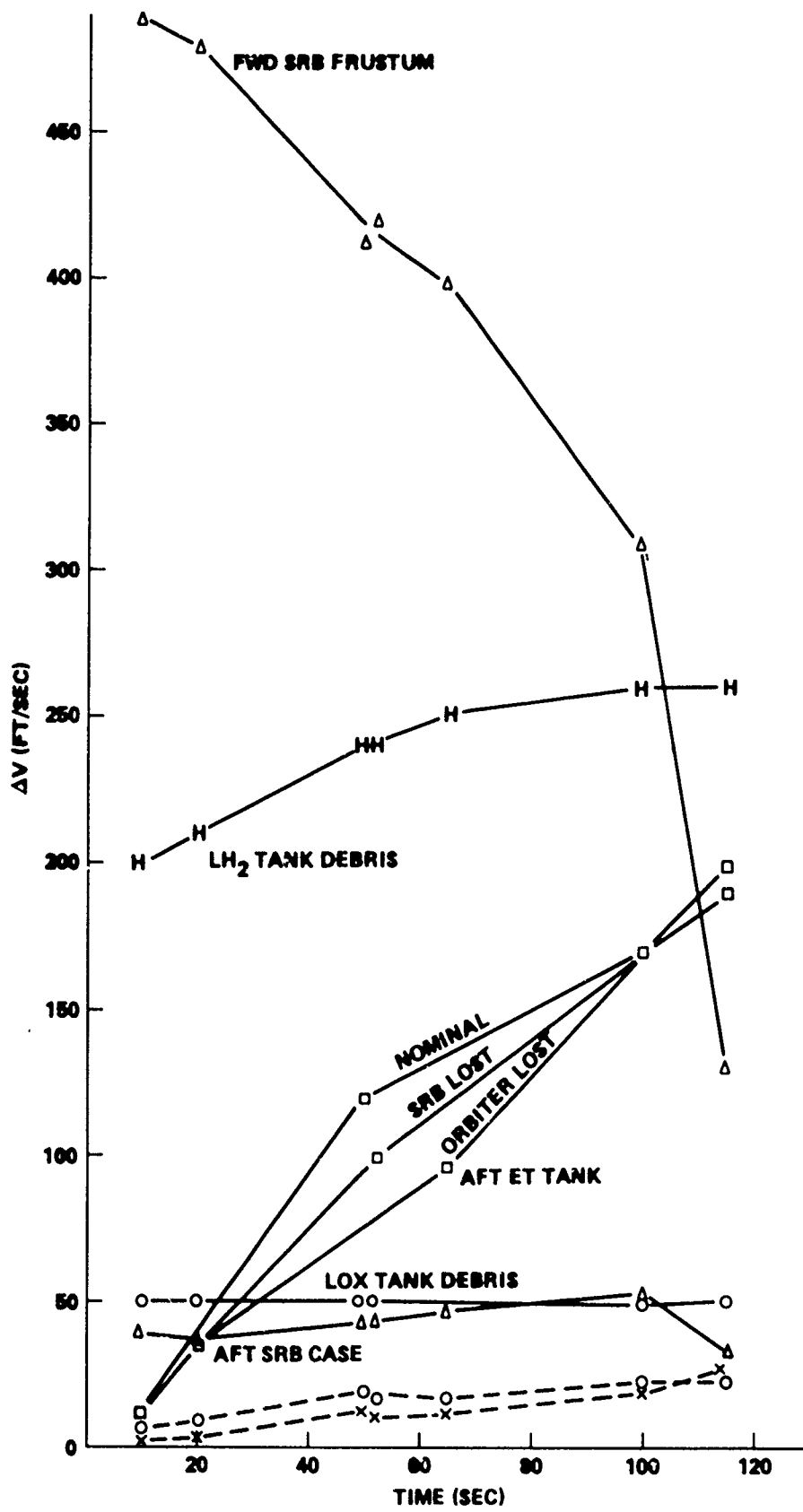


FIGURE 4-25 ΔV VS. DESTRUCT ACTION TIME FOR SELECTED FRAGMENTS

the thrust load of the orbiter subjects the LH₂ tank skin in the vicinity of the 3rd bay cable tray to a slight axial compressive load. Termination of orbiter thrust prior to destruct action would eliminate this condition. But for this analysis, it will be assumed the thrust persists at the instant of LSC initiation. Since the rationale for holing was predicated on preflawed pressure vessel test observations under a biaxial tension-tension stress state, branching or turning of a longitudinal crack at the X_T 1624 and X_T 1871 ring frames under a stress state of hoop tension and axial compression cannot be assured. However, local axial stresses at the tip of the crack will be tensile in all cases suggesting the possibility of circumferential extension regardless of general axial stress state.

Due to the high heating environment for the cable tray along the aft bay during reentry, elimination of the LSC from that area is necessary to minimize the weight penalty imposed by insulation requirements. External tank (ET) response to an optional LSC destruct system for the LH₂ tank has been studied and is presented here. The system consists of a 10-foot LSC centered at X_T 1624 and spanning 5 feet of each of the 2nd and 3rd bays (Fig. 4-26).

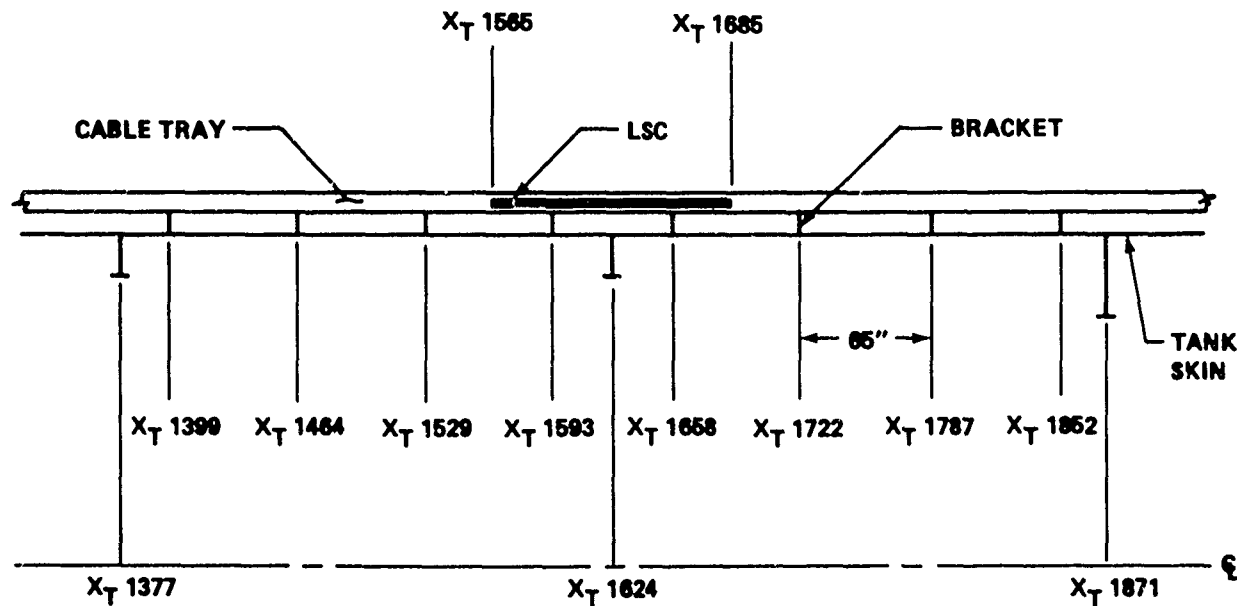


FIGURE 4-26 10-FT INSTALLATION SPANNING RING FRAME X_T 1624

Figure 4-26 illustrates placement of the LSC and locations of the cable tray brackets along the 2nd and 3rd bays. Design changes in the LSC and brackets now suggest that complete severance of the brackets will occur, but skin ligaments under the brackets will still remain. With orbiter thrusting, the ΔP across the tank wall will be in excess of 15 psi. A ΔP of 15 psi gives a gross ligament stress of

$$\sigma = \frac{F}{A} = \frac{\Delta P R (2C_1)}{A} = 139,000 \text{ psi}$$

where $A = 0.5 \text{ in}^2$ (ligament stress area for 0.143-inch wall thickness), $R = 165 \text{ in}$ (tank radius), and $2C_1 = 28 \text{ in}$ (length of each of four cuts in skin, separated by skin ligaments at cable tray brackets and X_T 1624 ring frame). This is significantly above the 95,000 psi ultimate strength of the 2219-T87 aluminum at LH_2 temperature. Ligament failure will occur by gross yielding, producing two 60-inch cracks separated by the ring frame at X_T 1624.

Hahn, et al give the critical loop stress for crack extension in thin-walled cylindrical pressure vessels ($R/t > 50$) with long cracks as:¹

$$\sigma_h^* = \frac{K_c}{(\pi C \phi_3)^{1/2}} \left[1 + 1.61 \frac{C^2}{R^2} \left(50 \tanh \frac{R}{50t} \right) \right]^{-1/2}$$

where

$$\begin{aligned}\phi_3 &= 1.0 (\sigma^* \ll \sigma_0) \\ 2C &= 2C_2 = \text{crack length (60 in)} \\ R &= \text{vessel radius (165 in)} \\ t &= \text{wall thickness (0.143 in)}\end{aligned}$$

For $K_c = 110 \text{ ksi} \sqrt{\text{in}}$ (maximum stress intensity factor for 2219-T87 aluminum) the above equation gives the critical hoop stress as

$$\sigma_h^* = 5900 \text{ psi}$$

The ΔP across the tank wall required to generate this stress is

$$\Delta P^* = \frac{\sigma_h^*}{R/t} = 5 \text{ psi}$$

At a ΔP of 15 psi, the cracks will easily propagate longitudinally to the forward end of the 2nd bay and the aft end of the 3rd bay producing two 20-foot cuts.

Recent tests have shown that the LSC will cut a total of about 1/2-inch of aluminum in the cable tray installation; 0.125-inch cable tray bottom plus more than 0.340-inch of tank wall. While this is not sufficient to completely sever the outer chord of the ring frame at X_T 1624 (Fig. 4-27), the remaining cross sectional area of the web and chords is less than 3.025 in^2 . For conservatism, consider a cut of 0.340-inch in the tank wall. The stress on the uncut section is

¹Hahn, G. T., Sarrate, H., and Rosenfield, A. R., "Criteria for Crack Extension in Cylindrical Pressure Vessels," Journal of Fracture Mechanics, Vol. 5, No. 3, 1969, p. 187.

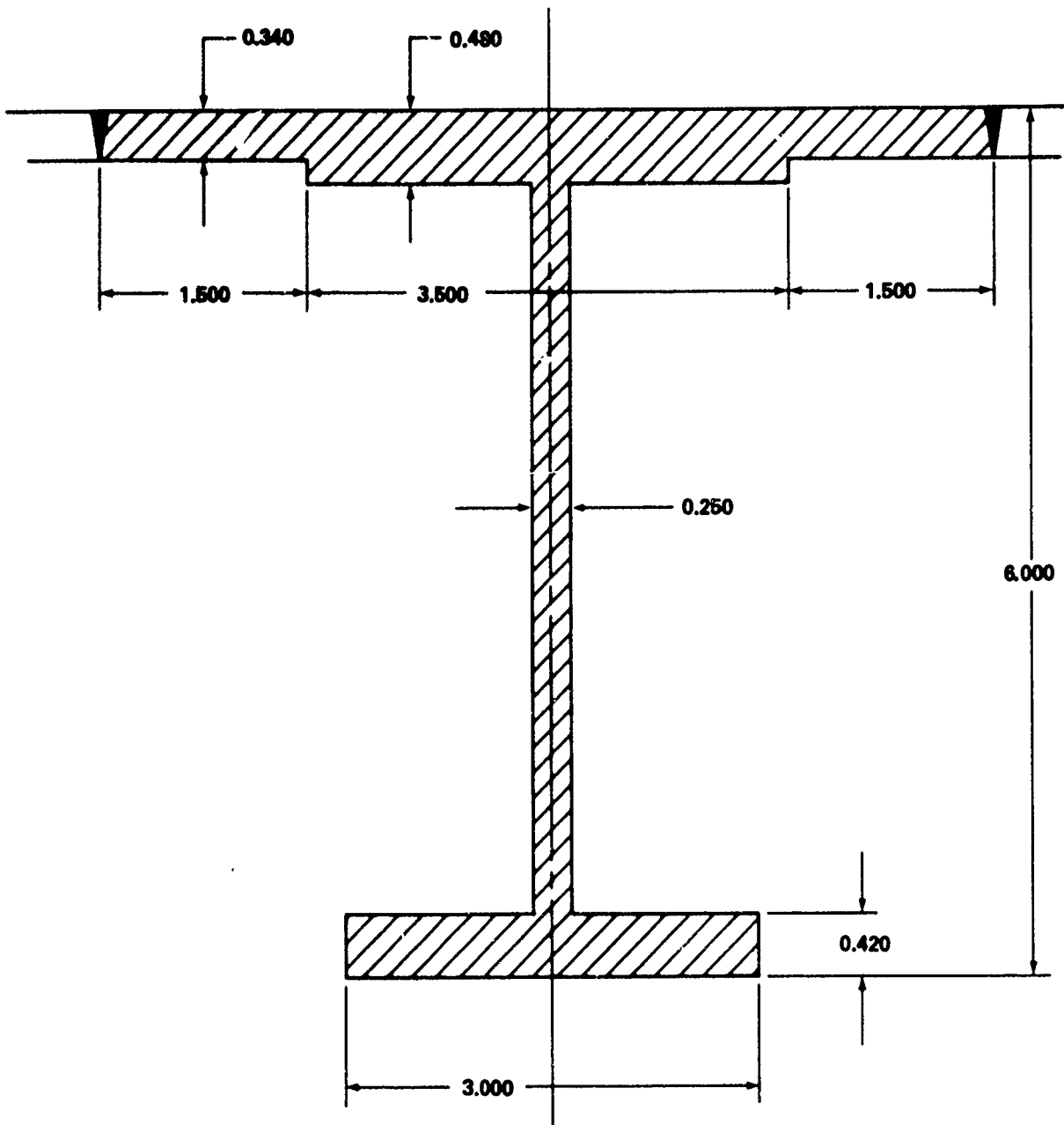


FIGURE 4-27 X_T 1624 FRAME CROSS SECTION AT LSC

$$\sigma = \frac{F}{A} = \frac{\Delta P R (2C_3)}{A} = 196,000 \text{ psi}$$

where $2C_3$ is now 240 inches. This is >2 times the ultimate strength of the frame material. Complete rupture of the frame will occur by gross yielding resulting in one continuous 40-foot cut extending from X_T 1377 to X_T 1871.

Of course, the failure and subsequent response of the frame is predicated on the assumption that the shear strength of the skin/frame intersection is sufficient to transfer the pressure load to the frame. The circumferential running load is

$$N = \Delta PC = 15 (120) = 1800 \text{ lb/in}$$

The shear stress then becomes

$$T = \frac{N}{t} = \frac{1800}{0.143} = 12,600 \text{ psi}$$

Assuming the shear strength of the 2219-T87 aluminum is one-half of the ultimate tensile strength yields a shear strength of about 47,000 psi. The load will be transferred to the frame.

The previous section established the length of continuous crack formed in the LH₂ tank wall. The next step is to predict the hole size formed by gross deformation of the severed skin and frame. The pressure load will apply a bending moment to the frame and skin and will unroll them if the bending moment exceeds the fully plastic bending moment of the severed structure. The skin has very low bending stiffness and will not contribute significantly to the stiffness of the structure around X_T 1624. Therefore, the X_T 1624 frame must carry the total bending moment. While the frame cross section varies with circumferential position, a good average value for the fully plastic bending moment of the section is about 500,000 in-lb.

Consider a short section of the frame, bounded on one end by the cut and fixed at the other end; that is, a cantilever beam having the cross sectional properties of the ring frame. At what distance from the free end will the fully plastic bending moment be exceeded? The applied moment is given by

$$M = (NL)(L/2)$$

when N is the running load and L is the distance from the free end. Equating the applied moment to the fully plastic bending moment yields

$$M_p = NL^2/2$$

Solving for L gives

$$L = \sqrt{\frac{2M}{P}} \quad N$$

The running load is now twice that used in the shear calculation since the frame is loaded by the skin on both sides. L then becomes

$$L = 17 \text{ in}$$

All sections of the frame at distances greater than 17 inches from the cut would see a bending moment greater than the fully plastic moment if the load remained constant. In reality, the load decays rapidly with time and the frame portals open, coming to rest when the driving force falls below the resistance. The hole formed is illustrated in Figure 4-28. It has an area of about 500 feet. The corresponding vent times are given below.

Flight Time (sec)	T (90%) (sec)	T (Stop) (sec)	F (Stop) (sec)
10	0.62	1.83	0.31

The escaping LOX and LH₂ form lateral jets centered at X_T 795 and X_T 1624, respectively. Initial thrust loads are high but decay with time. In the case considered here, the orbiter remains attached to the ET at the time of destruct action and the LH₂ jet impinges on the underside of the orbiter. A dynamic analysis of the response of the orbiter to the LH₂ jet formed using the original destruct system predicted failure of the forward orbiter/ET attach structure within 35 msec of destruct action. The optional system presented here will impose higher loads on the orbiter and locate them closer to the forward attach point. Failure of the forward attach point will not occur in less elapsed time.

Failure of the forward orbiter/ET attach point permits rotation of the orbiter about the aft attach points. However, rotations in excess of 3.5 degrees will fail the separation bolts and free the orbiter. Hence, the initial structure to consider is that of the ET, hinged at the two hole locations, and coupled to the orbiter at the aft attach point only. A dynamic analysis, tracking the motion of the various connected links, and incorporating the thrust-time and mass-time properties of the fluids, predicts relative orbiter to ET rotation of 3.5 degrees in 0.2 second.

The subsequent response of the ET is predicted via a three-link model. Complete failure of the tank at a hinge is assumed to occur when rotations bring the ends of the hole into contact and place the skin diametrically opposite the hole into tension. The failure criteria are 0.3 radians and 1.7 radians for the LOX and LH₂ tanks, respectively. Failure of the LH₂ tank at X_T 1624 is predicted first, occurring 2.7 seconds after destruct action. Failure of the LOX tank occurs immediately thereafter, at 2.9 seconds after destruct action. Hence, the ET breaks into three sections within 3 seconds of destruct action, if destruct action is initiated at 10 seconds after lift-off.

The optional LSC destruct system considered here is at least equivalent to the original system in terms of rapid dispersal of fluids. The LOX is expelled at the same rate with either the original system or the optional system. The LH₂ is expelled more rapidly with the optional system. The fragments formed during breakup of the ET are the same as those predicted for the original placement of the LSC.

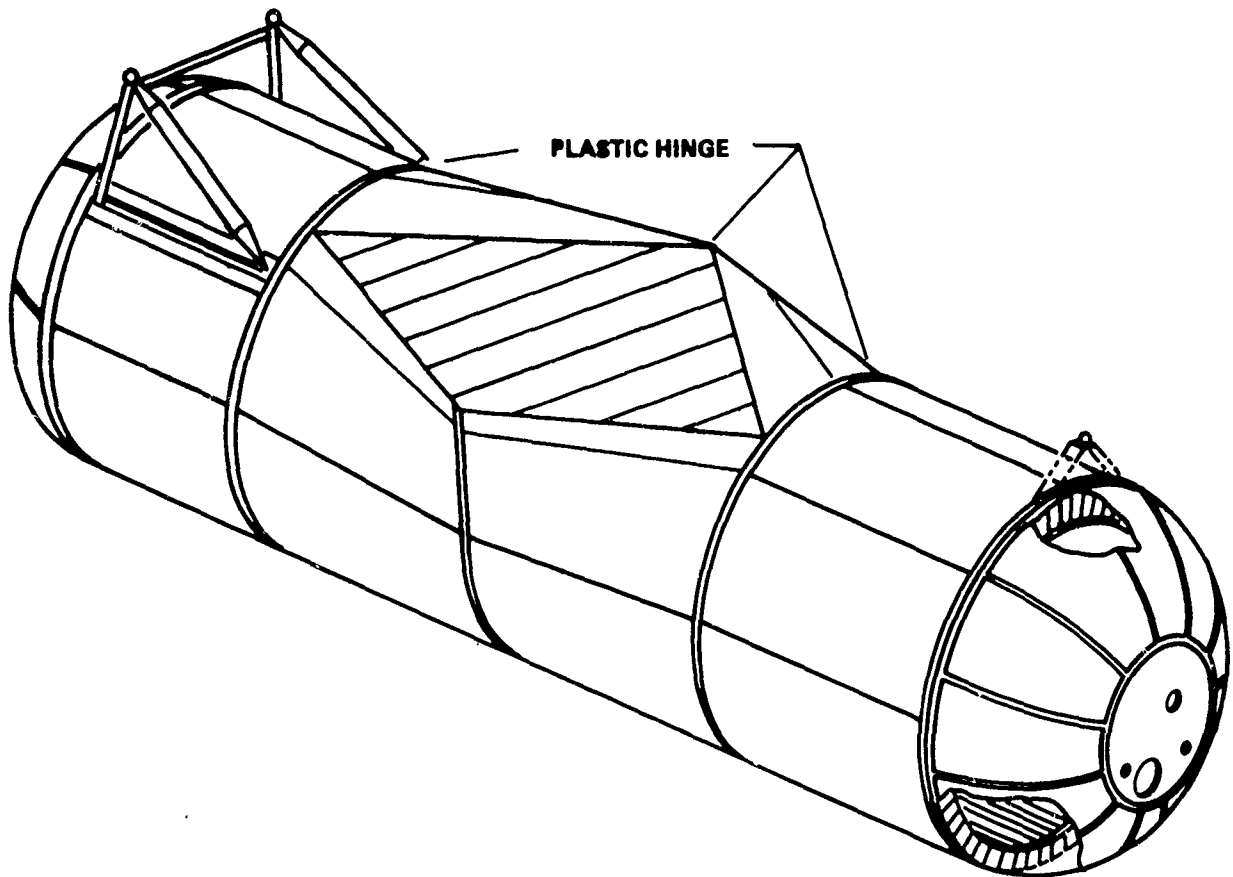


FIGURE 4-28 LH₂ TANK RESPONSE TO LSC CUT AT EARLY TIMES DURING ASCENT

BIBLIOGRAPHY

Belles, F.E., "Detonability and Chemical Kinetics: Prediction of Limits of Detonability of Hydrogen," Combustion Symposium, Vol. 7, 1962, p. 745.

Boggs, W.H., "Physical Processes Causing LOX/LH₂ Autoignition," Minutes of the Seventeenth Explosives Safety Seminar, Denver, Colorado, Vol. 1, Sep 1976, p. 135.

Cassutt, L.H., Maddocks, F.E., and Sawyer, W.A., "A Study of the Hazards in the Storage and Handling of Liquid Hydrogen," Advances in Cryogenic Engineering, Vol. 5, 1960, p. 55.

Dergarabedian, P., "Observations on Bubble Growths in Various Superheated Liquids," Journal of Fluid Mechanics, Vol. 9, 1960, p. 39.

Dergarabedian, P., "The Rate of Growth of Vapor Bubbles in Superheated Water," Journal of Applied Mechanics, Vol. 20, 1953, p. 537.

Farber, E.A., Smith, J.H., and Watts, E.H., "Prediction of Explosive Yield and Other Characteristics of Liquid Rocket Propellant Explosions, Final Report," University of Florida, N74-20589, Jun 30, 1973.

Forstall, W., Jr., and Shapiro, A.H., "Momentum and Mass Transfer in Coaxial Gas Jets," Journal of Applied Mechanics, Vol. 17, 1950, p. 399.

Kaye, S., "Hazard Studies with Hydrogen and Oxygen in the Liquid and Solid Phases," Advances in Cryogenic Engineering, Vol. 11, 1966, p. 277.

Lewis, B., and von Elbe, G., Combustion, Flames and Explosions of Gases, 2nd ed. (New York: Academic Press, 1961), pp. 382, 399.

Mayer, E., "Theory of Liquid Atomization in High Velocity Gas Streams," American Rocket Society Journal, Dec 1961, p. 1783.

"Ordnance Options for a Space Shuttle Range Safety Command Destruct System," Naval Surface Weapons Center, White Oak Laboratory, Silver Spring, Maryland, for George C. Marshall Space Flight Center, Marshall Space Flight Center, Alabama, under NASA-Defense Purchase Request H-13047 B, Amendment 3, 8 Mar 1976. Report dated 10 Dec 1976.

Perry, J.H., Ed., Chemical Engineer's Handbook, 3rd ed. (New York: McGraw-Hill, 1950.)

Schlichting, H., Boundary Layer Theory, 4th ed. (New York: McGraw-Hill, 1960).

"Study Report on Space Shuttle Range Safety Command Destruct System Analysis and Verification," Naval Surface Weapons Center, White Oak Laboratory, Silver Spring, Maryland, for George C. Marshall Space Flight Center, Marshall Space Flight Center, Alabama, under NASA-Defense Purchase Request H-13047 B, 15 May 1975. Report dated 2 Feb 1976.

Hahn, G. T., Sarrate, H., and Rosenfield, A. R., "Criteria for Crack Extension in Cylindrical Pressure Vessels," Journal of Fracture Mechanics, Vol. 5, No. 3, 1969.

APPENDIX A
LISTING OF SRB DEBRIS FRAGMENTS

CONFIGURATION: Integrated Vehicle

Sheet 1 of 2

COMPONENT: Solid Rocket Booster (Left or Right) (Forward Velocity = 180 fps)

TIME OF DESTRUCT ACTION (SEC): 10

Piece Description and Remarks	Number of Pieces	Weight of Each Piece (lb)	Total Weight (lb)	Reference Area (ft ²)	Ballistic Factor (W/CDA) (1b/ft ²)	Velocity Increment (ft/sec)	Figure Number
							C _D
							C _L
(1) Aft Case, Nozzle and Propellant (248,000 lb)	1	320,000	320,000	116	1,600-3,400	-41	A-1 -
(2) Forward Frustum and Skirt	1	21,800	21,800	237	77-530	490	A-2 -
(3) Aft Attach Struts	3	128	385	1.9	96-340	-20	A-3 -
(4) Motor Case Segments (Tumbling)	12	6,080	73,000	250	10-17	380	A-4 -
(5) Clevis Pins	1,260	0.33	416	0.010	24-110	380-1,500	A-5 -
(6) SRM Case (Between LSC's)	6	24	144	1.1	18-27	1,800	A-6 -
(7) Systems Tunnel Segments							
(a) 12-in Length Cover	14-28	0.5-1.0	14	0.67	0.9-2.6	150-2,500	A-7 -
(b) 150-in Length	48-60	1.6-12	200	1.1-8.3	1.2-1.8	150-2,500	A-6 -
(8) LSC Sheath Segments	150-600	0.006-0.05	6	0.01-0.08	0.5-0.8	2,300	A-6 -
(9) Miscellaneous (Cabling, Bolts, Brackets, Insulation, Inhibitor, etc.)	4,000-6,000	0.01-2	6,040	0.001-0.1	1-20	2,500*	** -
(10) Propellant Fragments, 1- to 5-in Cubes	21,800	0.06-7.9	39,900	0.007-0.17	12-62	2,500-1,000*	A-8 -
(11) Propellant Fragments, 5- to 10-in Cubes	8,030	7.9-64	191,100	0.17-0.69	58-124	1,000-490*	A-8 -

*Maximum velocities (e.g., maximum velocity for 1-in cube = 2,500 fps; for 5-in cube = 1,000 fps).

**C_D ≈ 1.

CONFIGURATION: Integrated Vehicle

COMPONENT: Solid Rocket Booster (Left or Right) (Forward Velocity = 180 fps) TIME OF DESTRUCT ACTION (SEC): 10

Sheet 2 of 2

NSWC TR 80-417

Piece Description and Remarks	Number of Pieces	Weight of Each Piece (1lb)	Total Weight (1lb)	Reference Area (ft ²)	Ballistic Factor (W/CDA) (1b/ft ²)	Velocity Increment (ft/sec)	Figure Number	
							C _D	C _L
(12) Propellant Fragments, 10- to 15-in Cubes	2,000	64-214	225,000	0.69-1.56	116-185	490-380*	A-8	-
(13) Propellant Fragments, 15- to 20-in Cubes	500	214-508	156,900	1.56-2.78	174-247	380*	A-8	-
(14) Propellant Fragments, 20- to 25-in Cubes	124	508-992	84,300	2.78-4.34	231-309	380*	A-8	-
(15) Propellant Fragments, 25- to 30-in Cubes	32	992-1,720	38,700	4.34-6.25	289-371	380*	A-8	-
(16) Propellant Fragments, 30- to 35-in Cubes	8	1,720-2,720	16,000	6.25-8.51	347-432	380*	A-8	-
(17) Propellant Fragments, 35- to 38.4-in Cubes	3	2,720-3,590	4,800	8.51-10.2	405-474	380*	A-8	-
TOTAL				1,178,700				

*Maximum velocities (e.g., maximum velocity for 1-in cube = 2,500 fps; for 5-in cube = 1,000 fps).

CONFIGURATION: Right SRB Separated

COMPONENT: Solid Rocket Booster (Left) (Forward Velocity = 300 fps)

TIME OF DESTRUCT ACTION (SEC): 20

Sheet 1 of 2

Piece Description and Remarks	Number of Pieces	Weight of Each Piece (1b)	Total Weight (lb)	Reference Area (ft ²)	Ballistic Factor (W/C _D ^A) (1b/ft ²)	Velocity Increment (ft/sec)	Figure Number	C _D	C _L
(1) Aft Case, Nozzle and Propellant (214,000 lb)	1	286,000	286,000	116	1,400-3,000	-38	A-1	-	
(2) Forward Frustum and Skirt	1	21,800	21,800	237	77-530	480	A-2	-	
(3) Aft Attach Struts	3	128	385	1.9	96-340	-20	A-3	-	
(4) Motor Case Segments (Tumbling)	12	6,080	73,000	250	10-17	410	A-4	-	
(5) Clevis Pins	1,260	0.33	416	0.010	24-110	410-1500	A-5	-	
(6) SRM Case (Between LSC's)	6	24	144	1.1	18-27	1,800	A-6	-	
(7) Systems Tunnel Segments									
(a) 12-in Length Cover	14-28	0.5-1.0	14	0.67	0.9-2.6	150-2,500	A-7	-	
(b) 150-in Length	48-60	1.6-1.2	200	1.1-8.3	1.2-1.8	150-2,500	A-6	-	
(8) LSC Sheath Segments	150-600	0.006-0.05	6	0.01-0.08	0.5-0.8	2,300	A-6	-	
(9) Miscellaneous (Cabling, Bolts, Brackets, Insulation, Inhibitor, etc.)	4,000-6,000	0.01-2	6,040	0.001-0.1	1-20	2,500*	**	-	
(10) Propellant Fragments, 1- to 5-in Cubes	29,500	0.06-7.94	51,600	0.007-0.17	12-62	2,400-960*	A-8	-	
(11) Propellant Fragments, 5- to 10-in Cubes	9,190	7.94-64	212,200	0.17-0.69	58-124	960-430*	A-8	-	

*Maximum velocities (e.g., maximum velocity for 1-in cube = 2,400 fps; for 5-in cube = 960 fps).

**C_D ≈ 1.

CONFIGURATION: Right SRB Separated

Sheet 2 of 2

COMPONENT: Solid Rocket Booster (Left) (Forward Velocity = 300 fps)

TIME OF DESTRUCT ACTION (SEC): 20

Piece Description and Remarks	Number of Pieces	Weight of Each Piece (lb)	Total Weight (lb)	Reference Area (ft ²)	Ballistic Factor Range (W/CDA) (1b/ft ²)	Velocity Increment (ft/sec)	Figure Number	C _D	C _L
(12) Propellant Fragments, 10- to 15-in Cubes	1,890	64-214	208,400	0.69-1.56	116-185	430-410*	A-8	-	
(13) Propellant Fragments, 15- to 20-in Cubes	387	214-508	120,400	1.56-2.78	174-247	410*	A-8	-	
(14) Propellant Fragments, 20- to 25-in Cubes	80	508-992	53,400	2.78-4.34	231-309	410*	A-8	-	
(15) Propellant Fragments, 25- to 30-in Cubes	16	992-1,720	20,200	4.34-6.25	289-371	410*	A-8	-	
(16) Propellant Fragments, 30- to 34.5-in Cubes	4	1,720-2,720	6,600	6.25-8.51	347-432	410*	A-8	-	
TOTAL			1,060,800						

*Maximum velocities (e.g., maximum velocity for 1-in cube = 2,400 fps; for 5-in cube = 960 fps).

CONFIGURATION: Right SRB Separated

COMPONENT: Solid Rocket Booster (Right) (Forward Velocity = 710 fps)

TIME OF DESTRUCT ACTION (SEC): 20

Piece Description and Remarks	Number of Pieces	Weight of Each Piece (1b)	Total Weight (1b)	Reference Area (ft ²)	Ballistic Range (W/C _D A) (1b/ft ²)	Velocity Increment (ft/sec)	Figure Number
							C _D C _L
(1) Aft Case, Nozzle and Propellant (214,000 1b)	1	286,000	286,000	116	1,400-3,000	-38	A-1 -
(2) Forward Frustum and Skirt	1	21,800	21,800	237	77-530	480	A-2 -
(3) Aft Attach Struts	3	128	385	1.9	96-340	-20	A-3 -
(4) Motor Case Segments (Tumbling)	12	6,080	73,000	250	10-17	410	A-4 -
(5) Clevis Pins	1,260	0.33	416	0.010	24-110	410-1,500	A-5 -
(6) SRM Case (Between LSC's)	6	24	144	1.1	18-27	1,800	A-6 -
(7) Systems Tunnel Segments							
(a) 12-in Length Cover	14-28	0.5-1.0	14	0.67	0.9-2.6	150-2,500	A-7 -
(b) 150-in Length	48-60	1.6-12	200	1.1-8.3	1.2-1.8	150-2,500	A-6 -
(8) LSC Sheath Segments	150-600	0.006-0.05	6	0.01-0.08	0.5-0.8	2,300	A-6 -
(9) Miscellaneous (Cabling, Bolts, Brackets, Insulation, Inhibitor, etc.)	4,000-6,000	0.01-2	6,040	0.001-0.1	1-20	2,500*	** -
(10) Propellant Fragments, 1- to 5-in Cubes	29,500	0.06-7.94	51,600	0.007-0.17	12-62	2,400-960*	A-8 -
(11) Propellant Fragments, 5- to 10-in Cubes	9,190	7.94-64	212,200	0.17-0.69	58-124	960-430*	A-8 -

*Maximum velocities (e.g., maximum velocity for 1-in cube = 2,400 fps; for 5-in cube = 960 fps).

**CD ≈ 1.

CONFIGURATION: Right SRB Separated

COMPONENT: Solid Rocket Booster (Right) (Forward Velocity = 710 fps)

TIME OF DESTRUCT ACTION (SEC): 20

Piece Description and Remarks	Number of Pieces	Weight of Each Piece (1b)	Total Weight (1b)	Reference Area (ft ²)	Ballistic Factor Range (W/C _{DA}) (1b/ft ²)	Velocity Increment (ft/sec)	Figure Number	
							C _D	C _L
(12) Propellant Fragments, ;0- to 15-in Cubes	1,890	64-214	208,400	0.69-1.56	116-185	430-410*	A-8	-
(13) Propellant Fragments, 15- to 20-in Cubes	387	214-508	120,400	1.56-2.78	174-247	410*	A-8	-
(14) Propellant Fragments, 20- to 25-in Cubes	80	508-992	53,400	2.78-4.34	231-309	410*	A-8	-
(15) Propellant Fragments, 25- to 30-in Cubes	16	992-1,720	20,200	4.34-6.25	289-371	410*	A-8	-
(16) Propellant Fragments, 30- to 34.5-in Cubes	4	1,720-2,720	6,600	6.25-8.51	347-432	410*	A-8	-
TOTAL			1,060,800					

*Maximum velocities (e.g., maximum velocity for 1-in cube = 2,400 fps; for 5-in cube = 960 fps).

CONFIGURATION: Orbiter Separated

COMPONENT: Solid Rocket Booster (Left or Right) (Forward Velocity = 360 fps) TIME OF DESTRUCT ACTION (SEC): 20

Sheet 1 of 2

NSWC TR 80-417

Piece Description and Remarks	Number of Pieces	Weight of Each Piece (1b)	Total Weight (1b)	Reference Area (Ft ²)	Ballistic Factor (W/CDA) (1b/Ft ²)	Velocity Increment (ft/sec)	Figure Number	
							C _D	C _L
(1) Aft Case, Nozzle and Propellant (214,000 lb)	1	286,000	286,000	116	1,400-3,000	-38	A-1	-
(2) Forward Frustum and Skirt	1	21,800	21,800	237	77-530	480	A-2	-
(3) Aft Attach Struts	3	128	385	1.9	96-340	-20	A-3	-
(4) Motor Case Segments (Tumbling)	12	6,080	73,000	250	10-17	410	A-4	-
(5) Clevis Pins	1,260	0.33	416	0.010	24-110	410-1,500	A-5	-
(6) SRM Case (Between LSC's)	6	24	144	1.1	18-27	1,800	A-6	-
(7) Systems Tunnel Segments								
(a) 12-in Length Cover	14-28	0.5-1.0	14	0.67	0.9-2.6	150-2,500	A-7	-
(b) 150-in Length	48-60	1.6-12	200	1.1-8.3	1.2-1.8	150-2,500	A-6	-
(8) LSC Sheath Segments	150-600	0.006-0.05	6	0.01-0.08	0.5-0.8	2,300	A-6	-
(9) Miscellaneous (Cabling, Bolts, Brackets, Insulation, Inhibitor, etc.)	4,000-6,000	0.01-2	6,040	0.001-0.1	1-20	2,500*	**	-
(10) Propellant Fragments, 1- to 5-in Cubes	29,500	0.06-7.94	51,600	0.007-0.17	12-62	2,400-960*	A-8	-
(11) Propellant Fragments, 5- to 10-in Cubes	9,190	7.94-64	212,200	0.17-0.69	58-124	960-430*	A-8	-

*Maximum velocities (e.g., maximum velocity for 1-in cube = 2,400 fps; for 5-in cube = 960 fps).

**C_D ≈ 1.

CONFIGURATION: Orbiter Separated

COMPONENT: Solid Rocket Booster (Left or Right) (Forward Velocity = 360 fps) TIME OF DESTRUCT ACTION (SEC): 20

Sheet 2 of 2

NSWC TR 80-417

Piece Description and Remarks	Number of Pieces	Weight of Each Piece (1lb)	Total Weight (1lb)	Reference Area (ft ²)	Ballistic Factor (W/CDA) (1b/ft ²)	Velocity Increment (ft/sec)	Figure Number	
							C _D	C _L
(12) Propellant Fragments, 10- to 15-in Cubes	1,890	64-214	208,400	0.69-1.56	116-185	430-410*	A-8	-
(13) Propellant Fragments, 15- to 20-in Cubes	387	214-508	120,400	1.56-2.78	174-247	410*	A-8	-
(14) Propellant Fragments, 20- to 25-in Cubes	80	508-992	53,400	2.78-4.34	231-309	410*	A-8	-
(15) Propellant Fragments, 25- to 30-in Cubes	16	992-1,720	20,200	4.34-6.25	289-371	410*	A-8	-
(16) Propellant Fragments, 30- to 34.5-in Cubes	4	1,720-2,720	6,600	6.25-8.51	347-432	410*	A-8	-
TOTAL			1,060,800					

*Maximum velocities (e.g., maximum velocity for 1-in cube = 2,400 fps; for 5-in cube = 960 fps).

CONFIGURATION: Integrated Vehicle

COMPONENT: Solid Rocket Booster (Left or Right) (Forward Velocity = 1,070 fps) TIME OF DESTRUCT ACTION (SEC): 50

Sheet 1 of 2

NSWC TR 80-417

Piece Description and Remarks	Number of Pieces	Weight of Each Piece (1lb)	Total Weight (lb)	Reference Area (ft ²)	Ballistic Factor Range (W/C _D A) (1b/ft ²)	Velocity Increment (ft/sec)	Figure Number	C _D	C _L
(1) Aft Case, Nozzle and Propellant (140,000 1b)	1	212,000	212,000	116	1,060-2,300	-43	A-1	-	
(2) Forward Frustum and Skirt	1	21,800	21,800	237	77-530	410	A-2	-	
(3) Aft Attach Struts	3	128	385	1.9	96-340	-20	A-3	-	
(4) Motor Case Segments (Tumbling)	12	6,080	73,000	250	10-17	520	A-4	-	
(5) Clevis Pins	1,260	0.33	416	0.010	24-110	520-1,400	A-5	-	
(6) SRM Case (Between LSC's)	6	24	144	1.1	18-27	1,700	A-6	-	
(7) Systems Tunnel Segments									
(a) 12-in Length Cover	14-28	0.5-1.0	14	0.67	0.9-2.6	75-2,500	A-7	-	
(b) 150-in Length	48-60	1.6-12	200	1.1-8.3	1.1-1.8	75-2,500	A-6	-	
(8) LSC Sheath Segments	150-600	0.006-0.05	6	0.01-0.08	0.5-0.8	2,300	A-6	-	
(9) Miscellaneous (Cabling, Bolts, Brackets, Insulation, Inhibitor, etc.)	4,000-6,000	0.01-2	6,040	0.001-0.1	1-20	2,500*	**	-	
(10) Propellant Fragments, 1- to 5-in Cubes	80,700	0.06-7.94	112,900	0.007-0.17	12-62	2,200-700*	A-8	-	
(11) Propellant Fragments, 5- to 10-in Cubes	11,600	7.94-64	231,400	0.17-0.69	58-124	700-520*	A-8	-	

*Maximum velocities (e.g., maximum velocity for 1-in cube = 2,200 fps; for 5-in cube = 700 fps).

**C_D ≈ 1.

CONFIGURATION: Integrated Vehicle

COMPONENT: Solid Rocket Booster (Left or Right) (Forward Velocity = 1,070 fps) TIME OF DESTRUCT ACTION (SEC): 50

Sheet 2 of 2

Piece Description and Remarks	Number of Pieces	Weight of Each Piece (1lb)	Total Weight (1lb)	Reference Area (ft ²)	Ballistic Factor Range (W/CDA) (1b/ft ²)	Velocity Increment (ft/sec)	Figure Number
							C _D C _L
(12) Propellant Fragments, 5- to 10-in Cubes	960	64-214	97,000	0.69-1.56	116-185	520*	A-8 -
(13) Propellant Fragments, 15- to 20-in Cubes	79	214-508	23,000	1.56-2.78	174-247	520*	A-8 -
(14) Propellant Fragments, 20- to 23.9-in Cubes	7	508-992	3,800	2.78-4.34	231-309	520*	A-8 -
TOTAL			782,100				

*Maximum velocities (e.g., maximum velocity for 1-in cube = .2,200 fps; for 5-in cube = 700 fps).

CONFIGURATION: Right SRB Separated

COMPONENT: Solid Rocket Booster (Left) (Forward Velocity = 1,070 fps)

TIME OF DESTRUCT ACTION (SEC): 52

Sheet 1 of 2

Piece Description and Remarks	Number of Pieces	Weight of Each Piece (1b)	Total Weight (lb)	Reference Area (ft ²)	Ballistic Factor (W/CDA) (lb/ft ²)	Velocity Increment (ft/sec)	Figure Number	C _D	C _L
(1) Aft Case, Nozzle and Propellant (135,000 1b)	1	207,000	207,000	116	1,040-2,200	-46	A-1	-	
(2) Forward Frustum and Skirt	1	21,800	21,800	237	77-530	420	A-2	-	
(3) Aft Attach Struts	3	128	385	1.9	96-340	-25	A-3	-	
(4) Motor Case Segments (Tumbling)	12	6,080	73,000	250	10-17	540	A-4	-	
(5) Clevis Pins	1,260	0.33	416	0.010	24-110	540-1,400	A-5	-	
(6) SRM Case (Between LSC's)	6	24	144	1.1	18-27	1,700	A-6	-	
(7) Systems Tunnel Segments									
(a) 12-in Length Cover	14-28	0.5-1.0	14	0.67	0.9-2.6	75-2,500	A-7	-	
(b) 150-in Length	48-60	1.6-12	200	1.1-8.3	1.2-1.8	75-2,500	A-6	-	
(8) LSC Sheath Segments	150-600	0.006-0.05	6	0.01-0.08	0.5-0.8	2,300	A-6	-	
(9) Miscellaneous (Cabling, Bolts, Brackets, Insulation, Inhibitor, etc.)	4,000-6,000	0.01-2	6,040	0.001-0.1	1-20	2,500*	**	-	
(10) Propellant Fragments, 1- to 5-in Cubes	86,700	0.06-7.94	118,700	0.007-0.17	12-62	2,200-700*	A-8	-	
(11) Propellant Fragments, 5- to 10-in Cubes	11,600	7.94-64	228,000	0.17-0.69	58-124	700-540*	A-8	-	

*Maximum velocities (e.g., maximum velocity for 1-in cube = 2,200 fps; for 5-in cube = 700 fps).

**C_D ≈ 1.

CONFIGURATION: Right SRB Separated

COMPONENT: Solid Rocket Booster (Left) (Forward Velocity = 1,070 fps)

TIME OF DESTRUCT ACTION (SEC): 52

Sheet 2 of 2

NSWC TR 80-417

Piece Description and Remarks	Number of Pieces	Weight of Each Piece (1b)	Total Weight (1b)	Reference Area (ft ²)	Ballistic Factor Range (W/CDA) (1b/ft ²)	Velocity Increment (ft/sec)	Figure Number	C _D	C _L
(12) Propellant Fragments, 10- to 15-in Cubes	874	64-214	88,000	0.69-1.56	116-185	540*	A-8	--	
(13) Propellant Fragments, 15- to 20-in Cubes	66	214-508	19,200	1.56-3.78	174-247	540*	A-8	--	
(14) Propellant Fragments, 20- to 23.3-in Cubes	6	508-992	2,700	2.78-4.34	231-309	540*	A-8	--	
TOTAL			765,600						

*Maximum velocities (e.g., maximum velocity for 1-in cube = 2,200 fps; for 5-in cube = 700 fps).

CONFIGURATION: Right SRB Separated

COMPONENT: Solid Rocket Booster (Right) (Forward Velocity = 1,160 fps)

TIME OF DESTRUCT ACTION (SEC): 52

Piece Description and Remarks	Number of Pieces	Weight of Each Piece (lb)	Total Weight (lb)	Reference Area (ft ²)	Ballistic Factor (W/C _D A) (1b/ft ²)	Velocity Increment (ft/sec)	Figure Number
							C _D C _L
(1) Aft Case, Nozzle and Propellant (135,000 lb)	1	207,000	207,000	116	1,040-2,200	-46	A-1 -
(2) Forward Frustum and Skirt	1	21,800	21,800	237	77-530	420	A-2 -
(3) Aft Attach Struts	3	128	385	1.9	96-340	-25	A-3 -
(4) Motor Case Segments (Tumbling)	12	6,080	73,000	250	10-17	540	A-4 -
(5) Clevis Pins	1,260	0.33	416	0.010	24-110	540-1,400	A-5 -
(6) SRM Case (Between LSC's)	6	24	144	1.1	18-27	1,700	A-6 -
(7) Systems Tunnel Segments							
(a) 12-in Length Cover	14-28	0.5-1.0	14	0.67	0.9-2.6	75-2,500	A-7 -
(b) 150-in Length	48-60	1.6-12	200	1.1-8.3	1.2-1.8	75-2,500	A-6 -
(8) LSC Sheath Segments	150-600	0.006-0.05	6	0.01-0.08	0.5-0.8	2,300	A-6 -
(9) Miscellaneous (Cabling, Bolts, Brackets, Insulation, Inhibitor, etc.)	4,000-6,000	0.01-2	6,040	0.001-0.1	1-20	2,500*	** -
(10) Propellant Fragments, 1- to 5-in Cubes	86,700	0.06-7.94	118,700	0.007-0.17	12-62	2,200-700*	A-8 -
(11) Propellant Fragments, 5- to 10-in Cubes	11,600	7.9-64	228,000	0.17-0.69	58-124	700-540*	A-8 -

*Maximum Velocities (e.g., maximum velocity for 1-in cube = 2,200 fps; for 5-in cube = 700 fps).

**C_D ≈ 1.

CONFIGURATION: Right SRB Separated

COMPONENT: Solid Rocket Booster (Right) (Forward Velocity = 1,160 fps) TIME OF DESTRUCT ACTION (SEC): 5.2

Piece Description and Remarks	Number of Pieces	Weight of Each Piece (lb)	Total Weight (lb)	Reference Area (ft ²)	Ballistic Factor Range (W/C _{DA}) (1b/ft ²)	Velocity Increment (ft/sec)	Figure Number
					C _D	C _L	
(12) Propellant Fragments, 10- to 15-in Cubes	874	64-214	88,000	0.69-1.56	116-185	540*	A-8 -
(13) Propellant Fragments, 15- to 20-in Cubes	66	214-508	19,200	1.56-2.78	174-247	540*	A-8 -
(14) Propellant Fragments, 20- to 23.3-in Cubes	6	508-992	2,700	2.78-4.34	231-309	540*	A-8 -
TOTAL			765,600				

*Maximum Velocities (e.g., maximum velocity for 1-in cube = 2,200 fps; for 5-in cube = 700 fps).

CONFIGURATION: Orbiter Separated

COMPONENT: Solid Rocket Booster (Left or Right) (Forward Velocity = 1,300 fps) TIME OF DESTRUCT ACTION (SEC): 65

Sheet 1 of 2

NSWC TR 80-417

Piece Description and Remarks	Number of Pieces	Weight of Each Piece (1b)	Total Weight (1b)	Referen.e Area (ft ²)	Ballistic Factor (W/CDA) (1b/ft ²)	Velocity Increment (ft/sec)	Figure Number	
							C _D	C _L
(1) Aft Case, Nozzle and Propellant (108,000 1b)	1	180,000	180,000	116	900-1,900	-48	A-1	-
(2) Forward Frustum and Skirt	1	21,700	21,700	237	77-530	400	A-2	-
(3) Aft Attach Struts	3	128	385	1.9	96-340	-25	A-3	-
(4) Motor Case Segments (Tumbling)	12	6,380	73,000	250	10-17	600	A-4	-
(5) Clevis Pins	1,260	0.33	416	0.010	24-110	600-1,400	A-5	-
(6) SRM Case (Between LSC's)	6	24	144	1.1	18-27	1,700	A-6	-
(7) Systems Tunnel Segments								
(a) 12-in Length Cover	14-28	0.5-1.0	14	0.67	0.9-2.6	75-2,500	A-7	-
(b) 150-in Length	48-30	1.6-12	200	1.1-8.3	1.2-1.8	75-2,500	A-6	-
(8) LSC Sheath Segments	150-600	0.006-0.05	6	0.01-0.08	0.5-0.8	2,300	A-6	-
(9) Miscellaneous (Cabling, Bolts, Brackets, Insulation, Inhibitor, etc.)	4,000-6,000	0.01-2	5,740	0.001-0.1	1-20	2,500	**	-
(10) Propellant Fragments, 1- to 5-in Cubes	140,000	0.06-7.9	159,400	0.007-0.17	12-62	2,100-600*	A-8	-
(11) Propellant Fragments, 5- to 10-in Cubes	10,100	7.9-64	179,300	0.17-0.69	58-124	600*	A-8	-

*Maximum velocities (e.g., maximum velocity for 1-in cube = 2,100 fps; for 5-in cube = 600 fps).

**C_D ≈ 1.

CONFIGURATION: Orbiter Separated

COMPONENT: Solid Rocket Booster (Left or Right) (Forward Velocity = 1,300 fps) TIME OF DESTRUCT ACTION (SEC): 65

Sheet 2 of 2

Piece Description and Remarks	Number of Pieces	Weight of Each Piece (lb)	Total Weight (lb)	Reference Area (ft ²)	Ballistic Factor Range (W/CDA) (lb/ft ²)	Velocity Increment (ft/sec)	Figure Number
							C _D C _L
(12) Propellant Fragments, 10- to 15-in Cubes	365	64-214	34,700	0.69-1.56	116-85	600*	A-8 -
(13) Propellant Fragments, 15- to 18.9-in Cubes	14	214-508	3,400	1.56-2.78	174-247	600*	A-8 -
TOTAL			658,400				

*Maximum velocities (e.g., maximum velocity for 1-in cube = 2,100 fps; for 5-in cube = 600 fps).

CONFIGURATION: Integrated Vehicle

COMPONENT: Solid Rocket Booster (Left or Right) (Forward Velocity = 3,200 fps) TIME OF DESTRUCT ACTION (SEC): 100

Sheet 1 of 1

NSWC TR 80-417

Piece Description and Remarks	Number of Pieces	Weight of Each Piece (1b)	Total Weight (1b)	Reference Area (ft ²)	Ballistic Factor Range (W/C _D A) (1b/ft ²)	Velocity Increment (ft/sec)	Figure Number	
							C _D	C _L
(1) Aft Case, Nozzle and Propellant (36,000 1b)	1	108,000	108,000	116	540-1,150	-52	A-1	-
(2) Forward Frustum and Skirt	1	21,500	21,500	237	76-520	310	A-2	-
(3) Aft Attach Struts	3	128	385	1.9	96-340	-25	A-3	-
(4) Motor Case Segments (Tumbling)	12	6,080	73,000	250	10-17	750	A-4	-
(5) Clevis Pins	1,260	0.33	416	0.010	24-110	750-1,100	A-5	-
(6) SRM Case (Between LSC's)	6	24	144	1.1	18-27	1,450	A-6	-
(7) Systems Tunnel Segments								
(a) 12-in Length Cover	14-28	0.5-1.0	14	0.67	0.9-2.6	5-2,000	A-7	-
(b) 150-in Length	48-60	1.6-12	200	1.1-8.3	1.2-1.8	5-2,000	A-6	-
(8) LSC Sheath Segments	150-600	0.006-0.05	6	0.01-0.08	0.5-0.8	2,300	A-6	-
(9) Miscellaneous (Cabling, Bolts, Brackets, Insulation, Inhibitor, etc.)	3,000-5,000	0.01-2	5,140	0.001-0.1	1-20	2,000	**	-
(10) Propellant Fragments, 1- to 5-in Cubes	449,000	0.06-7.94	125,400	0.007-0.17	12-62	1,600-750*	A-8	-
(11) Propellant Fragments, 5- to 7-in Cubes	30,800	7.94-64	800	0.17-0.69	58-124	750*	A-8	-
TOTAL			335,000					

*Maximum velocities (e.g., maximum velocity for 1-in cube = 1,600 fps; for 5-in cube = 750 fps).

**C_D ≈ 1.

CONFIGURATION: Right SRB Separated

COMPONENT: Solid Rocket Booster (Left) (Forward Velocity = 3,700 fps) TIME OF DESTRUCT ACTION (SEC): 115

Piece Description and Remarks	Number of Pieces	Weight of Each Piece (1lb)	Total Weight (1lb)	Reference Area (ft ²)	Ballistic Factor Range (W/C _D A) (1lb/ft ²)	Velocity Increment (ft/sec)	Figure Number	C _D	C _L
(1) Aft Case, Nozzle	1	72,000	72,000	116	360-770	-32	A-1	-	
(2) Forward Frustum and Skirt	1	21,400	21,400	237	76-520	130	A-2	-	
(3) Aft Attach Struts	3	128	385	1.9	96-340	-15	A-3	-	
(4) Motor Case Segments (Tumbling)									
(a) No Propellant	2	6,080	12,160	250	10-17	120	A-4	-	
(b) Propellant Adhering	10	9,250	92,500	250	15-26	75	A-4	-	
(5) Clevis Pins	1,260	0.33	416	0.010	24-110	75-750	A-5	-	
(6) SRM Case (Between LSC's)	6	24	144	1.1	18-27	1,000	A-6	-	
(7) Systems Turret Segments									
(a) 12-in Length Cover	14-28	0.5-1.0	14	0.67	0.9-2.6	5-2,000	A-7	-	
(b) 150-in Length	48-60	1.6-12	200	1.1-8.3	1.2-1.8	5-2,000	A-6	-	
(8) LSC Sheath Segments	150-600	0.006-0.05	6	0.01-0.08	0.5-0.8	2,300	A-6	-	
(9) Miscellaneous (Cabling, Bolts, Brackets, Insulation, Inhibitor, etc.)	3,000-5,000	0.01-2	4,740	0.001-0.1	1-20	2,000*	**	-	
TOTAL					204,000				

*Maximum velocity.

**C_D ≈ 1.

NSWC TR 80-417

CONFIGURATION: Right SRB Separated

COMPONENT: Solid Rocket Booster (Right) (Forward Velocity = 4,900 fps)

TIME OF DESTRUCT ACTION (SEC): 115

Sheet 1 of 1

NSWC TR 80-417

Piece Description and Remarks	Number of Pieces	Weight of Each Piece (1b)	Total Weight (1b)	Reference Area (ft ²)	Ballistic Factor Range (W/C _D A) (1b/ft ²)	Velocity Increment (ft/sec)	Figure Number	C _D	C _L
(1) Aft Case, Nozzle	1	72,000	72,000	116	360-770	-32	A-1	-	
(2) Forward Frustum and Skirt	1	21,400	21,400	237	76-520	130	A-2	-	
(3) Aft Attach Struts	3	128	385	1.9	96-340	-15	A-3	-	
(4) Motor Case Segments (Tumbling)									
(a) No Propellant	2	6,080	12,160	250	10-17	120	A-4	-	
(b) Propellant Adhering	10	9,250	92,500	250	15-26	75	A-4	-	
(5) Clevis Pins	1,260	0.33	416	0.010	24-110	75-750	A-5	-	
(6) SRM Case (Between LSC's)	6	24	144	1.1	18-27	1,000	A-6	-	
(7) Systems Tunnel Segments									
(a) 12-in Length Cover	14-28	0.5-1.0	14	0.67	0.9-2.6	5-2,000	A-7	-	
(b) 150-in Length	48-60	1.6-12	200	1.1-8.3	1.2-1.8	5-2,000	A-6	-	
(8) LSC Sheath Segments	150-600	0.006-0.05	6	0.01-0.08	0.5-0.8	2,300	A-6	-	
(9) Miscellaneous (Cabling, Bolts, Brackets, Insulation, Inhibitor, etc.)	3,000-5,000	0.01-2	4,740	0.001-0.1	1-20	2,000*	**	-	
TOTAL									
						204,000			

*Maximum velocity.

**C_D ≈ 1.

CONFIGURATION: Orbiter Separated

COMPONENT: Solid Rocket Booster (Left or Right) (Forward Velocity = 4,000 fps) TIME OF DESTRUCT ACTION (SEC): 115

Sheet 1 of 1

NSWC TR 80-417

Piece Description and Remarks	Number of Pieces	Weight of Each Piece (1b)	Total Weight (1b)	Reference Area (ft ²)	Ballistic Factor Range (W/CDA) (1b/ft ²)	Velocity Increment (ft/sec)	Figure Number	
							C _D	C _L
(1) Aft Case, Nozzle	1	72,000	72,000	116	360-770	-32	A-1	-
(2) Forward Frustum and Skirt	1	21,400	21,400	237	76-520	130	A-2	-
(3) Aft Attach Struts	3	128	385	1.9	96-340	-15	A-3	-
(4) Motor Case Segments (Tumbling)								
(a) No Propellant	2	6,080	12,160	250	10-17	120	A-4	-
(b) Propellant Adhering	10	9,250	92,500	250	15-26	75	A-4	-
(5) Clevis Pins	1,260	0.33	416	0.010	24-110	75-750	A-5	-
(6) SRM Case (Between LSC's)	6	24	144	1.1	1.8-27	1,000	A-6	-
(7) Systems Tunnel Segments								
(a) 12-in Length Cover	14-28	0.5-1.0	14	0.67	0.9-2.6	5-2,000	A-7	-
(b) 150-in Length	48-60	1.6-12	200	1.1-8.3	1.2-1.8	5-2,000	A-6	-
(8) LSC Sheath Segments	150-600	0.006-0.05	6	0.01-0.08	0.5-0.8	2,300	A-6	-
(9) Miscellaneous (Cabling, Bolts, Brackets, Insulation, Inhibitor, etc.)	3,000-5,000	0.01-2	4,740	0.001-0.1	1-20	2,000	*	-
TOTAL					204,000			

*C_D ≈ 1.

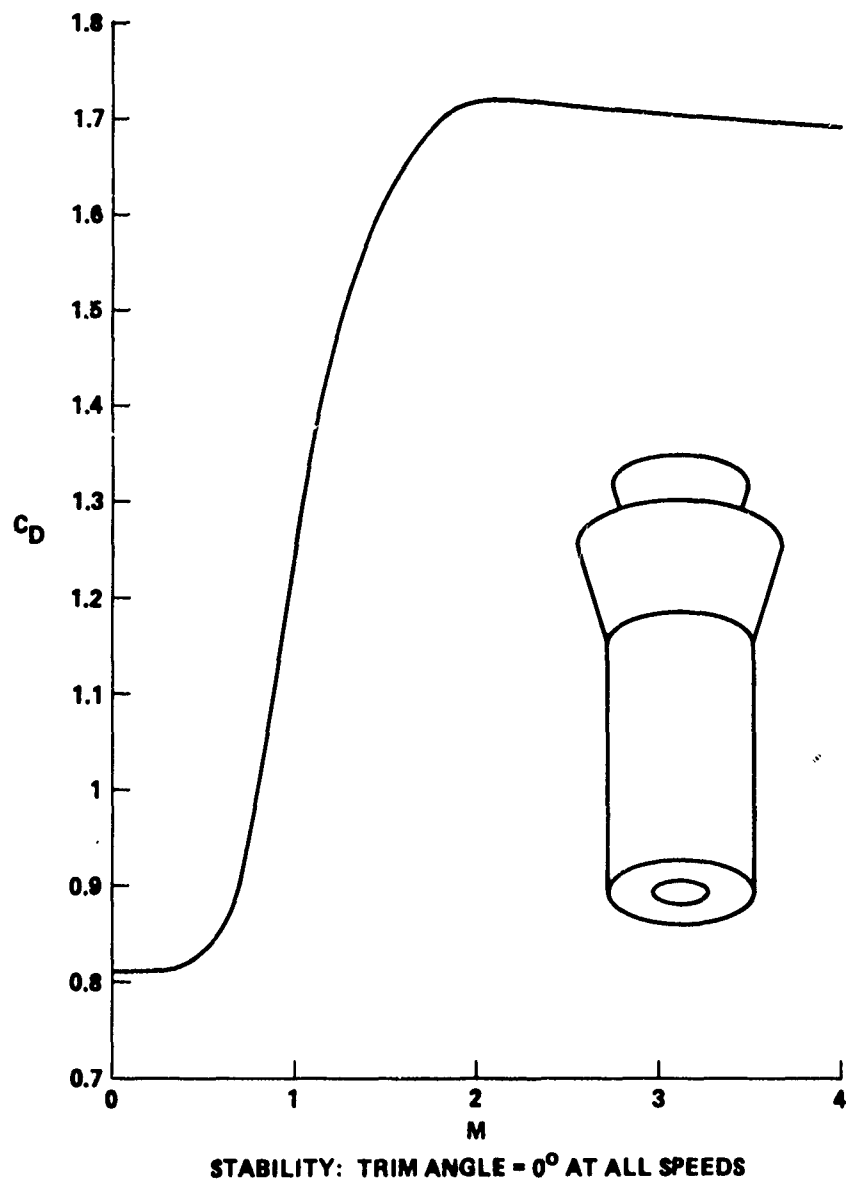


FIGURE A-1 DRAG COEFFICIENT FOR AFT CASE AND NOZZLE

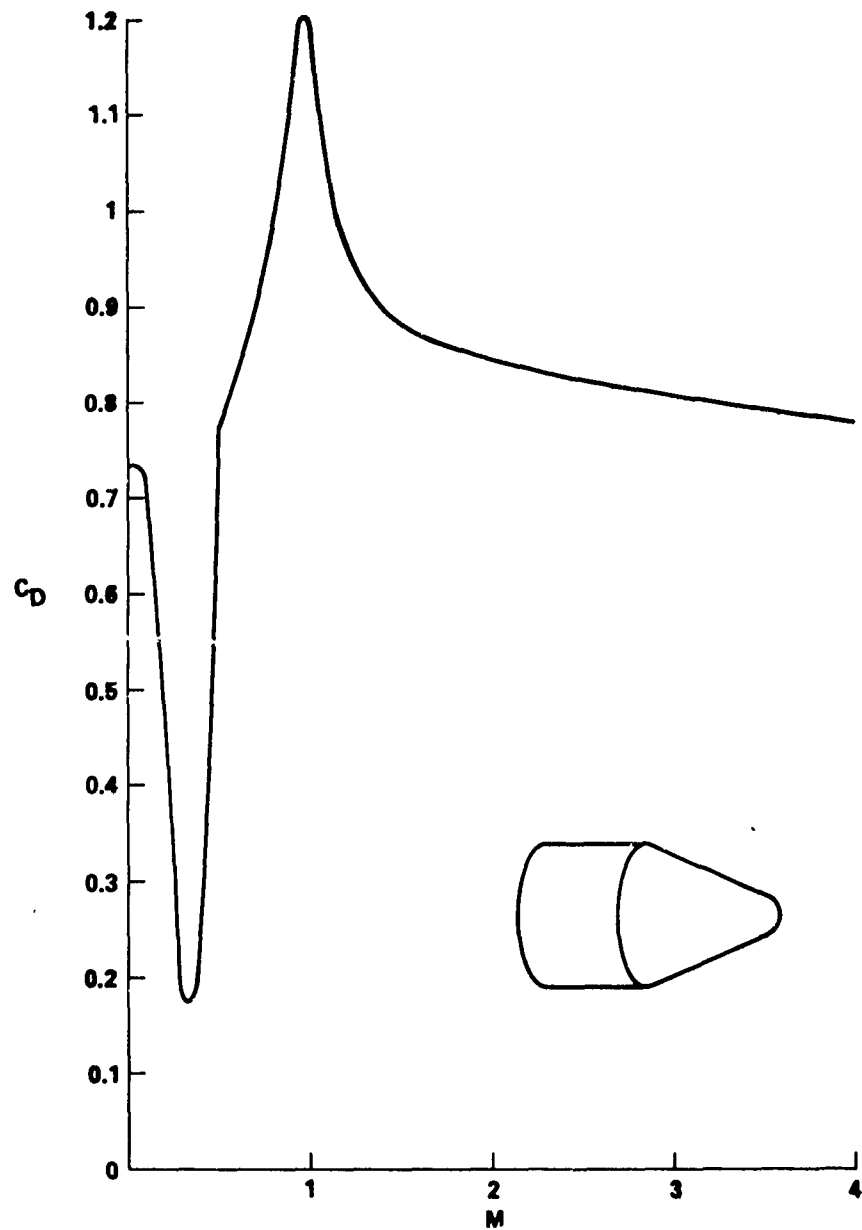


FIGURE A-2 DRAG COEFFICIENT FOR FORWARD FRUSTUM AND SKIRT

NSWC TR 80-417

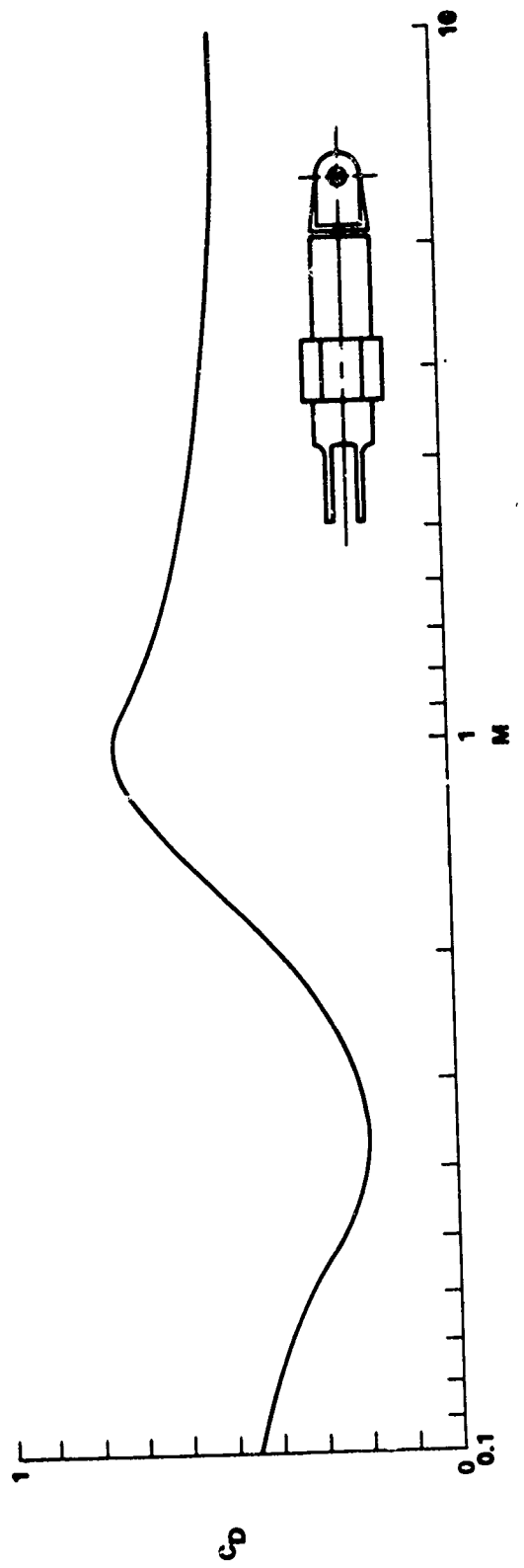


FIGURE A-3 DRAG COEFFICIENT FOR AFT SRB/ET ATTACH STRUTS

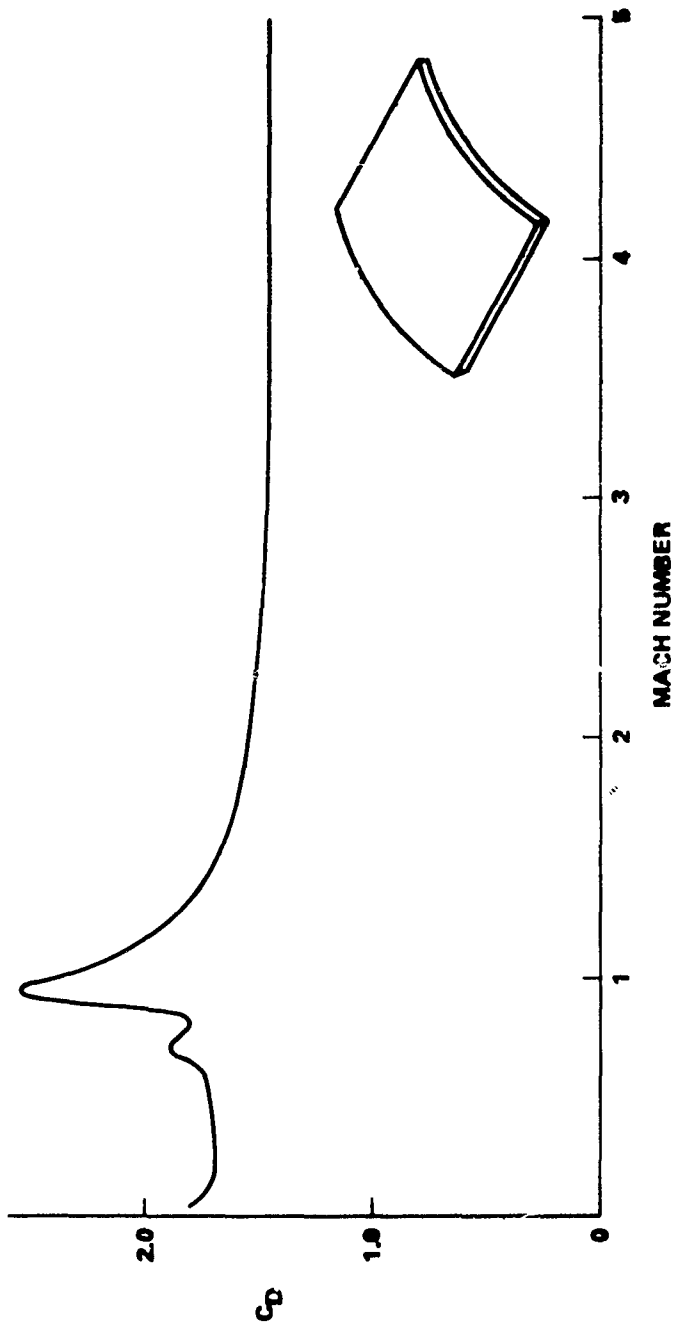


FIGURE A-4 DRAG COEFFICIENT FOR SRB MOTOR CASE SEGMENTS

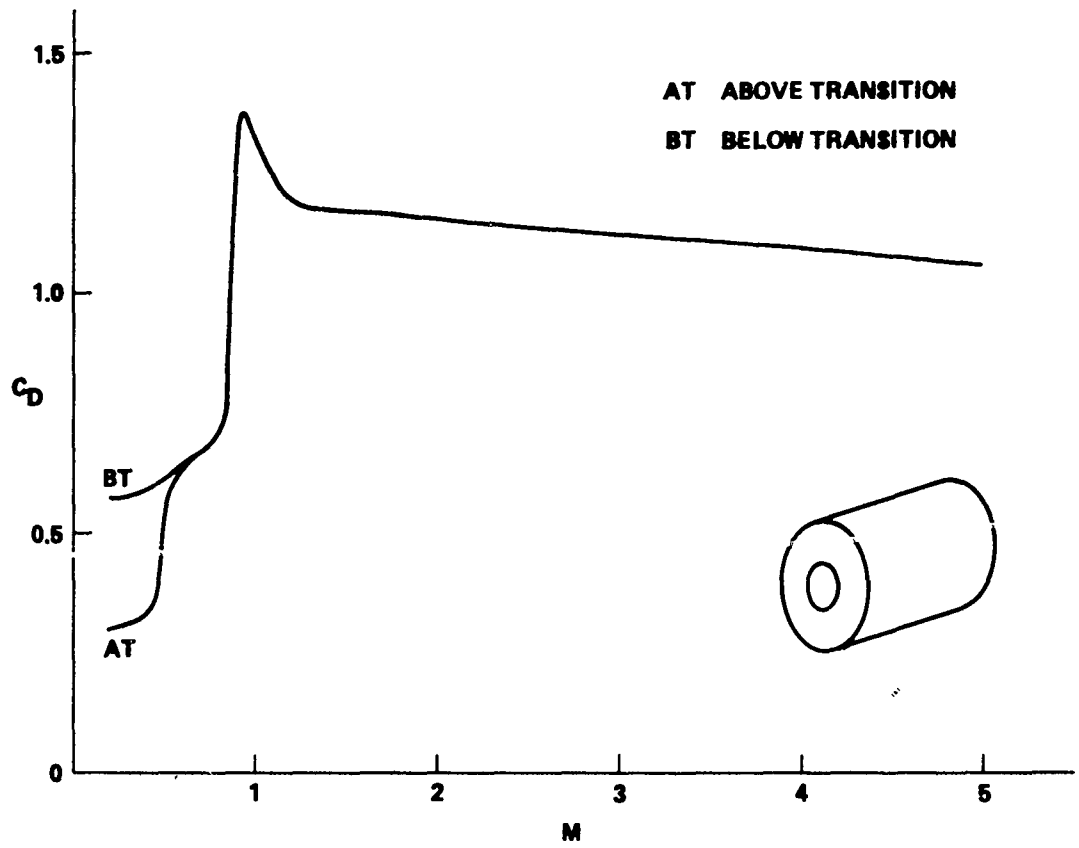


FIGURE A-5 DRAG COEFFICIENT FOR CLEVIS PINS

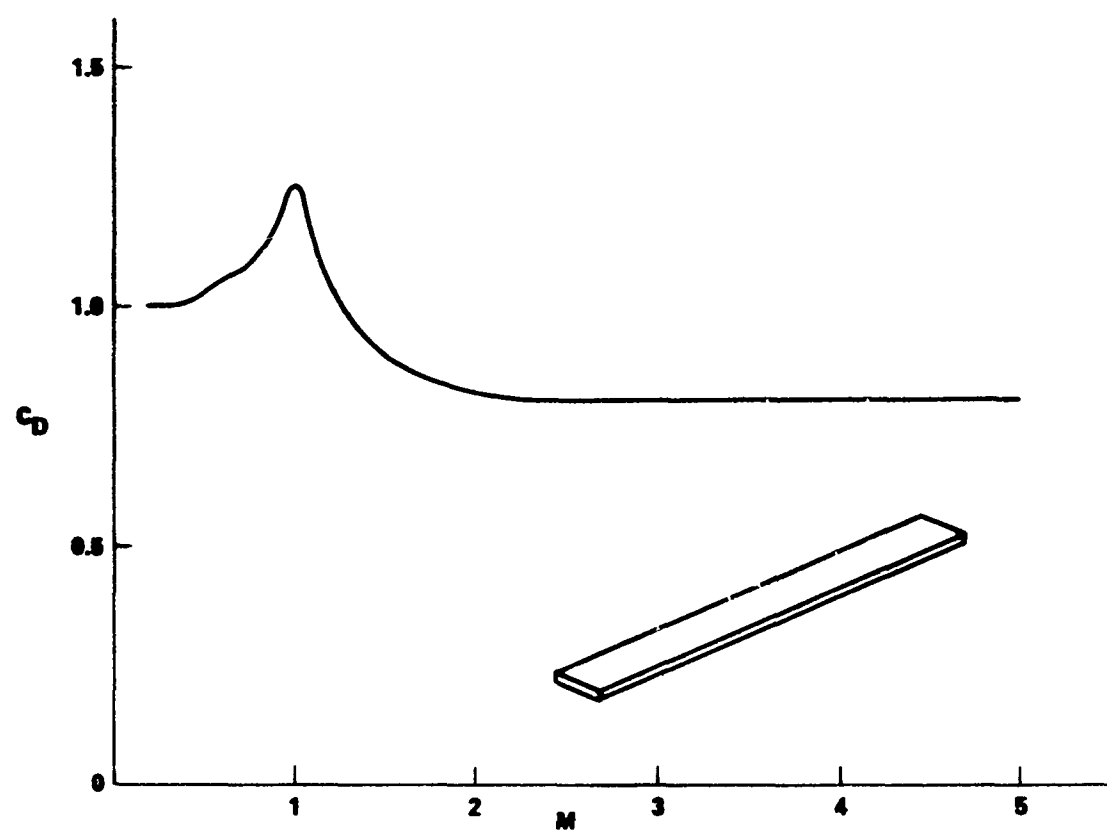


FIGURE A-6 DRAG COEFFICIENT FOR LONG, SLENDER SRM CASE,
SYSTEMS TUNNEL, AND LSC SEGMENTS

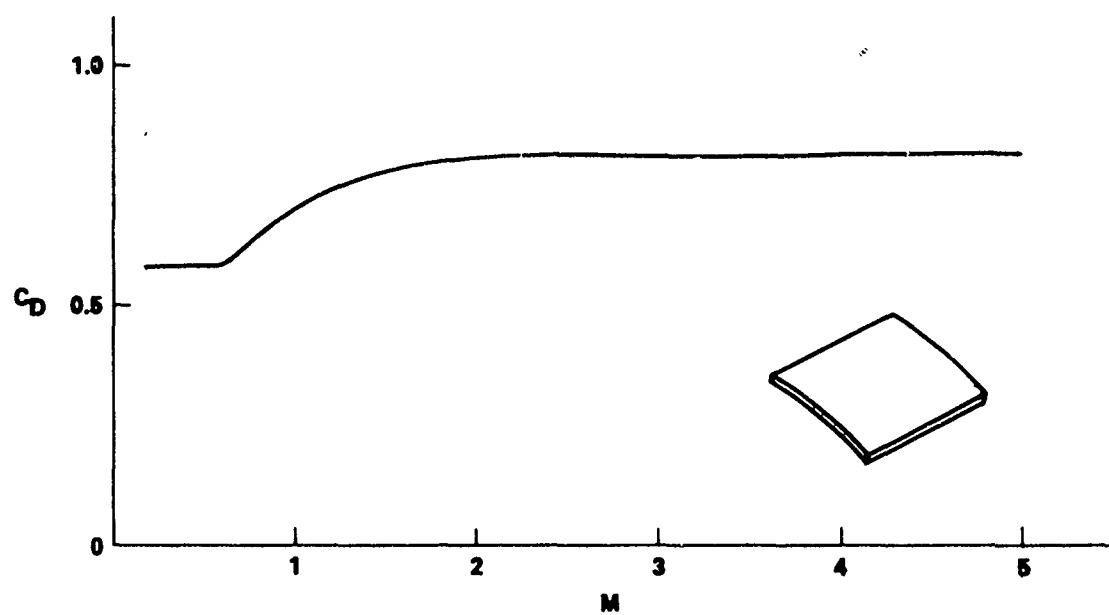


FIGURE A-7 DRAG COEFFICIENT FOR SHORT SRB SYSTEMS TUNNEL SEGMENTS

NSWC TR 80-417

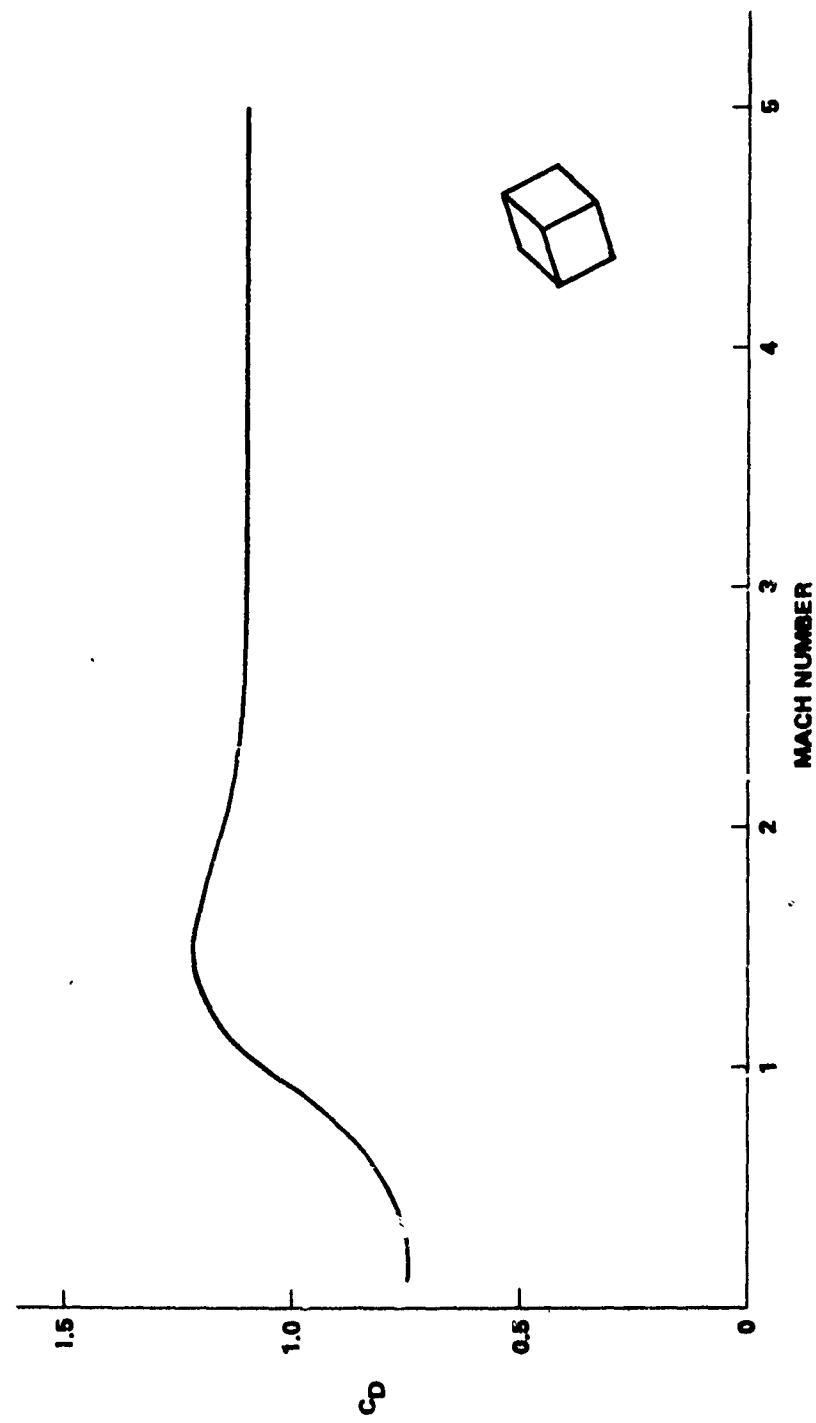


FIGURE A-8 DRAG COEFFICIENT FOR SRM PROPELLANT CUBES

NSWC TR 80-417

APPENDIX B

LISTING OF ET DEBRIS FRAGMENTS

CONFIGURATION: Integrated Vehicle

COMPONENT: External Tank (Forward Velocity = 180 fps)

TIME OF DESTRUCT ACTION (SEC): 10

Sheet 1 of 2

NSWC TR 80-417

Piece Description and Remarks	Number of Pieces	Weight of Each Piece (1b)	Total Weight (1b)	Reference Area (ft ²)	Ballistic Range (W/CDA) (1b/ft ²)	Velocity Increment (ft/sec)	C_D	C_L	Figure Number
(1) Forward Section - LOX Tank	1	6,500	6,500	594	8-16	3	B-1	B-1	
(2) Mid Section - Intertank and LH ₂ Tank	1	42,400	42,400	594	15-43	8	B-2	B-2	
(3) Aft Section - LH ₂ Tank	1	20,400	20,400	594	14-60	20	B-3	B-3	
(4) LOX Feedline Elbow	1	530	530	12	55-190	200	B-4	-	
(5) LOX Feedline Segment	2	135-325	460	12-30	14-54	200	B-4	-	
(6) LOX Antigeyser Line and Elbow	3	20-40	100	3-7	7-23	200	B-4	-	
(7) CO ₂ Pressurization Line	3	8-15	33	2-3.5	5-16	50-200	B-4	-	
(8) GH ₂ Pressurization Line	2	10-15	25	2.5-3.5	5-16	200	B-4	-	
(9) LOX Vent Valve Actuation Line	2	0.8	1.6	0.2	4-30	50	B-5	-	
(10) Nose Cap Purge Duct	2	0.8	1.6	0.2	4-30	50	B-5	-	
(11) Helium Injection Line	4	1.3	5.2	0.3	4-30	200	B-5	-	
(12) Skin Segment - LOX Tank (a) LOX Tank (b)	1 1	45 415	45 415	15 140	4	50	B-6	-	
LH ₂ Tank (a) LH ₂ Tank (b)	1 1	90 730	90 730	30 270	4	50 4	B-6	-	
(13) Ring Frame Stabilizer	8	0.1-5	20	0.04-1	2-32	200	B-7	-	
(14) Stability Ring Segment	14	4-22	98	2-9	1.6-3	200	B-8	-	
(15) Slosh Baffle Longitudinal Stringer	16-48	1-3	48	0.2-0.7	3.4-6	50	B-8	-	

CONFIGURATION: Integrated Vehicle

COMPONENT: External Tank (Forward Velocity = 180 fps)

TIME OF DESTRUCT ACTION (SEC): 10

Piece Description and Remarks	Number of Pieces	Weight of Each Piece (lb)	Total Weight (lb)	Reference Area (ft ²)	Ballistic Range (W/CDA) (1b/ft ²)	Velocity Increment (ft/sec)	Figure Number	C_D	C_L
(16) S1osh Baffle Segment	4-48	3.5-42	170	5-60	0.9-1.2	7	B-9	-	
(17) S1osh Baffle Tension Strap	160	0.1-0.2	24	0.2-0.3	0.4-0.7	50	B-8	-	
(18) S1osh Baffle Web	16-32	1.5-2.5	56	5.4	0.3-0.8	50	B-9	-	
(19) Cable Tray Segments	50	0.9-19	167	1-7	50-200	50-200	B-8	-	
(20) LSC Sheath Segments	50-200	0.006-0.05	2.2	0.01-0.08	0.5-0.8	2,300	B-8	-	
(21) Miscellaneous (Cabling, Bolts, Brackets, etc.)	100-500	0.01-5	~1,000	0.001-0.3	1-20	50-200	*	-	
	TOTAL		73,380						

* $C_D \approx 1.$

CONFIGURATION: Right SRB Separated

COMPONENT: External Tank (Forward Velocity = 300 fps)

TIME OF DESTRUCT ACTION (SEC): 20

Piece Description and Remarks	Number of Pieces	Weight of Each Piece (lb)	Total Weight (lb)	Reference Area (ft ²)	Ballistic Factor (W/CDA) (lb/ft ²)	Velocity Increment (ft/sec)	Figure Number
							CD
							C _L
(1) Forward Section - LOX Tank	1	6,500	6,500	594	8-16	5	B-1
(2) Mid Section - Intertank and LH ₂ Tank	1	42,000	42,000	594	15-43	11	B-2
(3) Aft Section - LH ₂ Tank	1	20,000	20,000	594	14-60	37	B-3
(4) LOX Feedline Elbow	1	530	530	12	55-190	210	B-4
(5) LOX Feedline Segment	2	135-325	460	12-30	14-54	210	B-4
(6) LOX Antigeyser Line and Elbow	3	20-40	100	3-7	7-23	210	B-4
(7) GO ₂ Pressurization Line	3	8-15	33	2-3.5	5-16	50-210	B-4
(8) GH ₂ Pressurization Line	2	10-15	25	2.5-3.5	5-16	210	B-4
(9) LOX Vent Valve Actuation Line	2	0.8	1.6	0.2	4-30	50	B-5
(10) Nose Cap Purge Duct	2	0.8	1.6	0.2	4-30	50	B-5
(11) Helium Injection Line	4	1.3	5.2	0.3	4-30	210	B-5
(12) Skin Segment - LOX Tank (a) LOX Tank (b) LH ₂ Tank (a) LH ₂ Tank (b) LH ₂ Tank (c)	1 1 1 1 1	45 415 90 730 860	45 415 90 730 860	15 140 30 270 320	4 4 4 4 4	50 50 210 210 210	B-6 B-6 B-6 B-6 B-6
(13) Ring Frame Stabilizer	8	0.1-5	20	0.04-1	2-32	210	B-7
(14) Stability Ring Segment	14	4-22	98	2-9	1.6-3	210	B-8

CONFIGURATION: Right SRB Separated

COMPONENT: External Tank (Forward Velocity = 300 fps)

TIME OF DESTRUCT ACTION (SEC): 20

Piece Description and Remarks	Number of Pieces	Weight of Each Piece (1b)	Total Weight (1b)	Reference Area (ft ²)	Ballistic Factor Range (W/C _D A) (1b/ft ²)	Velocity Increment (ft/sec)	C _D	Figure Number
(15) Slosh Baffle Longitudinal Stringer	16-48	1-3	48	0.2-0.7	3.4-6	50	B-8	-
(16) Slosh Baffle Segment	4-48	3.5-42	170	5-60	0.9-1.2	9	B-9	-
(17) Slosh Baffle Tension Strap	160	0.1-0.2	24	0.2-0.3	0.4-0.7	50	B-8	-
(18) Slosh Baffle Web	16-32	1.5-2.5	56	5.4	0.3-0.8	50	B-9	-
(19) Cable Tray Segments	50	0.9-19	167	1-7	50-200	50-210	B-8	-
(20) LSC Sheath Segments	50-200	0.006-0.05	2.2	0.01-0.08	0.5-0.8	2,300	B-8	-
(21) Miscellaneous (Cabling, Bolts, Brackets, etc.)	100-500	0.01-5	~1,000	0.001-0.3	1-20	50-210	*	-
TOTAL			73,380					

*C_D ≈ 1.

CONFIGURATION: Orbiter Separated

COMPONENT: External Tank (Forward Velocity = 360 fps)

TIME OF DESTRUCT ACTION (SEC): 20

Sheet 1 of 2

NSWC TR 80-417

Piece Description and Remarks	Number of Pieces	Weight of Each Piece (lb)	Total Weight (lb)	Reference Area (ft ²)	Ballistic Factor (W/CDA) (lb/ft ²)	Velocity Increment (ft/sec)	Figure Number
							C _D C _L
(1) Forward Section - LOX Tank	1	6,500	6,500	594	8-16	4	B-1 B-1
(2) Mid Section - Intertank and LH ₂ Tank	1	42,000	42,000	594	15-43	11	B-2 B-2
(3) Aft Section - LH ₂ Tank	1	20,000	20,000	594	4-60	35	B-3 B-3
(4) LOX Feedline Elbow	1	530	530	12	55-190	210	B-4 -
(5) LOX Feedline Segment	2	135-325	460	12-30	14-54	210	B-4 -
(6) LOX Antigeyser Line and Elbow	3	20-40	100	3-7	7-23	210	B-4 -
(7) CO ₂ Pressurization Line	3	8-15	33	2-3.5	5-16	50-210	B-4 -
(8) CH ₂ Pressurization Line	2	10-15	25	2.5-3.5	5-16	210	B-4 -
(9) LOX Vent Valve Actuation Line	2	0.8	1.6	0.2	4-30	50	B-5 -
(10) Nose Cap Purge Duct	2	0.8	1.6	0.2	4-30	50	B-5 -
(11) Helium Injection Line	4	1.3	5.2	0.3	4-30	210	B-5 -
(12) Skin Segment - LOX Tank (a) LOX Tank (b) LH ₂ Tank (a) LH ₂ Tank (b) LH ₂ Tank (c)	1 1 1 1 1	45 415 90 730 860	45 415 90 730 860	15 140 30 270 320	4 4 4 4 4	50 50 210 210 210	B-6 - B-6 - B-6 - B-6 - B-6 -
(13) Ring Frame Stabilizer	8	0.1-5	20	0.04-1	2-32	210	B-7 -
(14) Stability Ring Segment	14	4-22	98	2-9	1.6-3	210	B-8 -

CONFIGURATION: Orbiter Separated

COMPONENT: External Tank (Forward Velocity = 360 fps)

TIME OF DESTRUCT ACTION (SEC): 20

Sheet 2 of 2

NSWC TR 80-417

Piece Description and Remarks	Number of Pieces	Weight of Each Piece (lb)	Total Weight (lb)	Reference Area (ft ²)	Ballistic Factor Range (W/C _D A) (lb/ft ²)	Velocity Increment (ft/sec)	Figure Number
							C _D C _L
(15) Slosh Baffle Longitudinal Stringer	16-48	1-3	48	0.2-0.7	3.4-6	50	B-8 -
(16) Slosh Baffle Segment	4-48	3.5-42	170	5-60	0.9-1.2	9	B-9 -
(17) Slosh Baffle Tension Strap	160	0.1-0.2	24	0.2-0.3	0.4-0.7	50	B-8 -
(18) Slosh Baffle Web	16-32	1.5-2.5	56	5.4	0.3-0.8	50	B-9 -
(19) Cable Tray Segments	50	0.9-19	167	1-7	50-200	50-210	B-8 -
(20) LSC Sheath Segments	50-200	0.006-0.05	2.2	0.01-0.08	0.5-0.8	2,300	B-8 -
(21) Miscellaneous (Cabling, Bolts, Brackets, etc.)	100-500	0.01-5	~1,000	0.001-0.3	1-20	50-210	* --
TOTAL			73,380				

*C_D ≈ 1.

CONFIGURATION: Integrated Vehicle

COMPONENT: External Tank (Forward Velocity = 1,070 fps)

Sheet 1 of 2

TIME OF DESTRUCT ACTION (SEC): 50

Piece Description and Remarks	Number of Pieces	Weight of Each Piece (1b)	Total Weight (1b)	Reference Area (ft ²)	Ballistic Factor Range (W/C _D ^A /lb/ft ²)	Velocity Increment (ft/sec)	Figure Number
							C _D C _L
(1) Forward Section - LOX Tank	1	6,500	6,500	594	8-16	16	B-1 B-1
(2) Mid Section - Intertank and LH ₂ Tank	1	42,000	42,000	594	1.5-43	21	B-2 B-2
(3) Aft Section - LH ₂ Tank	1	20,000	20,000	594	14-60	120	B-3 B-3
(4) LOX Feedline Elbow	1	530	530	12	55-190	240	B-4 -
(5) LOX Feedline Segment	2	135-325	460	12-30	14-54	240	B-4 -
(6) LOX Antigeyser Line and Elbow	3	20-40	100	3-7	7-23	240	B-4 -
(7) CO ₂ Pressurization Line	3	8-15	33	2-3.5	5-16	50-240	B-4 -
(8) CH ₄ Pressurization Line	2	10-15	25	2.5-3.5	5-16	240	B-4 -
(9) LOX Vent Valve Actuation Line	2	0.8	1.6	0.2	4-30	50	B-5 -
(10) Nose Cap Purge Duct	2	0.8	1.6	0.2	4-30	50	B-5 -
(11) Helium Injection Line	4	1.3	5.2	0.3	4-30	240	B-5 -
(12) Skin Segment - LOX Tank (a)	1	45	45	15	4	50	B-6 -
LOX Tank (b)	1	41.5	41.5	140	4	50	B-6 -
LH ₂ Tank (a)	1	90	90	30	4	240	B-6 -
LH ₂ Tank (b)	1	730	730	270	4	240	B-6 -
LH ₂ Tank (c)	1	860	860	320	4	240	B-6 -
(13) Ring Frame Stabilizer	8	0.1-5	20	0.04-1	2-32	240	B-7 -
(14) Stability Ring Segment	14	4-22	98	2-9	1.6-3	240	B-8 -

CONFIGURATION: Integrated Vehicle

COMPONENT: External Tank (Forward Velocity = 1,070 fps)

TIME OF DESTRUCT ACTION (SEC): 50
Sheet 2 of 2

Piece Description and Remarks	Number of Pieces	Weight of Each Piece (1b)	Total Weight (1b)	Reference Area (ft ²)	Ballistic Factor Range (W/C _D A) (lb/ft ²)	Velocity Increment (ft/sec)	Figure Number	C_D	C_L
(15) Slosh Baffle Longitudinal Stringer	16-48	1-3	48	0.2-0.7	3.4-6	50	B-8	-	
(16) Slosh Baffle Segment	4-48	3.5-42	170	5-60	0.9-1.2	16	B-9	-	
(17) Slosh Baffle Tension Strap	160	0.1-0.2	24	0.2-0.3	0.4-0.7	50	B-8	-	
(18) Slosh Baffle Web	16-32	1.5-2.5	56	5.4	0.3-.8	50	B-9	-	
(19) Cable Tray Segments	50	0.9-19	167	1-7	50-200	50-240	B-8	-	
(20) LSC Sheath Segments	50-200	0.006-0.05	2.2	0.01-0.08	0.5-0.8	2,300	B-8	-	
(21) Miscellaneous (Cabling, Bolts, Brackets, etc.)	100-500	0.01-5	~1,000	0.001-0.3	1-20	50-240	*	-	
TOTAL			73,380						

* $C_D \approx 1.$

CONFIGURATION: Right SRB Separated

COMPONENT: External Tank (Forward Velocity = 1,070 fps)

Sheet 1 of 2

TIME OF DESTRUCT ACTION (SEC) : 52

Piece Description and Remarks	Number of Pieces	Weight of Each Piece (1lb)	Total Weight (1lb)	Reference Area (ft ²)	Ballistic Factor Range (W/C _{DA}) (1lb/ft ²)	Velocity Increment (ft/sec)	C _D	C _L	Figure Number
(1) Forward Section - LOX Tank	1	6,500	6,500	594	8-16	14	B-1	B-1	
(2) Mid Section - Intertank and LH ₂ Tank	1	42,000	42,000	594	15-43	1.9	B-2	B-2	
(3) Aft Section - LH ₂ Tank	1	20,000	20,000	594	14-60	100	B-3	B-3	
(4) LOX Feedline Elbow	1	530	530	12	55-190	240	B-4	-	
(5) LOX Feedline Segment	2	135-325	460	12-30	14-54	240	B-4	-	
(6) LOX Antigeyser Line and Elbow	3	20-40	100	3-7	7-23	240	B-4	-	
(7) CO ₂ Pressurization Line	3	8-15	33	2-3.5	5-16	50-240	B-4	-	
(8) CH ₂ Pressurization Line	2	10-15	25	2.5-3.5	5-16	240	B-4	-	
(9) LOX Vent Valve Actuation Line	2	0.8	1.6	0.2	4-30	50	B-5	-	
(10) Nose Cap Purge Duct	2	0.8	1.6	0.2	4-30	50	B-5	-	
(11) Helium Injection Line .	4	1.3	5.2	0.3	4-30	240	B-5	-	
(12) Skin Segment - LOX Tank (a) LOX Tank (b)	1	45	15	4	50	B-6	-		
LH ₂ Tank (a)	1	415	415	4	50	B-6	-		
LH ₂ Tank (b)	1	90	90	4	240	B-6	-		
LH ₂ Tank (c)	1	730	730	4	240	B-6	-		
860	860	860	320	4	240	B-6	-		
(13) Ring Frame Stabilizer	8	0.1-5	20	0.04-1	2-32	240	B-7	-	
(14) Stability Ring Segment	14	4-22	98	2-9	1.6-3	240	B-8	-	

CONFIGURATION: Right SRB Separated

COMPONENT: External Tank (Forward Velocity = 1,070 fps)

TIME OF DESTRUCT ACTION (SEC): 52

Sheet 2 of 2

NSWC TR 80-417

Piece Description and Remarks	Number of Pieces	Weight of Each Piece (1b)	Total Weight (1b)	Reference Area (ft ²)	Ballistic Factor (W/C _D A) (1b/ft ²)	Velocity Increment (ft/sec)	C _D	C _L	Figure Number
(15) Slosh Baffle Longitudinal Stringer	16-48	1-3	48	0.2-0.7	3.4-6	50	B-8	-	
(16) Slosh Baffle Segment	4-48	3.5-42	170	5-60	0.9-1.2	15	B-9	-	
(17) Slosh Baffle Tension Strap	160	0.1-0.2	24	0.2-0.3	0.4-0.7	50	B-8	-	
(18) Slosh Baffle Web	16-32	1.5-2.5	56	5.4	0.3-0.8	50	B-9	-	
(19) Cable Tray Segments	50	0.9-19	167	1-7	50-200	50-240	B-8	-	
(20) LSC Sheath Segments	50-200	0.006-0.05	2.2	0.01-0.08	0.5-0.8	2,300	B-8	-	
(21) Miscellaneous (Cabling, Bolts, Brackets, etc.)	100-500	0.01-5	~1,000	0.001-0.3	1-20	50-240	*	-	
TOTAL			73,380						

*C_D ≈ 1.

CONFIGURATION: Orbiter Separated

COMPONENT: External Tank (Forward Velocity = 1,300 fps)

TIME OF DESTRUCT ACTION (SEC): 65

Piece Description and Remarks	Number of Pieces	Weight of Each Piece (lb)	Total Weight (lb)	Reference Area (ft ²)	Ballistic Factor (W/CDA) (lb/ft ²)	Velocity Increment (ft/sec)	Figure Number	C _D	C _L
(1) Forward Section - LOX Tank	1	5,500	6,500	594	8-16	13	B-1	B-1	
(2) Mid Section - Intertank and LH ₂ Tank	1	42,000	42,000	594	15-43	17	B-2	B-2	
(3) Aft Section - LH ₂ Tank	1	20,000	20,000	594	14-60	96	B-3	B-3	
(4) LOX Feedline Elbow	1	530	530	12	55-190	250	B-4	-	
(5) LOX Feedline Segment	2	135-325	460	12-30	14-54	250	B-4	-	
(6) LOX Antigeyser Line and Elbow	3	20-40	100	3-7	7-23	250	B-4	-	
(7) CO ₂ Pressurization Line	3	8-15	33	2-3.5	5-16	50-250	B-4	-	
(8) GH ₂ Pressurization Line	2	10-15	25	2.5-3.5	5-16	250	B-4	-	
(9) LOX Vent Valve Actuation Line	2	0.8	1.6	0.2	4-30	50	B-5	-	
(10) Nose Cap Purge Duct	2	0.8	1.6	0.2	4-30	50	B-5	-	
(11) Helium Injection Line	4	1.3	5.2	0.3	4-30	250	B-5	-	
(12) Skin Segment - LOX Tank (a)	1	45	15	4	50	B-6	-		
LOX Tank (b)	1	415	140	4	50	B-6	-		
LH ₂ Tank (a)	1	90	30	4	250	B-6	-		
LH ₂ Tank (b)	1	730	270	4	250	B-6	-		
LH ₂ Tank (c)	1	860	320	4	250	B-6	-		
(13) Ring Frame Stabilizer	8	0.1-5	20	0.04-1	2-32	250	B-7	-	
(14) Stability Ring Segment	14	4-22	98	2-9	1.6-3	250	B-8	-	

Sheet 2 of 2

CONFIGURATION: Orbiter Separated
 COMPONENT: External Tank (Forward Velocity = 1,300 fps)

TIME OF DESTRUCT ACTION (SEC): 65

Piece Description and Remarks	Number of Pieces	Weight of Each Piece (1b)	Total Weight (1b)	Reference Area (ft ²)	Ballistic Factor (W/C _D A) (1b/ft ²)	Velocity Increment (ft/sec)	Figure Number
							C _D C _L
(15) Slosh Baffle Longitudinal Stringer	16-48	1-3	48	0.2-0.7	3.4-6	50	B-8 -
(16) Slosh Baffle Segment	4-48	3.5-42	170	5-60	0.9-1.2	14	B-9 -
(17) Slosh Baffle Tension Strap	160	0.1-0.2	24	0.2-0.3	0.4-0.7	50	B-8 -
(18) Slosh Baffle Web	16-32	1.5-2.5	56	5.4	0.3-0.8	50	B-9 -
(19) Cable Tray Segments	50	0.9-19	167	1-7	50-200	50-250	B-8 -
(20) LSC Sheath Segments	50-200	0.006-0.05	2.2	0.01-0.08	0.5-0.8	2,300	B-8 -
(21) Miscellaneous (Cabling, Bolts, Brackets, etc.)	100-500	0.01-5	~1,000	0.001-0.3	1-20	50-250	* -
TOTAL			73,380				

 $*C_D \approx 1.$

CONFIGURATION: Integrated Vehicle

COMPONENT: External Tank (Forward Velocity = 3,200 fps)

TIME OF DESTRUCT ACTION (SEC): 100

Sheet 1 of 2

Piece Description and Remarks	Number of Pieces	Weight of Each Piece (lb)	Total Weight (lb)	Reference Area (ft ²)	Ballistic Factor (W/CDA) (1lb/ft ²)	Velocity Increment (ft/sec)	Figure Number	C_D	C_L
(1) Forward Section - LOX Tank	1	6,500	6,500	594	8-16	21	B-1	B-1	
(2) Mid Section - Intertank and LH ₂ Tank	1	42,000	42,000	594	15-43	22	B-2	B-2	
(3) Aft Section - LH ₂ Tank	1	20,000	20,000	594	14-60	170	B-3	B-3	
(4) LOX Feedline Elbow	1	530	530	12	55-190	260	B-4	-	
(5) LOX Feedline Segment	2	135-325	460	12-30	14-54	260	B-4	-	
(6) LOX Antigeyser Line and Elbow	3	20-40	100	3-7	7-23	260	B-4	-	
(7) GO ₂ Pressurization Line	3	8-15	33	2-3.5	5-16	50-260	B-4	-	
(8) GH ₂ Pressurization Line	2	10-15	25	2.5-3.5	5-16	260	B-4	-	
(9) LOX Vent Valve Actuation Line	2	0.8	1.6	0.2	4-30	50	B-5	-	
(10) Nose Cap Purge Duct	2	0.8	1.6	0.2	4-30	50	B-5	-	
(11) Helium Injection Line	4	1.3	5.2	0.3	4-30	260	B-5	-	
(12) Skin Segment - LOX Tank (a)	1	45	45	15	4	50	B-6	-	
LOX Tank (b)	1	415	415	140	4	50	B-6	-	
LH ₂ Tank (a)	1	90	90	30	4	260	B-6	-	
LH ₂ Tank (b)	1	730	730	270	4	260	B-6	-	
LH ₂ Tank (c)	1	860	860	320	4	260	B-6	-	
(13) Ring Frame Stabilizer	8	0.1-5	20	0.04-1	2-32	260	B-7	-	
(14) Stability Ring Segment	14	4-22	98	2-9	1.6-3	260	B-8	-	

CONFIGURATION: Integrated Vehicle

COMPONENT: External Tank (Forward Velocity = 3,200 fps)

TIME OF DESTRUCT ACTION (SEC) : 100

Piece Description and Remarks	Number of Pieces	Weight of Each Piece (1b)	Total Weight (1b)	Reference Area (ft ²)	Ballistic Factor Range (W/C _D A) (1b/ft ²)	Velocity Increment (ft/sec)	Figure Number	C _L	C _D	Figure Number
(15) Slosh Baffle Longitudinal Stringer	16-48	1-3	48	0.2-0.7	3.4-6	50	B-8	-		
(16) Slosh Baffle Segment	4-48	3.5-42	170	5-60	0.9-1.2	1.6	B-9	-		
(17) Slosh Baffle Tension Strap	160	0.1-0.2	24	0.2-0.3	0.4-0.7	50	B-8	-		
(18) Slosh Baffle Web	16-32	1.5-2.5	56	5.4	0.3-0.8	50	B-9	-		
(19) Cable Tray Segments	50	0.9-19	167	1-7	50-200	50-260	B-8	-		
(20) LSC Sheath Segments	50-200	0.006-0.05	2.2	0.01-0.08	0.5-0.8	2,300	B-8	-		
(21) Miscellaneous (Cabling, Bolts, Brackets, etc.)	100-500	0.01-5	~1,000	0.001-0.3	1-20	50-260	*	-		
TOTAL			73,380							

*C_D ≈ 1.

CONFIGURATION: Right SRB Separated

COMPONENT: External Tank (Forward Velocity = 3,700 fps)

TIME OF DESTRUCT ACTION (SEC): 115

Piece Description and Remarks	Number of Pieces	Weight of Each Piece (lb)	Total Weight (lb)	Reference Area (ft ²)	Ballistic Factor Range (W/CDA) (lb/ft ²)	Velocity Increment (ft/sec)	Figure Number	C _D	C _L
(1) Forward Section - LOX Tank	1	6,500	6,500	594	8-16	28	B-1	B-1	
(2) Mid Section - Intertank and LH ₂ Tank	1	42,000	42,000	594	15-43	25	B-2	B-2	
(3) Aft Section - LH ₂ Tank	1	20,000	20,000	594	14-60	190	B-3	B-3	
(4) LOX Feedline Elbow	1	530	530	12	55-190	260	B-4	-	
(5) LOX Feedline Segment	2	135-325	460	12-30	14-54	260	B-4	-	
(6) LOX Antigeyser Line and Elbow	3	20-40	100	3-7	7-23	260	B-4	-	
(7) CO ₂ Pressurization Line	3	8-15	33	2-3.5	5-16	50-260	B-4	-	
(8) CH ₄ Pressurization Line	2	10-15	25	2.5-3.5	5-16	50-260	B-4	-	
(9) LOX Vent Valve Actuation Line	2	0.8	1.6	0.2	4-30	50	B-5	-	
(10) Nose Cap Purge Duct	2	0.8	1.6	0.2	4-30	50	B-5	-	
(11) Helium Injection Line	4	1.3	5.2	0.3	4-30	260	B-5	-	
(12) Skin Segment - LOX Tank (a) LOX Tank (b) LH ₂ Tank (a) LH ₂ Tank (b) LH ₂ Tank (c)	1 1 1 1 1	45 415 90 730 860	45 415 90 730 860	15 140 30 270 320	4 4 4 4 4	50 50 260 260 260	B-6 B-6 B-6 B-6 B-6	- - - - -	
(13) Ring Frame Stabilizer	8	0.1-5	20	0.04-1	2-32	260	B-7	-	
(14) Stability Ring Segment	14	4-22	98	2-9	1.6-3	260	B-8	-	

CONFIGURATION: Right SRB Separated

COMPONENT: External Tank (Forward Velocity = 3,700 fps)

Sheet 2 of 2

TIME OF DESTRUCT ACTION (SEC): 115

Piece Description and Remarks	Number of Pieces	Weight of Each Piece (1b)	Total Weight (1b)	Reference Area (ft ²)	Ballistic Factor Range (W/C _D A) (1b/ft ²)	Velocity Increment (ft/sec)	Figure Number
					C _D	C _L	
(15) Slosh Baffle Longitudinal Stringer	16-48	1-3	48	0.2-0.7	3.4-6	50	B-8
(16) Slosh Baffle Segment	4-48	3.5-42	170	5-60	0.9-1.2	22	B-9
(17) Slosh Baffle Tension Strap	160	0.1-0.2	24	0.2-0.3	0.4-0.7	50	B-8
(18) Slosh Baffle Web	16-32	1.5-2.5	56	5.4	0.3-0.8	50	B-9
(19) Cable Tray Segments	50	0.9-19	167	1-7	50-200	50-260	B-8
(20) LSC Sheath Segments	50-200	0.006-0.05	2.2	0.01-0.08	0.5-0.8	2,300	B-8
(21) Miscellaneous (Cabling, Bolts, Brackets, etc.)	100-500	0.01-5	~1,000	0.001-0.3	1-20	50-260	*
TOTAL			73,380				

*C_D ≈ 1.

CONFIGURATION: Orbiter Separated

COMPONENT: External Tank (Forward Velocity = 4,000 fps)

TIME OF DESTRUCT ACTION (SEC): 115

Sheet 1 of 2

NSWC TR 80-417

Piece Description and Remarks	Number of Pieces	Weight of Each Piece (lb)	Total Weight (lb)	Reference Area (ft ²)	Ballistic Factor (W/CDA) (lb/ft ²)	Velocity Increment (ft/sec)	Figure Number	C_D	C_L
(1) Forward Section - LOX Tank	1	6,500	6,500	594	8-16	24	B-1	B-1	
(2) Mid Section - Intertank and LH ₂ Tank	1	42,000	42,000	594	15-43	27	B-2	B-2	
(3) Aft Section - LH ₂ Tank	1	20,000	20,000	594	14-60	200	B-3	B-3	
(4) LOX Feedline Elbow	1	530	530	12	55-190	260	B-4	-	
(5) LOX Feedline Segment	2	135-325	460	12-30	14-54	260	B-4	-	
(6) LOX Antigeyser Line and Elbow	3	20-40	100	3-7	7-23	260	B-4	-	
(7) GO ₂ Pressurization Line	3	8-15	33	2-3.5	5-16	50-260	B-4	-	
(8) GH ₂ Pressurization Line	2	10-15	25	2.5-3.5	5-16	260	B-4	-	
(9) LOX Vent Valve Actuation Line	2	0.8	1.6	0.2	4-30	50	B-5	-	
(10) Nose Cap Purge Duct	2	0.8	1.6	0.2	4-30	50	B-5	-	
(11) Helium Injection Line	4	1.3	5.2	0.3	4-30	260	B-5	-	
(12) Skin Segment - LOX Tank (a) LOX Tank (b) LH ₂ Tank (a) LH ₂ Tank (b) LH ₂ Tank (c)	1 1 1 1 1	45 415 90 730 860	45 415 90 730 860	15 140 30 270 320	4 4 4 4 4	50 50 260 260 260	B-6 B-6 B-6 B-6 B-6	- - - - -	
(13) Ring Frame Stabilizer	3	0.1-5	20	0.04-1	2-32	260	B-7	-	
(14) Stability Ring Segment	14	4-22	98	2-9	1.6-3	260	B-8	-	

CONFIGURATION: Orbiter Separated

COMPONENT: External Tank (Forward Velocity = 4,000 fps)

TIME OF DESTRUCT ACTION (SEC): 115

Piece Description and Remarks	Number of Pieces	Weight of Each Piece (lb)	Total Weight (lb)	Reference Area (ft ²)	Ballistic Factor Range (W/CDA) (1b/ft ²)	Velocity Increment (ft/sec)	Figure Number	C_D	C_L
(15) Slosh Baffle Longitudinal Stringer	16-48	1-3	48	0.2-0.7	3.4-6	50	B-8	-	
(16) Slosh Baffle Segment	4-48	3.5-42	170	5-60	0.9-1.2	20	B-9	-	
(17) Slosh Baffle Tension Strap	160	0.1-0.2	24	0.2-0.3	0.4-0.7	50	B-8	-	
(18) Slosh Baffle Web	16-32	1.5-2.5	56	5.4	0.3-0.8	50	B-9	-	
(19) Cable Tray Segments	50	0.9-19	16?	1-7	50-200	50-260	B-8	-	
(20) LSC Sheath Segments	50-200	0.006-0.05	2.2	0.01-0.08	0.5-0.8	2,300	B-8	-	
(21) Miscellaneous (Cabling, Bolts, Brackets, etc.)	100-500	0.01-5	~1,000	0.001-0.3	1-20	50-260	*	-	
TOTAL			73,380						

* $C_D \approx 1.$

CONFIGURATION: SRB's and Orbiter Separated

COMPONENT: External Tank (Forward Velocity = 13,800 fps)

Sheet 1 of 2

TIME OF DESTRUCT ACTION (SEC): 350

Piece Description and Remarks	Number of Pieces	Weight of Each Piece (lb)	Total Weight (lb)	Reference Area (ft ²)	Ballistic Factor Range (W/CDA) (lb/ft ²)	Velocity Increment (ft/sec)	Figure Number	
							C _D	C _L
(1) Forward Section - LOX Tank	1	6,500	6,500	594	8-16	40	B-1	B-1
(2) Mid Section - Intertank and LH ₂ Tank	1	42,000	42,000	594	15-43	34	B-2	B-2
(3) Aft Section - LH ₂ Tank	1	20,000	20,000	594	14-60	180	B-3	B-3
(4) LOX Feedline Elbow	1	530	530	12	55-190	210	B-4	-
(5) LOX Feedline Segment	2	135-325	460	12-30	14-54	210	B-4	-
(6) LOX Antigeyser Line and Elbow	3	20-40	100	3-7	7-23	210	B-4	-
(7) GO ₂ Pressurization Line	3	8-15	33	2-3.5	5-16	75-210	B-4	-
(8) GH ₂ Pressurization Line	2	10-15	25	2.5-3.5	5-16	210	B-4	-
(9) LOX Vent Valve Actuation Line	2	0.8	1.6	0.2	4-30	75	B-5	-
(10) Nose Cap Purge Duct	2	0.8	1.6	0.2	4-30	75	B-5	-
(11) Helium Injection Line	4	1.3	5.2	0.3	4-30	210	B-5	-
(12) Skin Segment - LOX Tank (a)	1	45	45	15	4	75	B-6	-
LOX Tank (b)	1	415	415	140	4	75	B-6	-
LH ₂ Tank (a)	1	90	90	30	4	210	B-6	-
LH ₂ Tank (b)	1	730	730	270	4	210	B-6	-
LH ₂ Tank (c)	1	860	860	320	4	210	B-6	-
(13) Ring Frame Stabilizer	8	0.1-5	20	0.04-1	2-32	210	B-7	-
(14) Stability Ring Segment	14	4-22	98	2-9	1.6-3	210	B-8	-

CONFIGURATION: SRB's and Orbiter Separated

Sheet 2 of 2

COMPONENT: External Tank (Forward Velocity = 13,800 fps)

TIME OF DESTRUCT ACTION (SEC): 350

Piece Description and Remarks	Number of Pieces	Weight of Each Piece (lb)	Total Weight (lb)	Reference Area (ft ²)	Ballistic Factor (W/C _D A) (1b/ft ²)	Velocity Increment (ft/sec)	Figure Number	C _D	C _L
(15) Slosh Baffle Longitudinal Stringer	16-48	1-3	48	0.2-0.7	3.4-6	75	B-8	-	
(16) Slosh Baffle Segment	4-48	3.5-42	170	5-60	0.9-1.2	22	B-9	-	
(17) Slosh Baffle Tension Strap	160	0.1-0.2	24	0.2-0.3	0.4-0.7	75	B-8	-	
(18) Slosh Baffle Web	16-32	1.5-2.5	56	5.4	0.3-0.8	75	B-9	-	
(19) Cable Tray Segments	50	0.9-19	167	1-7	50-200	75-210	B-8	-	
(20) LSC Sheath Segments	50-200	0.006-0.05	2.2	0.01-0.08	0.5-0.8	2,300	B-8		
(21) Miscellaneous (Cabling, Bolts, Brackets, etc.)	100-500	0.01-5	~1,000	0.001-0.3	1-20	75-210	*	-	
TOTAL			73,380						

*C_D ≈ 1.

CONFIGURATION: SRB's and Orbiter Separated

COMPONENT: External Tank (Forward Velocity = 22,100 fps)

TIME OF DESTRUCT ACTION (SEC): 450

Piece Description and Remarks	Number of Pieces	Weight of Each Piece (lb)	Total Weight (lb)	Reference Area (ft ²)	Ballistic Factor Range (W/CDA) (1b/ft ²)	Velocity Increment (ft/sec)	Figure Number	C _D	C _L
(1) Forward Section - LOX Tank	1	6,500	6,500	594	8-16	27	B-1	B-1	
(2) Mid Section - Intertank and LH ₂ Tank	1	42,000	42,000	594	15-43	45	B-2	B-2	
(3) Aft Section - LH ₂ Tank	1	20,000	20,000	594	14-60	51	B-3	B-3	
(4) LOX Feedline Elbow	1	530	530	12	55-190	260	B-4	-	
(5) LOX Feedline Segment	2	135-325	460	12-30	14-54	260	B-4	-	
(6) LOX Antigeyser Line and Elbow	3	20-40	100	3-7	7-23	260	B-4	-	
(7) GO ₂ Pressurization Line	3	8-15	33	2-3.5	5-16	115-260	B-4	-	
(8) CH ₂ Pressurization Line	2	10-15	25	2.5-3.5	5-16	115-260	B-4	-	
(9) LOX Vent Valve Actuation Line	2	0.8	1.6	0.2	4-30	115	B-5	-	
(10) Nose Cap Purge Duct	2	0.8	1.6	0.2	4-30	115	B-5	-	
(11) Helium Injection Line	4	1.3	5.2	0.3	4-30	260	B-5	-	
(12) Skin Segment - LOX Tank (a) LOX Tank (b) LH ₂ Tank (a) LH ₂ Tank (b) LH ₂ Tank (c)	1 1 1 1 1	45 415 90 730 860	45 415 90 730 860	15 140 30 270 320	4 4 4 4 4	115 115 260 260 260	B-6 B-6 B-6 B-6 B-6	- - - - -	
(13) Ring Frame Stabilizer	8	0.1-5	20	0.04-1	2-32	260	B-7	-	
(14) Stability Ring Segment	14	4-22	98	2-9	1.6-3	260	B-7	-	

CONFIGURATION: SRB's and Orbiter Separated

COMPONENT: External Tank (Forward Velocity = 22,100 fps)

Sheet 2 of 2

TIME OF DESTRUCT ACTION (SEC): 4.50

Piece Description and Remarks	Number of Pieces	Weight of Each Piece (lb)	Total Weight (lb)	Reference Area (ft ²)	Ballistic Factor Range (W/C _D A) (lb/ft ²)	Velocity Increment (ft/sec)	Figure Number	C _D	C _L
(15) Slosh Baffle Longitudinal Stringer	16-48	1-3	48	0.2-0.7	3.4-6	115	B-8	-	
(16) Slosh Baffle Segment	4-48	3.5-42	170	5-60	0.9-1.2	43	B-9	-	
(17) Slosh Baffle Tension Strap	160	0.1-0.2	24	0.2-0.3	0.4-0.7	115	B-8	-	
(18) Slosh Baffle Web	16-32	1.5-2.5	56	5.4	0.3-0.8	115	B-9	-	
(19) Cable Tray Segments	50	0.9-19	167	1-7	50-200	115-260	B-8	-	
(20) LSC Sheath Segments	50-200	0.006-0.05	2.2	0.01-0.08	0.5-0.8	2,300	B-8	-	
(21) Miscellaneous (Cabling, Bolts, Brackets, etc.)	100-500	0.01-5	~1,000	0.001-0.3	1-20	115-260	*	-	
TOTAL			73,380						

*C_D ≈ 1.

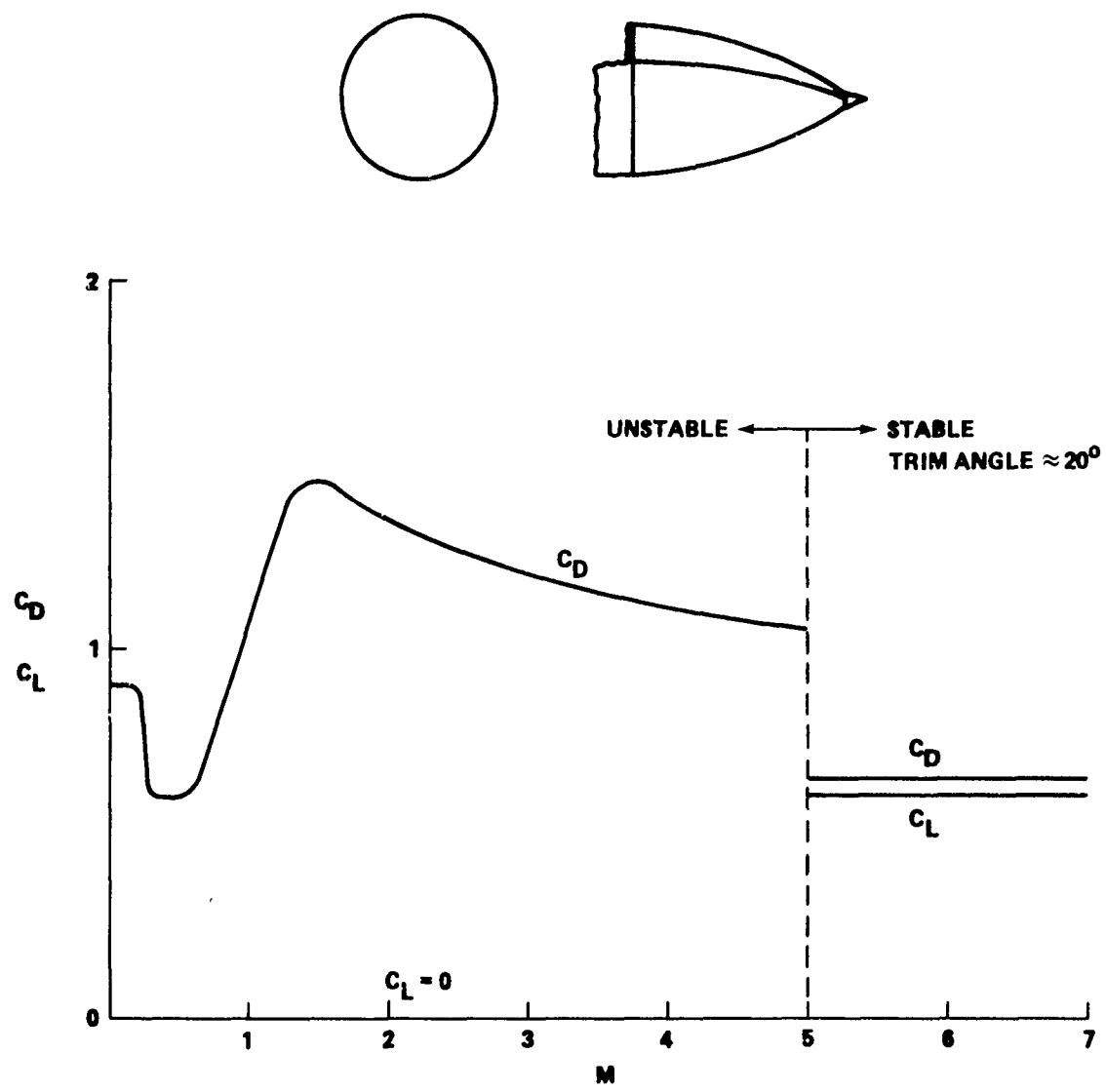


FIGURE B-1 LIFT AND DRAG COEFFICIENTS FOR FORWARD ET SECTION

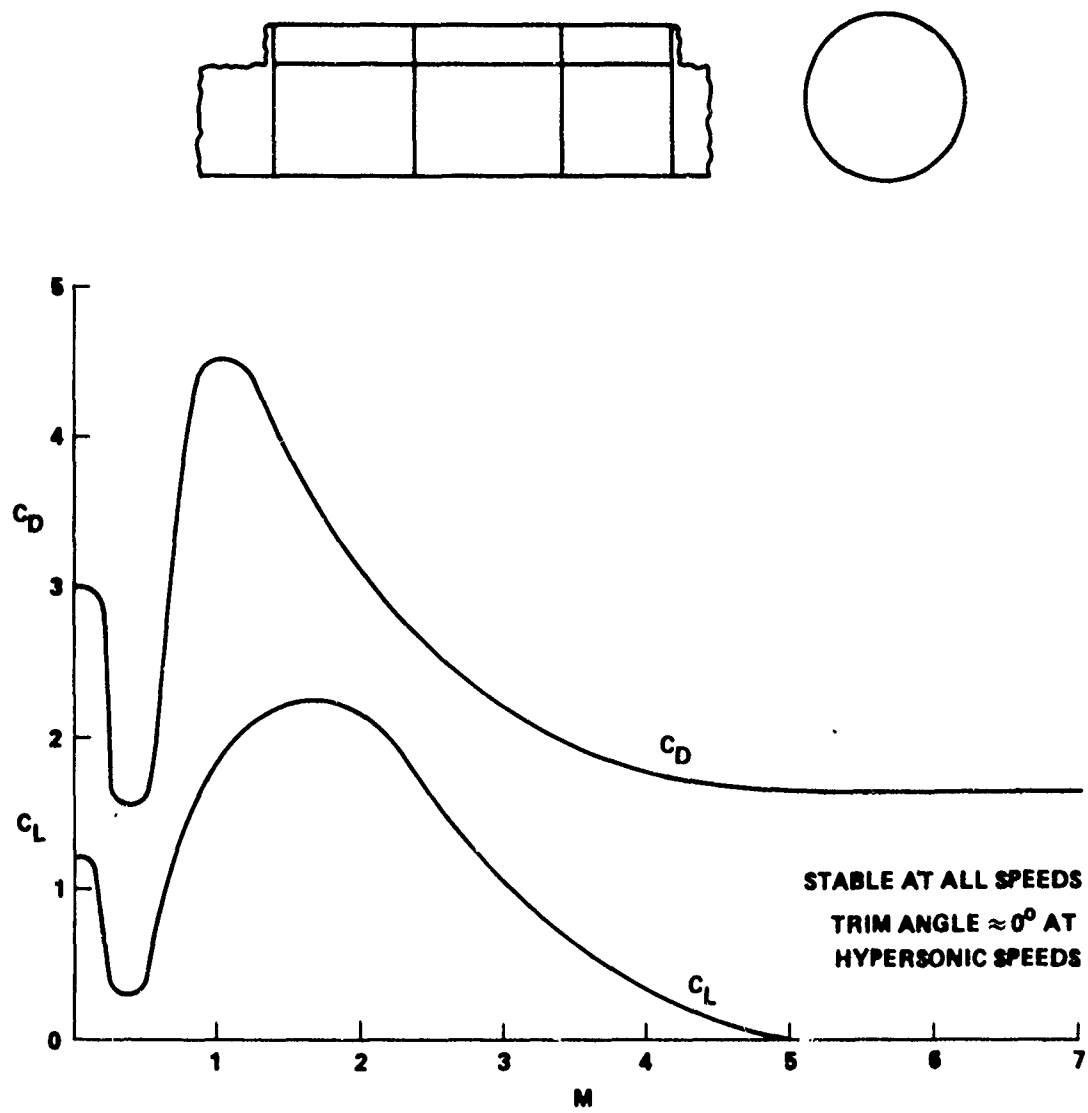


FIGURE B-2 LIFT AND DRAG COEFFICIENTS FOR MID ET SECTION

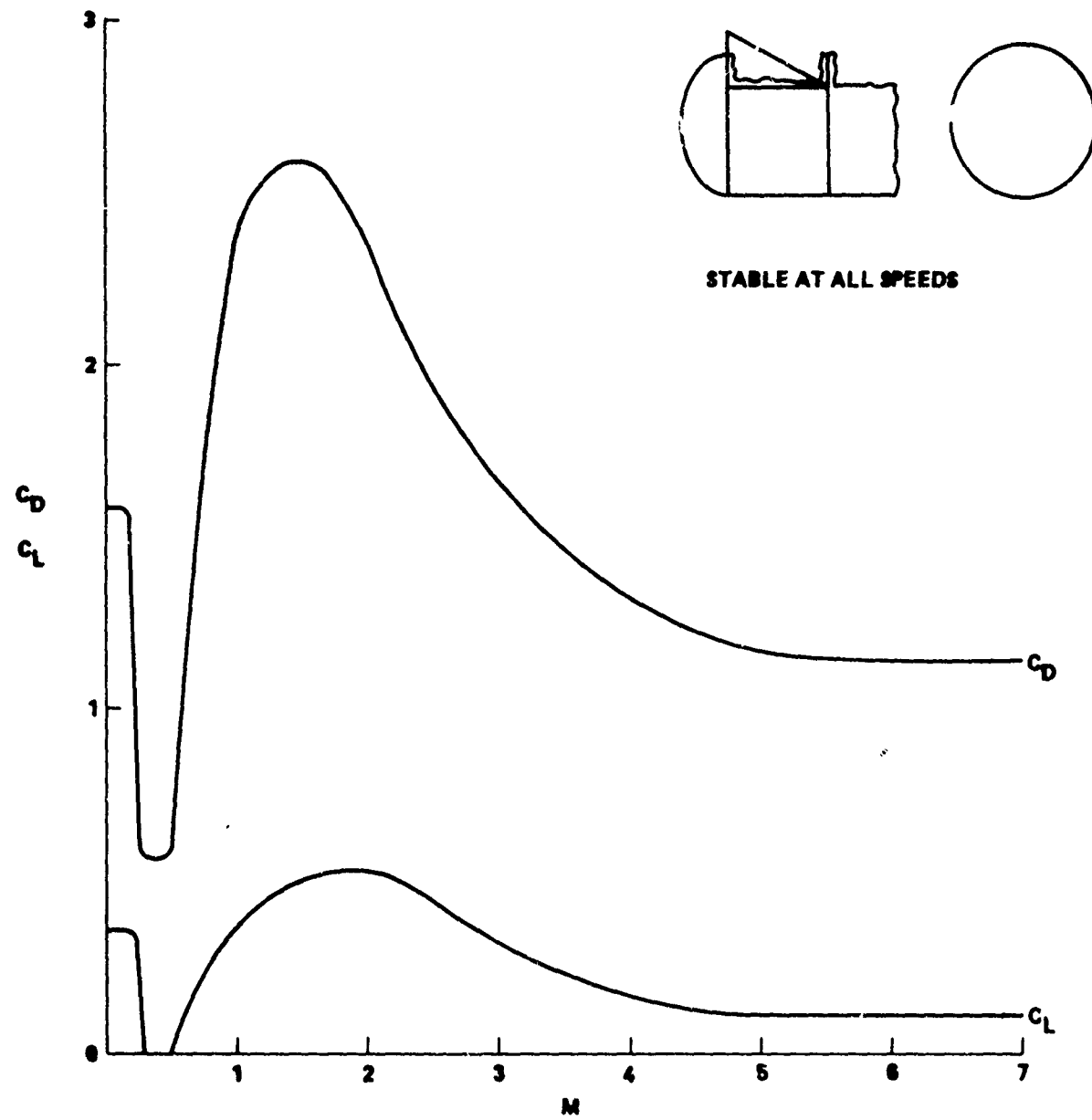


FIGURE B-3 LIFT AND DRAG COEFFICIENTS FOR AFT ET SECTION

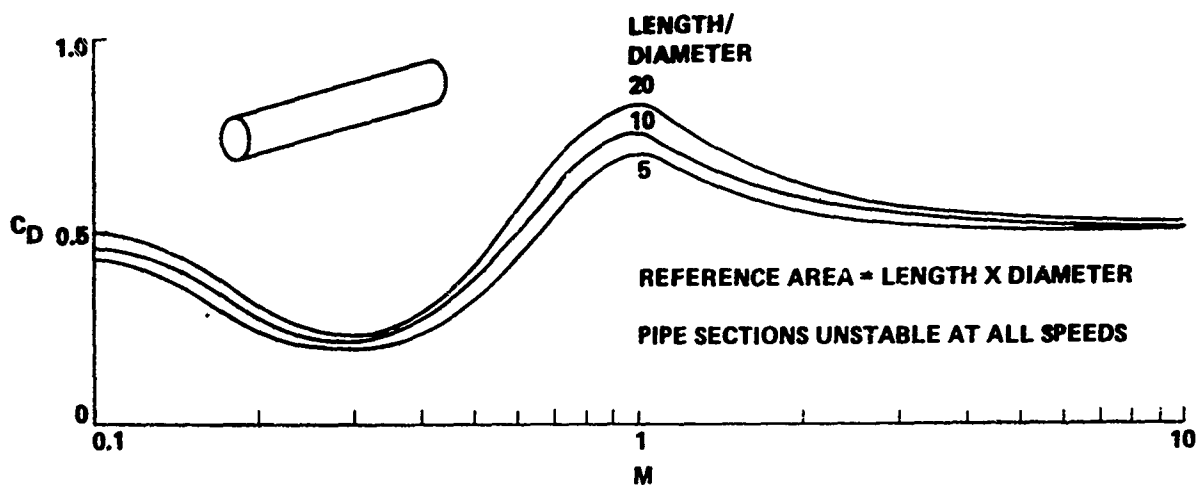


FIGURE B-4 DRAG COEFFICIENT FOR PIPE SECTIONS

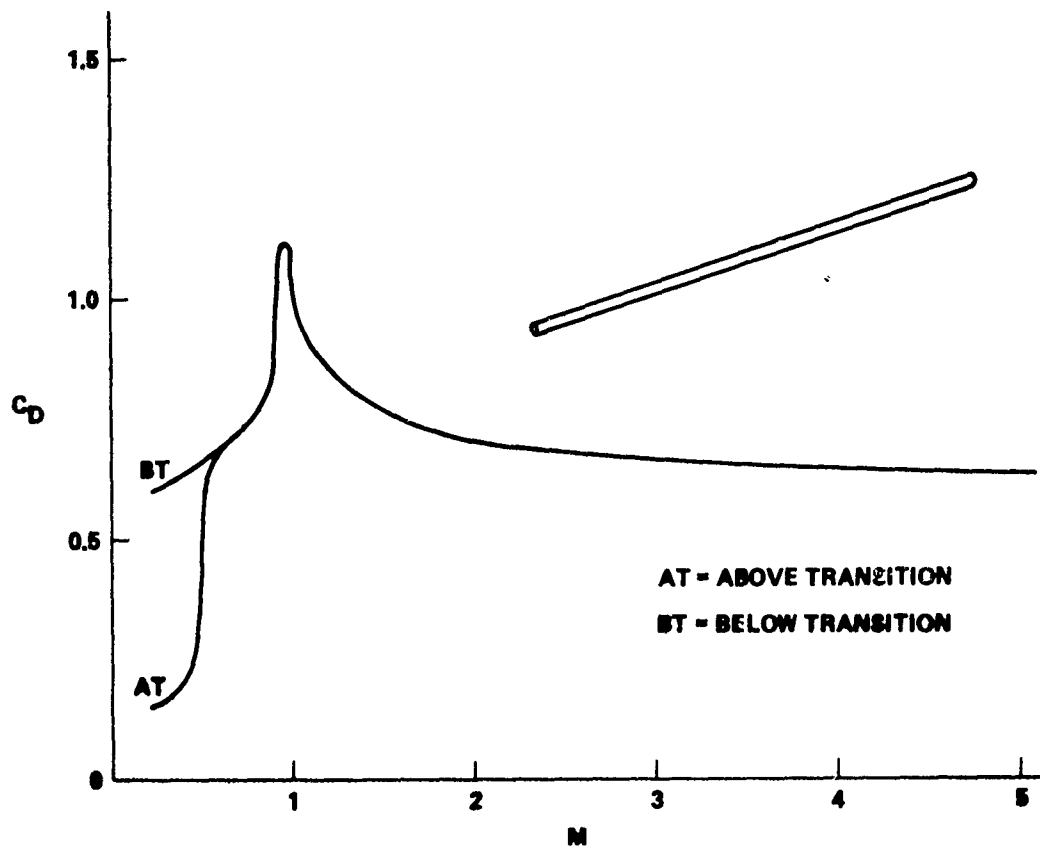


FIGURE B-5 DRAG COEFFICIENT FOR VENT VALVE, PURGE, AND HELIUM INJECTION LINES

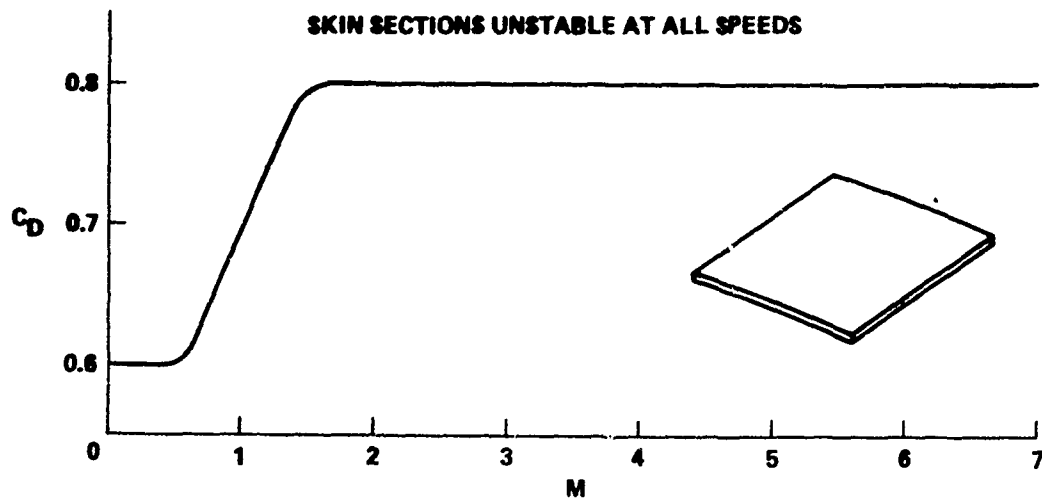


FIGURE B-6 DRAG COEFFICIENT FOR ET SKIN SECTIONS

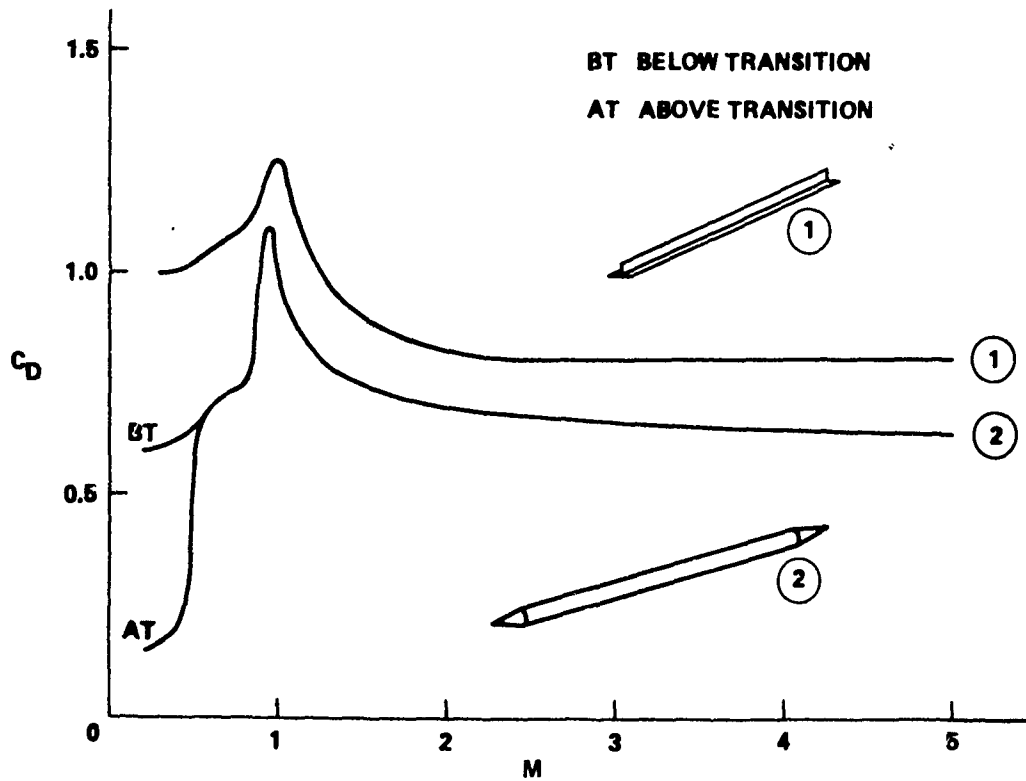


FIGURE B-7 DRAG COEFFICIENT FOR RING FRAME STABILIZERS (LH_2 TANK)

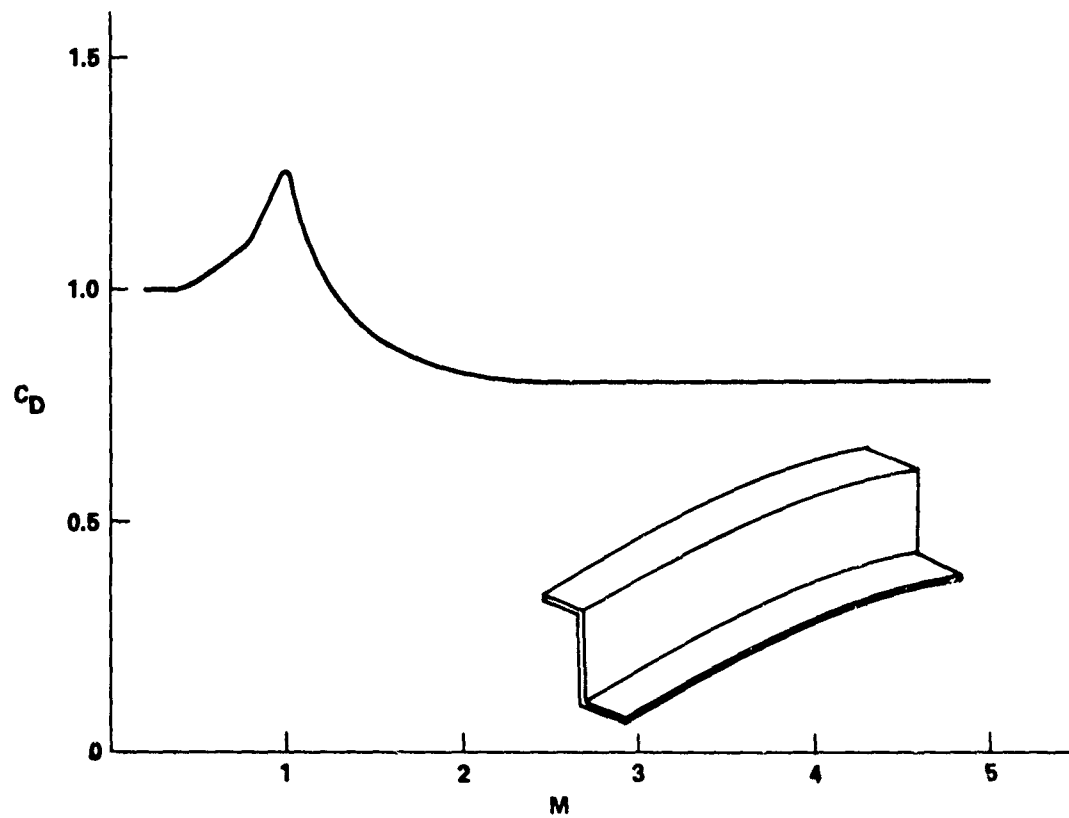


FIGURE B-8 DRAG COEFFICIENT FOR STABILITY RINGS (LH_2 TANK), STRINGERS AND TENSION STRAPS (SLOSH BAFFLE), CABLE TRAY SEGMENTS, AND LSC SHEATH SEGMENTS

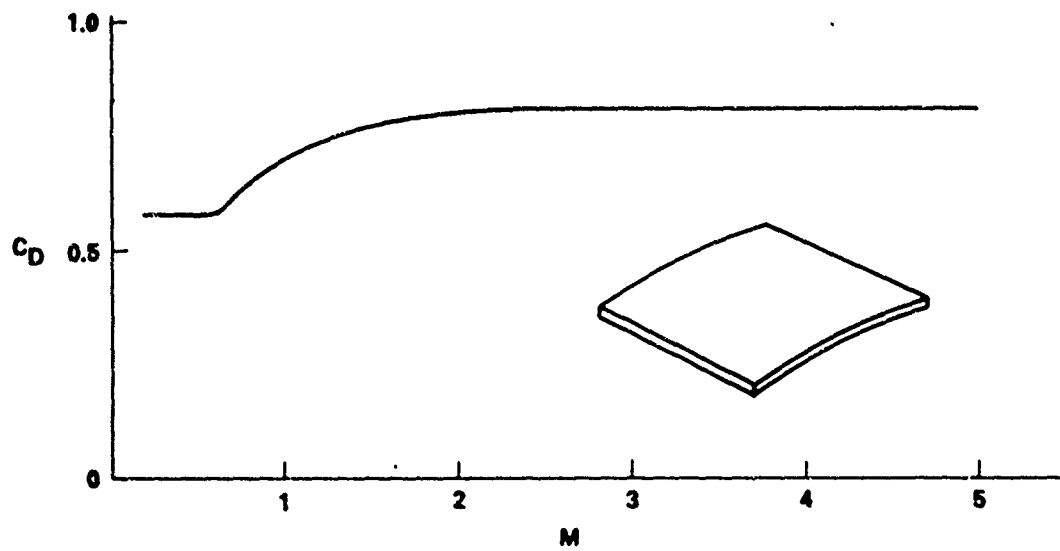


FIGURE B-9 DRAG COEFFICIENT FOR SLOSH BAFFLE SEGMENTS AND INDIVIDUAL BAFFLE WEBS

NSWC TR 80-417

APPENDIX C

LISTING OF ORBITER DEBRIS FRAGMENTS

CONFIGURATION: Integrated Vehicle

COMPONENT: Orbiter (Forward Velocity = 180 fps)

TIME OF DESTRUCT ACTION (SEC): 10

Piece Description and Remarks	Number of Pieces	Weight of Each Piece (lb)	Total Weight (lb)	Reference Area (ft ²)	Ballistic Factor Range (W/CDA) (lb/ft ²)	Velocity Increment (ft/sec)	Figure Number	C_D	C_L
(1) Fuselage (Mid Section)	1	63,200	63,200	1,000	50-290	16	C-1	-	
(2) Fuselage (Aft Section)	1	179,000	179,000	335	310-670	16	C-2	-	
(3) Nose Landing Gear	1	500	500	8	30-200	0-16	C-3	-	
(4) RCS Nozzles	14	50	700	0.2	130-250	0-16	C-4	-	
(5) RCS Press Tanks	2	75	150	2.2	34-340	0-16	C-5	-	
(6) RCS Fuel Tanks	2	200	400	8.7	23-230	0-16	C-5	-	
(7) Fwd Orbiter/ET Attach Struts	2	90	180	3	33-110	8	C-6	-	
(8) Beams, Trusses, Pipes	40-70	1.5-50	700	0.2-0.6	6-100	0-16	C-7	-	
(9) Payload Bay Doors	8	375	3,000	140	3.3-4.5	16	C-8	-	
(10) Landing Gear Doors	2	80	160	20	5-6.7	0-16	C-8	-	
(11) Skin Sections	40-400	2-20	800	1-10	2.5-3.3	0-16	C-8	-	
(12) Thermal Tiles	2,500-5,000	0.1-0.7	500-1,000	0.35	0.36-3.3	0-200	C-8	-	
(13) C-C Thermal Material	~1,000	0.06	60	0.01	5-7	0-16	C-9	-	
(14) Miscellaneous	1,000-5,000	0.01-10	6,500	0.001-1	1-20	0-200	*	-	
	TOTAL				256,400				

 $*C_D \approx 1$

CONFIGURATION: Right SRB Separated

COMPONENT: Orbiter (Forward Velocity = 300 fps)

TIME OF DESTRUCT ACTION (SEC): 20

Piece Description and Remarks	Number of Pieces	Weight of Each Piece (lb)	Total Weight (lb)	Reference Area (ft ²)	Ballistic Factor (W/C _D A) (1b/ft ²)	Velocity Increment (ft/sec)	Figure Number
					C _D	C _L	
(1) Fuselage (Mid Section)	1	63,200	63,200	1,000	50-290	40	C-1 -
(2) Fuselage (Aft Section)	1	179,000	179,000	335	310-670	40	C-2 -
(3) Nose Landing Gear	1	500	500	8	30-200	0-40	C-3 -
(4) RCS Nozzles	14	50	700	0.2	130-250	0-40	C-4 -
(5) RCS Press Tanks	2	75	150	2.2	34-340	0-40	C-5 -
(6) RCS Fuel Tanks	2	200	400	8.7	23-230	0-40	C-5 -
(7) Fwd Orbiter/ET Attach Struts	2	90	180	3	33-110	20	C-6 -
(8) Beams, Trusses, Pipes	40-70	1.5-50	700	0.2-0.6	6-100	0-40	C-7 -
(9) Payload Bay Doors	8	375	3,000	140	3.3-4.5	40	C-8 -
(10) Landing Gear Doors	2	80	160	20	5-6.7	0-40	C-8 -
(11) Skin Sections	40-400	2-20	800	1-10	2.5-3.3	0-40	C-8 -
(12) Thermal Tiles	2,500-5,000	0.1-0.7	500-1,000	0.35	0.36-3.3	0-210	C-8 -
(13) C-C Thermal Material	~1,000	0.06	60	0.01	5-7	0-40	C-9 -
(14) Miscellaneous	1,000-5,000	0.01-10	6,500	0.001-1	1-20	0-210	*
TOTAL			256,400				

*C_D ≈ 1.

CONFIGURATION: Integrated Vehicle

COMPONENT: Orbiter (Forward Velocity = 1,070 fps)

TIME OF DESTRUCT ACTION (SEC): 50

Piece Description and Remarks	Number of Pieces	Weight of Each Piece (lb)	Total Weight (lb)	Reference Area (ft ²)	Ballistic Factor Range (W/C _D A) (1lb/ft ²)	Velocity Increment (ft/sec)	Figure Number	C _D	C _L
(1) Fuselage (Mid Section)	1	63,200	63,200	1,000	50-290	100	C-1	-	
(2) Fuselage (Aft Section)	1	179,000	179,000	335	310-670	100	C-2	-	
(3) Nose Landing Gear	1	500	500	8	30-200	0-100	C-3	-	
(4) RCS Nozzles	14	50	700	0.2	130-250	0-100	C-4	-	
(5) RCS Press Tanks	2	75	150	2.2	34-340	0-100	C-5	-	
(6) RCS Fuel Tanks	2	200	400	8.7	23-230	0-100	C-5	-	
(7) Fwd Orbiter/ET Attach Struts	2	90	180	3	33-110	50	C-6	-	
(8) Beams, Trusses, Pipes	40-70	1.5-50	700	0.2-0.6	6-100	0-100	C-7	-	
(9) Payload Bay Doors	8	375	3,000	140	3.3-4.5	100	C-8	-	
(10) Landing Gear Doors	2	80	160	20	5-6.7	0-100	C-8	-	
(11) Skin Sections	40-400	2-20	800	1-10	2.5-3.3	0-100	C-8	-	
(12) Thermal Tiles	2,500-5,000	0.1-0.7	500-1,000	0.35	0.36-3.3	0-240	C-8	-	
(13) C-C Thermal Material	~1,000	0.06	60	0.01	5-7	0-100	C-9	-	
(14) Miscellaneous	1,000-5,000	0.01-10	6,500	0.001-1	1-20	0-240	*	-	
	TOTAL		256,400						

C-4

*C_D ≈ 1.

CONFIGURATION: Right SRB Separated

COMPONENT: Orbiter (Forward Velocity = 1,070 fps)

TIME OF DESTRUCT ACTION (SEC): 52

Piece Description and Remarks	Number of Pieces	Weight of Each Piece (lb)	Total Weight (lb)	Reference Area (ft ²)	Ballistic Factor (W/C _{DA}) (1b/ft ²)	Velocity Increment (ft/sec)	Figure Number	C _D	C _L
(1) Fuselage (Mid Section)	1	63,200	63,200	1,000	50-290	100	C-1	-	
(2) Fuselage (Aft Section)	1	179,000	179,000	335	310-670	100	C-2	-	
(3) Nose Landing Gear	1	500	500	8	30-200	0-100	C-3	-	
(4) RCS Nozzles	14	50	700	0.2	130-250	0-100	C-4	-	
(5) RCS Press Tanks	2	75	150	2.2	34-340	0-100	C-5	-	
(6) RCS Fuel Tanks	2	200	400	8.7	23-230	0-100	C-5	-	
(7) Fwd Orbiter/ET Attach Struts	2	90	180	3	33-110	50	C-6	-	
(8) Beams, Trusses, Pipes	40-70	1.5-50	700	0.2-0.6	6-100	0-100	C-7	-	
(9) Payload Bay Doors	8	375	3,000	140	3.3-4.5	100	C-8	-	
(10) Landing Gear Doors	2	80	160	20	5-6.7	0-100	C-8	-	
(11) Skin Sections	40-400	2-20	800	1-10	2.5-3.3	0-100	C-8	-	
(12) Thermal Tiles	2,500-5,000	0.1-0.7	500-1,000	0.35	0.36-3.3	0-240	C-8	-	
(13) C-C Thermal Material	~1,000	0.06	60	0.01	5-7	0-100	C-9	-	
(14) Miscellaneous	1,000-5,000	0.01-10	6,500	0.001-1	1-20	0-240	*	-	
	TOTAL			256,400					

*C_D ≈ 1.

CONFIGURATION: Integrated Vehicle

COMPONENT: Orbiter (Forward Velocity = 3,200 fps)

TIME OF DESTRUCT ACTION (SEC): 100

Piece Description and Remarks	Number of Pieces	Weight of Each Piece (1lb)	Total Weight (1lb)	Reference Area (ft ²)	Ballistic Factor Range (W/CDA) (1lb/ft ²)	Velocity Increment (ft/sec)	Figure Number	C_D	CL
(1) Fuselage (Mid Section)	1	63,200	63,200	1,000	50-290	140	C-1	-	
(2) Fuselage (Aft Section)	1	179,000	179,000	335	310-670	140	C-2	-	
(3) Nose Landing Gear	1	500	500	8	30-200	0-140	C-3	-	
(4) RCS Nozzles	14	50	700	0.2	130-250	0-140	C-4	-	
(5) RCS Press Tanks	2	75	150	2.2	34-340	0-140	C-5	-	
(6) RCS Fuel Tanks	2	200	400	8.7	23-230	0-140	C-5	-	
(7) Fwd Orbiter/ET Attach Struts	2	90	180	3	33-110	70	C-6	-	
(8) Beams, Trusses, Pipes	40-70	1.5-50	700	0.2-0.6	6-100	0-140	C-7	-	
(9) Payload Bay Doors	8	375	3,000	140	3.3-4.5	140	C-8	-	
(10) Landing Gear Doors	2	80	160	20	5-6.7	0-140	C-8	-	
(11) Skin Sections	40-400	2-20	800	1-10	2.5-3.3	0-140	C-8	-	
(12) Thermal Tiles	2,500-5,000	0.1-0.7	500-1,000	0.35	0.36-3.3	0-260	C-8	-	
(13) C-C Thermal Material	~1,000	0.06	60	0.01	5-7	0-140	C-9	-	
(14) Miscellaneous	1,000-5,000	0.01-10	6,500	0.001-1	1-20	0-260	*	-	
	TOTAL		256,400						

CONFIGURATION: Right SRB Separated

COMPONENT: Orbiter (Forward Velocity = 3,700 fps)

Piece Description and Remarks	Number of Pieces	Weight of Each Piece (1b)	Total Weight (1b)	Reference Area (ft ²)	Ballistic Factor Range (W/C _D A) (1b/ft ²)	Velocity Increment (ft/sec)	TIME OF DESTRUCT ACTION (SEC): 115	
							Figure Number	C _D
(1) Fuselage (Mid Section)	1	63,200	63,200	1,000	50-290	150	C-1	-
(2) Fuselage (Aft Section)	1	179,000	179,000	335	310-670	150	C-2	-
(3) Nose Landing Gear	1	500	500	8	30-200	0-160	C-3	-
(4) RCS Nozzles	14	50	700	0.2	130-250	0-160	C-4	-
(5) RCS Press Tanks	2	75	150	2.2	34-340	0-160	C-5	-
(6) RCS Fuel Tanks	2	200	400	8.7	23-230	0-160	C-5	-
(7) Fwd Orbiter/ET Attach Struts	2	90	180	3	33-110	80	C-6	-
(8) Beams, Trusses, Pipes	40-70	1.5-50	700	0.2-0.6	6-100	0-160	C-7	-
(9) Payload Bay Doors	8	375	3,000	140	3.3-4.5	160	C-8	-
(10) Landing Gear Doors	2	80	160	20	5-6.7	0-160	C-8	-
(11) Skin Sections	40-400	2-20	800	1-10	2.5-3.3	0-160	C-8	-
(12) Thermal Tiles	2,500-5,000	0.1-0.7	500-1,000	0.35	0.36-3.3	0-260	C-8	-
(13) C-C Thermal Material	~1,000	0.06	60	0.01	5-8	0-160	C-9	-
(14) Miscellaneous	1,000-5,000	0.01-10	6,500	0.001-1	1-20	0-260	*	-
	TOTAL			256,400				

*C_D ≈ 1.

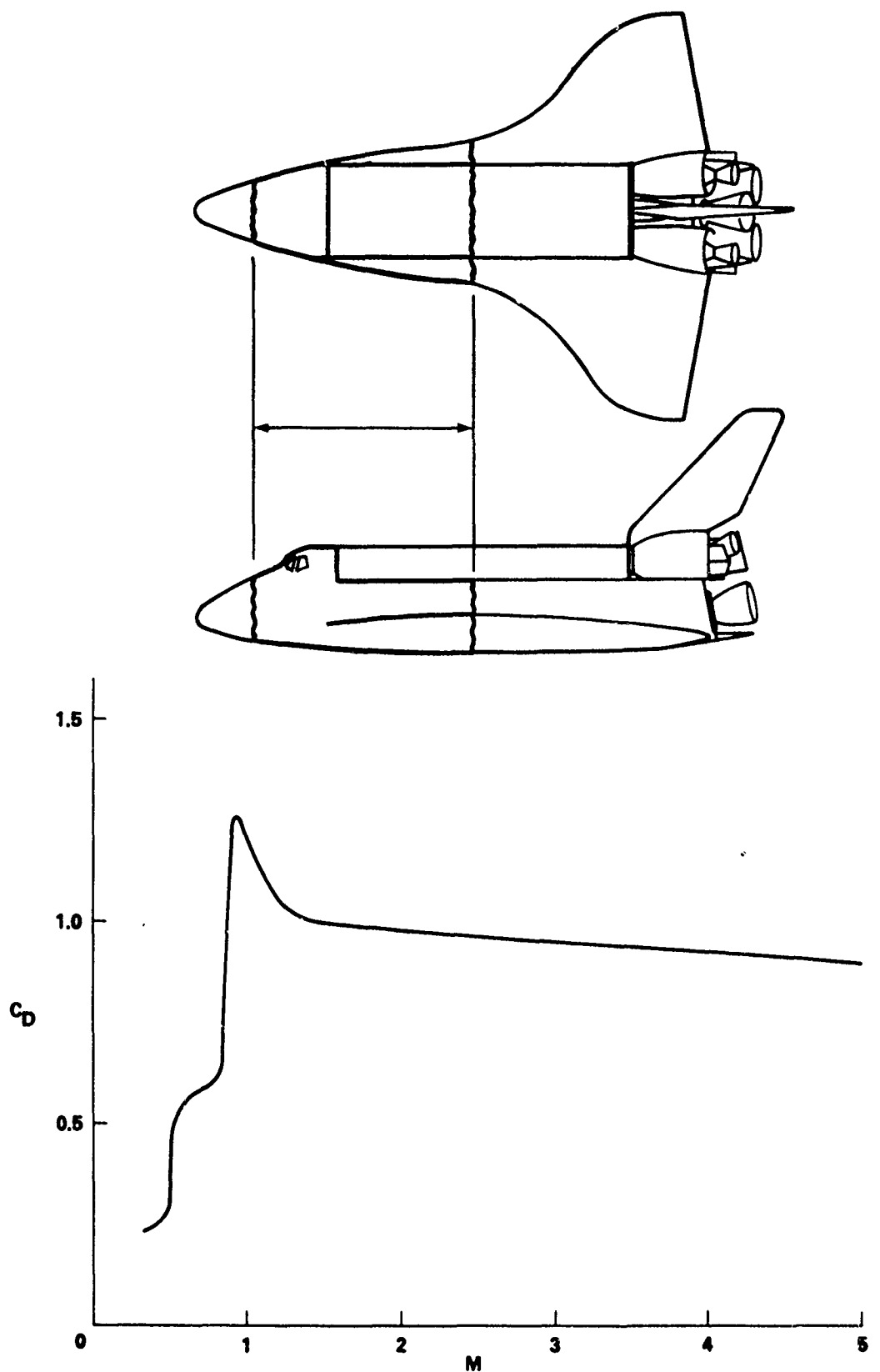


FIGURE C-1 DRAG COEFFICIENT FOR FUSELAGE MID SECTION

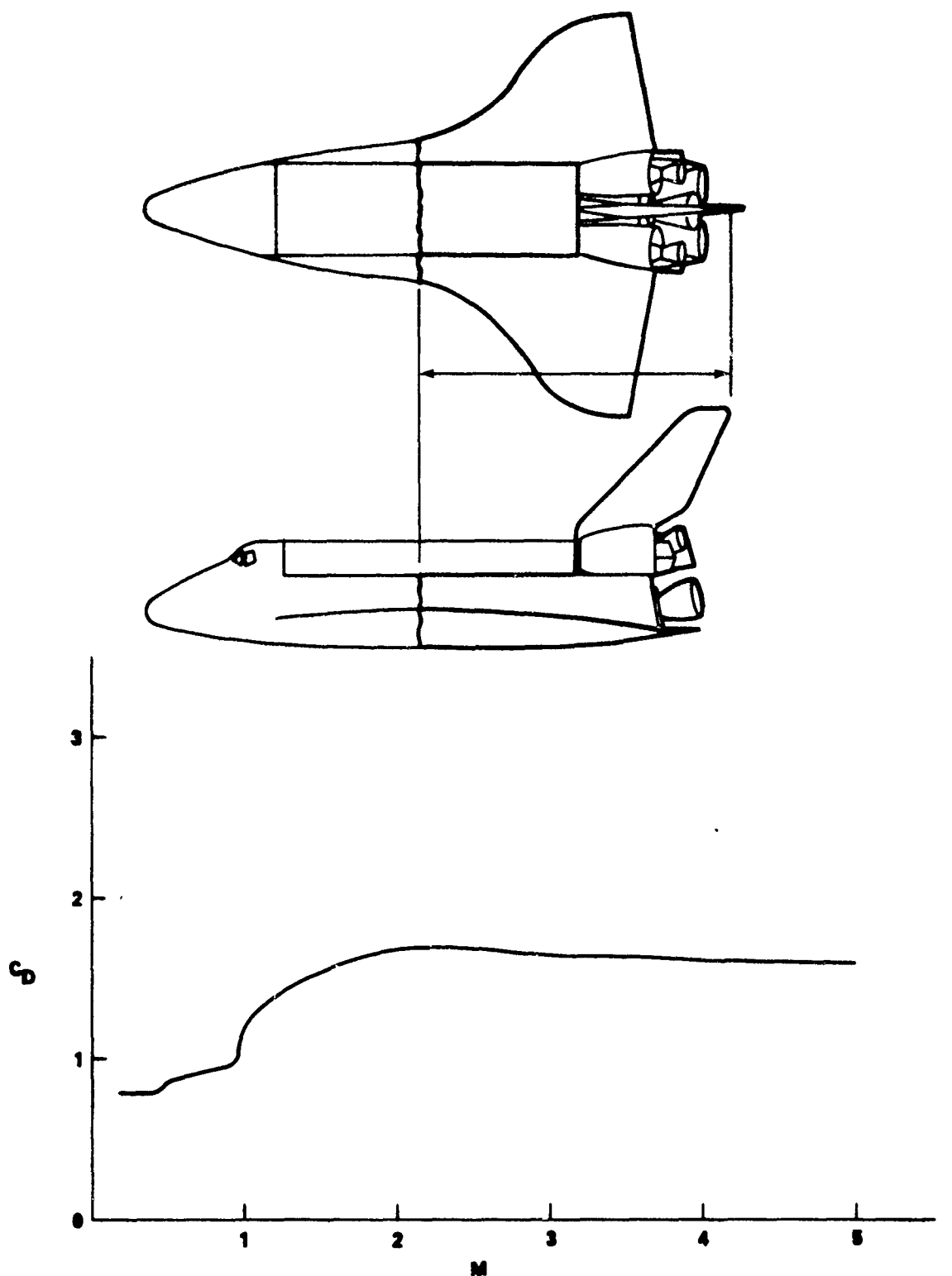


FIGURE C-2 DRAG COEFFICIENT FOR FUSELAGE AFT SECTION
(BODY, WING, TAIL, NOZZLES)

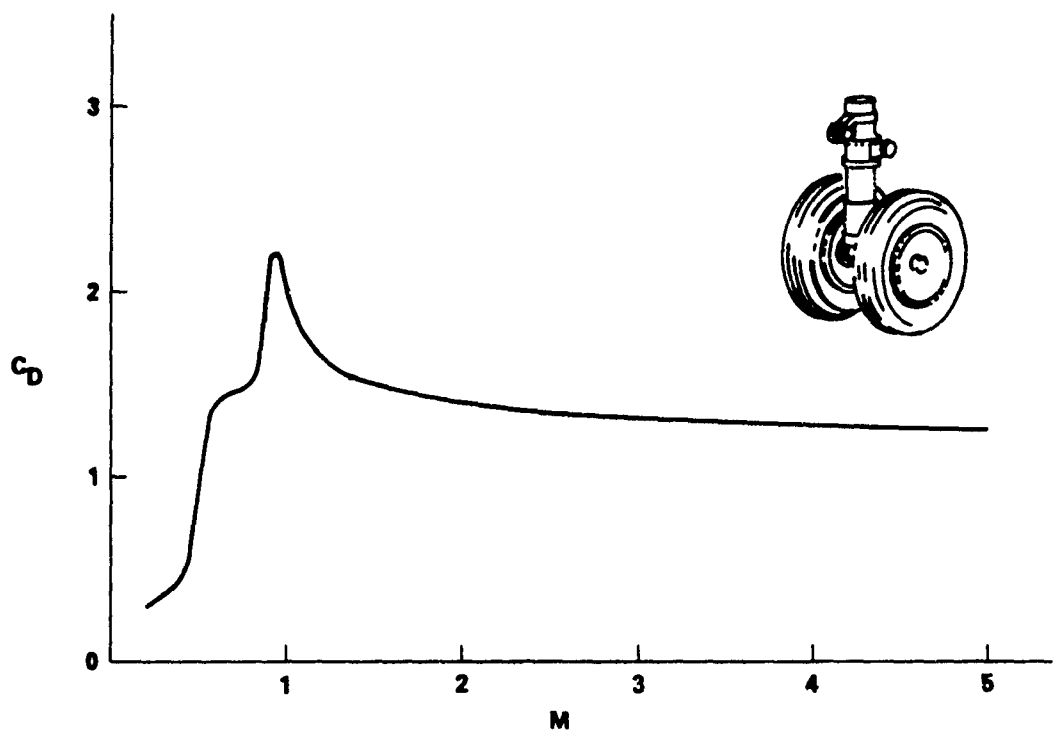


FIGURE C-3 DRAG COEFFICIENT FOR NOSE LANDING GEAR

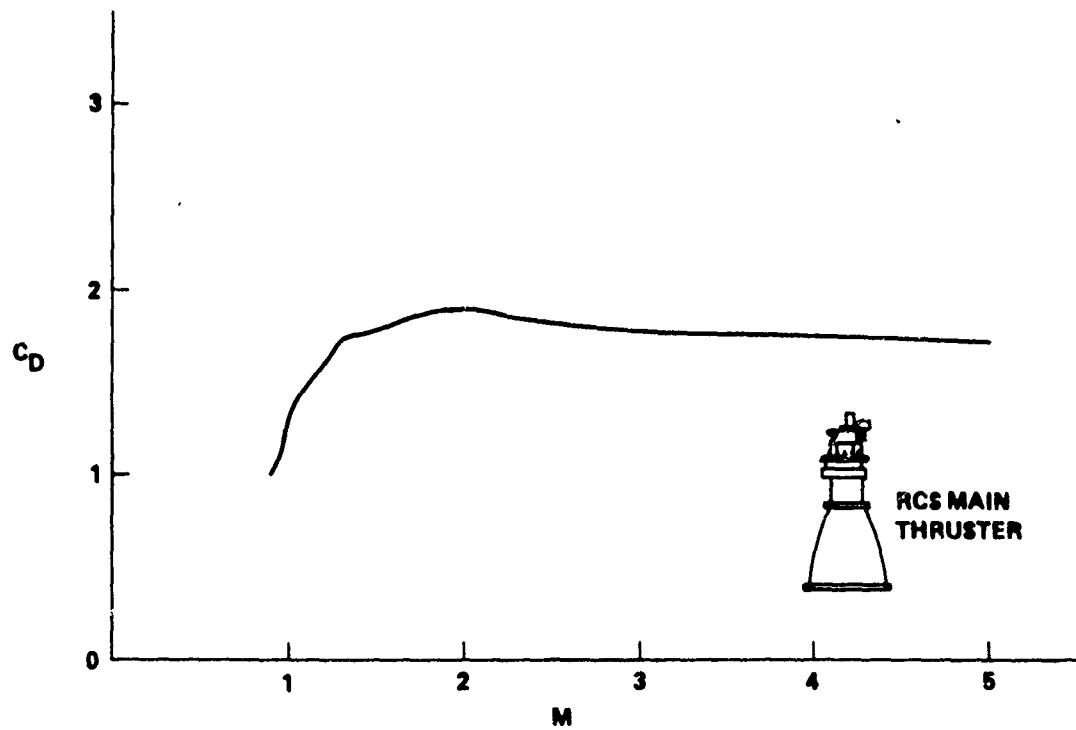


FIGURE C-4 DRAG COEFFICIENT FOR RCS NOZZLES

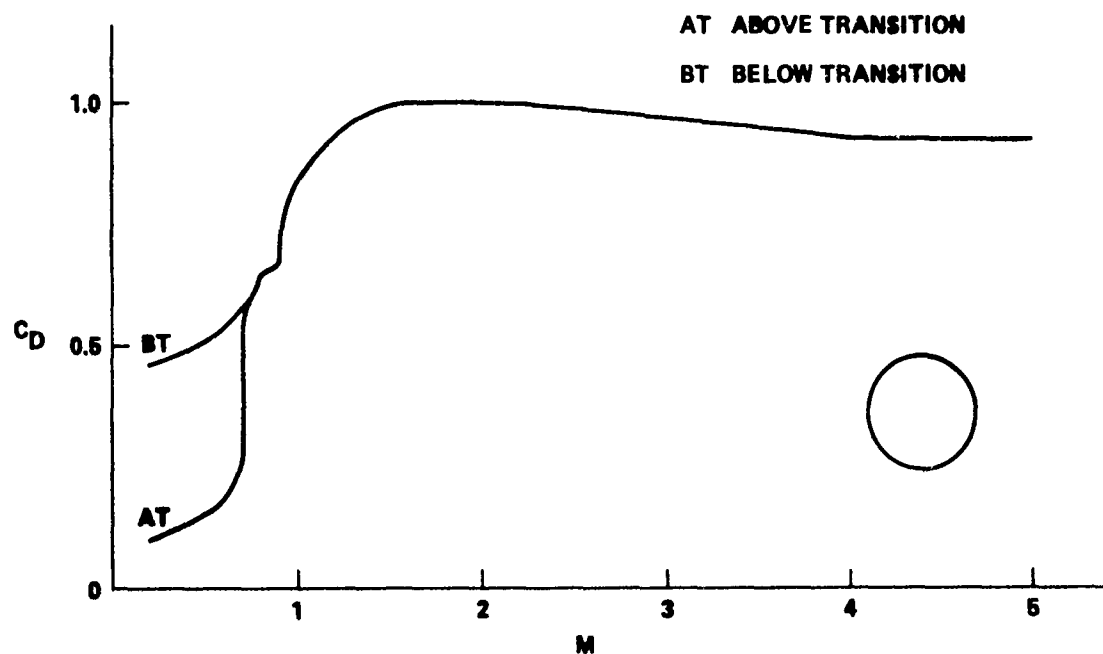


FIGURE C-5 DRAG COEFFICIENT FOR RCS FUEL, OXIDIZER, AND PRESSURIZATION TANKS

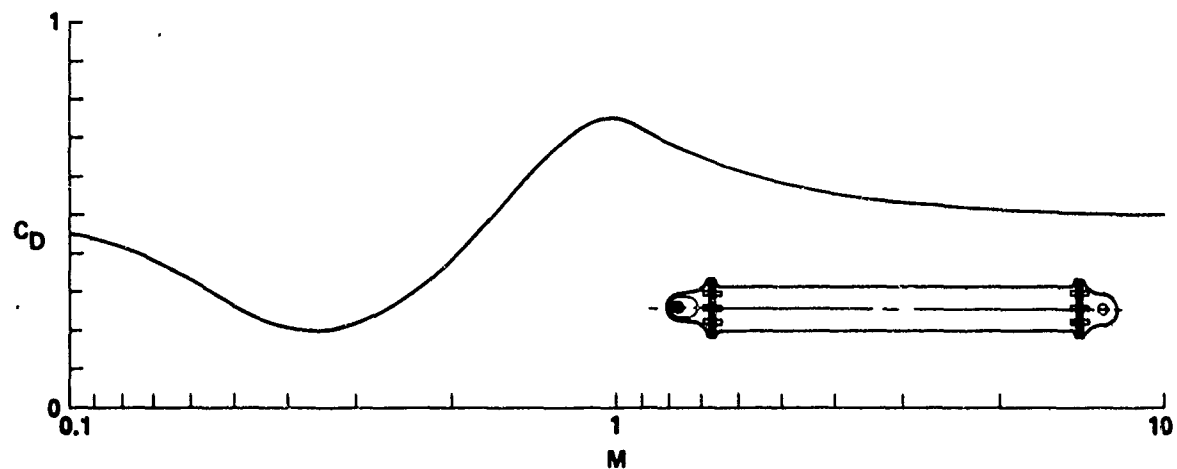


FIGURE C-6 DRAG COEFFICIENT FOR ORBITER/ET ATTACH STRUTS

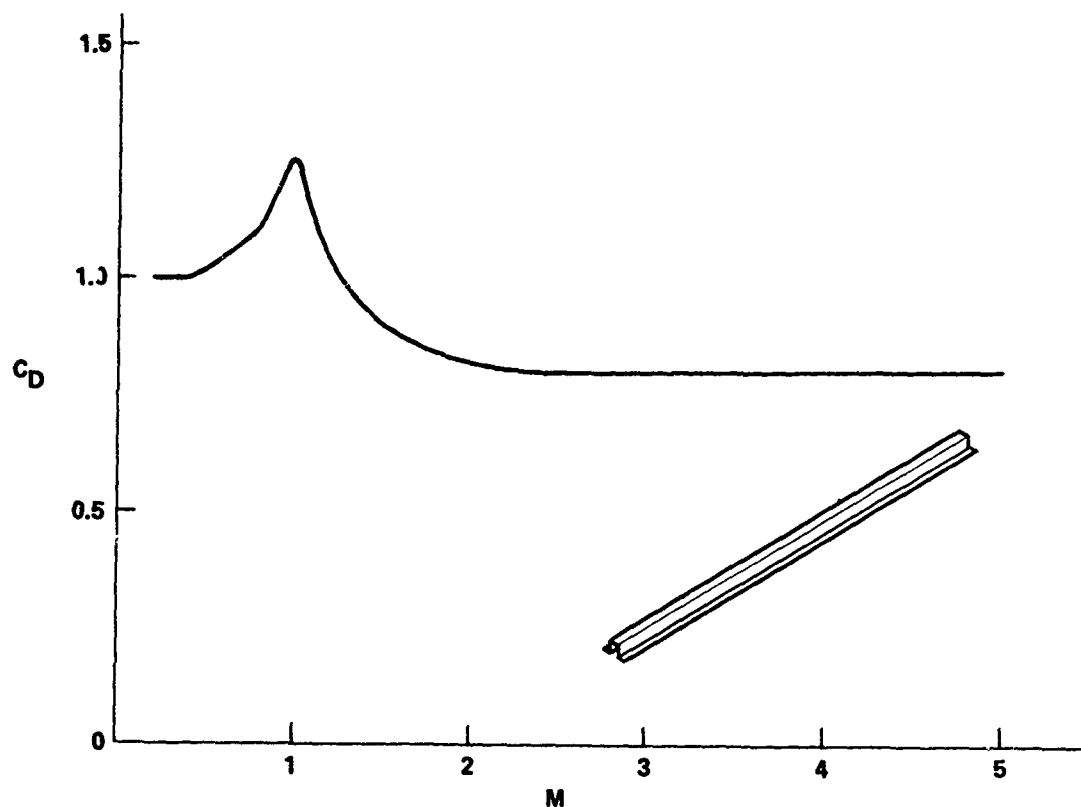


FIGURE C-7 DRAG COEFFICIENT FOR BEAMS, TRUSSES, AND PIPES

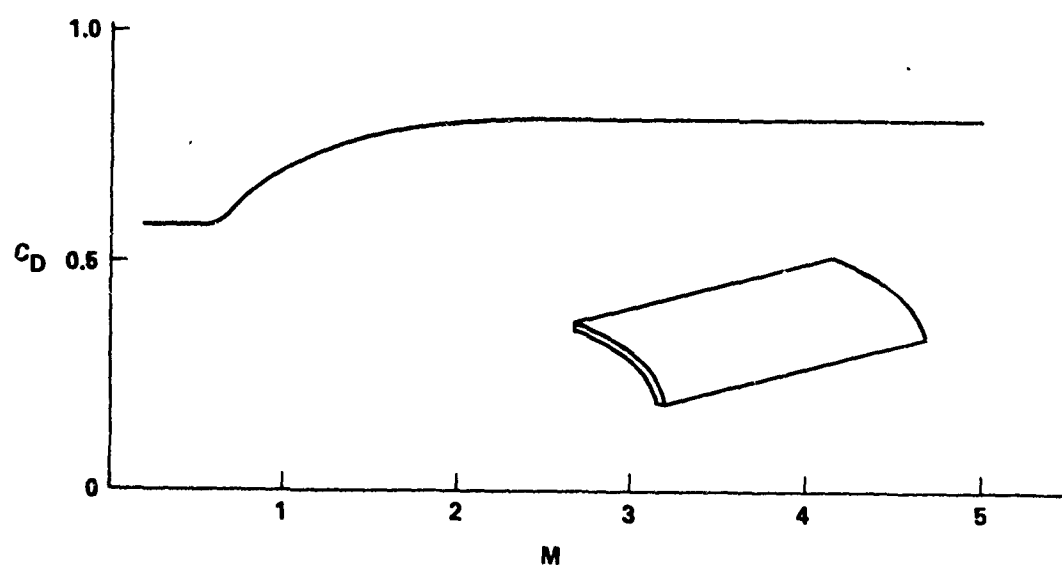
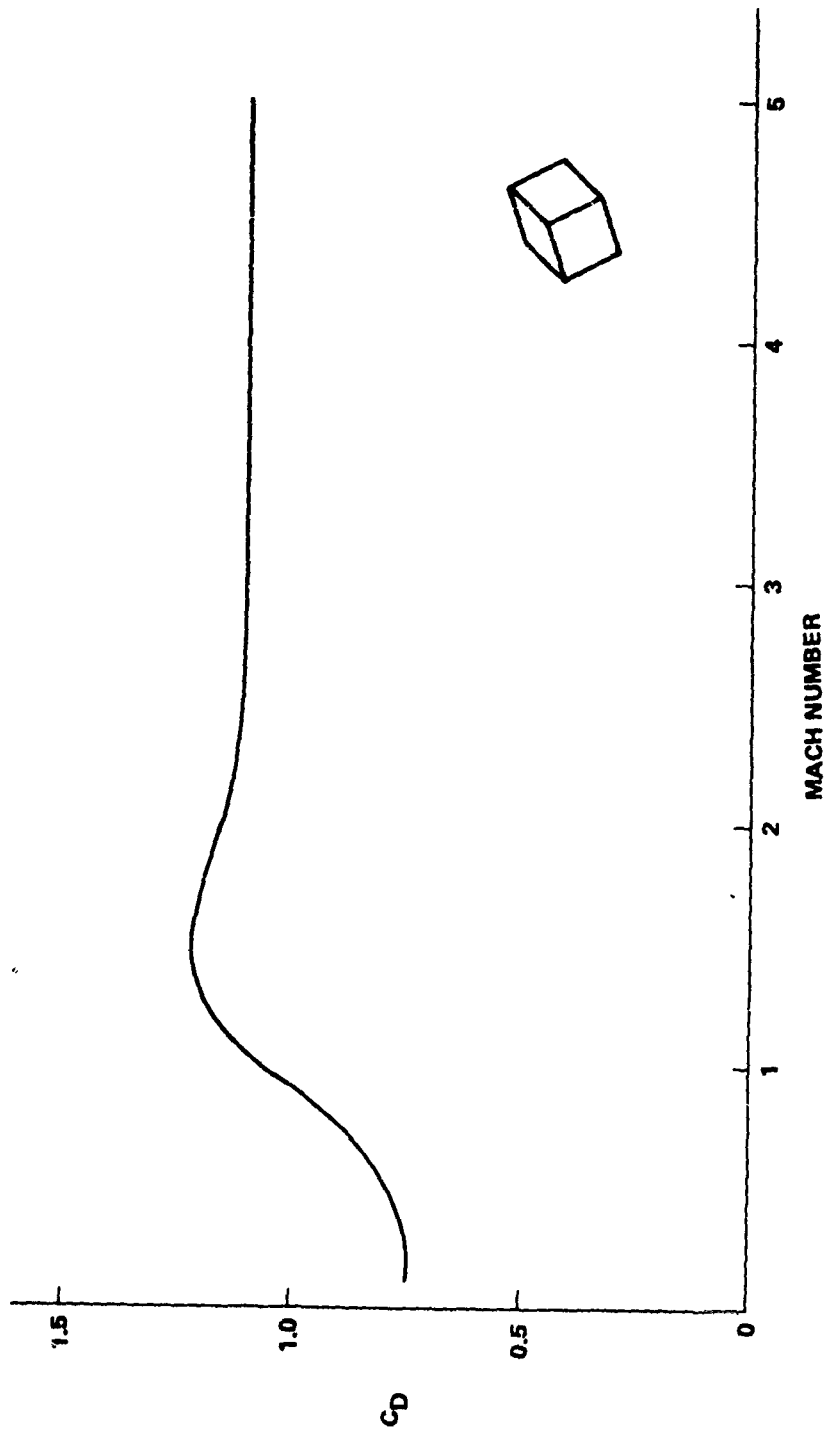


FIGURE C-8 DRAG COEFFICIENT FOR PAYLOAD BAY DOORS, LANDING GEAR DOORS,
SKIN SECTIONS, AND THERMAL TILES



C-13

FIGURE C-9 DRAG COEFFICIENT FOR C-C THERMAL MATERIAL

DISTRIBUTION

Copies

National Aeronautics and Space
Administration
Marshall Space Flight Center
ATTN: J. A. Roach (EL-42)
Alabama 35812

National Aeronautics and Space
Administration
Kennedy Space Center
ATTN: B. Rock (SF-ENG)
Florida 32899

National Aeronautics and Space
Administration
Lyndon B. Johnson Space Center
ATTN: R. Rose
Houston, TX 77058

President
Naval War College
Newport, RI .02840

Superintendent
Naval Postgraduate School
ATTN: Library
Montery, CA 93940

Superintendent
Naval Academy
Annapolis, MD 21402

Commander
Harry Diamond Laboratories
2800 Powder Mill Road
ATTN: Technical Library
Adelphi, MD 20783

40 Commandant
Army War College
ATTN: Library
Carlisle Barracks, PA 17013

Commandant
Industrial College of the Armed Forces
Ft. Leslie J. McNair
ATTN: Document Control
Washington, DC 20315

Commandant
National War College
Ft. Leslie J. McNair
ATTN: Class. Rec. Library
Washington, DC 20315

Directorate of Safety Headquarters
Eastern Space and Missile Center
Patrick Air Force Base
ATTN: L. Ullian (SEM)
Florida 32925

SAMTEC/ROSF
ATTN: Colin Gardner
Vandenberg AFB, CA 93437

Commander
Air Force Weapons Laboratory
ATTN: Lt. N. Clemens (DYVS)
Kirtland Air Force Base, NM 87117

Air University Library
ATTN: Documents Section
Maxwell Air Force Base, AL 26112

Copies

Institute for Defense Analysis
 400 Army-Navy Drive
 ATTN: Library
 Arlington, VA 22202

Chairman
 Department of Defense Explosives
 Safety Board
 Room 856-C Hoffman Bldg. 1
 2461 Eisenhower Avenue
 ATTN: R. Perkins
 R. Scott
 T. Zaker
 Alexandria, VA 22331

Director
 Defense Nuclear Agency
 ATTN: Technical Library
 Washington, DC 20305

Commander
 Field Command
 Defense Nuclear Agency
 ATTN: FCTA
 Kirtland Air Force Base, NM 87115

Defense Technical Information Center
 Cameron Station
 Alexandria, VA 22314

Library of Congress
 ATTN: Gift and Exchange Division
 Washington, DC 20540

Thiokol/Wasatch Division
 P. O. Box 524
 ATTN: Technical Library
 Brigham City, Utah 84302

Martin Marietta Corp.
 Michoud Operations
 ATTN: B. Elam
 New Orleans, Louisiana

Rockwell International Space Division
 12214 Lakewood Blvd.
 ATTN: Technical Library
 Downey, CA 90241

Battelle Memorial Institute
 505 King Avenue
 ATTN: E. Rice
 Columbus, OH 43201

Denver Research Institute
 Mechanical Sciences and
 Environmental Engineering
 University of Denver
 ATTN: J. Wisotski
 Denver, CO 80210

Falcon Research
 ATTN: D. Parks
 Denver, CO 80210

General American Transportation
 Corporation
 General American Research Div.
 7449 North Natchez Avenue
 ATTN: Technical Library
 Niles, IL 60648

General Electric Company - TEMPO
 816 State Street
 ATTN: W. Chan/DASIAC
 Santa Barbara, CA 93102

Hercules Incorporated
 Box 98
 ATTN: D. Richardson
 Magna, UT 84044

IIT Research Institute
 10 West 35th Street
 ATTN: Technical Library
 Chicago, IL 60616

Kaman Sciences Corp.
 P. O. Box 7463
 Colorado Springs, CO 80907

Los Alamos Scientific Laboratory
 P. O. Box 1663
 ATTN: LASL Library
 Los Alamos, NM 87544

12

New Mexico Institute of Mining
and Technology

TERA

ATTN: M. L. Kempton
J. P. McLain
Socorro, NM 87801

Pacific Technology
P. O. Box 148
Del Mar, CA 92016

Physics International Company
2700 Merced Street
ATTN: Technical Library
San Leandro, CA 94577

R and D. Associates
P. O. Box 3580
ATTN: Technical Library
Santa Monica, CA 90403

Sandia Laboratories
P. O. Box 5800
ATTN: Library
J. Reed
L. Vortman
Albuquerque, NM 87115

Sandia Laboratories
Livermore Laboratory
P. O. Box 969
Livermore, CA 94550

Director

Scripps Institution of Oceanography
La Jolla, CA 92037

Shock Hydrodynamics Incorporated
15010 Ventura Boulevard
ATTN: Technical Library
Sherman Oaks, CA 91403

Southwest Research Institute
8500 Culebra Road
ATTN: W. Baker
San Antonio, TX 78206

Systems, Science and Software
P. O. Box 1620
La Jolla, CA 92037

Teledyne Energy Systems
110 W. Timonium Road
ATTN: T. Olsen
Lutherville, MD 21093

University of California
Lawrence Livermore Laboratory
ATTN: Technical Library
Livermore, CA 94550

URS Corporation
155 Bonet Road
ATTN: Document Control
San Mateo, CA 94402

Director
Woods Hole Oceanographic Institute
Woods Hole, MA 02543

J. H. Wiggins Corporation
1650 S. Pacific Coast Highway
ATTN: J. Baeker
Redondo Beach, CA 90277